UNIVERSITY OF CALIFORNIA

Santa Barbara

Insights into South American Native Ungulate and Caviomorph Paleobiology

A dissertation submitted in partial satisfaction of the

requirements for the degree Doctor of Philosophy

in Earth Science

by

Andrew John McGrath

Committee in Charge:

Professor André Wyss, Chair

Professor Susannah Porter

Professor Bruce Tiffney

June 2021

The dissertation of Andrew John McGrath is approved.

_____
Susannah Porter

_____
Bruce Tiffney

_____
André Wyss, Committee Chair

June 2021

Insights into South American Native Ungulate and Caviomorph Paleobiology

by

Andrew John McGrath

ACKNOWLEDGEMENTS

To my family and friends who supported me through this journey. Thank you to all those who collected, prepared, and curated the fossils on which this thesis is based. Thank you to my committee members and research collaborators whose revisions and suggestions improved the quality of this dissertation.

VITA OF ANDREW JOHN MCGRATH

June 2021

EDUCATION

Bachelor of Arts in Biology, Case Western Reserve University, May 2016
Bachelor of Arts in Evolutionary Biology, Case Western Reserve University, May 2016
Doctor of Philosophy in Earth Science, University of California, Santa Barbara, June 2021 (expected)

PROFESSIONAL EMPLOYMENT

2016–21: Teaching Assistant; Departments of Earth Science, Ecology, Evolution, & Marine Biology, and Summer Sessions; University of California, Santa Barbara
2018–21: Teaching Associate: Departments of Earth Science and Ecology, Evolution, & Marine Biology; University of California, Santa Barbara

PUBLICATIONS

McGrath, A. J., Anaya, F., & Croft, D. A. 2020. New proterotheriids (Litopterna, Mammalia) from the middle Miocene of Quebrada Honda, Bolivia, and trends in diversity and body size of proterotheriid and macraucheniid litopterns. *Ameghiniana*, 57(2): 159–188.

McGrath, A. J., Flynn, J. J., & Wyss, A. R. 2020. Proterotheriids and macraucheniids (Litopterna: Mammalia) from the Pampa Castillo fauna, Chile (early Miocene, Santacrucian SALMA) and a new phylogeny of Proterotheriidae. *Journal of Systematic Palaeontology*, 18(9), 717–738.

McGrath, A. J., Anaya, F., & Croft, D. A. 2018. Two new macraucheniids (Mammalia: Litopterna) from the late middle Miocene (Laventan South American Land Mammal Age) of Quebrada Honda, Bolivia. *Journal of Vertebrate Paleontology*, 38(3), e1461632.

FELLOWSHIPS & AWARDS

Alumni Graduate Award for Research Excellence, UCSB Earth Science 2021
Wendell Phillips Woodring Memorial Graduate Fellowship, UCSB Earth Science 2020
Lloyd and Mary Edwards Field Studies Fellowship, UCSB Earth Science 2017
Regents Fellowship in Earth Science, UCSB 2016

FIELDS OF STUDY

Major Field: Vertebrate Paleobiology
Systematics and Phylogeny with Professor André Wyss
Diversity and Morphological Evolution with Professors André Wyss and Darin Croft

Faunal Similarity with Professors André Wyss, Darin Croft, and John Flynn
Geometric Morphometrics with Professor André Wyss

ABSTRACT

Insights into South American Native Ungulate and Caviomorph Paleobiology

By

Andrew John McGrath

In the five chapters of this dissertation, I investigate the paleobiology of South American native ungulates (SANUs) and caviomorph rodents. Although these studies involve different taxonomic groups and employ disparate methods, most rely on previously undescribed fossils to interrogate broader evolutionary questions.

In the first chapter, I describe early Miocene litopterns (a group of SANUs) from Pampa Castillo, Aysén Region, Chile, and perform a phylogenetic analysis of one of its subgroups, Proterotheriidae. Litoptern taxa from Pampa Castillo include the macraucheniid *Theosodon* and proterotheriids *Thoatherium* and *Picturotherium*, corroborating the fauna's assignment to the Santacrucian South American land mammal age (SALMA). My phylogenetic analysis, which indicates that "Anisolambdidae" forms a non-monophyletic cluster within Proterotheriidae, is the foundation of a new stem-based definition for Proterotheriidae. This chapter was published in the *Journal of Systematic Palaeontology* in 2020.

My second chapter describes two new proterotheriids from the middle Miocene of Quebrada Honda, Tarija Department, Bolivia, and analyzes litoptern diversity and body-

size evolution in a phylogenetic context. These taxa, *Olisanophus riorosarioensis* gen. et sp. nov. and *Olisanophus akilachuta* gen. et sp. nov., greatly clarify proterotheriid evolution in mid-latitude South America. The diversity analysis indicates that these groups were more diverse than previously appreciated, particularly during the Paleogene. Macraucheniids increased in body size throughout the Cenozoic, whereas proterotheriids followed a similar trend during the Paleogene, but did not change in size during the Neogene. This chapter was published in *Ameghiniana* in 2020.

Cavioid, chinchilloid, and erethizontoid caviomorph rodents from Pampa Castillo are described in the third chapter. Cavioids are represented by *Luantus minor*, *Eocardia* cf. *excavata*, and *Neoreomys australis*, the last of which is the most abundantly represented mammal in the Pampa Castillo fauna. Chinchilloids are represented by four species of *Perimys* (*P. erutus*, *P. onustus*, *P. intermedius*, and a yet unnamed species previously described from the Pinturas Formation), *Prolagostomus pusillus*, *Scleromys quadrangulatus*, and a probable new species of *Scleromys*. This assemblage represents a mixture of two well-known, contemporaneous fossil faunas previously recognized from the lower + middle sequences of the Pinturas Formation and the Santa Cruz Formation. The phylogenetic affinities and relative abundance of these taxa suggest the paleoenvironment of Pampa Castillo was similarly intermediate between these two better-known faunas.

In the fourth chapter, I describe the octodontoid caviomorphs from Pampa Castillo and conduct a faunal similarity analysis of Pampa Castillo and ten other early to middle Miocene (Colhuehuapian–Friasian/Colloncuran SALMAs) Patagonian rodent faunas. Eight octodontoids occur at Pampa Castillo, three of them likely representing

new species of *Caviocricetus*, *Dudumus*, and *Prostichomys*. The other five are referred to previously described taxa: *Acarechimys minutus*, *Acarechimys constans*, *Acarechimys* cf. *minutissimus*, *Acaremys* cf. *murinus*, and *Spaniomys* cf. *riparius*. Faunal similarity analyses yielded inconsistent results depending on whether genus- or species-level data were used. The combined results of these analyses and recently published geochronological data suggest that the 'Pinturan' biochronologic interval is not valid; faunas referred to it should instead be assigned to the Santacrucian SALMA.

I analyze the proximal ankle bones of litoptern and notoungulate (another SANU group) from the early Miocene Santa Cruz Formation, Argentina with the aim of assessing their utility in systematic studies and whether linear measurements or two-dimensional (2D) landmarks are more effective for assessing morphological differences. The ultimate goal of this research is to allow robust inferences about the locomotory habits of the sampled taxa. These results suggest that isolated tarsals may be identified to family and genus-level, but this conclusion needs further testing. Quantitative tests show that tarsals of different SANU taxa may be slightly more reliably distinguished by 2D landmarks than by linear measurements. However, 2D landmarks are clearly superior from the perspective of ease of measurement, replicability, and applicability to taxonomically diverse samples. Although the lack of modern taxa in the sample limited the paleobiological inferences that could be drawn, body mass, phylogeny, and possibly locomotor behavior, clearly influence tarsal morphology.

Throughout this dissertation, I have used the description of new taxa and specimens as the foundation for phylogenetic, paleoenvironmental, biochronological,

and ecomorphological analyses. These studies have advanced our knowledge of mammal evolution in South America, particularly in the early and middle Miocene.

TABLE OF CONTENTS

LIST OF FIGURES

CHAPTER 1

PROTEROTHERIIDS AND MACRAUCHENIIDS (LITOPTERNA: MAMMALIA) FROM THE PAMPA CASTILLO FAUNA, CHILE (EARLY MIOCENE, SANTACRUCIAN SALMA) AND A NEW PHYLOGENY OF PROTEROTHERIIDAE

ABSTRACT

Here we describe the litopterns, a diverse and temporally long-ranging clade of South American native ‘ungulates’, of the early Miocene Pampa Castillo fauna from the Galera Formation in the Andean Cordillera of southern Chile and present a new phylogeny of Proterotheriidae, the most speciose litoptern subgroup.

Two proterotheriids occur at Pampa Castillo (Fig. 1), *Thoatherium*, the northernmost and first record of this taxon outside Santa Cruz Province, Argentina, and *Picturotherium*, known previously solely from the Pinturas Formation of northwestern Santa Cruz Province. Macraucheniidae are represented at Pampa Castillo by *Theosodon*. Collectively, these three taxa suggest an early Miocene (Santacrucian SALMA) age for the fossil mammal fauna from Pampa Castillo, reinforcing previous biochronologic interpretations.

Results of a comprehensive phylogenetic analysis identify *Megadolodus molariformis* as the earliest-diverging member of Proterotheriidae, a name for which we propose a stem-based definition. Few multi-species proterotheriid genera were recovered as monophyletic in our analysis. Three ‘anisolambdid’ litopterns, initially assumed to represent outgroups, instead nest deeply within Proterotheriidae, implying long ghost lineages. The phylogenetic placement of the four proterotheriids from the middle Miocene La Venta fauna of Colombia sheds light on the poorly understood long-term isolation of tropical faunas and their degree of exchange with high-latitude regions.

Santacrucian SALMA assemblages in Patagonia are notable in that older localities preferentially produce earlier-diverging proterotheriids. Older sites are also marked by a mix of brachyodont and hypsodont taxa, whereas younger sites yield strictly hypsodont forms, supporting the notion of increasing aridity in Patagonia through this interval. Proterotheriids alone cannot be used to discriminate between an early or late Santacrucian age for the Pampa Castillo fauna, but the brachydonty of *Picturotherium* suggests a humid climate and closed habitats.

KEYWORDS

Chile; Proterotheriidae; Macraucheniidae; Miocene; Santacrucian SALMA; South American Native Ungulates (SANUs).

INTRODUCTION

During its lengthy isolation from other continents spanning most of the Cenozoic, South America hosted a highly endemic mammal fauna (Simpson 1980), including several native herbivorous lineages. These forms, South American native 'ungulates' (SANUs), are conventionally considered to constitute a monophyletic group, Meridiungulata (*sensu* McKenna and Bell, 1997), or to have arisen independently from multiple 'condylarth' precursors (Muizon and Cifelli, 2000; Horovitz, 2004; O'Leary et al., 2013; Gelfo et al., 2016) (quotation marks indicate questionable monophyly). Recent proteomic and genetic work suggests that the two most diverse SANU subgroups, notoungulates and litopterns, form a monophyletic pair closely related to perissodactyls (Buckley, 2015; Welker et al., 2015; Westbury et al., 2017).

Litopterna, the second-most diverse SANU clade after notoungulates, ranged from the Paleocene to the early Holocene (Kerber et al., 2011; Prado et al., 2015; Croft, 2016; Gelfo et al., 2016). Three major litoptern sub-clades, Macraucheniidae, Adianthidae, and Proterotheriidae, were present in the early Miocene (Cifelli, 1983; Muizon and Cifelli, 2000; Soria, 2001; Croft, 2016; Gelfo et al., 2016). Macraucheniids, the largest-bodied litopterns, ranged from the middle or late Eocene (Mustersan South American Land Mammal 'Age' [SALMA]) to the early Holocene (Cifelli, 1983; Kerber et al., 2011). Adianthids (*sensu* Cifelli, 1991, i.e., excluding Indaleciidae), among the most poorly understood litoptern groups, spanned the late Oligocene (Deseadan SALMA) to middle Miocene (Colloncuran/'Friasian' SALMA;

Cifelli and Soria, 1983; Cifelli, 1991). Proterotheriids (*sensu* Soria, 2001), are known from the late Oligocene (Deseadan SALMA) to the late Pleistocene (Lujanian SALMA; Soria, 2001; Ubilla et al., 2009).

Given their substantial phylogenetic distance from extant ungulates, proterotheriids hold the potential to inform hypotheses concerning the evolution of modern ungulate groups. For example, proterotheriids are notable for their functional, and in the case of *Thoatherium* Ameghino, 1887, true, monodactyly (the degree of which, remarkably, exceeds even that of modern equids) (Scott, 1910; Soria, 2001; Cassini et al., 2012a). Digit reduction in equids and artiodactyls has been variously ascribed to increasing body size (Thomason, 1986; McHorse et al., 2017), open habitats (Simpson, 1951), or locomotor efficiency (Gregory, 1912; Howell, 1944; Janis and Wilhelm, 1993). Conversely, proterotheriids remained relatively small-bodied throughout their history (Soria, 2001; Cassini et al., 2012a, b), and are thought to have favoured closed habitats based on their craniomandibular morphology and inferred browsing diet (Cifelli and Guerrero, 1997; Cassini, 2013; Morosi and Ubilla, 2017). Proterotheriids are counterpoints, therefore, to arguments that digit reduction is advantageous in the contexts of large body size and open habitats.

Proterotheriid relationships have not previously been addressed comprehensively using modern cladistic methods. In his thorough revision of the group, Soria (2001) recognized two major proterotheriid lineages using non-cladistic means. Subsequent analyses (Kramarz and Bond, 2005; Villafañe et al., 2012; Schmidt, 2015) employed phylogenetic methods but geographically restricted

datasets, excluding taxa from the low-latitudes. The dataset assembled here includes all species known from adequate material, including four from the middle Miocene La Venta fauna of Colombia, none of which have been subjected to rigorous phylogenetic analysis until now (Fig. 1; Cifelli and Guerrero Diaz, 1989; Cifelli and Guerrero, 1997; Cifelli and Villarroel, 1997). Two taxa from La Venta, *Lambdaconus colombianus* Hoffstetter and Soria, 1986, and *Megadolodus molariformis* McKenna, 1956, were originally interpreted as late-surviving 'condylarths' (McKenna, 1956; Hoffstetter and Soria, 1986) but are currently regarded as proterotheriids (Cifelli and Guerrero Diaz, 1989; Cifelli and Villarroel, 1997). The present analysis, therefore, provides the first comprehensive basis for assessing the biogeographic history of proterotheriids.

Herein we first describe the litopterns from the early Miocene (Santacrucian SALMA) Pampa Castillo fauna from the Andes Mountains of southern Chile (Fig. 1; Flynn et al., 2002). Although the Cenozoic mammal fauna of Argentina has been studied for nearly two centuries (e.g., Owen, 1838) the Chilean record is comparatively poorly understood. The fossil mammals from Pampa Castillo are similar in age to the well-sampled Santa Cruz fauna best known from the coast of Santa Cruz Province, Argentina, some 475 km to the east, though other localities occur further inland (Fig. 1; e.g., Fleagle et al., 2012; Vizcaíno et al., 2012; Croft, 2016). The Santacrucian SALMA of Patagonia records 13 proterotheriid species placed in seven genera (Soria, 2001; Villafañe et al., 2006). Other litopterns occurring during this interval include an uncertain number of species of the macraucheniid *Theosodon* Ameghino, 1887, and the adianthid *Adianthus buccatus*

Ameghino, 1891a, (Scott, 1910; Cassini et al., 2012a). The Santacrucian SALMA captures a period of climatic change in Patagonia including the onset of the mid-Miocene climatic optimum (Raigemborn et al., 2018a; Cuitiño et al., 2019; Trayler et al., 2020). As the northwestern-most Santacrucian fauna in Patagonia (Fig. 1), Pampa Castillo offers the opportunity to understand this climatic change, and the mammalian community's response to it, in a broader context.

MATERIALS AND METHODS

Geological Setting

Detailed accounts of the stratigraphy and chronology of the mammal-bearing strata at Pampa Castillo and the taxonomic composition of the Pampa Castillo fauna are given in Flynn et al. (2002). The locality occurs above tree line at roughly 1350 m elevation in the Andes Mountains of southern Chile (Aisén Province; ~47°S, 72.5°W) between Lago General Carrera (=Lago Buenos Aires) and Lago Cochrane (=Lago Pueyrredón; Fig. 1). The mammal-bearing beds have been variably assigned to the Río Zeballos (Niemeyer, 1975), Santa Cruz (de la Cruz et al., 2004), Galera (Niemeyer et al., 1984), or Pampa Castillo (Scalabrino, 2009) Formations [see discussion in Flynn et al. (2002) and Folguera et al. (2018)]. Pending formal naming, designation of a type section, and a published description of the Pampa Castillo formation, we continue to refer to these beds to the Galera Formation, consistent with previous work (Flynn et al., 2002). The sequence has been correlated

stratigraphically and temporally to the Santa Cruz Formation in Argentina (Niemeyer et al., 1984; Flynn et al., 2002). Folguera et al. (2018) recently provided a LA-ICP-MS U/Pb date of 18.7 ± 0.3 Ma on zircons from a reworked tuff about 10 m above the contact between the terrestrial fossil-bearing unit and the gradationally and conformably underlying marine Guadal Formation at Meseta Guadal. A U/Pb (SHRIMP) age of ~18 Ma from a tuff within the fossil-bearing unit (Suárez et al., 2015) is consistent with the known age range of the Santacrucian SALMA and Santa Cruz Formation deposits and faunas (Flynn and Swisher, 1995; Croft et al., 2004; Cuitiño et al., 2016; and discussion below). No litopterns have been reported from the Galera Formation at Pampa Guadal, ~20 km northwest of Pampa Castillo (Bostelmann and Buldrini, 2012). The Pampa Castillo fauna is referred to the Santacrucian SALMA, although only the rodents (Dodson, 1994; Chick et al., 2010) and palaeothentids (Flynn et al., 2002) have been described comprehensively. This study represents the first detailed assessment of the fauna's SANUs.

Phylogenetic Analysis Methods

Our phylogenetic analysis encompasses all proterotheriid species known from adequate material (Supplementary File 1). Taxa excluded due to incompleteness are: *Bounodus enigmaticus* Carlini et al., 2006, *Diadiaphorus*? *caniadensis*, *Diadiaphorus* (or *Epitherium*) *eversus* Ameghino, 1891b, *Epecuenia thoatherioides* Cabrera, 1939, *Lambdaconus inaequifacies* Ameghino, 1904, *Neolicaphrium major* Soria, 2001, and *Paramacrauchenia inexspectata* Soria, 2001.

Synonymies and taxonomy follow Soria (2001), except as noted below. We recognize *Tetramerorhinus fleaglei* Soria, 2001 [considered a subspecies of *T.*

cingulatum Ameghino, 1891b, by Soria (2001)] as a distinct species, following Kramarz and Bond (2005). Following Schmidt (2015), *Brachytherium cuspidatum* Ameghino, 1883, [a *nomen dubium* per Soria (2001)] is considered a valid senior synonym of *Lophogonodon gradatum* Ameghino, 1891b, and *Lophogonodon paranensis* Ameghino, 1904. We follow Carrillo et al. (2018) in recognizing *Lambdaconus colombianus* as such, rather than as *Neodolodus colombianus* (Hoffstetter and Soria, 1986) or *Prothoatherium colombianus* (Cifelli and Guerrero Diaz, 1989). Soria (2001) considered *Prothoatherium* Ameghino, 1902, invalid, dividing its species between *Lambdaconus* and *Paramacrauchenia*, but did not discuss *L. colombianus*.

The six outgroup taxa in our analysis included three ‘anisolambdids’, one protolipternid (both litoptern subgroups, but see Gelfo et al., 2016), one indaleciid (possible litoptern subgroup), and one didolodontid (a ‘condylarth’, but see Gelfo et al., 2016). Specimens examined and literature consulted in assembly of the character-taxon matrix (Supplementary File 1) are listed in Supplementary File 2.

Our phylogenetic analysis included 38 taxa and 92 characters, 8 of which are continuous (Appendix 1). Nine characters pertain to cranial morphology, three to the mandible 69 to the dentition, and one to the postcranium. Continuous characters were rescaled to result in a range of 0–1 (Supplementary File 3) and were additive (ordered; see Goloboff et al., 2006). Continuous characters were scored as a range if measurements were taken from multiple specimens (Supplementary File 1; Supplementary File 3). Discrete characters were non-additive. All characters were unweighted. Hypsodonty indices were calculated as m3 crown height divided by m3

linguolabial width, following Janis (1988). We recorded hypsodonty indices only on relatively unworn teeth (i.e., where the lophids were distinguishable from/thinner than the cuspids). Hypsodonty index (char. 85; Appendix 1) was treated as a discrete rather than a continuous character because the latter option would require a large sample size for each taxon to yield meaningful results given that crown height changes due to wear. Moderate differences in hypsodonty among specimens may therefore be the result of differences in age at the time of death rather than evolution. We discretized this character to mitigate these age-related variations. The discrete states employed here (HI < 0.85, 0.85 < HI < 1.00, and HI > 1.00) were determined by qualitatively binning the variation between sampled taxa.

The analysis was performed in TNT version 1.5 (Goloboff and Catalano, 2016) using a driven, new technology search, and ratchet and tree-fusing. The minimum-length tree was generated ten times. Taxa were scored for between 25 (*Proterotherium cervioides* Ameghino, 1883) and 89 (*Thoatherium minusculum*) characters, with a median of 62 characters scored across all taxa (Supplementary File 1). *Didolodus multicuspis* Ameghino, 1897, (Didolodontidae) was specified as the outgroup. Bremer nodal support values were calculated for each analysis. Two follow-up analyses were run after excluding taxa scored for fewer than 33% and 50% of the characters, resulting in the elimination of four and ten taxa, respectively (Supplementary File 1).

Anatomical Abbreviations

C/**c**: canine; **Dp**/**dp**: deciduous premolar; **I**/**i**: incisor; **L**: left; **M**/**m**: molar; **P**/**p**: premolar; **R**: right.

Institutional Abbreviations

ACM: Beneski Museum of Natural History, Amherst, MA, USA; **AMNH FM**, Fossil Mammal Collections, American Museum of Natural History, New York, USA; **DGM**: Divisao de Geologia e Mineralogia, Departamento Nacional da Producao Mineral, Rio de Janeiro, Brazil; **Duke-ING**: Joint expeditions of Duke University and IGM; **FMNH P**: Paleontology Collections, Field Museum of Natural History, Chicago, USA; **IGM**: Museo Geológico Nacional, Servicio Geológico Colombiano (formerly INGEOMINAS), Bogotá D.C., Colombia; **MACN A**: Ameghino collection, Museo Argentino de Ciencias Naturales 'Bernardino Rivadavia', Buenos Aires, Argentina; **MACN PV**: Vertebrate Paleontology collections, Museo Argentino de Ciencias Naturales 'Bernardino Rivadavia', Buenos Aires, Argentina; **MLP**: Museo de La Plata, La Plata, Argentina; **MNHN**: Muséum national d'Histoire naturelle, Paris, France; **MNRJ**: Museu Nacional, Rio de Janeiro, Brazil; **SGOPV**: Vertebrate Paleontology collections, Museo Nacional de Historia Natural, Santiago, Chile; **TATAC**: Tatacoa Desert Collections, Departamento de Geociencias, Universidad Nacional de Colombia, Bogotá, Colombia; **UCMP**: University of California Museum of Paleontology, Berkeley, California, USA; **YPM PU**: Princeton Collections, Yale Peabody Museum, New Haven, CT, USA.

SYSTEMATIC PALEONTOLOGY

Mammalia Linnaeus, 1758

Eutheria Huxley, 1880

Litopterna Ameghino, 1889

Lopholipterna Cifelli, 1983

Proterotheriidae Ameghino, 1887

Thoatherium Ameghino, 1887

Thoatherium cf. *T. minusculum* Ameghino, 1887

Figures 2A–C, 3

Type Species. *Thoatherium minusculum*.

Material. SGOPV 2015, complete LP3 (Fig. 2A) and mandibular fragment with two partial left molariform teeth, either m1–2 or m2–3; SGOPV 2095, complete RM1 (Fig. 2B); SGOPV 2210, partial mandible preserving Ldp2–4, Lm1, and Rdp2–3 in various states of completeness and complete Rdp4 and Rm1 (Fig. 3); SGOPV 2395, complete Lm3 (Fig. 2C).

Occurrence. Early Miocene (Burdigalian; Santacrucian SALMA) Santa Cruz Formation, Santa Cruz Province, Argentina, and Pampa Castillo fauna, Galera Formation, Chile.

Locality and Horizon. Pampa Castillo, Galera Formation, Chile.

Description. SGOPV 2015 includes a left upper molariform (Fig. 2A), likely P3, and parts of two left lower molariforms. The upper tooth bears three well-developed labial styles, and a weak paraconular fold, but no metaconular fold. The paraconule,

protocone, and hypocone are well-developed. No sulcus occurs on the crest connecting the protocone and hypocone. The highly reduced metaconule is connected by a faint crest to the crest between the protocone and hypocone. The weak mesiolingual cingulum is isolated from the protocone. A distal cingulum is present, but the presence or absence of a labial cingulum cannot be determined due to breakage.

The lower molariforms of SGOPV 2015 (likely m1–2 or m2–3) are incomplete. Both teeth appear to lack paraconids, and their paralophids fail to reach the lingual margin of the tooth. The protoconid and hypoconid on each tooth are positioned equally far labially. Neither tooth preserves a hypoconulid. A labial cingulid is present on the more mesial tooth. Both teeth possess a weak lingual cingulid that is interrupted at the base of the metaconid. The entoflexid is missing, making it uncertain whether the cingulid continued distal of the metaconid.

SGOPV 2095 is a right upper molariform tooth, probably M1 (Fig. 2B). The three labial styles and the paraconule, protocone, and hypocone are well-developed; para- and metaconular folds are absent. The crest joining the protocone and hypocone bears a small sulcus. The metaconule is extremely small, linguolabially elongated, and connected to the crest between the protocone and hypocone as well as to the metacone. Although damaged, the mesiolingual cingulum appears to have reached the protocone. Cingula occur distally and labially.

SGOPV 2210 [errantly referred to as SGOPV 2209 by Flynn et al. (2002)] preserves parts of both mandibular rami bearing dp2–4 and m1, of which only Rdp4 and Rm1 are complete (Fig. 3). The dp2 is double-rooted and bears a prominent

protoconid. A cristid extends distal of the metaconid. The molariform dp3 bears well-developed trigonid and talonid crescents. The strong paraconid lies on the same labiolingual plane as the metaconid. The hypoconid is positioned more labially than the protoconid, making the talonid crescent appear higher and narrower than that of the trigonid. A well-developed hypoconulid is present, but the entoconid is absent. The dp3 bears a labial cingulid, while a weak lingual cingulid crosses the metaflexid. In contrast to dp3, the two crescents of the dp4 are roughly symmetrical. Due to wear, the presence or absence of a paraconid is unknown. The paralophid fails to reach the tooth's lingual border. As in dp3, the entoconid is absent on dp4, a strong labial cingulid is present, and a lingual cingulid crosses the metaflexid. The m1 appears to lack a paraconid, but the paralophid reaches the lingual edge of the tooth. The talonid basin is slightly longer mesiodistally than the trigonid. The hypoconulid is well-developed, and the entoconid is absent. No labial cingulid occurs. The lingual cingulid originates at the mesial edge of the tooth, dips root-ward, and ends below the metaconid. Neither the mandibular symphysis nor any mandibular foramina are preserved.

SGOPV 2395 consists of a single Lm3 in a mandibular fragment (Fig. 2C). The paralophid terminates midway between the labial and lingual edges of the tooth, and the paraconid is weak. The trigonid exceeds the talonid in length. No entoconid occurs, but the hypoconulid is prominent. A weak labial cingulid surrounds the base of the protoconid but not the hypoconid. A weak lingual cingulid originates at the paraconid and ends at the metaconid.

Remarks. SGOPV 2015 is assigned to *Thoatherium* based on its small size (Table 1), the highly reduced metaconule and lack of strong interstylar folds on P3, and the lack of an entoconid and distal lingual cingulid on the lower cheek teeth. This combination of features rules out assignment to other proterotheriid genera. The teeth of SGOPV 2015 fall within the size range reported for *T. minusculum* (Soria, 2001, table 12), with the trivial exception that the more complete lower molariform is 0.2 mm (~2%) wider labiolingually than the maximum value reported by Soria (2001). We do not assign SGOPV 2015 to *T. minusculum* definitively however, given the specimen's fragmentary nature.

SGOPV 2095 is assigned to *Thoatherium* based on its small, linguolabially elongate metaconule, which connects the metacone to the crest between the protocone and hypocone. A similar feature occurs in *Diadiaphorus majusculus* Ameghino, 1887*,* but SGOPV 2095 is much smaller, falling within the range of *T. minusculum* (Table 1; Soria, 2001, table 12). The upper molars of *T. minusculum* are generally labiolingually wider than those of SGOPV 2095. For this reason, and because SGOPV 2095 consists of a single tooth, we qualify our identification of it as *Thoatherium* cf. *T. minusculum*.

SGOPV 2210 is assigned to *Thoatherium* based on its size, lack of entoconid on dp3–4 and m1, and weak lingual cingulid on m1 (Table 1; Scott, 1910, pl. 13, figs. 16, 16a; Soria, 2001). This combination of features excludes assignment to other proterotheriid genera. The m1 of SGOPV 2210 falls within the size range of *T. minusculum*, while the dp3–4 are slightly smaller than the two specimens reported by Soria (2001). The presence of only a single successional (permanent) tooth in

SGOPV 2210 precludes a more definitive assignment than to *Thoatherium* cf. *T. minusculum*.

SGOPV 2395 is also assigned to *Thoatherium* cf. *T. minusculum* on the basis of size, lack of entoconid, and short lingual cingulid (Table 1). An interdental wear facet occurs mesially but not distally, indicating that this tooth is Lm3. *Thoatherium* and *Diadiaphorus* are the only proterotheriids lacking entoconids on m3, and the size of SGOPV 2395 supports its assignment to *T.* cf. *T. minusculum.*

cf. *Thoatherium* sp.

Figure 2D

Material. SGOPV 2167, complete Lm1? (Fig. 2D) and fragment of second lower molariform tooth

Locality and Horizon. Pampa Castillo, Galera Formation, Chile.

Description. SGOPV 2167 includes one complete and one partial lower molariform tooth. The complete tooth likely represents Lm1 (Fig. 2D), but the locus of the fragment cannot be established definitively. The paraconid of m1 is well-developed, and the paralophid reaches the tooth's lingual edge. The protoconid and hypoconid are positioned equally far labially. The trigonid crescent is shorter mesiodistally than the talonid crescent. An entoconid is absent, but the hypoconulid is well-developed. A labial cingulid encircles the base of both labial cuspids. The lingual cingulid originates below the paraconid, dips root-ward, and ends mesial of the metaconid.

Remarks. SGOPV 2167 is assigned to cf. *Thoatherium* based on its size, strong paraconid, short lingual cingulid, and lack of entoconid, recalling SGOPV 2015 and SGOPV 2210 assigned above to *Thoatherium* cf. *T. minusculum* (Table 1). Despite these similarities, we only tentatively assign SGOPV 2167 to *Thoatherium* as it most closely resembles m1 of *T. minusculum* but also recalls the lower premolars of *Tetramerorhinus* spp. Ameghino, 1894, and *Anisolophus* spp. Burmeister, 1885. Uncertainty about the tooth's locus precludes unequivocal assignment to *Thoatherium*.

Picturotherium Kramarz and Bond, 2005

Picturotherium sp.

Figures 4, S1

Type Species. *Picturotherium migueli* Kramarz and Bond, 2005.

Material. SGOPV 2158, complete Rm3 (Fig. 4) and lower molariform tooth fragments (Fig. S1).

Occurrence. Early Miocene (Burdigalian; Santacrucian ['Pinturan'?] SALMA), Pinturas Formation, Santa Cruz Province, Argentina, and Pampa Castillo fauna, Chile.

Locality and Horizon. Pampa Castillo, Galera Formation, Chile.

Description. SGOPV 2158 includes a complete, low-crowned Rm3 (Fig. 4). The paralophid nearly reaches the tooth's lingual border, and the paraconid is weak. The

hypoconulid is medially positioned and forms a third, ‘distal’ lobe. The hypolophid folds lingually between the hypoconid and hypoconulid, effectively forming an additional flexid, termed the hypoflexid hereafter. A small entoconid joins the hypolophid basally rather than through a cristid. The weak labial cingulid is better developed around the base of the protoconid than the hypoconid. A lingual cingulid runs the length of the tooth, interrupted only by the metaconid. The associated tooth fragments provide no taxonomically diagnostic information.

Remarks. SGOPV 2158 is referred to *Picturotherium* based on a combination of features supporting this assignment to the exclusion of other proterotheriids. The presence of an entoconid rules out *Thoatherium minusculum* and *Diadiaphorus majusculus.* In *Anisolophus minusculus* Roth, 1899, *Lambdaconus* spp. Ameghino, 1897, *Paramacrauchenia* spp. Bordas, 1936, and *Prolicaphrium specillatum* Ameghino, 1902, the m3 entoconid and hypoconulid are subequal in size, whereas in SGOPV 2158 the former is much smaller. In contrast to SGOPV 2158, the molar paraconids of *Tetramerorhinus* spp., *T. minusculum*, and *D. majusculus* are well-developed. The hypoflexid of SGOPV 2158 is stronger than in *Lambdaconus* spp., *P. specillatum*, *Diadiaphorus*? *caniadensis* Kramarz and Bond, 2005, *Anisolophus floweri* Ameghino, 1887, and *A. minusculus.* The basal connection between the entoconid and hypolophid of SGOPV 2158 differs from *Tetramerorhinus* spp., *Anisolophus* spp., and *D.*? *caniadensis* where the entoconid is either independent or associated with the hypoconulid (Supplementary File 1). Although SGOPV 2158 is too worn to determine a crown height (see Appendix 1, char. 85), it seems less

hypsodont than *Diadiaphorus* spp., *T. minusculum*, *Tetramerorhinus* spp., *Anisolophus* spp., and *Paramacrauchenia* spp.

We assign SGOPV 2158 to *Picturotherium* sp. rather than *P. migueli* because it differs from the paratypes of *P. migueli* in several respects. The paralophid of SGOPV 2158 extends farther lingually than in *P. migueli* (MACN PV SC119b). The lingual cingulid extends the length of the tooth in SGOPV 2158 but ends at the metaconid in *P. migueli.* Additionally, SGOPV 2158 is larger than m3s attributed to *P. migueli* (Table 1). Given the fragmentary nature of SGOPV 2158, possible sexual dimorphism, as has been suggested for proterotheriids (Soria, 2001; Schmidt, 2015), or intraspecific variation, it forms an inadequate basis for recognizing a new species. Both SGOPV 2158 and MACN PV SC119b resemble the m3 of the late Oligocene (Deseadan SALMA) adianthid *Thadanius hoffstetteri* Cifelli and Soria, 1983, highlighting the remarkable degree of convergence between the lower molars of various litopterns, further cautioning against recognizing new taxa on the basis lower molars.

Proterotheriidae indet.

Figures S2–S3

Material. SGOPV 2220, maxillary and mandibular fragments with roots of a molariform tooth and fragments of one upper and one lower molariform tooth (Fig. S2); SGOPV 2416, lower molariform tooth fragment (Fig. S3).

Locality and Horizon. Pampa Castillo, Galera Formation, Chile.

Description and Remarks. SGOPV 2220 consists of an upper and lower jaw fragment, each preserving the roots of two teeth (Fig. S2). The crowns are almost completely eroded. In the maxillary fragment, a labial cingulum skirts the presumed paracone, but no other morphological details are preserved. On the mandibular fragment, a single trigonid basin, the only coronal element preserved, bears a labial cingulid encircling the base of the protoconid. SGOPV 2220 likely represents a third proterotheriid taxon in the Pampa Castillo fauna, given its large size compared to the taxa discussed above.

SGOPV 2416 consists of one crescent of a lower molariform (Fig. S3). The specimen's small size compared to macraucheniids, and relatively straight lophid (paralophid or hypolophid) compared to adianthids, argue for its proterotheriid affinities, but it cannot be identified more precisely.

Macraucheniidae Gervais, 1855

Theosodon Ameghino, 1887

Theosodon sp.

Figure 5

Type Species. *Theosodon lydekkeri* Ameghino, 1887.

Material. SGOPV 2064, mandible preserving roots of Li1–m1, Lm3, Ri1–c, Rp3–m3, complete Lm2, and incomplete Lm3 (Fig. 5).

Occurrence. Early Miocene (Burdigalian) to middle Miocene (Serravallian) (Colhuehuapian to Laventan SALMAs) of Argentina (Santa Cruz, Chubut, and Mendoza Provinces), Chile (Pampa Castillo, Chucal, and Río Frías faunas), Bolivia (Quebrada Honda fauna and Yecua Formation), and Colombia (La Venta fauna).

Locality and Horizon. Pampa Castillo, Galera Formation, Chile.

Description. The i1–p1 are single-rooted, and p2–m3 are double-rooted (Fig. 5). A heavily worn Lm2 is the only tooth crown preserved; it agrees in size (Table 1) and all recognizable morphology with most *Theosodon* species. The shape of the anterior edge of the mandibular symphysis, an important diagnostic feature for species of *Theosodon*, cannot be determined.

Remarks. SGOPV 2064 is assigned to *Theosodon* sp. based on size and morphology. Assignment to species is precluded by its lack of diagnostic features, and the problematic taxonomy of the genus (Bond and López, 1995; Cifelli and Guerrero, 1997; Schmidt and Ferrero, 2014; McGrath et al., 2018).

PHYLOGENETIC ANALYSIS

Our phylogenetic analysis identified twelve most-parsimonious trees (MPT) of 339.616 steps with a consistency index of 0.382 and a retention index of 0.607 (Fig. 6). Of the 35 nodes in the majority consensus tree, 13 had Bremer support greater

than 1.000 (indicated by black dots in Figure 6) and 11 Bremer supports between 0.500 and 1.000 (white dots).

The ‘anisolambdids’, *Anisolambda* spp. Ameghino, 1901, *Paranisolambda prodromus* Paula Couto, 1952, and *Protheosodon coniferus* Ameghino, 1897, initially included as outgroups, were instead recovered at disparate positions within Proterotheriidae (Fig. 6; see name definition below). Of the six multi-species genera included in our analysis, only *Diplasiotherium* Rovereto, 1914, was recovered as monophyletic. *Tetramerorhinus*, the most speciose proterotheriid genus, was identified as paraphyletic, though three of its five species formed an exclusive clade. The proterotheriids from La Venta were distributed broadly across the strict consensus tree – marked by stars in Figure 6. *Megadolodus molariformis* was identified as the earliest-diverging proterotheriid. *Lambdaconus colombianus* paired with the ‘anisolambdid’ *Protheosodon coniferus*, several nodes removed from other *Lambdaconus* species. *Prolicaphrium sanalfonensis* Cifelli and Guerrero, 1997, plotted as the sister taxon to *Diplasiotherium* spp., and only distantly related to *Prolicaphrium specillatum*. *Villarroelia totoyoi* Cifelli and Guerrero, 1997, was recovered basal to the clade including *Tetramerorhinus* spp., *Diadiaphorus majusculus*, *Thoatherium minusculum*, and most late Miocene and younger proterotheriids.

The analysis excluding the four taxa scored for fewer than 33% of characters produced six MPTs of 331.636 steps (Fig. S4A). The 50% cut-off analysis, eliminating six additional taxa, yielded a single MPT of 300.017 steps (Fig. S4B). Both analyses excluding less-complete taxa produced strict consensus trees

identical in topology to the strict consensus tree of the full analysis (Fig. 6), apart from the pruned taxa.

DISCUSSION

Phylogenetic Analysis

Definition of Proterotheriidae and the Group's Broader Relationships— Employing the methods of phylogenetic taxonomy (de Queiroz and Gauthier, 1992), we propose a stem-based definition of Proterotheriidae. Proterotheriidae is defined as the clade composed of *Tetramerorhinus lucarius* Ameghino, 1894, (*sensu* Soria, 2001) and all litopterns more closely related to it than to *Macrauchenia patachonica* Owen, 1838, *Tricoelodus bicuspidatus* Ameghino, 1897, or *Protolipterna ellipsodontoides* Cifelli, 1983 (node P in Figure 6). *Tetramerorhinus lucarius* was selected as a specifier because it is a well-known, morphologically 'typical' proterotheriid, whereas *Proterotherium cervioides,* classically the type genus and species of Proterotheriidae, is limited to fragmentary material (Supplementary File 1; Soria, 2001). *Macrauchenia patachonica* and *P. ellipsodontoides* are employed in the definition to represent Macraucheniidae and Protolipternidae, respectively [see Gelfo et al. (2016) regarding the validity of Protolipternidae]. *Tricoelodus bicuspidatus* was chosen to represent the Adianthidae because it is better-known than the type species, *Adianthus buccatus* (Cifelli and Soria, 1983).

Previous authors have employed de facto equivalents of apomorphy-based definitions for Proterotheriidae, citing craniodental and postcranial characters (Cifelli, 1983; Soria, 2001). Both previous conceptions of the group cite molarization of P/p3 (e.g., protoconule, metaconule, and well-developed metacone on P3 and crescentic trigonid and talonid lophids on p3). Soria's (2001) definition cited additional characters that typify the group classically (e.g., a single, tusk-like upper incisor and reduced digits II and IV). Though they did not define Proterotheriidae explicitly, Cifelli and Villarroel (1997) provided additional, largely postcranial, proterotheriid synapomorphies supporting their placement of *Megadolodus molariformis* within the group. Many of Soria's (2001) and Cifelli and Villarroel's (1997) characters are not applicable to taxa unknown from postcrania or anterior dentitions (e.g., *Anisolambda* and *Picturotherium migueli*; Supplementary File 1) limiting their utility for most Paleogene taxa. Our proposed definition of Proterotheriidae is generally more inclusive than previous conceptions of the group.

Future analyses may alter the membership of Proterotheriidae as here defined. Macraucheniids and adianthids (*sensu* Cifelli, 1991), groups traditionally considered more closely related to Proterotheriidae than *P. ellipsodontoides* (Cifelli, 1983; Soria, 2001), were not included in this study. Accordingly, several taxa here considered basal members of Proterotheriidae, such as *M. molariformis* and *Adiantoides leali* Simpson and Minoprio, 1949, may cease to be members of the clade bearing that name (Fig. 6) once macraucheniids and adianthids are analyzed alongside typical proterotheriids.

The affinities of indaleciids, represented in this analysis by *Adiantoides leali*, are enigmatic. Originally considered a subgroup of Adianthidae (=Indaleciinae; Bond and Vucetich, 1983), indaleciids have also been variously linked with sparnotheriodontid litopterns (Cifelli, 1993), notopterns (Soria, 1989), and notoungulates and astrapotheres (García-López and Babot, 2014). Indaleciids are members of the Proterotheriidae, as the latter name is defined here (Fig. 6).

Comparison to Previous Studies—Soria (2001) offered a hypothesis of proterotheriid relationships following his extensive taxonomic revision of the group, considering *Lambdaconus* the 'ancestral' proterotheriid. In the present analysis, *Megadolodus molariformis* was recovered as the earliest-diverging proterotheriid, though *Lambdaconus suinus* and *Lambdaconus lacerum* Ameghino, 1902, fell in early-diverging positions (Fig. 6). Soria (2001) divided most proterotheriids between two main lineages, termed the *Thoatherium*- and *Diadiaphorus*-lines. Ameghino (1904) and Friant (1967) proposed a threefold basal split among proterotheriids. In contrast, we find little support for a basal split between diverse subgroups of proterotheriids.

Schmidt's (2015) phylogenetic analysis of Proterotheriidae, based on modified datasets of Kramarz and Bond (2005) and Villafañe et al. (2012), recovered *Anisolophus minusculus* and *Anisolophus floweri* as the earliest-diverging proterotheriids. Our results indicate these taxa to be more deeply nested within Proterotheriidae (Fig. 6). Schmidt (2015) viewed *Prolicaphrium specillatum*, *Proterotherium cervioides*, *Picturotherium migueli*, *Lambdaconus lacerum*, and *Paramacrauchenia scamnata* Ameghino, 1902, as forming an exclusive clade,

whereas we recovered these taxa (except *P. cervioides*) sequentially near the base of Proterotheriidae (Fig. 6). As with our analysis, all previous analyses centred on craniodental characters.

Proterotheriid Interrelationships—Contrary to Soria's (2001) findings, *Thoatherium minusculum* and *Diadiaphorus majusculus* were recovered as sister taxa in our analysis (Fig. 6). These taxa share a reduced, lophoid metaconule on M1–2 (char. 43-2, Supplementary File 1), and (uniquely among proterotheriids) lack an entoconid on m1–3 (chars. 79-2, 87-4, Supplementary File 1). This close relationship is somewhat counterintuitive in that *T. minusculum* is a small, gracile form, whereas *D. majusculus* is large and robust (Scott, 1910; Soria, 2001; Cassini et al., 2012a, b), suggesting that these attributes are highly plastic. Although *Diadiaphorus caniadensis* was not included in this analysis due to its extremely fragmentary remains (Kramarz and Bond, 2005), perhaps complicating the inferred *D. majusculus* and *T. minusculum* relationship. *Diadiaphorus eversus*, a species placed in *Diadiaphorus* by some authors (Ameghino, 1891a; Schmidt, 2015) and *Epitherium* by Soria (2001), is only known from a single upper molar. Additional material of *D. caniadensis* and *D. eversus* is needed to clarify whether they are members of *Diadiaphorus*, implying that *D. majusculus* and *T. minusculum* acquired their distinctive shared dental morphology independently.

Our phylogenetic analysis is relevant to several ongoing questions about the taxonomy and age of certain proterotheriids. Our results corroborate recognizing *Tetramerorhinus fleaglei* as a distinct species. Named as *Tetramerorhinus cingulatum fleaglei* Soria, 2001, it included all specimens of *T. cingulatum* known

from the Pinturas Formation at the time. In elevating it to *T. fleaglei,* Kramarz and Bond (2005) considered it more closely related to *Tetramerorhinus prosistens* Ameghino, 1899 (also from the Pinturas Formation) than to *T. cingulatum* from the Santa Cruz Formation (=*T. cingulatum cingulatum* per Soria, 2001). Our analysis separates *T. fleaglei* and *T. cingulatum* by several nodes (Fig. 6), rather than recovering them as sister taxa as would be expected of subspecies. Although not exclusively related, the similarities of *T. fleaglei* and *T. prosistens* noted by Kramarz and Bond (2005) are reflected by their proximate phylogenetic placements (Fig. 6).

The holotype and only specimen of *Thoatheriopsis mendocensis* Soria, 2001 (MLP 81-XI-28-1) is either from the early Miocene Areniscas Entrecruzadas Member or the middle Miocene Estratos de Mariño Member of the Mariño Formation in Mendoza Province, Argentina (Irigoyen et al., 2000; Villafañe et al., 2012). The phylogenetic placement *T. mendocensis* recovered here is more compatible with a middle Miocene age, given that shorter ghost lineages would need to be invoked through the middle Miocene (Fig. 6).

The non-monophyly of many proterotheriid genera suggests that extensive taxonomic revision is warranted. In particular, *Lambdaconus colombianus*, *Neobrachytherium ameghinoi* Soria, 2001, and *Prolicaphrium sanalfonensis* require new combinations given their distant relationships to the type species of their currently assigned genera. The two species of *Diplasiotherium* represented the only non-monotypic genus recovered as monophyletic, but its two species are represented by fragmentary lower dental remains (Supplementary File 1; Soria, 2001; Schmidt et al., 2018), so their placement in the broader phylogeny should be

treated warily (Fig. 6). These two species were the sole outliers of a clade including all other late Miocene and younger (Chasicoan to Lujanian SALMAs) proterotheriids; removing *Diplasiotherium* from the analysis leaves the remaining late Miocene and younger forms united (Figs 6; S4).

Status and Affinities of Anisolambdidae—The three ‘anisolambdids’ considered here, *Paranisolambda prodromus*, *Anisolambda* spp., and *Protheosodon coniferus*, initially included as outgroups, fell on distinct branches within Proterotheriidae (Fig. 6). Anisolambdinae, encompassing various Paleocene to Oligocene taxa considered ‘condylarths’ and early-diverging macraucheniids and proterotheriids by earlier workers, was originally named as a subgroup of Proterotheriidae by Cifelli (1983). Soria (2001) argued that this assemblage, which he elevated in rank to Anisolambdidae, was only distantly related to proterotheriids (=Proterotheriinae *sensu* Cifelli, 1983).

Several advanced, ‘proterotheriid-like’ features of the dentition (e.g., mesiolingual cingula, paralophids, and premolar cuspids) have been cited in support of ‘anisolambdid’ monophyly and, thus, precluding these taxa from an “ancestral” position within Proterotheriidae (Soria, 2001; Gelfo et al., 2016). In our analysis, ‘Anisolambdidae/inae’ is not identified as monophyletic, nor do its constituents solely represent early-diverging proterotheriids, rather, they are distributed disparately across clade X (Fig. 6), the least-inclusive clade that includes all proterotheriids (=Proterotheriidae *sensu* Soria, 2001).

Constraining the analysis to sequentially exclude *Anisolambda* spp. (Fig. S5A) and *P. prodromus* (Fig. S5B) from clade X produced MPTs roughly two steps

longer than the unconstrained tree (Table 2; Fig. 6). Permitting *P. prodromus* and *Anisolambda* spp. to be members of clade X requires acceptance of several lengthy ghost lineages (up to ~25 Myr) given the late Paleocene or middle Eocene ages of these taxa (Itaboraian, Vacan, and Barrancan SALMAs; Cifelli, 1983; Flynn and Swisher, 1995; Gelfo et al., 2009; Dunn et al., 2013; Croft, 2016). The next oldest members of clade X, *P. coniferus* and *Lambdaconus suinus*, are from the late Oligocene (Deseadan SALMA; Loomis, 1914; Soria, 2001). Whether these long ghost lineages reflect a highly incomplete fossil record, or shortcomings of our phylogenetic hypothesis, is uncertain.

The topology of the proterotheriid tree, and thus the transformation sequence of many characters, is particularly sensitive to the in- or exclusion of the 'anisolambdid' *P. coniferus*. For example, excluding *P. coniferus* from clade X, *Lambdaconus colombianus* forms the proximal outgroup of clade X (Fig. S5C). The branching arrangement at the base of clade X is altered substantially as well, including the emergence of a clade comprising *Picturotherium migueli*, *P. prodromus*, *Lambdaconus lacerum*, *Paramacrauchenia scamnata*, *Lambdaconus suinus*, and *Anisolambda* spp. from the basal dichotomy. (Fig. S5C; Table 2). Excluding *P. coniferus* from the analysis entirely leaves *L. colombianus* as a member of clade X, but *Prolicaphrium sanalfonensis*, *Diplasiotherium* spp., and *Villarroelia totoyoi*, shift several nodes basally. Considered in isolation, several features of *P. coniferus* would seem to call into question its membership in clade X (=Proterotheriidae *sensu* Soria, 2001), including its ostensibly plesiomorphic lower dentition (i1–p1 present and spatulate, no large diastemata), and well-developed

second and fourth metatarsals (Supplementary File 1; Loomis, 1914). *Lambdaconus suinus*, an earlier-diverging member of clade X (Fig. 6), bears a 'typical proterotheriid' lower anterior dentition (i.e., two simple incisors, reduced canine, and large diastemata between i2, canine, and p1) (Fig. 6; Supplementary File 1; Soria, 2001). The position of *P. coniferus* in Figure 6 requires reversals of these dental features or their independent acquisition by *L. suinus* and later-diverging proterotheriids. Moreover, the pedal digits of *P. coniferus* are well-developed, whereas the lateral metacarpals of *L. colombianus,* the sister taxon of *P. coniferus* (Fig. 6), are reduced as in all other members of clade X for which these elements are known (Cifelli and Guerrero Diaz, 1989). Although not preserved in *P. coniferus*, its manual digits were likely unreduced as well, since digits are not known to reduce in the fore and hind limbs of litopterns differentially. Accordingly, the topology of Figure 6 requires convergent digit reduction in *L. colombianus* and other members of clade X, or reacquisition of unreduced digits in *P. coniferus* (Supplementary File 1). These implied morphological reversals highlight the importance of recovering additional anterior dentitions and postcranial data to clarify litoptern relationships.

Relationships of *Lambdaconus colombianus*—The phylogenetic relationships of *Lambdaconus colombianus*, variously considered a 'condylarth' (Hoffstetter and Soria, 1986) or a proterotheriid (Cifelli and Guerrero Diaz, 1989), have never previously been tested. Our analysis paired *L. colombianus* with the 'anisolambdid' *Protheosodon coniferus* (Fig. 6), a topology requiring a long ghost lineage (Deseadan–Laventan SALMAs, ~15 myr). *Lambdaconus colombianus* is only distantly related to *Lambdaconus suinus* and *Lambdaconus lacerum,* suggesting

that *L. colombianus* is more properly placed in a new or different genus. Excluding *P. coniferus* from clade X, recovers *L. colombianus* as the sister group to clade X (Fig. S5C), a topology that requires a ghost lineage (Deseadan to Laventan SALMAs) as long as that in the original analysis (Fig. 6). Excluding all three 'anisolambdids' from clade X produces similar results (Fig. S5D). Our confidence in the phylogenetic placement of *L. colombianus* is lessened by its dependence on the placement of *P. coniferus* (Figs. 6, S5C), which is itself enigmatic (see above discussion).

Relationships of Megadolodinae—*Megadolodus molariformis* (like *Lambdaconus colombianus*) was originally considered a 'condylarth' based on its bunodont dentition (McKenna 1956) but is now considered a proterotheriid based largely on tarsal and pedal morphology (Cifelli and Villarroel, 1997). Our analysis recovered *M. molariformis* as the earliest-diverging proterotheriid (Fig. 6), supporting the view that megadolodines (*M. molariformis* + *Bounodus enigmaticus*) represent a lineage distinct from all other proterotheriids (=Proterotheriinae + Anisolambdinae *sensu* Cifelli, 1983; Cifelli and Villarroel, 1997). Future analyses may show that macraucheniids or adianthids are more closely related to *Tetramerorhinus lucarius* than is *M. molariformis*, excluding megadolodines from Proterotheriidae by definition. Ideally, such analyses should include some of the postcranial characters identified by Cifelli and Villarroel (1997).

Other La Venta Proterotheriids—*Prolicaphrium sanalfonensis* was recovered in a clade with *Diplasiotherium* (Fig. 6). As noted, however, the precarious placement of *Diplasiotherium*, argues against drawing strong taxonomic or biogeographic

conclusions from this grouping. Excluding *Diplasiotherium* from the phylogenetic analysis left the phylogenetic position of *P. sanalfonensis* unchanged (Fig. S4). The placement of *P. sanalfonensis* within *Prolicaphrium* warrants re-examination given that *P. specillatum* is more closely related to two species of *Anisolophus* than to *'P.' sanalfonensis* (Fig. 6). *Villarroelia totoyoi* was recovered as an outgroup to a clade including the Santacrucian taxa *Tetramerorhinus* spp., *Diadiaphorus majusculus*, and *Thoatherium minusculum*, plus most late Miocene and younger proterotheriids (Fig. 6).

Proterotheriid Biogeography—As the first phylogenetic analysis including taxa from the low latitudes, our results shed much needed light on the biogeographic history of proterotheriids. *Megadolodus molariformis* and *Lambdaconus colombianus* have lengthy ghost lineages (Fig. 6), implying poorly understood histories from at least the early Eocene (Itaboraian SALMA) and late Oligocene (Deseadan SALMA), respectively. The lack of pre-Laventan (middle Miocene) members of these lineages in the comparatively well-sampled high latitude assemblages suggests that these lineages persisted in the tropics long after their nearest southern relatives became extinct. If proterotheriids were indeed closed-habitat browsers (Cifelli and Villarroel, 1997; Cassini et al., 2011, 2012; Cassini, 2013; Morosi and Ubilla, 2017; Corona et al., 2019), high diversity in low-latitude forests would not be unexpected.

Prolicaphrium sanalfonensis and *Villarroelia totoyoi*, both from La Venta, were recovered deep within Proterotheriidae, on separate branches bracketed by high-latitude early Miocene taxa (Fig. 6). This topology implies multiple dispersals between northern and southern South America during the early Miocene. The

ancestors of *P. sanalfonensis* and *V. totoyoi* may have dispersed north from Patagonia during the Colhuehuapian or Santacrucian SALMAs. Alternatively, the early Miocene Patagonian lineages may have originated in the lower latitudes and then radiated in the south (i.e., *P. sanalfonensis* and *V. totoyoi* evolved *in situ* in the north, rather than immigrating there. *Megadolodus molariformis* and *L. colombianus* indicate the likely existence of two poorly known proterotheriid lineages in northern South America during the early Miocene, lending credence to this second scenario.

Proterotheriid interrelationships (Fig. 6) imply that little to no exchange occurred between high and low latitudes in South America during the middle Miocene, in contrast to the early Miocene. Only one post-Santacrucian dispersal event is required by the topology, for the lineage including *Diplasiotherium* spp. from northern and eastern Argentina (Cifelli and Guerrero, 1997; Soria, 2001; Schmidt et al., 2018). Given weak support for the phylogenetic placement of *Diplasiotherium*, conceivably no lineages moved between low and high latitudes during the middle Miocene. Rodents and sparassodonts (Walton, 1997; Croft, 2007; Tejada-Lara et al., 2015; Engelman et al., 2018) exhibited latitudinal provincialism during the middle Miocene, when the Pebas mega-wetland covered much of western Amazonia and potentially limited dispersal (Hoorn et al., 2010; Tejada-Lara et al., 2015). Alternatively, biotic provinciality may simply reflect latitudinal climatic differences (Croft, 2012; Flynn et al., 2012).

Biostratigraphic Implications of Santacrucian SALMA Proterotheriidae

Three formations in Patagonia have yielded Santacrucian SALMA proterotheriids (Fig. 1; Table 3): the Galera Formation (Pampa Castillo, described

herein), Santa Cruz Formation (> 10 localities; e.g., Scott 1910; Soria 2001; Bostelmann et al., 2013; Raigemborn et al., 2018a; Cuitiño et al., 2019), and Pinturas Formation (two localities; Kramarz and Bond, 2005).

Proterotheriids from the lower and middle sequences of the Pinturas Formation (*sensu* Kramarz and Bellosi, 2005; lmPF) tend to occupy more basal positions in our phylogeny than taxa from the upper Pinturas Formation and Santa Cruz Formation (SCF; Fig. 6). *Tetramerorhinus fleaglei*, *Tetramerorhinus prosistens*, *Picturotherium migueli*, and *Lambdaconus lacerum* occur at various lmPF localities in the upper Pinturas River Valley (Fig. 1; Table 3). Kramarz and Bond (2005) recognized *Diadiaphorus*? *caniadensis*, *Diadiaphorus* sp., and *Tetramerorhinus cingulatum* from Estancia la Cañada, tentatively attributed to the upper part of the Pinturas Formation (Bown and Fleagle, 1993). The stratigraphic and phylogenetic positions of proterotheriids from the upper and lower Pinturas Formation are generally congruent. *Picturotherium migueli* (lmPF) and *L. lacerum* (lmPF and Colhuehuapian SALMA) were recovered as early-diverging proterotheriids (Fig. 6). *Tetramerorhinus fleaglei* (lmPF) and *T. prosistens* (lmPF) are successive outgroups to a clade including taxa from the upper Pinturas Formation and the SCF. The lower and middle levels of the Pinturas Formation are likely ~18 Ma, coeval with Pampa Castillo (Folguera et al., 2018) and the oldest levels of the SCF which outcrop in western Patagonia [e.g., lower beds of Lago Posadas (=Lago Pueyrredón), Sierra Baguales, Karaiken (Fig. 1; Perkins et al., 2012; Bostelmann et al., 2013; Cuitiño et al., 2016; Trayler et al., 2019)]. The upper Pinturas Formation appears to be coeval with much of the SCF, including the better-studied levels exposed on the Atlantic

Coast [e.g., Monte León, Cerro Observatorio (Fleagle et al., 2012)]. Later-diverging taxa such as *Diadiaphorus majusculus*, *Tetramerorhinus lucarius*, and *Tetramerorhinus mixtum* Ameghino, 1894, occur exclusively in the SCF, whereas *T. minusculum* is tentatively known from the Galera Formation (*T.* cf. *T. minusculum*; present study) and the SCF (Table 3; Soria, 2001). Other SCF proterotheriids (*Anisolophus* spp. and *Paramacrauchenia scamnata*) however, were recovered basal to these lmPF taxa (Fig. 6), though we note that SCF localities are not entirely synchronous.

At western sites of the SCF such as Lago Posadas and Karaiken deposition commenced earlier than at eastern sites but continued through the deposition of the eastern sites (Fig. 1; Blisniuk et al., 2005; Perkins et al., 2012, Cuitiño et al., 2016). Historically, the precise stratigraphic provenance of vertebrate fossils was not recorded at these sites, so any stratigraphic patterns in proterotheriid distribution within these western sites remain obscure. One exception is Sierra Baguales, in western Patagonia; preliminarily correlated with the SCF (Fig. 1; Bostelmann et al., 2013), it has yielded detrital zircon ages of 18–19 Ma, indicating that these strata are slightly older than the SCF in eastern Patagonia (Fleagle et al., 2012; Bostelmann et al., 2013; Cuitiño et al., 2016). *Paramacrauchenia scamnata*, the only proterotheriid from Sierra Baguales, was identified as the most basal SCF proterotheriid in our phylogenetic analysis (Fig. 6). This species also occurs in Colhuehuapian-aged beds of the Sarmiento Formation, but is unknown elsewhere in the SCF (Soria, 2001).

The biostratigraphic utility of proterotheriids in the Santacrucian SALMA of Patagonia is currently unknown, although the occurrence of generally more basal

taxa in the lmPF and in the ‘older’ SCF at Sierra Baguales is promising (Fig. 6; Table 3). Currently, the lmPF is known only from the upper Pinturas River Valley, making it uncertain whether its distinct proterotheriid assemblage reflects a discrete ‘Pinturan’ biochronologic interval (e.g., Kramarz and Bellosi, 2005; Vucetich et al., 2016) or if the upper Pinturas River Valley merely records an unusual local fauna. The only proposed ‘Pinturan’ site outside of the upper Pinturas River Valley, the Upper Faunal Zone of the Colhue-Huapi Member at Gran Barranca, has produced a partial LM1 or LM2 assigned to *Tetramerorhinus* sp. (Kramarz et al., 2010), providing no additional context. Additional collecting, with precise stratigraphic control, is needed to better assess proterotheriid faunal change during the Santacrucian SALMA.

Paleoenvironmental Implications of Santacrucian Proterotheriidae

Faunal differences between lmPF and western SCF localities (e.g., Karaiken, Lago Posadas, and Sierra Baguales) and eastern SCF localities (e.g., Cerro Observatorio, Monte León, Killik Aike, Coy Inlet, Sehuén) may reflect paleoenvironmental influences (Fig. 1). Proterotheriids from the eastern SCF tend to be larger-bodied than those from the western SCF and lmPF and are exclusively hypsodont (Table 3; Soria, 2001). (Although proterotheriids are all brachyodont relative to many other ‘ungulates’, we employ ‘hypsodont’ here relative to other proterotheriids.) Various proxies suggest that the eastern swath of the SCF was deposited in mixed semi-arid and humid temperate forests with seasonal rainfall (Brea et al., 2012; Kay et al., 2012; Raigemborn et al., 2015, 2018a, b; Zapata et al., 2016).

Many species are common to localities in the eastern and western SCF. *Paramacrauchenia scamnata*, known only from Sierra Baguales in the SCF, is a noteworthy exception, Sierra Baguales being the only western SCF site considered distinctly older than eastern localities (Table 3; Soria, 2001; Bostelmann et al., 2013). The SCF is time transgressive, deposition beginning earlier in the west than in the east, though the upper strata of western localities are coeval with those in the east (Perkins et al., 2012; Cuitiño et al., 2016; Trayler et al., 2019). Historically, the precise stratigraphic provenance of fossils from these sites was not recorded, making the stratigraphic range of most taxa within the SCF uncertain. *Paramacrauchenia scamnata* is known from Sierra Baguales, the only western SCF site considered to be clearly older than eastern localities (Blisniuk et al., 2005; Bostelmann et al., 2013; Cuitiño et al., 2015). The brachydonty of *P. scamnata* and the lack of hypsodont forms at Sierra Baguales are perhaps indicative of a more humid paleoenvironment than is recorded elsewhere in the SCF.

Proterotheriids of the lmPF (upper Pinturas River Valley, Fig. 1) include brachyodont (*Picturotherium migueli* and *Lambdaconus lacerum*) and hypsodont (*Tetramerorhinus fleaglei* and *Tetramerorhinus prosistens*) forms (Table 3; Kramarz and Bond, 2005). *Diadiaphorus*? *caniadensis*, and possibly *T. cingulatum*, from the upper Pinturas Formation (Estancia La Cañada; Fig. 1), which is partially coeval with eastern exposures of the SCF (Perkins et al., 2012; Cuitiño et al., 2016), are hypsodont (Kramarz and Bond, 2005). Sedimentological evidence, as well as the greater abundance of forest-adapted mammals (e.g., erethizontid rodents, primates, caenolestoid marsupials) in the lmPF relative to the SCF suggest that sediments in

the upper Pinturas River Valley record a more humid climate than those of Atlantic coastal sites of the SCF, supporting the notion that brachyodont proterotheriids are indicators of humid climates (Bown and Larriestra, 1990; Kramarz and Bellosi, 2005; Kay et al., 2012; Raigemborn et al., 2018b).

Pampa Castillo Fauna: Litopterna

Pampa Castillo records the northernmost occurrence of *Thoatherium,* as well as the taxon's first occurrence outside the SCF of Santa Cruz Province, Argentina (Figs. 1–3; Soria, 2001; Villafañe et al., 2006; Bostelmann et al., 2013). The nearest previously published record of *Thoatherium* comes from Lago Posadas (=Lago Pueyrredón), ~70 km southeast of Pampa Castillo (Soria, 2001).

Picturotherium was previously restricted to the lower Pinturas Formation in the upper Pinturas River Valley (Loma de Lluvia and Cerro de los Monos localities), ~130 km east of Pampa Castillo (Figs. 1, 4; Table 3; Kramarz and Bond, 2005). The fauna of the lmPF may represent a distinct 'Pinturan' (=Astrapothericulense, per Ameghino, 1906) sub-age, with taxa having a more 'primitive' character than conventional Santacrucian faunas (Kramarz and Bellosi, 2005; Kramarz et al., 2010). Three rodent species occur exclusively in the Pampa Castillo fauna and the Pinturas Formation (Chick et al., 2010). Further descriptions of both faunas (e.g., notoungulates, xenarthrans) are needed to fully assess their degree of similarity which may inform the debate regarding the validity of the proposed 'Pinturan' SALMA. In terms of paleoenvironments, the brachydonty of *Picturotherium* sp. suggests a more humid paleoclimate at Pampa Castillo relative to most localities in the eastern SCF.

Proterotheriids support assignment of the Pampa Castillo fauna to the Santacrucian SALMA (Flynn et al., 2002), but do not resolve its age within this interval, assuming previously proposed temporal distinctions are valid. The occurrence of *Picturotherium* sp. suggests temporal correspondence with the lower Pinturas Formation, consistent with radioisotopic data from both areas. *Thoatherium* was previously restricted to the SCF [Atlantic Coast, Sehuén, Lago Posadas, and Karaiken (Table 3; Soria, 2001)]. Its presence at Pampa Castillo suggests that the site may be partially coeval with the SCF.

Theosodon (Fig. 5) is a geographically (Argentina, Bolivia, Chile, Colombia, possibly Peru) and temporally (Colhuehuapian [earliest Miocene] to Laventan [late middle Miocene] SALMAs) widespread taxon (Scott, 1910; Soria, 1981, 1983; Cifelli and Guerrero, 1997; Croft et al., 2004; Forasiepi et al., 2011; Tejada-Lara et al., 2015; McGrath et al., 2018). Accordingly, its occurrence sheds little light on the age or paleoenvironment of Pampa Castillo.

Adianthids, while not recovered at Pampa Castillo, are known from the SCF in eastern Santa Cruz Province (Cifelli and Soria, 1983), and from the middle Miocene (Colloncuran/‘Friasian’ SALMA) of Río Cisnes, Chile (Cifelli, 1991). Adianthids would be expected at Pampa Castillo given this distribution, but they are generally scarce in faunas from which they are known (Cifelli and Soria, 1983).

Folguera et al. (2018) dated a reworked tuff 10 m above the base of the ’Pampa Castillo’ (=Galera) Formation at 18.7 ± 0.3 Ma suggesting that the Pampa Castillo fauna is approximately coeval or slightly older than the lmPF and western SCF localities (Blisniuk et al., 2005; Bostelmann et al., 2013; Cuitiño et al., 2015;

Trayler et al., 2019). The litoptern taxa present at Pampa Castillo are consistent with this age estimate as *Thoatherium* is known from the western SCF (Soria, 2001) and *Picturotherium* is known from the lmPF (Kramarz and Bond, 2005).

CONCLUSIONS

At least two proterotheriid and one macraucheniid litopterns are recorded in the Pampa Castillo fauna of southern Chile (Fig. 1). Pampa Castillo provides the northernmost record of the proterotheriid *Thoatherium*, and its first outside of the Santa Cruz Formation and Santa Cruz Province, Argentina (Figs. 2–3). *Picturotherium,* previously reported only from the Pinturas Formation of the upper Pinturas River Valley, is represented by an isolated m3 (Fig. 4), which is ~50% larger than its counterpart in the type species *P. migueli*. Crownless mandibular and maxillary fragments likely represent a third proterotheriid at Pampa Castillo, as it is too large to be referred to *Thoatherium* or *Picturotherium* (Fig. S2). The macraucheniid *Theosodon* is represented by a mandible preserving nearly all tooth roots and the crown of Lm2 (Fig. 5). The litoptern assemblage supports a Santacrucian age for the Pampa Castillo fauna. The co-occurrence of *Picturotherium* in the Pampa Castillo fauna and in the lower and middle Pinturas Formation may indicate a close temporal correspondence of these strata, as is also suggested by rodent assemblages (Chick et al., 2010).

Using a comprehensive phylogenetic analysis as a framework, we propose a stem-based phylogenetic definition for the Proterotheriidae in an effort to stabilize use of this name. Our analysis failed to recover many traditionally recognized genera as monophyletic, suggesting that several warrant revision. The unexpectedly close relationship between *Thoatherium minusculum* and *Diadiaphorus majusculus* (Fig. 6) suggests that body size and 'robustness' are highly plastic features of proterotheriids.

Three 'anisolambdids' fell in disparate positions within Proterotheriidae, calling into question the validity of 'Anisolambdidae' and implying the existence of several ghost lineages up to ~25 million years in length. Constraining the phylogeny to exclude Paleocene and Eocene 'anisolambdids' from Proterotheriidae as traditionally conceived (clade X, Fig. 6; first known from the late Oligocene), lengthened the MPT by two or fewer steps (Figs. S5A–B; Table 2). The phylogenetic position of *Protheosodon coniferus* requires the acceptance of several seemingly implausible morphological reversals or convergences, highlighting the need for further study of this taxon's affinities.

The four proterotheriid species from the tropical middle Miocene assemblage of La Venta, Colombia are not closely related. *Megadolodus molariformis* and *L. colombianus* originate from long ghost lineages, highlighting our inadequate understanding of tropical-latitude faunas during the Paleogene and early Neogene (Fig. 6). The phylogenetic placement of the other proterotheriids from La Venta, *Villarroelia totoyoi* and *Prolicaphrium sanalfonensis*, imply multiple early Miocene dispersal events of uncertain direction between the high and low latitudes.

Proterotheriids hold potential biostratigraphic and paleoecologic importance for the early Miocene of Patagonia. Earlier-diverging species of *Tetramerorhinus*, *T. fleaglei* and *T. prosistens*, occur in the lower and middle Pinturas Formation, whereas later-diverging species, *T. cingulatum*, *T. lucarius*, and *T. mixtum*, occur in the upper Pinturas and upper Santa Cruz Formations (Fig. 6; Table 3). The two proterotheriids from the Santacrucian and Colhuehuapian SALMAs, *Paramacrauchenia scamnata* and *Lambdaconus lacerum*, are recovered only from older Santacrucian strata, at Sierra Baguales and from the lower Pinturas Formation (Fig. 1). Lower levels of the Pinturas Formation and strata at Sierra Baguales produce hypsodont and brachyodont proterotheriids (Table 3), suggesting that a more humid climate and closed habitat are recorded at these sites compared to other Santacrucian localities in Patagonia where only 'hypsodont' proterotheriids occur. The occurrence of the brachyodont *Picturotherium* sp. at Pampa Castillo suggests that this fauna inhabited a more humid climate than did its contemporaries from the Santa Cruz Formation.

Acknowledgements

This manuscript was previously published in the *Journal of Systematic Palaeontology* in 2020 with John Flynn and André Wyss as co-authors.

We are grateful to the following institutions for providing access to their collections: American Museum of Natural History, Field Museum of Natural History, Museo Argentino de Ciencias Naturales 'Bernardino Rivadavia', Museo de La Plata, University of California Museum of Paleontology, and Yale Peabody Museum. We also thank Richard Cifelli and the Oklahoma Museum of Natural History for providing

study casts of specimens from La Venta. This study was partly funded by the University of California Regents' Fellowship, Tanya Atwater Global Field Travel Fund, and an American Museum of Natural History Richard Gilder Graduate School Collections Study Grant. Field work was funded by a grant from the Eppley Foundation for Scientific Research and the AMNH. We thank Greg Buckley, René Burgos, Roger Carpenter, Paul Raty, Paul Sereno, Carlos de Smet, Cruz Vargas, and members and friends of the de Smet family for their assistance in the field. Jeanne Kelly and Jane Shumsky of the American Museum of Natural History prepared the specimens. We thank Javier Gelfo and Alejandro Kramarz for helpful conversations that improved the manuscript.

REFERENCES

Ameghino, F. 1883. Sobre una nueva colección de mamíferos fósiles recogidos por el profesor Pedro Scalabrini en las barrancas del río Paraná. Boletín de La Academia Nacional de Ciencias de Córdoba 5:257–306.

Ameghino, F. 1887. Enumeración sistemática de las Ameghino, F. 1887. Enumeración sistemática de las especies de mamíferos fósiles coleccionados por Carlos Ameghino en los terrenos eocenos de la Patagonia austral y depositados en el Museo de La Plata. Boletín Museo de La Pla. Boletín Museo de La Plata 5:445–469.

Ameghino, F. 1889. Contribución al conocimiento de los mamíferos fósiles de la República Argentina. Actas de La Academia Nacional de Ciencias de Córdoba 6:1–1027.

Ameghino, F. 1891a. Caracteres diagnósticas de cincuenta epécias nuevas de mamíferos fósiles argentinos. Revista Argentina de Historia Natural 1:129–167.

Ameghino, F. 1891b. Nuevos restos de mamíferos fósiles recogidos por Carlos Ameghino en el Eoceno inferior de la Patagonia austral. Especies nuevas: adiciones y corecciones. Revista Argentina de Historia Natural 1:289–328.

Ameghino, F. 1894. Ennumération synoptique des espéces de mammiféres fossilies des formations éocénes de Patagonie. Boletín de La Academia Nacional de Ciencias de Córdoba 13:259–445.

Ameghino, F. 1897. Mammiféres crétacés de l'Argentine (Deuxiéme contribution á la connaissance de la faune mammologique des couces á Pyrotherium). Boletín Del Instituto Geográfico Argentino 18:405–521.

Ameghino, F. 1899. Sinópsis Geológico-Paleontológica. Suplemento (Adiciones y Corecciones) 1. La Plata, Argentina, 13 pp.

Ameghino, F. 1901. Notices préliminaires sur des ongulés nouveaux des terrains crétacés de Patagonie. Boletín de La Academia Nacional de Ciencias de Córdoba 16:349–426.

Ameghino, F. 1902. Premiére contribution a la connaisance de la faune mammalogique des couches a Colpodon. Boletín de La Academia Nacional de Ciencias de Córdoba 17:71–138.

Ameghino, F. 1904. Nuevas especies de mamíferos Cretáceos y Terciarios de la República Argentina. Anales de La Sociedad Cientifica Argentina 57:327.

Ameghino, F. 1906. Les formations sédimentaires du Crétacé Supérieur et du Tertiaire de Patagonie avec un parallelé entre leurs faunes mammalogiques et celles de l'ancien continent. Anales Del Museo Nacional de Buenos Aires (Tercera Serie) 8:1–568.

Blisniuk, P. M., L. A. Stern, C. P. Chamberlain, B. D. Idleman, and P. K. Zeitler. 2005. Climatic and ecologic changes during Miocene surface uplift in the southern Patagonian Andes. Earth and Planetary Science Letters 230:125–142.

Bond, M., and M. G. Vucetich. 1983. *Indalecia grandensis* gen. et sp. nov. del Eoceno temprano del noroeste Argentino, tipo de una nueva subfamilia de los Adianthidae (Mammalia, Litopterna). Revista de La Asociación Geológica de Argentina 38:107–117.

Bond, M., and G. M. López. 1995. Los Macraucheniidae (Mammalia, Litopterna) de la Formación Arroyo Chasicó (Partido de Vallarino, Pcia. de Buenos Aires). IV Jornadas Geologicas y Geofisicas Bonaerenses 23–27.

Bordas, A. F. 1936. Un nuevo mamífero del Colpodon de Gaiman (*Proheptaconus trelewense* gen et. sp. nov.). Physis 12:110–112.

Bostelmann, E., J. P. Le Roux, A. Vásquez, N. M. Gutiérrez, J. L. Oyarzún, C. Carreño, T. Torres, R. Otero, A. Llanos, C. M. Fanning, and F. Hervé. 2013. Burdigalian deposits of the Santa Cruz Formation in the Sierra Baguales, Austral (Magallanes) Basin: age, depositional environment and vertebrate fossils. Andean Geology 40:458–489.

Bostelmann, J. E., R. Bobe, G. Carrasco, B. V. Alloway, P. Santi-Malnis, A. Mancuso, B. Agüero, Z. Alemseged, and Y. Godoy. 2012. The Alto Río Cisnes fossil fauna (Río Frías Formation, early middle Miocene, Friasian SALMA): a

keystone and paradigmatic vertebrate assemblage of the South American fossil record. Abriendo Ventanas Al Pasado: III Simposio Paleontología En Chile 42–45.

Bown, T. M., and C. N. Larriestra. 1990. Sedimentary paleoenvironments of fossil platyrrhine localities, Miocene Pinturas Formation, Santa Cruz Province, Argentina. Journal of Human Evolution 19:87–119.

Bown, T. M., and J. G. Fleagle. 1993. Systematics, biostratigraphy, and dental evolution of the Palaeothentidae, later Oligocene to early-middle Miocene (Deseadan-Santacrucian) caenolestoid marsupials of South America. Journal of Paleontology 67:1–76.

Brea, M., A. F. Zucol, and A. Iglesias. 2012. Fossil plant studies from late Early Miocene of the Santa Cruz Formation: paleoecology and paleoclimatology at the passive margin of Patagonia, Argentina; pp. 104–129 in S. F. Vizcaíno, R. F. Kay, and M. S. Bargo (eds.), Early Miocene Paleobiology in Patagonia: High-Latitude Paleocommunities of the Santa Cruz Formation. Cambridge University Press, Cambridge, UK.

Buckley, M. 2015. Ancient collagen reveals evolutionary history of the endemic South American “ungulates.” Proceedings of the Royal Society B: Biological Sciences 282:2014–2671.

Burmeister, H. 1885. Examen crítico de los mamíferos y reptiles fósiles denominados por D. Augusto Bravard y mencionados en su obra pecedente. Anales Del Museo Nacional de Buenos Aires 3:95–174.

Cabrera, A. 1939. Los géneros de la familia Typotheriidae. Physis 14:359–372.

Carrillo, J. D., E. Amson, C. Jaramillo, R. Sánchez, L. Quiroz, and C. Cuartas. 2018. The Neogene record of northern South American native ungulates. Smithsonian Contributions to Paleobiology 1–80.

Cassini, G. H. 2013. Skull geometric morphometrics and paleoecology of Santacrucian (late early Miocene; Patagonia) native ungulates (Astrapotheria, Litopterna, and Notoungulata). Ameghiniana 50:193–216.

Cassini, G. H., S. F. Vizcaíno, and M. S. Bargo. 2012a. Body mass estimation in early Miocene native South American ungulates: a predictive equation based on 3D landmarks. Journal of Zoology 287:53–64.

Cassini, G. H., M. Mendoza, S. F. Vizcaíno, and M. S. Bargo. 2011. Inferring habitat and feeding behaviour of Early Miocene notoungulates from Patagonia. Lethaia 44:153–165.

Cassini, G. H., E. Cerdeño, A. L. Villafañe, and N. A. Muñoz. 2012b. Paleobiology of Santacrucian native ungulates (Meridiungulata: Astrapotheria, Litopterna and Notoungulata); pp. 243–287 in S. F. Vizcaíno, R. F. Kay, and M. S. Bargo (eds.), Early Miocene Paleobiology in Patagonia: High-Latitude Paleocommunities of the Santa Cruz Formation. Cambridge University Press,

Cambridge, UK.

Chick, J., D. A. Croft, H. E. Dodson, J. J. Flynn, and A. R. Wyss. 2010. The early Miocene rodent fauna of Pampa Castillo, Chile. Society of Vertebrate Paleontology Annual Meeting, Program and Abstracts Book 71A-72A.

Cifelli, R. L. 1983. The origin and affinities of the South American Condylarthra and early Tertiary Litopterna (Mammalia). American Museum Novitates 1–49.

Cifelli, R. L. 1991. A new adianthid litoptern (Mammalia) from the Miocene of Chile. Revista Chilena de Historia Natrual 64:119–125.

Cifelli, R. L. 1993. The phylogeny of the native South American ungulates; pp. 195–214 in F. S. Szalay, M. J. Novacek, and M. C. McKenna (eds.), Mammal Phylogeny, Placentals. Springer-Verlag, New York, New York, USA.

Cifelli, R. L., and M. F. Soria. 1983. Systematics of the Adianthidae (Litopterna, Mammalia). American Museum Novitates 1–25.

Cifelli, R. L., and J. Guerrero Diaz. 1989. New remains of *Prothoatherium columbianus* (Litopterna, Mammalia) from the Miocene of Colombia. Journal of Vertebrate Paleontology 9:222–231.

Cifelli, R. L., and J. Guerrero. 1997. Litopterns; pp. 289–302 in R. F. Kay, R. H. Madden, R. L. Cifellii, and J. J. Flynn (eds.), Vertebrate Paleontology in the Neotropics: The Miocene Fauna of La Venta, Colombia. Smithsonian Institution Press, Washington, D.C., USA.

Cifelli, R. L., and C. Villarroel. 1997. Paleobiology and affinities of *Megadolodus*; pp. 265–288 in R. F. Kay, R. H. Madden, R. L. Cifelli, and J. J. Flynn (eds.), Vertebrate Paleontology in the Neotropics: The Miocene Fauna of La Venta, Colombia. Smithsonian Institution Press, Washington, D.C., USA.

Corona, A., M. Ubilla, and D. Perea. 2019. New records and diet reconstruction using dental microwear analysis for *Neolicaphrium recens* Frenguelli, 1921 (Litopterna, Proterotheriidae). Andean Geology 46:153–167.

Croft, D. A. 2007. The middle Miocene (Laventan) Quebrada Honda fauna, southern Bolivia and a description of its notoungulates. Palaeontology 50:277–303.

Croft, D. A. 2012. Punctuated isolation: the making and mixing of South America's mammals; pp. 9–19 in B. D. Patterson and L. P. Costa (eds.), Bones, Clones and Biomes: The History and Geography of Recent Neotropical Mammals. University of Chicago Press, Chicago, Illinois, USA.

Croft, D. A. 2016. Horned Armadillos and Rafting Monkeys: The Fascinating Fossil Mammals of South America. Indiana University Press, Bloomington, Indiana, USA, 304 pp.

Croft, D. A., J. J. Flynn, and A. R. Wyss. 2004. Notoungulata and Litopterna of the early Miocene Chucal Fauna, northern Chile. Fieldiana Geology 1–52.

Cuitiño, J. I., R. Ventura Santos, P. J. Alonso Muruaga, and R. A. Scasso. 2015. Sr-stratigraphy and sedimentary evolution of early Miocene marine foreland deposits in the northern Austral (Magallanes) Basin, Argentina. Andean Geology 43:364–385.

Cuitiño, J. I., S. F. Vizcaíno, M. S. Bargo, and I. Aramendía. 2019. Sedimentology and fossil vertebrates of the Santa Cruz Formation (early Miocene) in Lago Posadas, southwestern Patagonia, Argentina. Andean Geology 46:383–420.

Cuitiño, J. I., J. C. Fernicola, M. J. Kohn, R. Trayler, M. Naipauer, M. S. Bargo, R. F. Kay, and S. F. Vizcaíno. 2016. U-Pb geochronology of the Santa Cruz Formation (early Miocene) at the Río Bote and Río Santa Cruz (southernmost Patagonia, Argentina): implications for the correlation of fossil vertebrate localities. Journal of South American Earth Sciences 70:198–210.

Dodson, H. E. 1994. Miocene rodents from Pampa Castillo, Chile: Implications for refining the Santacrucian (early middle Miocene) and “Friasian” (middle Miocene) South American land mammal ages. University of California, Santa Barbara, 155 pp.

Dunn, R. E., R. H. Madden, M. J. Kohn, M. D. Schmitz, C. A. E. Strömberg, A. A. Carlini, G. H. Ré, and J. Crowley. 2013. A new chronology for middle Eocene-early Miocene South American Land Mammal Ages. Bulletin of the Geological Society of America 125:539–555.

Engelman, R. K., F. Anaya, and D. A. Croft. 2018. *Australogale leptognathus*, gen. et sp. nov., a second species of small sparassodont (Mammalia: Metatheria) from the middle Miocene locality of Quebrada Honda, Bolivia. Journal of Mammalian Evolution 1–18.

Fleagle, J. G., M. E. Perkins, M. T. Heizler, A. a. Tauber, B. Nash, T. M. Bown, M. T. Dozo, and M. F. Tejedor. 2012. Absolute and relative ages of fossil localities in the Santa Cruz and Pinturas Formations; pp. 41–58 in S. F. Vizcaíno, R. F. Kay, and M. S. Bargo (eds.), Early Miocene Paleobiology in Patagonia: High-Latitude Paleocommunities of the Santa Cruz Formation. Cambridge University Press, Cambridge, UK.

Flynn, J. J., and C. C. Swisher. 1995. Cenozoic South American Land Mammal Ages: correlation to global geochronologies. Geochronology Time Scales and Global Stratigraphic Correlation, SEPM Special Publication 54:317–333.

Flynn, J. J., R. Charrier, D. A. Croft, and A. R. Wyss. 2012. Cenozoic Andean faunas: shedding new light on South American mammal evolution, biogeography, environments, and tectonics; pp. 51–75 in B. D. Patterson and L. P. Costa (eds.), Bones, Clones and Biomes: The History and Geography of Recent Neotropical Mammals. University of Chicago Press, Chicago, Illinois, USA.

Flynn, J. J., M. J. Novacek, H. E. Dodson, D. Frassinetti, M. C. McKenna, M. A. Norell, K. E. Sears, C. C. Swisher, and A. R. Wyss. 2002. A new fossil mammal

assemblage from the southern Chilean Andes: implications for geology, geochronology, and tectonics. Journal of South American Earth Sciences 15:285–302.

Folguera, A., A. Encinas, A. Echaurren, G. Gianni, and D. Orts. 2018. Constraints on the Neogene growth of the central Patagonian Andes at the latitude of the Chile triple junction (45–47° S) using U/Pb geochronology in synorogenic strata. Tectonophysics 744:134–154.

Forasiepi, A. M., A. G. Martinelli, M. S. de la Fuente, S. Dieguez, and M. Bond. 2011. Paleontology and stratigraphy of the Aisol Formation (Neogene), San Rafael, Mendoza; pp. 135–154 in J. A. Salfity and R. A. Marquillas (eds.), Cenozoic Geology of the Central Andes of Argentina. SCS Publisher, Salta, Argentina.

Friant, M. 1967. Sur les molaires de Condylarthrea et des Litopternes Sud-Americains. Mem. Geopaleontol. Dell'Universitá Di Ferrara 2:135–155.

García-López, D. A., and J. Babot. 2014. The auditory region of the middle Eocene Litopterna Indalecia grandensis Bond & Vucetich 1983: anatomical and phylogenetic approach. IV International Paleontological Congress 183.

Gelfo, J. N., G. M. López, and M. Lorente. 2016. Los ungulados arcaicos de América del Sur: "Condylarthra" y Litopterna. Contribuciones Científicas Del Museo Argentino de Ciencias Naturales "Bernardino Rivadavia" 6:285–291.

Gelfo, J. N., F. J. Goin, M. O. Woodburne, and C. de Muizon. 2009. Biochronological relationships of the earliest South American Paleogene mammalian faunas. Palaeontology 52:251–269.

Gervais, P. 1855. Recherches Sur Les Mammiféres Fossiles de l'Amérique Méridonale. P. Bertrand, Paris, France, 62 pp.

Goloboff, P. A., and S. A. Catalano. 2016. TNT version 1.5, including a full implementation of phylogenetic morphometrics. Cladistics 32:221–238.

Goloboff, P. A., C. I. Mattoni, and A. S. Quinteros. 2006. Continuous characters analyzed as such. Cladistics 22:589–601.

Gregory, W. K. 1912. Notes on the principles of quadrupedal locomotion and on the mechanism of the limbs in hoofed animals. Annals of the New York Academy of Sciences 22:267–294.

Hoffstetter, R., and M. F. Soria. 1986. *Neodolodus colombianus* gen. et sp. nov., un nouveau Condylarthre (Mammalia) dans le Miocene de Colombie. Comptes Rendus de l'Acadamie Des Sciences 303:1619–1622.

Hoorn, C., F. P. Wesselingh, J. Hovikoski, and J. Guerrero. 2010. The development of the Amazonian mega-wetland (Miocene; Brazil, Colombia, Peru, Bolivia); pp. 123–142 in C. Hoorn and F. P. Wesselingh (eds.), Amazonia: Landscape and Species Evolution: A Look into the Past. Blackwell Scientific Publications.

Horovitz, I. 2004. Eutherian mammal systematics and the origins of South American ungulates as based on postcranial osteology. Bulletin of Carnegie Museum of Natural History 36:63–79.

Howell, A. B. 1944. Speed in Animals, Their Specializations for Running and Leaping. Hafner Publishing Company, New York, New York, USA, 268 pp.

Huxley, T. 1880. On the application of the laws of evolution to the arrangement of the Vertebrata, and more particularly of the Mammalia. Proceedings of the Zoological Society, London 43:649–662.

Irigoyen, M. V, K. L. Buchan, and R. L. Brown. 2000. Magnetostratigraphy of Neogene Andean foreland-basin strata, latitude 33°S, Mendoza Province, Argentina. Geological Society of America Bulletin 112:803–816.

Janis, C. M. 1988. An estimation of tooth volume and hypsodonty indices in ungulate mammals and the correlation of these factors with dietary preferences. Proceedings of the VIIth International Symposium on Dental Morphology 367–387.

Janis, C. M., and P. B. Wilhelm. 1993. Were there mammalian pursuit predators in the tertiary? Dances with wolf avatars. Journal of Mammalian Evolution 1:103–125.

Kay, R. F., S. F. Vizcaíno, and M. S. Bargo. 2012. A review of the paleoenvironment and paleoecology of the Miocene Santa Cruz Formation; pp. 331–364 in S. F. Vizcaíno, R. F. Kay, and M. S. Bargo (eds.), Early Miocene paleobiology in Patagonia: High-latitude paleocommunities of the Santa Cruz Formation. Cambridge University Press, Cambridge, UK.

Kerber, L., A. Kinoshita, F. A. José, A. M. Graciano Figueiredo, É. V. Oliveira, and O. Baffa. 2011. Electron spin resonance dating of the southern Brazilian Pleistocene mammals from Touro Passo Formation, and remarks on the geochronology, fauna and palaeoenvironments. Quaternary International 245:201–208.

Kramarz, A. G., and E. S. Bellosi. 2005. Hystricognath rodents from the Pinturas Formation, early-middle Miocene of Patagonia, biostratigraphic and paleoenvironmental implications. Journal of South American Earth Sciences 18:199–212.

Kramarz, A. G., and M. Bond. 2005. Los Litopterna (Mammalia) de la Formación Pinturas, Mioceno temprano-medio de Patagonia. Ameghiniana 42:611–625.

Kramarz, A. G., M. G. Vucetich, A. A. Carlini, M. R. Ciancio, M. A. Abello, C. M. Deschamps, and J. N. Gelfo. 2010. A new mammal fauna at the top of the Gran Barranca sequence and its biochronological significance; pp. 260–273 in R. H. Madden, A. A. Carlini, M. G. Vucetich, and R. F. Kay (eds.), The Paleontology of Gran Barranca: Evolution and Environmental Change through the Middle Cenozoic of Patagonia. Cambridge University Press, Cambridge, UK.

de la Cruz, R., D. Welkner, M. Suárez, and D. Quiroz. 2004. Geología del area Oriental de la Hojas Cochrane y Villa O'Higgins, Región Aisén del General Carlos Ibáñez del Campo. Carta Geológica de Chile 57.

Linnaeus, C. 1758. Systema Naturae per Regna Tri Naturae, 10th ed. Laurentii Salvii, Stockholm, Sweden, 824 pp.

Loomis, F. B. 1914. The Deseado Formation of Patagonia. The Rumford Press, Concord, NH, 232 pp.

McGrath, A. J., F. Anaya, and D. A. Croft. 2018. Two new macraucheniids (Mammalia: Litopterna) from the late middle Miocene (Laventan South American Land Mammal Age) of Quebrada Honda, Bolivia. Journal of Vertebrate Paleontology 38:e1461632.

McHorse, B. K., A. A. Biewener, and S. E. Pierce. 2017. Mechanics of evolutionary digit reduction in fossil horses (Equidae). Proceedings of the Royal Society B: Biological Sciences 284:20171174.

McKenna, M. C. 1956. Survival of primitive notoungulates and condylarths into the Miocene of Colombia. American Journal of Science 254:736–743.

McKenna, M. C., and S. K. Bell. 1997. Classification of Mammals Above the Species Level. Columbia University Press, New York, New York, USA, 631 pp.

Morosi, E., and M. Ubilla. 2017. Dietary and palaeoenvironmental inferences in *Neolicaphrium recens* Frenguelli, 1921 (Litopterna, Proterotheriidae) using carbon and oxygen stable isotopes (Late Pleistocene; Uruguay). Historical Biology 1–7.

Muizon, C. de, and R. L. Cifelli. 2000. The "condylarths" (archaic Ungulata, Mammalia) from the early Palaeocene of Tiupampa (Bolivia): implications on the origin of the South American ungulates. Geodiversitas 22:47–150.

Niemeyer, J., R. F. Skarmeta, and W. Espinosa. 1984. Hojas Peninsula de Taitao y Puerto Aysen Servicio Nacional de Geológica y Mineria. Carta Geológica de Chile 80.

Niemeyer, R. H. 1975. Geología de la región comprendida entre el Lago General Carrera y el Río Chacabuco, Aisén. Universidad de Chile, 309 pp.

O'Leary, M. A., J. I. Bloch, J. J. Flynn, T. J. Gaudin, A. Giallombardo, N. P. Giannini, S. L. Goldberg, B. P. Kraatz, Z. Luo, J. Meng, X. Ni, M. J. Novacek, F. A. Perini, Z. S. Randall, G. W. Rougier, E. J. Sargis, M. T. Silcox, N. B. Simmons, M. Spaulding, P. M. Velazco, M. Weksler, J. R. Wible, and A. L. Cirranello. 2013. The placental mammal ancestor and the post-K-Pg radiation of placentals. Science 339:662–667.

Owen, R. 1838. Fossil Mammalia; pp. 81–111 in C. Darwin (ed.), The Zoology of the Voyage of the H.M.S. Beagle. Smith, Elder and Co., London, UK.

Paula Couto, C. 1952. Fossil mammals from the beginning of the Cenozoic in Brazil:

Condylarthra, Litopterna, Xenungulata, and Astrapotheria. Bulletin of American Museum of Natural History 99:355–394.

Perkins, M. E., J. G. Fleagle, M. T. Heizler, B. Nash, T. M. Brown, A. A. Tauber, and M. T. Dozo. 2012. Tephrochronology of the Miocene Santa Cruz and Pinturas Formations, Argentina; pp. 23–40 in S. F. Vizcaíno, R. F. Kay, and M. S. Bargo (eds.), Early Miocene paleobiology in Patagonia: High-Latitude Paleocommunities of the Santa Cruz Formation. Cambridge University Press, Cambridge, UK.

Prado, J. L., C. Martinez-Maza, and M. T. Alberdi. 2015. Megafauna extinction in South America: a new chronology for the Argentine Pampas. Palaeogeography, Palaeoclimatology, Palaeoecology 425:41–49.

de Queiroz, K., and J. Gauthier. 1992. Phylogenetic taxonomy. Annual Review of Ecology and Systematics 23:449–480.

Raigemborn, M. S., V. Krapovickas, A. F. Zucol, L. Zapata, E. Beilinson, N. Toledo, J. Perry, S. Lizzoli, L. Martegani, D. E. Tineo, and E. Passeggi. 2018a. Paleosols and related soil-biota of the early Miocene Santa Cruz Formation (Austral-Magallanes Basin, Argentina): a multidisciplinary approach to reconstructing ancient terrestrial ecosystems. Latin American Journal of Sedimentology and Basin Analysis 25:117–148.

Raigemborn, M. S., E. Beilinson, J. M. Krause, A. N. Varela, E. Bellosi, S. D. Matheos, and N. Sosa. 2018b. Paleolandscape reconstruction and interplay of controlling factors of an Eocene pedogenically-modified distal volcaniclastic succession in Patagonia. Journal of South American Earth Sciences 1–22.

Raigemborn, M. S., S. D. Matheos, V. Krapovickas, S. F. Vizcaíno, M. S. Bargo, R. F. Kay, J. C. Fernicola, and L. Zapata. 2015. Paleoenvironmental reconstruction of the coastal Monte Léon and Santa Cruz formations (early Miocene) at Rincón del Buque, southern Patagonia: a revisited locality. Journal of South American Earth Sciences 60:31–55.

Roth, S. 1899. Aviso preliminar sobre mamíferos mesozóicos encontrados en Patagonia. Revista Del Museo de La Plata 9:381–388.

Rovereto, C. 1914. Los estratos araucanos y su fósiles. Anales Del Museo Nacional de Buenos Aires 25:1–250.

Scalabrino, B. 2009. Déformation d'un continent audessus d'une dorsale océanique active en subduction. Université Montpellier, 388 pp.

Schmidt, G. I. 2015. Actualización sistemática y filogenia de los Proterotheriidae (Mammalia, Litopterna) del "Mesopotamiense" (Mioceno tardío) de Entre Ríos, Argentina. Revista Brasileira de Paleontologia 18:521–546.

Schmidt, G. I., and B. S. Ferrero. 2014. Taxonomic reinterpretation of *Theosodon hystatus* Cabrera and Kraglievich, 1931 (Litopterna, Macraucheniidae) and phylogenetic relationships of the family. Journal of Vertebrate Paleontology

34:1231–1238.

Schmidt, G. I., C. I. Montalvo, R. Sostillo, and E. Cerdeño. 2018. Proterotheriidae (Mammalia, Litopterna) from the Cerro Azul Formation (late Miocene), La Pampa Province, Argentina. Journal of South American Earth Sciences.

Scott, W. B. 1910. Mammalia of the Santa Cruz beds. Part I. Litopterna. Princeton University Expedition to Patagonia 7:1–156.

Simpson, G. G. 1951. Horses: The Story of the Horse Family in the Modern World and through Sixty Million Years. Oxford University Press, Oxford, UK, 247 pp.

Simpson, G. G. 1980. Splendid Isolation: The Curious History of South Americna Mammals. Yale University Press, New Haven, Connecticut, USA, 275 pp.

Simpson, G. G., and J. L. Minoprio. 1949. A new adianthine liptotern and associated mammals from a Deseadan faunule in Mendoza, Argentina. American Museum Novitates 1–28.

Soria, M. F. 1981. Los Litopterna del Colhuehuapense (Oligoceno tardio) de la Argentina. Revista Del Museo Argentino de Ciencias Naturales Bernardino Rivadavia 3:1–54.

Soria, M. F. 1983. Vertebrados fosiles y edad de la Formación Aisol, provincia de Mendoza. Revista de La Asociación Geológica Argentina 38:299–306.

Soria, M. F. 1989. Notopterna: un nuevo orden de mamíferos ungulados eogenos de América del Sur. Parte II. *Notonychops powelli* gen. et sp. nov. (Notonychopidae nov.) de la Formación Río Loro (Paleoceno medio), provincia de Tucumán, Argentina. Ameghiniana 25:259–272.

Soria, M. F. 2001. Los Proterotheriidae (Litopterna, Mammalia), sistemática, origen y filogenia. Monografias Del Museo Argentino de Ciencias Naturales 1–171.

Suárez, C., A. M. Forasiepi, F. J. Goin, and C. Jaramillo. 2016. Insights into the Neotropics prior to the Great American Biotic Interchange: new evidence of mammalian predators from the Miocene of northern Colombia. Journal of Vertebrate Paleontology 36:e1029581.

Tejada-Lara, J. V., R. Salas-Gismondi, F. Pujos, P. Baby, M. Benammi, S. Brusset, D. De Franceschi, N. Espurt, M. Urbina, and P.-O. Antoine. 2015. Life in proto-Amazonia: middle Miocene mammals from the Fitzcarrald Arch (Peruvian Amazonia). Palaeontology 58:341–378.

Thomason, J. J. 1986. The functional morphology of the manus in the tridactyl equids *Merychippus* and *Mesohippus*: paleontological inferences from neontological models. Journal of Vertebrate Paleontology 6:143–161.

Trayler, R. B., M. D. Schmitz, J. I. Cuitiño, M. J. Kohn, M. S. Bargo, R. F. Kay, C. A. E. Strömberg, and S. F. Vizcaíno. 2020. An improved approach to age-modeling in deep time: implications for the Santa Cruz Formation, Argentina. Geological Society of America Bulletin 132:233–244.

Ubilla, M., D. Perea, A. Rinderknecht, and A. Corona. 2009. Pleistocene mammals from Uruguay: biostratigraphic, biogeographic and environmental connotations; pp. 217–230 in A. M. Ribeiro, S. Girardi, and C. Scherer (eds.), Quaternario do Rio Grande do Sul: integrando conhecimentos. Porto Alegre, Brazil.

Villafañe, A. L., E. Ortiz-Jaureguizar, and M. Bond. 2006. Cambios en la riqueza taxonómica y en las tasas de primera y última aparición de los Proterotheriidae (Mammalia, Litopterna) durante el Cenozoico. Estudios Geológicos 62:155–166.

Villafañe, A. L., G. I. Schmidt, and E. Cerdeño. 2012. Consideraciones sistematicas y bioestratigraficas acerca de *Thoatheriopsis mendocensis* Soria, 2001 (Litopterna, Proterotheriidae). Ameghiniana 49:365–374.

Vizcaíno, S. F., M. S. Bargo, and R. F. Kay. 2012. Background for a paleoecological study of the Santa Cruz Formation (late Early Miocene) on the Atlantic Coast of Patagonia; pp. 1–22 in S. F. Vizcaíno, R. F. Kay, and M. S. Bargo (eds.), Early Miocene Paleobiology in Patagonia: High-Latitude Paleocommunities of the Santa Cruz Formation. Cambridge University Press, Cambridge, UK.

Vucetich, M. G., M. E. Pérez, M. Arnal, C. M. Deschamps, and E. C. Vieytes. 2016. Caviomorph rodents: main features of their evolution. Contribuciones Científicas Del Museo Argentino de Ciencias Naturales “Bernardino Rivadavia” 6:347–358.

Walton, A. H. 1997. Rodents; pp. 392–409 in R. F. Kay, R. H. Madden, R. L. Cifellii, and J. J. Flynn (eds.), Vertebrate Paleontology in the Neotropics: The Miocene Fauna of La Venta, Colombia. Smithsonian Institution Press, Washington, D.C., USA.

Welker, F., M. J. Collins, J. A. Thomas, M. Wadsley, S. Brace, E. Cappellini, S. T. Turvey, M. A. Reguero, J. N. Gelfo, A. G. Kramarz, J. Burger, J. Thomas-Oates, D. A. Ashford, P. D. Ashton, K. Rowsell, D. M. Porter, B. Kessler, R. Fischer, C. Baessmann, S. Kaspar, J. V. Olsen, P. Kiley, J. A. Elliott, C. D. Kelstrup, V. Mullin, M. Hofreiter, E. Willerslev, J.-J. Hublin, L. Orlando, I. Barnes, and R. D. E. MacPhee. 2015. Ancient proteins resolve the evolutionary history of Darwin’s South American ungulates. Nature 522:81–84.

Westbury, M., S. Baleka, A. Barlow, S. Hartmann, J. L. A. Paijmans, A. Kramarz, A. M. Forasiepi, M. Bond, J. N. Gelfo, M. A. Reguero, P. López-Mendoza, M. Taglioretti, F. Scaglia, A. Rinderknecht, W. Jones, F. Mena, G. Billet, C. de Muizon, J. L. Aguilar, R. D. E. MacPhee, and M. Hofreiter. 2017. A mitogenomic timetree for Darwin’s enigmatic South American mammal *Macrauchenia patachonica*. Nature Communications 8:1–8.

Wyss, A. R., J. J. Flynn, M. A. Norell, C. C. Swisher, M. J. Novacek, M. C. McKenna, and R. Charrier. 1994. Paleogene mammals from the Andes of central Chile: A preliminary taxonomic, biostratigraphic, and geochronologic assessment. American Museum Novitates 1–31.

Zapata, L., V. Krapovickas, M. S. Raigemborn, and S. D. Matheos. 2016. Bee cell

trace fossils associations on paleosols from the Santa Cruz Formation: palaeoenvironmental and palaeobiological implications. Palaeogeography, Palaeoclimatology, Palaeoecology 459:153–169.

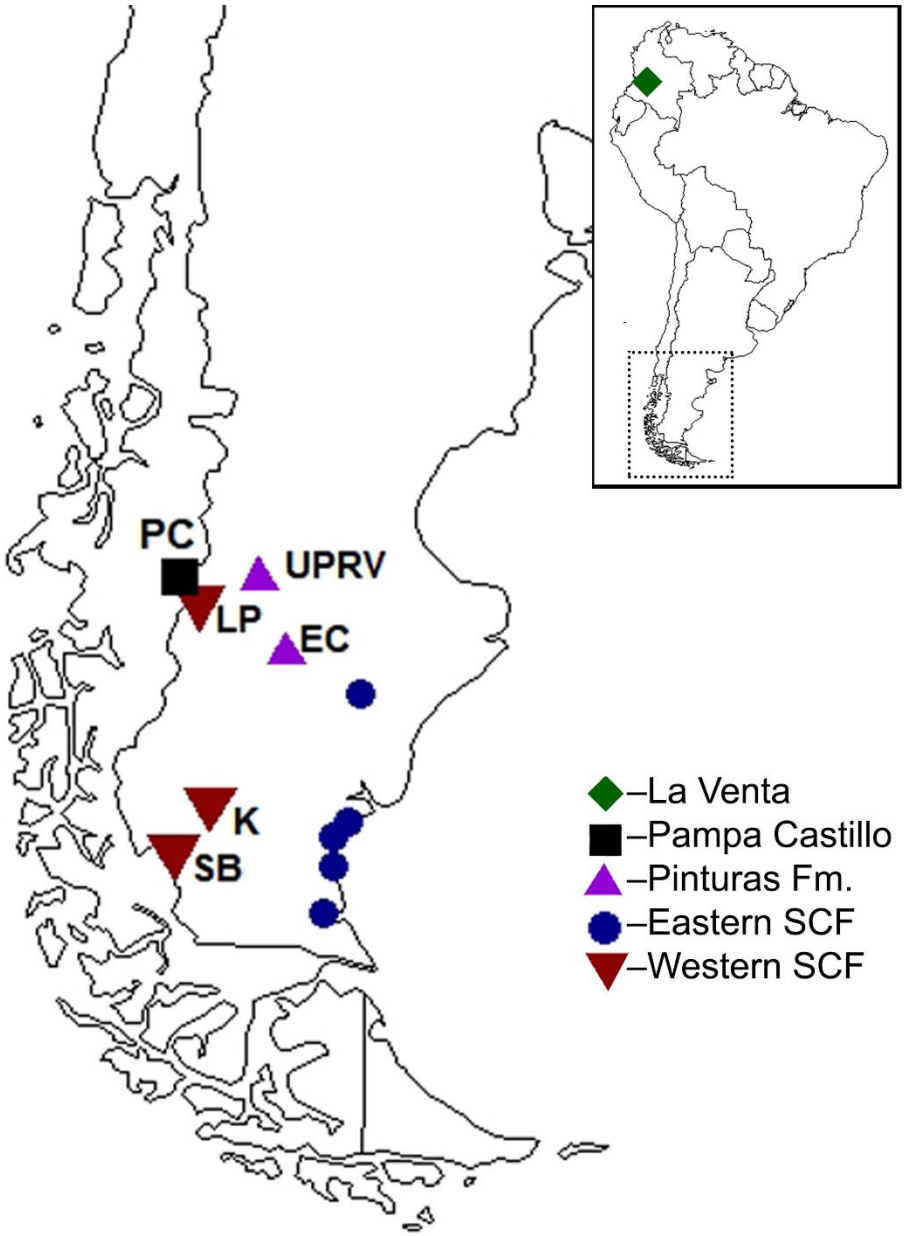

Figure 1. Map showing Pampa Castillo and other fossil localities mentioned in text. Many fossil localities are present in the eastern Santa Cruz Formation (see Vizcaíno *et al.,* 2012), but only four representative localities are plotted here. **Abbreviations: EC**, Estancia la Cañada; **K**, Karaiken; **LP**, Lago Posadas; **PC**, Pampa Castillo; **SB**, Sierra Baguales; **UPRV**, upper Pinturas River Valley.

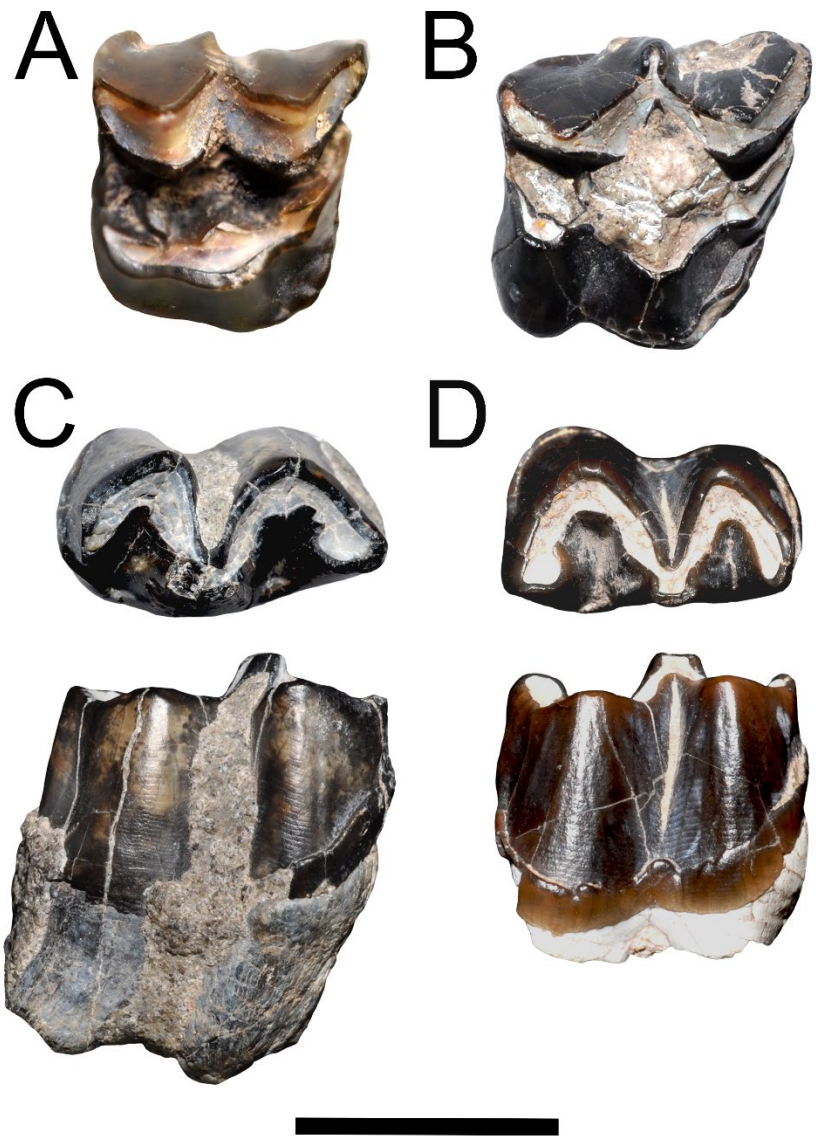

Figure 2. Isolated teeth of *Thoatherium* cf. *T. minusculum* and cf. *Thoatherium* sp. from Pampa Castillo. *Thoatherium* cf. *T. minusculum*: **A**, SGOPV 2015, LP3 in occlusal view (reversed); **B**, SGOPV 2095, RM1 in occlusal view; **C**, SGOPV 2395, Lm3? in occlusal (above) and labial (below; reversed) views. In all views, mesial is to the right. In occlusal views, labial is up. Cf. *Thoatherium* sp.: **D**, SGOPV 2167, Lm1? in occlusal (above) and labial (below; reversed) views. Scale bar equals 1 cm.

Figure 3. Mandible of *Thoatherium* cf. *T. minusculum* (SGOPV 2210) preserving partial Rdp2–3 and complete Ldp2–4, Lm1, Rdp4, and Rm1 in occlusal (above) and left labial (below; reversed) views. Anterior is to the right. Scale bar equals 5 cm.

Figure 4. Rm3 of *Picturotherium* sp. (SGOPV 2158) in occlusal (top) and labial (bottom; reversed) views. Mesial is to the left. Scale bar equals 1 cm.

Figure 5. Three mandibular fragments of *Theosodon* sp. (SGOPV 2064) preserving roots of Li1–m1, Ri1–c, and Rp3–m3; complete Lm2; and partial Lm3; in occlusal view. Scale bar equals 5 cm.

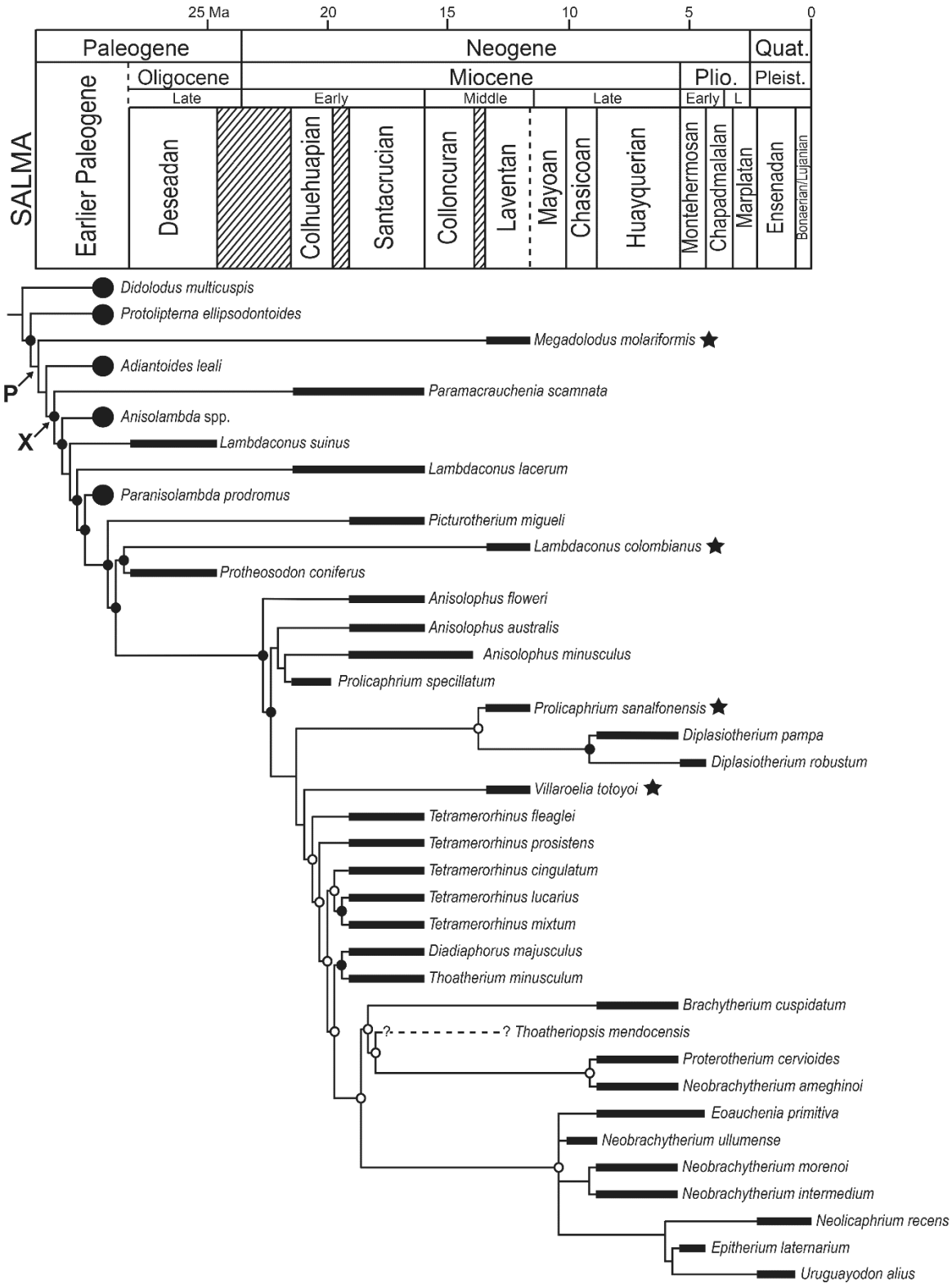
25 Ma
20
15
10
5
0
Paleogene
Neogene
Quat.
Oligocene
Miocene
Plio.
Pleist.
Late
Early
Middle
Late
Early
L
SALMA
Earlier Paleogene
Deseadan
Colhuehuapian
Santacrucian
Colloncuran
Laventan
Mayoan
Chasicoan
Huayquerian
Montehermosan
Chapadmalalan
Marplatan
Ensenadan
Bonaerian/Lujanian
Didolodus multicuspis
Protolipterna ellipsodontoides
Megadolodus molariformis
Adiantoides leali
P
Paramacrauchenia scamnata
Anisolambda spp.
X
Lambdaconus suinus
Lambdaconus lacerum
Paranisolambda prodromus
Picturotherium migueli
Lambdaconus colombianus
Protheosodon coniferus
Anisolophus floweri
Anisolophus australis
Anisolophus minusculus
Prolicaphrium specillatum
Prolicaphrium sanalfonensis
Diplasiotherium pampa
Diplasiotherium robustum
Villaroelia totoyoi
Tetramerorhinus fleaglei
Tetramerorhinus prosistens
Tetramerorhinus cingulatum
Tetramerorhinus lucarius
Tetramerorhinus mixtum
Diadiaphorus majusculus
Thoatherium minusculum
Brachytherium cuspidatum
? Thoatheriopsis mendocensis
Proterotherium cervioides
Neobrachytherium ameghinoi
Eoauchenia primitiva
Neobrachytherium ullumense
Neobrachytherium morenoi
Neobrachytherium intermedium
Neolicaphrium recens
Epitherium laternarium
Uruguayodon alius

Figure 6 (from previous page). Majority consensus of the twelve most-parsimonious trees (339.616 steps). Thick black bars represent known stratigraphic range of taxon. Taxa that lived prior to the Deseadan SALMA (late Oligocene) are represented by black dots. Thin lines approximate implied ghost lineages. Dotted line represents the unknown temporal provenance of *T. mendocensis* (see Villafañe *et al.,* 2012). Black dots mark nodes with Bremer support ≥ 1.000 steps. White dots signify nodes with Bremer support between 0.500 and 1.000 steps. Node P represents Proterotheriidae as defined in text. Node X represents the least-inclusive clade that includes all proterotheriids *sensu* Soria (2001). Stars signify taxa from La Venta, Colombia. SALMA scale follows Croft (2016). **Abbreviation**: **SALMA**, South American Land Mammal 'Age'.

Table 1. Dental measurements of Pampa Castillo litopterns and select specimens of *Picturotherium migueli*. *-uncertain measurement due to damaged tooth. †-data from Kramarz & Bond (2005). **Abbreviations: MD**, mesiodistal length; **LL**, linguolabial width. All measurements reported in mm.

Taxon	**Specimen**	**Tooth**	**MD**	**LL**
Thoatherium cf. *minusculum*	SGO PV 2015	LP3	10.6	11.7
		Lm?	11.7	10.0
	SGO PV 2095	RM1	12.1	12.8
	SGO PV 2210	Rdp3	12.2	7.5*
		Rdp4	10.9	7.7
		Rm1	11.0	7.2
		Lm1	11.7*	7.2*
	SGO PV 2395	Lm3	13.5	7.6
cf. *Thoatherium* sp.	SGO PV 2167	Lm1?	12.1	7.2
Picturotherium sp.	SGO PV 2158	Rm3	14.2	9.0
Picturotherium migueli	MACN PV SC119a†	m3	11.1	7.2
	MACN PV SC119b†	Lm3	10.95	6.75
Theosodon sp.	SGO PV 2064	Lm2	23.2	15.9

Table 2. Summary of phylogenetic analyses in which the three 'anisolambdid' taxa were constrained to fall outside of the clade of 'traditional' proterotheriids (clade X; Fig. 6). **Abbreviation**: **MPT**, most parsimonious tree(s).

Excluded Taxa	**Length of MPT**	**# Steps Relative to Unconstrained Analysis**	**Ref.**
Anisolambda spp.	341.616	+2.000	Fig. S4A
Paranisolambda prodromus	341.547	+1.931	Fig. S4B
Protheosodon coniferus	343.571	+3.955	Fig. S4C
All 3 'anisolambdids'	345.616	+6.000	Fig. S4D

Table 3. Stratigraphic and geographic distribution of early Miocene proterotheriids in Patagonia. **Abbreviations**: **lmPF**, lower and middle Pinturas Formation; **uPF**: upper Pinturas Formation; **eSCF**: eastern Santa Cruz Formation; **wSCF**: western Santa Cruz Formation; **Col**: Colhuehuapian SALMA; **PC**: Pampa Castillo.

Taxon	**lmPF**	**uPF**	**eSCF**	**wSCF**	**Col**	**PC**
Anisolophus australis			X			
Anisolophus floweri			X	X		
Anisolophus minusculus			X			
Diadiaphorus majusculus			X			
Diadiaphorus caniadensis		X				
Lambdaconus lacerum	X				X	
Paramacrauchenia scamnata				X	X	
Picturotherium migueli	X					
Picturotherium sp.						X
Prolicaphrium specillatum					X	
Tetramerorhinus cingulatum		?	X			
Tetramerorhinus fleaglei	X					
Tetramerorhinus lucarius			X	X		
Tetramerorhinus mixtum			X	X		
Tetramerorhinus prosistens	X					
Thoatherium minusculum			X	X		
Thoatherium sp.			X	X		X

CHAPTER 2

NEW PROTEROTHERIIDS FROM THE MIDDLE MIOCENE OF QUEBRADA HONDA, BOLIVIA, AND BODY SIZE AND DIVERSITY TRENDS IN PROTEROTHERIID AND MACRAUCHENIID LITOPTERNS (MAMMALIA)

ABSTRACT

In this work, we describe two new species of proterotheriid litopterns, *Olisanophus riorosarioensis* gen. et sp. nov. and *Olisanophus akilachuta* sp. nov. from the middle Miocene (Laventan SALMA) of Quebrada Honda, Bolivia. When incorporated into a recently published phylogenetic analysis (40 taxa; 92 characters), they plot as sister taxa, partially supported by their connected metaconule and protocone on M3. Additionally, we revise the taxonomy of two contemporaneous proterotheriids from La Venta, Colombia. '*Prolicaphrium*' *sanalfonensis* is reassigned to *Mesolicaphrium* gen. nov., with a prominent protocone on M3 as a synapomorphy of the genus. We revalidate the genus *Neodolodus* for *Neodolodus colombianus*, a species previously referred to '*Prothoatherium*' or *Lambdaconus* by previous authors. We used the paleotree R package to examine evolutionary trends in diversity and body size (using m1 length as a proxy) in proterotheriid and macraucheniid litopterns in a phylogenetic context. Proterotheriids were more diverse in the Paleogene than their fossil record indicates; their diversity peaked in the early Miocene and gradually declined until the Pleistocene. Macraucheniids experienced two peaks in diversity, in the early and late Miocene, but were still fairly diverse in the Pleistocene, unlike proterotheriids. Multiple proterotheriid lineages became larger during the Paleogene, but body size was roughly static during the Neogene, with no obvious link between phylogeny and size. Macraucheniids can be grouped into three size classes that are phylogenetically conserved and roughly correspond temporally to Eocene (small

Polymorphis spp.), Miocene–Pliocene (medium-sized ‘cramaucheniines’ and early macraucheniines, *e.g., Theosodon*, *Promacrauchenia*), and Pleistocene (large macraucheniines, *e.g., Macrauchenia*) species.

KEYWORDS

South America. Laventan. Ungulate. Proterotheriidae. Macraucheniidae. Body Size. Diversity. Evolution.

INTRODUCTION

South America was isolated from other landmasses for much of the Cenozoic, leading to the development of a largely endemic mammalian fauna including a variety of hoofed mammals called South American native ungulates (SANUs) (Patterson and Pascual, 1968; Simpson, 1980; Croft, 2016; Croft et al., 2020). Litopterns were the second-most diverse SANU group after notoungulates, though the exact composition of the clade is uncertain, with authors disagreeing about the phylogenetic placement of certain Paleogene taxa like Didolodontidae, Protolipternidae, and Amilnedwardsiidae (Cifelli, 1983; Soria, 1989; Gelfo et al., 2016). They existed from the Paleocene until the late Pleistocene (Bonaparte and Morales, 1997; Bond et al., 2001; Soria, 2001; Gelfo et al., 2016). A variety of litoptern subgroups are known, but two, Proterotheriidae and Macraucheniidae, vastly exceed the others (e.g., Adianthidae, Protolipternidae, Sparnotheriodontidae) in terms of diversity and longevity. Proterotheriids, the most diverse subgroup, existed from the early Eocene (Itaboraian South American Land Mammal Age [SALMA]) until the late Pleistocene (Bond et al., 2001; Soria, 2001; McGrath et al., 2020). Macraucheniids are first known from the late Eocene (Mustersan SALMA), and several species reached gigantic sizes (~1000 kg) in the Pleistocene (Fariña et al., 1998; Schmidt and Ferrero, 2014). Proterotheriids and macraucheniids were very diverse in the early Miocene (Colhuehuapian and Santacrucian SALMAs) and late Miocene (Chasicoan and Huayquerian SALMAs) (Soria, 2001; Villafañe et al.,

2006; Schmidt and Ferrero, 2014; Croft, 2016; Croft et al., 2020), but their middle Miocene diversity is poorly known.

Recently published phylogenies of Proterotheriidae (McGrath et al., 2020) and Macraucheniidae (Schmidt and Ferrero, 2014; Forasiepi et al., 2016; McGrath et al., 2018) have provided new contexts for understanding diversity and morphological evolution in these groups. Examining diversity in a phylogenetic context, as opposed to simply counting taxa recorded during a given interval (e.g., SALMA), improves our understanding of diversity because it takes ghost lineages (lineages inferred based on a phylogeny) into account. In this way, true drops in diversity can be better distinguished from artificial ones that are due to incomplete sampling. Studying the evolution of a continuous feature, such as body size, in a phylogenetic context provides a more accurate picture of the timing of evolutionary changes and whether such changes characterize individual lineages or evolved convergently multiple times within a clade.

In recent years, Quebrada Honda (Fig. 7) has become one of the best-studied middle Miocene fossil localities in South America and has yielded many new mammal species (e.g., Croft, 2007; Pujos et al., 2011, 2014; Engelman and Croft, 2014; Engelman et al., 2017; Brandoni et al., 2018; McGrath et al., 2018).The fossil-bearing layers have been dated to 13.0–12.7 Ma, partially contemporaneous with the well-studied La Venta Fauna in Colombia (MacFadden et al., 1990; Kay et al., 1997). Proterotheriids have been reported previously from Quebrada Honda, but none have been identified to the species level. In his initial report on the site, Hoffstetter (1977) described indeterminate proterotheriid remains that included two

lower molars, an astragalus that he thought resembled *Epecuenia thoatherioides* Cabrera, 1939, and a calcaneus comparable in size to *Proterotherium australe* (=*Tetramerorhinus mixtum* Ameghino, 1894, per Soria, 2001). Takai et al. (1984) referred two partial mandibles to *Diadiaphorus* sp. Ameghino, 1887, though Soria (2001) disputed this assignment, stating that one of the specimens resembled *Tetramerorhinus lucarius* Ameghino, 1894, or *Anisolophus australis* Burmeister, 1879, and the other was indeterminate.

The goal of the present study is to describe and identify new proterotheriid remains from the Quebrada Honda region that have been collected in recent years through a research collaboration between Case Western Reserve University (Cleveland, Ohio, USA) and the Universidad Autónoma “Tomás Frías” (Potosí, Bolivia) as well as remains collected by earlier expeditions (Hoffstetter, 1977; Takai et al., 1984). We identify these remains as representing two new species of a new genus (*Olisanophus riorosarioensis* gen. et sp. nov. and *Olisanophus akilachuta* sp. nov.), which we include in a phylogenetic analysis of the family. Based on the results of this phylogenetic analysis, we revise the taxonomy of two proterotheriids from La Venta, ‘*Prolicaphrium*’ *sanalfonensis* Cifelli and Guerrero, 1997, and ‘*Lambdaconus*’ *colombianus* Hoffstetter and Soria, 1986. We also examine trends in diversity and body size in Proterotheriidae and Macraucheniidae in the context of these groups’ phylogenies.

MATERIALS AND METHODS

Anatomical Abbreviations

C/c, upper/lower canine; **I/i**, upper/lower incisor; **L**, left; **M/m**, upper/lower molar; **P/p**, upper/lower premolar; **R**, right.

Institutional Abbreviations

AMNH, American Museum of Natural History, New York, New York, USA; **FMNH**, Field Museum of Natural History, Chicago, Illinois, USA; **GB Naz**, Nazareno collections, Servicio Geológico de Bolivia, La Paz, Bolivia; **IGM**, Museo Geológico Nacional, Servicio Geológico Colombiano (formerly INGEOMINAS), Bogotá D.C., Colombia; **MACN**, Museo Argentino de Ciencias Naturales “Bernardino Rivadavia”, Buenos Aires, Argentina; **MLP**, Museo de La Plata, La Plata, Argentina; **MNHN,** Muséum national d’Histoire naturelle, Paris, France; **RIEB CM**, Research Institute of Evolutionary Biology, Tokyo, Japan; **UATF-V**, Vertebrate Paleontology Collections, Universidad Autónoma Tomás Frías, Potosí, Bolivia; **UCMP**, University of California Museum of Paleontology, Berkeley, California, USA; **YPM**, Yale Peabody Museum, New Haven, Connecticut, USA.

Each numbered specimen in the UATF-V collections includes only those remains collected in a limited area (typically less than one square meter) that most likely pertain to a single individual (i.e., represent a single taxon, are of similar ontogenetic age, and include no duplicated elements). Dental terminology follows McGrath et al. (2020), and postcranial terminology follows Scott (1910). These

specimens were compared with other proterotheriids through firsthand observation and examination of the primary literature.

Phylogenetic Analysis

The two new species were added to the character-taxon matrix of McGrath et al. (2020), bringing the total number of taxa to 40, including *Didolodus multicuspis* Ameghino, 1897, as the outgroup (Supplementary File 4). These taxa were scored for 92 characters, eight of which were coded as continuous (Appendix 1). *Olisanophus riorosarioensis* was scored for 55 characters, and *O. akilachuta* was scored for 40. As in McGrath et al. (2020), the phylogenetic analysis was conducted in TNT v. 1.5 (Goloboff and Catalano, 2016) using a New Technology search with tree-fusing and ratchet options on their default settings. The minimum-length trees were found 100 times. Continuous characters were rescaled to have a range of 0–1 and were treated as additive (*i.e.*, ordered; see Goloboff *et al.*, 2006). All discrete characters were non-additive and unweighted.

Diversity and Morphological Evolution

Estimates of proterotheriid and macraucheniid diversity and phenograms depicting their body size evolution were constructed using the paleotree package v. 3.1.3 (Bapst, 2012) for RStudio v.1.1.414 (RStudioTeam, 2016). Trees were built using the "bin_timePaleoPhy" command. This command calibrates a given phylogeny by time and randomly selects a first and last appearance date for each taxon within its given temporal interval (*i.e.,* SALMA). Minimum branch length, which must be > 0 to prevent concurrent divergences of multiple lineages, was arbitrarily

set to 0.5 million years (type = “mbl”, vartime = 0.5); thus, the divergence date for a particular taxon was 0.5 million years before its earliest occurrence, and each internodal branch (*i.e.,* a node leading to another node) was 0.5 million years. To create minimum required diversity curves, 100 evolutionary histories were generated (ntrees = 100), and the curves were then made with the “multiDiv” command. The phenograms were created using the “plotTraitgram” command, which requires a single tree input (ntrees = 1). For this analysis, taxa were presumed to survive for the duration of their given SALMA(s) (nonstoch.bin = TRUE). Also due to the requirements of this command, all polytomies were resolved in the manner that requires the minimum total ghost lineages (timeres = TRUE). The values of the internal nodes in the phenograms were constructed using maximum likelihood.

Temporal ranges of individual taxa (Table 4) were taken from the literature and based on data from museum collections (AMNH, FMNH, MACN, MLP, UCMP, YPM). Temporal ranges of taxa were based on SALMAs (or equivalent stages) rather than absolute ages because more precise information about age is lacking for many fossils, particularly ones from historical collections. For this reason, the “bin_timePaleoPhy” command was used rather than “timePaleoPhy” (see Bapst, 2012). SALMA ages (Supplementary File 5) were taken from Flynn and Swisher (1995), Dunn et al. (2013), Tomassini et al. (2013), Woodburne et al. (2014a, b), and Krause et al. (2017). The Pleistocene SALMAs (Ensenadan and Lujanian/Bonaerian) were combined into one ‘Pleistocene’ unit due to uncertain provenance of some Pleistocene taxa (Soria, 2001; Corona *et al.*, 2019a) and to make the duration of this unit closer to that of other SALMAs. *Thoatheriopsis*

mendocensis Soria, 2001, a proterotheriid from the early or middle Miocene levels of the Mariño Formation (Villafañe et al., 2012), was assumed to come from the Laventan SALMA, an age that implies shorter ghost lineages (McGrath et al., 2020).

The phylogeny used for proterotheriid diversity and body size evolution was that generated by the analysis described above with the addition of seven species omitted by McGrath et al. (2020) due to incompleteness (Supplementary File 6). Five of these species (*Adiantoides magnus* Cifelli and Soria, 1983, *Diadiaphorus caniadensis* Kramarz and Bond, 2005, *Lambdaconus inaequifacies* Ameghino, 1904, *Neolicaphrium major* Soria, 2001, and *Paramacrauchenia inexspectata* Soria, 2001) were assumed to be the sister taxon of the type species of their respective genus, though the monophyly of these genera was not tested in this analysis and is therefore uncertain. A sixth species, *Bounodus enigmaticus* Carlini et al., 2006, was considered to be the sister taxon of *Megadolodus molariformis* McKenna, 1956, because they are the only named members of Megadolodinae (Cifelli and Villarroel, 1997; Carlini et al., 2006). The seventh, *Indalecia grandensis* Bond and Vucetich, 1983, was presumed to be the sister taxon of *Adiantoides* spp. because these taxa are generally believed to comprise the Indaleciidae, a subgroup of Proterotheriidae per McGrath et al. (2020) (Cifelli and Soria, 1983). *Anisolambda amel* Simpson, 1948, and *Anisolambda fissidens* Ameghino, 1901, were treated separately in these analyses as opposed to collectively as *Anisolambda* spp. in McGrath et al. (2020). Several other “anisolambdids” (*sensu* Soria, 2001) such as *Wainka tshotshe* Simpson, 1935, and *Lambdaconops porcus* Ameghino, 1901, were left out of these analyses. The fragmentary remains of these taxa are not scorable for a sufficient

amount of characters to include them in the phylogenetic analysis of McGrath et al. (2020; see Appendix 1). Additionally, there are no obvious relatives in the phylogeny of McGrath et al. (2020) to ally with taxa such as *Wainka tshotshe* or *Lambdaconops porcus* because they are monotypic genera that do not belong to known monophyletic subgroups of Proterotheriidae (McGrath et al. [2020] recovered "Anisolambdidae" as polyphyletic). The paleotree analyses require every taxon to be part of the input phylogeny, so these taxa had to be excluded entirely.

For analyses of macraucheniid diversity, we used the phylogeny of McGrath et al. (2018), which was based on the analyses of Schmidt and Ferrero (2014) and Forasiepi et al. (2016) (Supplementary File 7; Fig. S6). Those phylogenetic analyses considered taxa at the genus level, so multispecific genera were treated as polytomies in the present analysis. The validity of many species referred to *Theosodon* Ameghino, 1887, and *Promacrauchenia* Ameghino, 1904, are uncertain (Cifelli and Guerrero, 1997; Cassini et al., 2012; Schmidt and Ferrero, 2014; McGrath et al., 2018), but we included the best-known species, which presumably are the most likely to be valid. Although *Promacrauchenia* (*Pseudomacrauchenia*) *yepesi* Kraglievich, 1930, is not well-known, it was included due to its Pleistocene occurrence (Castellanos, 1950; Reguero et al., 2007), which represents a temporal extension for its genus. "*Theosodon* sp. nov." from La Venta, Colombia (Cifelli and Guerrero, 1997) was included and treated as a distinct species of the genus.

Measurements were taken directly from the literature or from photographs using the Fiji platform for ImageJ (Schindelin et al., 2012). Mesiodistal length of m1 was used as a proxy for size because it is a commonly preserved element and is

often used to infer body size in fossil mammals (see Hopkins, 2018). Average m1 length for each taxon is listed in Table 4, and data for individual specimens is listed in Supplementary File 8. In cases where no m1 has been referred to a particular taxon, mesiodistal m1 length was estimated based on other tooth dimensions or on other, similarly-sized taxa (see Supplementary File 8). We did not use body mass due to inherent difficulties in calculating the mass of an extinct group such as litopterns that is not closely related to any extant species (see McGrath et al., 2018) and because we were interested in relative trends in body size through time in these clades rather than each taxon's absolute mass.

GEOGRAPHIC AND GEOLOGIC CONTEXT

The specimens described herein were collected from outcrops of the Honda Group (unnamed formation) in western Tarija Department, southern Bolivia, in the vicinity of the village of Quebrada Honda (Fig. 7). Specifically, they derive from three particularly productive areas of outcrops are known as the Quebrada Honda, Río Rosario, and Huayllajara local areas (see MacFadden et al., 1990; Brandoni et al., 2018). In this work, 'Quebrada Honda' refers to the outcrops collectively (including all local areas) unless specified as Quebrada Honda Local Area. See Croft (2007) and Croft (2016) for overviews of the paleontology of Quebrada Honda.

The holotype of *Olisanophus riorosarioensis* (UATF-V-001287) and three specimens referred to *O. akilachuta* (UATF-V-00967, UATF-V-00978, UATF-V-

001613) were collected from the Río Rosario Local Area. The holotype of *Olisanophus akilachuta* (UATF-V-001780) and one other specimen referred to this species (UTAF-V-001613) were collected from the Quebrada Honda Local Area in levels stratigraphically equivalent to those where the specimens from Río Rosario were found. These strata lie below the tuff dated by MacFadden et al. (1990) at 12.83 ± 0.11 Ma. Another specimen referred to *O. akilachuta* (RIEB-CM-423), and one referred to *O. riorosarioensis* (MNHN BLV 20) apparently were also collected from this area (Hoffstetter, 1977; Takai et al., 1984), but their stratigraphic provenance is unknown. MacFadden et al. (1990) correlated these basal levels in both local areas to Polarity Chrons C5AAn and C5Ar.3r of the Geomagnetic Polarity Time Scale (GPTS), which span 13.183–12.887 Ma (Ogg, 2012). One poorly preserved partial dentary referred to *Olisanophus* sp. (UATF-V-00181) was collected from relatively high in section at the Huayllajara Local Area. It is likely younger than other specimens referred to the genus, but exactly how much younger is the subject of ongoing geochronological investigations.

SYSTEMATIC PALEONTOLOGY

Mammalia Linnaeus, 1758

Eutheria Huxley, 1880

Panperissodactyla Welker et al., 2015

Litopterna Ameghino, 1889

Lopholipterna Cifelli, 1983

Proterotheriidae Ameghino, 1887

Olisanophus gen. nov.

Type species. *Olisanophus riorosarioensis* sp. nov.

Derivation of name. Anagram of *Anisolophus* Burmeister, 1885, a proterotheriid from the early and middle Miocene of Argentina.

Referred species. The type and *Olisanophus akilachuta* sp. nov.

Geographic distribution and age. Unnamed formation of the Honda Group (Quebrada Honda), Department of Tarija, southern Bolivia; late middle Miocene (Serravallian Age), Laventan SALMA.

Diagnosis. Mid-sized proterotheriid with weak interstylar folds on P4–M3 as in *Anisolophus*, *Paranisolambda prodromus* Paula Couto, 1952, *Prolicaphrium specillatum* Ameghino, 1902, *Tetramerorhinus fleaglei* Soria, 2001, *Tetramerorhinus prosistens* Ameghino, 1899, and *Villarroelia totoyoi* Cifelli and Guerrero, 1997; P3 with hypocone and small metaconule but lacking paraconule unlike all known proterotheriids; P3–M2 with mesiolingual cingula joined to protocone as in *Anisolophus australis, Anisolophus floweri* Ameghino, 1887, *Lambdaconus lacerum* Ameghino, 1902, and *Tetramerorhinus mixtum*; ; M1–3 with strong labial cingula; metaconule on M2 connected to protocone; M2 protocone and hypocone separated by sulcus; M3 with small or absent hypocone and a parastyle that is more prominent

than mesostyle or metastyle; M3 protocone significantly larger than paraconule, metaconule, and hypocone, if present; M3 metaconule closely connected to protocone at its base or by slight postprotocrista; entoconid and hypoconulid of p4–m3 subequal in size; p4–m3 hypoconulid more labial than entoconid; m1–3 lack paraconids as in *Anisolophus* spp., *Lambdaconus lacerum*, *Megadolodus molariformis*, *Neobrachytherium ameghinoi* Soria, 2001, *Neobrachytherium intermedium* Ameghino, 1891, *Paramacrauchenia scamnata* Ameghino, 1902, *Picturotherium migueli* Kramarz and Bond, 2005, *Prol. specillatum*, and *V. totoyoi*; m3 with entoconid isolated or weakly connected to hypolophulid; and m3 with a slight sulcus between the hypoconid and hypoconulid.

Olisanophus riorosarioensis sp. nov.

Figures 2, S2

Type material. UATF-V-001287, elements of right and left upper and lower dentitions including partial isolated RP3–4, partial RM1 and RM3, and complete RM2 in a maxillary fragment (Fig. 8.1, isolated partial LM3 (Fig. S7.1), partial left mandible including symphysis, roots of Lp1–2, partial Lp3, and complete Lp4–m3 (Figs. 8.2, S7.3), partial right mandible including roots of Rp3–4, partial Rm1–2, and complete Rm3 (Fig. S7.2).

Derivation of name. In reference to the type locality, Río Rosario.

Referred material. Type only.

Geographic and stratigraphic occurrence. Unnamed formation of the Honda Group, Quebrada Honda, Department of Tarija, southern Bolivia: locality B-07-23,

Río Rosario Local Area, unspecified lower levels equivalent to Units 2–4 of MacFadden and Wolff (1981).

Diagnosis. P3 with preparaconular crista but no paraconule; P3–M2 with very large, curved mesiolingual cingula. M1–2 with small lingual cingulum between protocone and hypocone; M3 with continuous cingulum around entire mesial, lingual, and distal edges of tooth similar to, but stronger than, some specimens of *Diadiaphorus majusculus* Ameghino, 1887; M3 with highly reduced metaconule and no hypocone as in *Lambdaconus suinus* Ameghino, 1897, and *Thoatherium minusculum* Ameghino, 1897; p4–m3 with labial cingulids; and m3 entoconid connected to hypolophulid by a weak crest.

Description. The RP3 of UATF-V-001287 is worn and missing its labial edge, so only the lingual half of the ectoloph is present (Fig. 8.1; Table 5). A small paraconule is present, though it is quite a bit smaller than the protocone and hypocone. Though the tooth is worn, a slight bulge distal to the protocone suggests that a metaconule is present on P3. The mesiolingual cingulum is prominent and joins the protocone at the cusp's lingual edge.

RP4 is very similar to RP3 except for its larger size and lesser degree of wear (Fig. 8.1; Table 5). Like P3, it lacks the labial edge of the ectoloph. This tooth differs from P3 in its larger metaconule and the presence of a paraconule. The distolingual sulcus separates the hypocone and protocone. A thin band of enamel between the hypocone and metaconule shows that the distolingual sulcus once extended distally and labially to separate these cusps but has been shortened by wear. The mesiolingual cingulum resembles that of P3.

The RM1 of UATF-V-001287 exhibits little morphology because it is highly worn and missing the labial edge of the ectoloph (Fig. 8.1). The hypocone appears to be as large as the protocone. The mesiolingual cingulum is joined to the base of the protocone, as in P3–4, but is less prominent. Despite the high degree of wear in M1, the mesiolingual cingulum remains unworn except for the most lingual portion, where it joins the paraconule. The paraconule is visible due to its rounded mesiolingual border. The preparaconular crista is more pronounced in M1 than in P3–4 and projects labially to join the parastyle. A small cingulum or conule is located on the lingual edge between the protocone and hypocone and is separated from these cusps by sulci.

RM2 is complete and less worn than M1 (Fig. 8.1). The hypocone is slightly lingual with respect to the protocone and is separated from it by a deep sulcus. Though the hypocone is completely covered by enamel, a polygonal wear facet is present on its distal surface. The distal cingulum is strong and projects up from the hypocone to join the metastyle. The metaconule is smaller than the paraconule; it is closely connected to the protocone at the base rather than by a short postprotocrista and is separated from the hypocone by a sulcus. All three labial styles are present, with the metastyle less developed than the others. Between the labial styles, very weak interstylar folds are present, with the paracone fold being slightly more prominent. Labial cingula are also present on M2 though interrupted by the mesostyle. The mesiolingual cingulum resembles that of M1 and encloses a deep basin. As in M1, a small lingual cingulum/conule is located on the lingual edge of the tooth between the protocone and hypocone.

Both M3s of UATF-V-001287 are present and lack their labial borders (Figs. 8.1, S7.1). The paraconule is reduced relative to other proterotheriids, such as *Diadiaphorus*, *Tetramerorhinus*, *Villarroelia totoyoi*, and *Picturotherium migueli* (Cifelli and Guerrero, 1997; Soria, 2001; Kramarz and Bond, 2005), and it is joined to the protocone by a short preprotocrista. The metaconule is small and connected to the protocone by a very short postprotocrista, unlike M2. A continuous cingulum encircles the entire mesial, lingual, and distal borders of M3. In the distolingual corner of the tooth, this cingulum rises slightly This feature is positioned where one would expect a hypocone, but it does not rise to the level of the para- and metaconules, much less the protocone, nor is it significantly differentiated from the surrounding cingulum. The cingulum varies slightly in height and width throughout its length and has an additional high point near the mesiolingual corner.

The left ramus of UATF-V-001287 preserves a single alveolus for p1 and two alveoli for p2 (Fig. 8.2). Alveoli representing the external incisor and canine may be present, though it is uncertain whether these features merely represent damage to the mandible. If these features truly represent alveoli, the external incisor appears to be large and procumbent, and the canine appears to be single-rooted and approximately the same size as p1. Both of these teeth would resemble other known proterotheriids in morphology but would differ in position. Most proterotheriids possess a diastema between the canine and p1, but the alveoli of UATF-V-001287 are next to each other, suggesting that these teeth were in contact. The mandibular symphysis extends posteriorly to the mesial border of the p2 alveolus (Fig. 8.2). The symphysis appears to have broken postmortem rather than representing an unfused

symphysis in life, which would distinguish *O. riorosarioensis* from other proterotheriids. The left ramus preserves two mandibular foramina, one below p1 and the other below the mesial alveolus of p3 (Fig. S7.3). The mandible is roughly elliptical in cross-section (12.2 mm wide x 21.3 mm deep at the border of m1–2). It becomes dorsoventrally shallower anteriorly (16.5 mm at the border of p3–4).

UATF-V-001287 preserves the labial edge of p3 (Fig. 8.2), which appears to have been molariform (i.e., bicrescentic). No labial cingulid is present on p3, but as in the p4, the talonid seems to be labiolingually longer than the trigonid.

The p4 of UATF-V-001287 is molariform (Fig. 8.2). The paralophid is straight and obliquely oriented and terminates in a small paraconid. The hypoconid extends further labially than the protoconid as in p3. The hypolophid ends in a small entoconid. A weak labial cingulid encircles the protoconid and hypoconid (Fig. S7.3). A very weak lingual cingulid extends from the paraconid but does not reach the metaconid.

The Lm1 of UATF-V-001287 is complete (Fig. 8.2), and the Rm1 preserves the hypoconid (Fig. S7.2). The labial cingulid is much stronger than that of p4 and is more prominent around the base of the protoconid than the hypoconid (Supplementary Fig 2.3). Wear obscures all other morphology of m1.

The Lm2 of UATF-V-001287 is complete (Fig. 8.2), and Rm2 lacks the distolingual portion (Fig. S7.2). The paralophid ends at the labiolingual midline, and the paraconid is absent. The metaconid is mesial of the midline, resulting in the talonid basin being longer than the trigonid. The hypoconulid and entoconid are

subequal in size and closely connected. The labial cingulid resembles that of m1 but is slightly more pronounced (Fig. S7.3). The lingual cingulid is strong on the mesiolingual corner of the tooth and continues very weakly around the base of the metaconid.

Both m3s are complete in UATF-V-001287 (Figs. 8.2, S7.2). As in m2, the paralophid terminates before the lingual edge of the tooth, and the paraconid is absent. The metaconid is roughly circular in cross-section. The entoconid and hypoconulid are equal in size and are separated by a sulcus. A weak crest connects the entoconid and hypolophulid, though this connection only appears via wear. The entoconid is distal with respect to the hypoconid and lingual of the hypoconulid. A labial cingulid encircles the base of the protoconid (Fig. S7.3). The base of the hypoconid is not fully erupted, so the presence of the labial cingulid around the base of this cuspid cannot be determined. A lingual cingulid encircles the mesiolingual corner of m3.

Overall, the enamel of *O. riorosarioensis* appears thicker than in other (non-megadolodine) proterotheriids such as *Tetramerorhinus*, *Brachytherium cuspidatum* Ameghino, 1883, *Thoatherium minusculum*, *Paramacrauchenia* Bordas, 1936, and *Prolicaphrium specillatum* (Soria, 2001; Schmidt, 2015). Trends in enamel thickness have not been analyzed broadly among litopterns, but this may represent an alternative strategy to hypsodonty for prolonging the effectiveness of the cheek teeth.

Remarks. *Olisanophus riorosarioensis* clearly differs from all other Laventan proterotheriids (Table 4). It is much larger than *Neodolodus colombianus* from La

Venta, Colombia, and its teeth bear more developed lophs (Fig. 8; Table 5; Hoffstetter and Soria, 1986; Cifelli and Guerrero Diaz, 1989). Another La Venta taxon, *Villarroelia totoyoi*, has much larger metaconules and paraconules relative to the other upper molar cusps and is slightly larger than *O. riorosarioensis* (Cifelli and Guerrero, 1997). The continuous cingulum around the mesial, lingual, and distal edges of M3 and small cingulum/conule on the lingual edge of M1–2 distinguish *O. riorosarioensis* from *Olisanophus akilachuta* and *Mesolicaphrium sanalfonensis* (as well as all other proterotheriids) (Figs. 2.1, 3.3; Cifelli and Guerrero, 1997). *Thoatheriopsis mendocensis*, a proterotheriid of uncertain - possibly middle Miocene - age, differs from *O. riorosarioensis* in its lack of interstylar folds on P3–M3 and broader mesiolingual cingula on P3–4 (Villafañe et al., 2012).

Olisanophus cf. *O. riorosarioensis*

=*Diadiaphorus* sp. Takai et al., 1984 [*partim*]

Referred Material. RIEB CM 423, partial right horizontal ramus of mandible preserving p1–m3.

Geographic and Stratigraphic Occurrence. Unnamed formation of the Honda Group, Quebrada Honda, Department of Tarija, southern Bolivia: unspecified locality and stratigraphic layer of Quebrada Honda Local Area (Fig. 7).

Description and Remarks. We were unable to study this specimen directly and relied solely on the description and photograph in Takai *et al.* (1984). The teeth of this specimen are highly worn, with only m3 preserving useful coronal morphology.

This tooth lacks a paraconid, and the paralophid terminates near the labiolingual midpoint. The distolingual corner of the m3 is damaged, though a remnant of the entoconid appears to be present. The lower molars bear strong labial cingulids.

Takai et al. (1984) referred RIEB-CM 423 to *Diadiaphorus* sp., but they cited no particular features to support this conclusion. The specimen appears to have an entoconid on m3 (Takai et al., 1984: pl. 27), unlike *Diadiaphorus majusculus*; however, another species questionably referred to the genus, *Diadiaphorus caniadensis*, does possess a small entoconid (Kramarz and Bond, 2005). Takai et al. (1984) reported p1–m3 length as 68 mm, making this specimen much smaller than *D. majusculus* (~120 mm; pers obs.). A complete p1–m3 series is not known for either *D. caniadensis* nor *Diadiaphorus eversus* Ameghino, 1891 (Schmidt, 2015), but these species are only slightly smaller than *D. majusculus* in other respects and therefore are also significantly larger than the species represented by RIEB-CM 423 (Soria, 2001; Kramarz and Bond, 2005; Schmidt, 2015). Although p1–2 are not preserved in the holotype of *O. riorosarioensis* (Fig. 8.2), RIEB-CM 423 is approximately the right size for this taxon. Based on Takai et al. (1984: pl. 27), we estimate the mesiodistal length of m1–3 of RIEB-CM 423 to be 35.5 mm; the same measurement of UATF-V-001287 is 36.0 mm. The morphology of this specimen is compatible with that of *O. riorosarioensis* in all other respects including the presence of strong labial cingulids, which distinguish this species from *Olisanophus akilachuta* (described below). We refer RIEB-CM 423 to *O. riorosarioensis* with reservation because we could only observe the specimen through low-quality photographs.

Olisanophus akilachuta sp. nov.

Figures 3, S3–S6

Type Material. UATF-V-001780, partial RP3? (Fig. 9.1), complete RM2–3 (Fig. 9.2–3), partial LM2 (Fig. S8.1), complete LM3, partial Lm3 (Fig. 9.4).

Referred Material. UATF-V-000967, partial right upper molariform (likely P4 or M1) (Fig. S8.2); UATF-V-000978, partial mandible preserving partial Lm1–3 (Fig. S9); UATF-V-001613, maxillary fragment with heavily worn M1–3, distal right tibia, fragmentary phalanx, other limb bone fragments (Fig. S10); UATF-V-001770, mandibular fragment preserving roots of Lp3 and complete Lp4–m2 (Fig. 9.5); MNHN BLV 20, partial Lm1 and complete Lm2 (Fig. S11).

Derivation of Name. From akila, meaning ‘fast,’ and ch’uta, meaning ‘resident of the Altiplano,’ in Quechua, an indigenous language of the Quebrada Honda region, in reference to the location of Quebrada Honda and the cursorial adaptations of many proterotheriids.

Geographic and Stratigraphic Occurrence. Unnamed formation of the Honda Group (Quebrada Honda), Department of Tarija, southern Bolivia (Fig. 7): localities B-13-02 (UATF-V-001780) and B-07-17 (UATF-V-001770), red beds below first gray interval, Unit 2 of MacFadden and Wolff (1981), Quebrada Honda Local Area; unspecified locality, Quebrada Honda Local Area (MNHN BLV 20); Locality B-07-22, lower red beds approximately equivalent to Unit 2 of MacFadden and Wolff (1981), Río Rosario Local Area (UATF-V-000967, UATF-V-000978, UATF-V-001613).

Diagnosis. P3 lacks paraconule; P3–M3 with less pronounced mesiolingual cingula than *O. riorosarioensis* and *Mesolicaphrium sanalfonensis*; M3 metaconule slightly larger than *O. riorosarioensis*; M3 with small or absent hypocone; M3 lacks continuous cingulum around mesial, lingual, and distal edges unlike *O. riorosarioensis*; Lower p4–m3 lacking labial cingulids unlike *O. riorosarioensis*; and m3 entoconid separated from hypoconulid and hypolophulid by sulcus as in *Mes. sanalfonensis*.

Description. The holotype of *O. akilachuta*, UATF-V-001780, includes a mesiolingual fragment of a molariform tooth that probably represents RP3 (Fig. 9.1; Table 5). This fragment lacks a paraconule, instead the protocone bears a small mesially-extending crest. The mesiolingual cingulum is weak and connected to the base of the protocone. The distinct paracone and metacone rule out P1 and P2. The paraconule and mesiolingual cingulum would likely be more prominent if this represented a more distal tooth such as P4 or M1. Since only isolated teeth are preserved in the holotype, we cannot be certain of the identity of this fragment.

An isolated partial right upper molariform tooth (UATF-V-000967; Fig. S8.2) may represent P4 or M1. It exhibits very little wear and its labial edge is broken. A hypocone is present; it is lingual of the protocone and is separated from it by a sulcus. Both the paraconule and metaconule are present and are noticeably smaller than the protocone. There are no cristae related to the metaconule, which is closely connected to the protocone and separated from the hypocone by a sulcus. From the paraconule, a preparaconular crista projects towards the parastyle. The mesiolingual cingulum is relatively straight and not connected to the protocone. The presence of a

paraconule and a strong hypocone rule out the possibility that UATF-V-000967 represents P3 or M3, respectively. UATF-V-001780 demonstrates that the mesiolingual cingulum of M2 (described below) is connected to the base of the protocone, unlike the condition in UATF-V-000967, which suggests it does not represent that locus. Although M1 and M2 generally resemble each other, the shape of the mesiolingual cingulum varies between these teeth in some proterotheriids (*e.g.*, *Anisolophus minusculus* Roth, 1899, *Epitherium laternarium* Ameghino, 1888, and *T. minusculum*; Supplementary File 4). As noted above, UATF-V-001780 does not appear to preserve M1. This tooth is present in a referred specimen, UATF-V-001613 (Fig. S10), but all of its coronal morphology has been destroyed by wear, and its borders are damaged.

UATF-V-001780 preserves a complete RM2 (Fig. 9.2) and a partial LM2 (Fig. S8.1) that includes the paracone, paraconule, mesiolingual cingulum, and part of the protocone. The paraconule is separate from and smaller than the protocone. A preparaconular crista projects mesiolabially as in UATF-V-000967 (Fig. S8.2). The metaconule is notably smaller than the paraconule. The protocone, paraconule, and metaconule are connected to each other at the base, and these three cusps are separated from the paracone, metacone, and hypocone by deep sulci. The hypocone is directly distal of the protocone and separated from it by a sulcus. A mesiolingual cingulum joins the protocone at its base, enclosing a small basin. The three labial styles are present, with the metastyle being slightly reduced relative to the others. Weak interstylar folds are present between the labial styles. Two labial

cingula connect the bases of the labial styles. RM2 is also preserved in UATF-V-001613 (Fig. S10), but wear has obscured its coronal morphology.

Both left and right M3 are complete in UATF-V-001780 (Fig. 9.3). The protocone is the most prominent cusp on the tooth. The paraconule is smaller than the protocone and separated from it by a sulcus. The preparaconular crista is also reduced in M3 compared to M2, in part because the paraconule is positioned more mesiolabially in M3. The metaconule is equal in size to the paraconule and closely connected to the protocone. The mesiolingual cingulum joins the protocone at its base. In UATF-V-001780 (the holotype), the distal cingulum curves to connect to the protocone, and there is no noticeable enlargement in this cingulum to suggest a hypocone. Contrastingly, a small hypocone, subequal in size to the para- and metaconules, is present in UATF-V-001613 (Fig. S10.1). All three labial styles are present, and they decrease in size distally (parastyle > mesostyle > metastyle). A weak paracone fold is present, but no metacone fold is present. Two labial cingula connect the labial styles, and the cingulum connecting the parastyle and mesostyle is more prominent.

The crown of Lp3 of UATF-V-001770 is missing, but its roots are preserved (Fig. 9.5). The Lp4 of UATF-V-001770 has a paralophid that reaches the lingual edge of the tooth and terminates in a paraconid approximately the same size as the hypoconulid and entoconid (Fig. 9.5; Table 5). The paraconid is slightly lingual and distal to the paralophid, giving the appearance that the paralophid curves ‘inward’ at its end. A similar morphology is seen in the lower molars of some sparnotheriodontid litopterns such as *Sparnotheriodon* Soria, 1978 and *Victorlemoinea* Ameghino, 1901

(Paula Couto, 1952; Soria, 1978). The hypoconid is slightly labial of the protoconid. The metaconid is slightly mesial of the midline, making the trigonid basin shorter mesiodistally than the talonid basin. The hypolophulid does not reach the lingual edge of the tooth; rather, it is connected to the entoconid by a small cristid. No hypoconulid is present, and labial and lingual cingulids are also absent.

As in other proterotheriid taxa, the m1 and m2 of UATF-V-001770 (Fig. 9.5) and MNHN BLV 20 (Fig. S11) closely resemble each other except for the greater wear of m1. The paralophid does not reach the lingual edge of the tooth, and the paraconid is absent. Similar to p4, the trigonid basin is slightly shorter in these anterior molars than the talonid. The entoconid is slightly larger than the hypoconulid, and the two cuspids are separated by a slight sulcus that, as evidenced by m1, disappears with wear. A small cristid continues distal of the hypoconulid in the same orientation as the hypolophulid. Both teeth lack labial and lingual cingulids in UATF-V-001770, but the m2 of MNHN BLV 20 bears a small lingual cingulid (the mesiolingual corner of m1 in this specimen is damaged). UATF-V-000978 (Fig. S9) preserves the roots of Rm1 and a partial Rm2. This specimen exhibits more wear than UATF-V-001770 or MNHN BLV 20, but the specimen's morphologies are identical in all observable respects.

The only part of the lower dentition preserved in the holotype of *O. akilachuta*, UATF-V-001780, is a partial Lm3 (Fig. 9.4). Much of the trigonid basin is missing, so the extent of the paralophid and presence of a paraconid cannot be determined. The hypoconulid and entoconid are equal in size and separated by a sulcus. A slight sulcus separates the hypoconid and hypoconulid, splitting the hypolophulid. This

sulcus is also reflected on the labial border of the tooth. No labial cingulid is observed, but because the junction between the crown and roots is not preserved, this cannot be determined with certainty. The Rm3 of UATF-V-000978 preserves the trigonid basin and cristid obliqua, and the labial cingulid is absent in this tooth (Fig. S9). There is no evidence of m3 in UATF-V-001770. The vertical ramus of the mandible begins posterior of Lm2 (Fig. 9.5). No mandibular foramina are visible, but the imperfectly preserved surface of the mandible may obscure their presence. The cross-section and relative depth of the horizontal ramus are distorted by compression along the labiolingual axis.

The distal right tibia of UATF-V-001613 (Fig. S10) is of typical proterotheriid morphology (Scott, 1910; Soria, 2001). The distal surface is divided into two concavities to articulate with the astragalar condyles. The mesial concavity is shifted dorsally with respect to the lateral concavity and has a stronger ‘lip’ around its external edge. The dorsal intercondylar tongue is larger and more hook-like than the ventral intercondylar tongue. The maximum mediolateral width of the distal epiphysis is 19.2 mm at its greatest.

Part of the proximal end of a proximal phalanx (UATF-V-001613) is preserved. Based on its size (proximal epiphysis is approximately 13.3 mm dorsoventrally), it most likely represents digit III.

Olisanophus sp.

Figures S7–S8

=*Diadiaphorus* sp. Takai et al., 1984 [*partim*]

Referred Material. RIEB-CM 424, partial mandible preserving left external incisor and roots of Lc–p3; UATF-V-001181, partial mandible preserving bases of Rm1–3? (Fig. S12.1); UATF-V-001562, partial mandible preserving partial Lp3–4 (Fig. S13); UATF-V-001907, distal right femur and distal right tibia (Fig. S12.2, 7.4; UATF-V-001999, distal third metapodial (Fig. S12.3).

Geographic and Stratigraphic Occurrence. Unnamed formation of the Honda Group (Quebrada Honda), Department of Tarija, southern Bolivia (Fig. 7): unspecified provenance (RIEB-CM 424) and locality B-07-17 (UATF-V-001999), Quebrada Honda Local Area; locality B-07-22, Rio Rosario Local Area (UATF-V-001562, UATF-V-001907); B-10-05, Huayllajara Local Area (UATF-V-001181).

Description. RIEB-CM 424 preserves a partially erupted left external incisor (Takai et al., 1984: pl. 27). The mandible is broken at this point, so it is uncertain whether the tooth had yet erupted in life. The crowns of Lc–p3 are absent, but their roots are preserved. Two mandibular foramina are present below the root of the canine and the distal edge of the root of p1. As with RIEB-CM 423, this specimen was described as *Diadiaphorus* sp. (Takai et al., 1984), but it preserves no diagnostic morphology of this genus and is smaller than the type species, *Diadiaphorus majusculus*. The morphology and size of RIEB-CM 424 agrees with its tentative referral to *Olisanophus*.

UATF-V-001181 preserves the bases of three right molariform teeth (Fig. S12.1). They are most likely m1–3, but due to their increasing size (moving distally),

they could also represent p4–m2 or dp3–m1. The mesiodistal length of these three teeth is approximately 35 mm. We refer this specimen to *Olisanophus* sp. because it falls within the size range of *O. riorosarioensis* and *O. akilachuta*, the only proterotheriids currently identified at Quebrada Honda.

UATF-V-001562 preserves Lp3–4 (Fig. S13). The teeth are slightly worn, but their crowns are mostly covered by hard calcareous matrix. The trigonid basin of p3 is much longer mesiodistally and narrower labiolingually than the talonid. This tooth bears a strong paraconid. The p3 is approximately 14 mm long mesiodistally and 7.5 mm labiolingually. The paraconid of p4 is also prominent. The hypoconulid is slightly larger than the entoconid and these cuspids are incipient on each other. This tooth is approximately 13 mm long mesiodistally and 9 mm labiolingually. Measurements of both teeth should be viewed with caution due to their state of preparation (Fig. S13). We assign this specimen to *Olisanophus* because it resembles *O. riorosarioensis* and *O. akilachuta* in all observable aspects. Unfortunately, there are no known criteria to distinguish the p4s of these species, and the p3 of *O. akilachuta* is unknown, so we must refer UATF-V-001562 to *Olisanophus* sp.

UATF-V-001907 includes the distal epiphysis of a right femur (Fig. S12.2) and the distal end of a right tibia (Fig. S12.4). These elements resemble those of well-known Santa Cruz proterotheriids such as *Tetramerorhinus* spp. and *Diadiaphorus majusculus* (Scott, 1910) and are similar in size to *Tetramerorhinus* spp. which, based on dental measurements, were approximately the same size as *Olisanophus* (Tabs. 1, 2; Soria, 2001).

UATF-V-001999 is a third (i.e., central) metapodial (Fig. S12.3). We believe this pertains to a proterotheriid rather than a small macraucheniid, such as the sympatric *Llullataruca shockeyi* McGrath et al., 2018, for multiple reasons. UATF-V-001999 presents a rather large articular surface when viewed dorsally, unlike macraucheniid metatarsals (Scott, 1910: pl. XX; McGrath et al., 2018: fig. 6D*)*, and the shaft of UATF-V-001999 is relatively thicker. In palmar (inferior) view, the keel does not continue as a ridge extending up the shaft as in *Theosodon* (Scott, 1910). We are unable to determine whether UATF-V-001999 is a metacarpal or metatarsal. The transverse width of UATF-V-001999 at the distal epiphysis is 17.7 mm.

Mesolicaphrium gen. nov.

=*Prolicaphrium* Ameghino, 1902 [*partim*]

Type species. *Mesolicaphrium sanalfonensis* (Cifelli and Guerrero, 1997).

Derivation of Name*.* Modification of *Prolicaphrium*, the genus to which this species was previously referred. *Meso-* refers to its middle Miocene age, between that of *Prolicaphrium* (early Miocene) and *Neolicaphrium* Frenguelli, 1921 (Pliocene–Pleistocene).

Referred Species. The type only.

Geographic Distribution and Age. La Victoria and Villavieja formations, Honda Group (La Venta), Huila Department, Colombia. See Cifelli and Guerrero (1997) for additional details.

Diagnosis. Mid-sized proterotheriid with weak interstylar folds on P3–M3 as in *Anisolophus*, *Olisanophus*, *Paranisolambda prodromus*, *Prolicaphrium specillatum*, *Tetramerorhinus fleaglei*, *Tetramerorhinus prosistens*, and *Villarroelia totoyoi*. P3 molariform with well-developed labial styles, paraconule, and metaconule but no hypocone as in *Anisolophus*, *Megadolodus molariformis*, *Neodolodus colombianus*, *Paramacrauchenia scamnata*, and *Protheosodon coniferus* Ameghino, 1897; M2 protocone and paraconule subequal in size; M3 with well-developed metaconule not connected to other cusps; M3 protocone significantly larger than metaconule and paraconule; M3 with distal cingulum that turns mesially to join protocone but no hypocone; M3 with thin, lophate paraconule; relatively straight lophids on p4–m3 that cause the trigonid and talonid crescents to appear more triangular than in other proterotheriids; entoconid in p4–m3 more lingual than hypoconulid; m1–2 trigonid basin mesiodistally shorter than talonid basin; m1–3 lack paraconids; m1–3 with labial cingulids; and m3 with sulcids separating hypoconid, hypoconulid, and entoconid.

Mesolicaphrium sanalfonensis comb. nov.

=*Prolicaphrium sanalfonensis* Cifelli and Guerrero, 1997

Type Material. IGM 182852, symphysis and right horizontal ramus of mandible preserving c (interpreted as i2 by Cifelli and Guerrero (1997); see remarks below), p2–m3.

Referred Material. IGM 184499, right horizontal ramus of mandible preserving p2–m3; IGM 183246 and 183620, associated RP3 and LM1–2; IGM 250873, RM3; UCMP 39254, isolated tooth fragments; UCMP 39256, fragmentary and highly worn upper and lower teeth.

Diagnosis. Same as for genus.

Remarks. Cifelli and Guerrero (1997) provided a detailed and thorough description of this taxon to which we have relatively little to add. However, we interpret the mesialmost tooth of the holotype (IGM 182852) as Rc rather than Ri2 because of its small size, simple morphology, and position on the mandible. Proterotheriids generally possess two lower incisors that many authors refer to simply by their relative positions, internal and external, due to uncertain homologies (*i.e.*, it is not known which incisor was lost; Soria, 2001). The i2 of Cifelli and Guerrero (1997) would correspond to the external incisor of other authors, which is generally large and procumbent, unlike the mesialmost tooth of IGM 182852. Additionally, the long axes of proterotheriid incisors are oriented more or less perpendicular to the mandibular ramus unlike the small tooth of IGM 182852, which is parallel to the ramus.

Mesolicaphrium sanalfonensis was originally assigned to *Prolicaphrium* based on its similarity to the type and only species, *Prolicaphrium specillatum*, rather than shared unique apomorphies (Cifelli and Guerrero, 1997). Upon further examination, these species differ in many respects, warranting their placement in separate genera. The P3 of *Prol. specillatum* lacks a hypocone and has a distal cingulum that turns mesially to meet the lophate protocone. The P3 of *Mes. sanalfonensis* has a

small hypocone and a sulcus that separates this cusp from the protocone. The mesiolingual cingulum of the P3 of *Prol. specillatum* does not connect to the protocone, whereas it does in *Mes. sanalfonensis*. The metaconule of M1 and M2 of *Prol. specillatum* is isolated from all other cusps and is subequal in size to the paraconule, protocone, and hypocone. The only known M1 of *Mes. sanalfonensis* is heavily worn, but the metaconule of M2 is connected to the protocone by a crest and is smaller than the protocone, hypocone, and paraconule. The lower teeth of these two species differ primarily in the curvature of the lophids, which are straighter in *Mes. sanalfonensis*. The m1–3 of *Mes. sanalfonensis* bear strong cingulids, unlike the molars of *Prol. specillatum*.

Our phylogenetic analysis (see below) recovers *Mes. sanalfonensis* as the sister taxon to *Diplasiotherium* spp. Rovereto, 1914, inside of a larger clade that includes *O. riorosarioensis* and *O. akilachuta* (Fig. 10). *Diplasiotherium robustum* Rovereto, 1914, and *Diplasiotherium pampa* Soria, 2001, are both known solely from fairly worn lower dentitions (Soria, 2001; Schmidt et al., 2018). The position of these two species in the phylogeny (Fig. 10), and therefore their close relationship with *Mes. sanalfonensis*, should be treated with caution until additional material is discovered. If *Diplasiotherium* spp. are excluded from the analysis, the position *Mes. sanalfonensis* does not change and it forms an exclusive clade with *Olisanophus* spp.

Neodolodus Hoffstetter and Soria, 1986

Type and Only Species. *Neodolodus colombianus* Hoffstetter and Soria, 1986.

Geographic and Stratigraphic Occurrence. Castilletes Formation and Honda Group (La Victoria and Villavieja formations), Guajira and Huila Departments, Colombia. Middle Miocene (Langhian to Serravallian ages), Colloncuran–Laventan SALMAs.

Diagnosis. Brachydont proterotheriid smaller than all other Neogene proterotheriids. Mesostyle absent in P3–4 unlike *Lambdaconus lacerum*, *Lambdaconus suinus*, *Paramacrauchenia scamnata*, *Picturotherium migueli*, and *Proterotherium cervioides* Ameghino, 1883. Hypocone absent in P3–4 unlike *Protero. cervioides*. P3–M3 with strong interstylar folds as in *Lambdaconus* spp., *Paramacrauchenia* spp. P3 with a continuous cingulum around the lingual edge of the tooth. P4 with distal cingulum that turns mesially and joins protocone. M1–3 with labial cingula. M1–3 with mesiolingual cingula that join the base of the protocone unlike *Pa. scamnata* and *Pi. migueli*. M1–2 with metaconule and hypocone subequal to protocone in size unlike *L. suinus*, *Paramacrauchenia* spp., *Pi. migueli*, and *Protero. cervioides.* M1–2 with metaconule not connected to protocone or hypocone unlike *Pa. scamnata*, *Pi. migueli*, and *Protero. cervioides*. M3 with a small hypocone connected to the protocone by a crest and an isolated metaconule unlike *L. suinus*, *Pa. scamnata*, and *Pi. migueli*. M3 with smaller paraconule and stronger mesiolingual cingulum than *Lambdaconus inaequifacies* and *Pi. migueli*. Entoconid absent in p3. Paraconid absent in p4–m3, and paralophid terminates at or labial to the labiolingual midline of the tooth unlike *Paramacrauchenia* spp. p4–m3 with strong labial cingulids unlike *L. lacerum*, *L. suinus*, *Pa. scamnata*, and *Pi. migueli*. Entoconid of m1–2 larger than

hypoconulid. Sulci separating the hypoconid, hypoconulid, and entoconid on m3 unlike *L. suinus*.

Neodolodus colombianus Hoffstetter and Soria, 1986

=*Prothoatherium colombianus* Cifelli and Guerrero Diaz, 1989

=*Lambdaconus colombianus* Carrillo et al., 2018

Type Material. MNHN VIV 9, right mandibular ramus preserving p3–m3.

Referred Material. Nine specimens representing most upper and lower teeth (including upper incisor) and elements of fore- and hind limbs. See Cifelli and Guerrero Diaz (1989) for full details.

Diagnosis. Same as for genus due to monotypy.

Remarks. See Cifelli and Guerrero Diaz (1989) for a full description of this taxon.

Neodolodus colombianus was first described by Hoffstetter and Soria (1986) as a late-surviving didolodontid “condylarth” on the basis of a single specimen, a partial dentary bearing p3–m3. Following the discovery of additional material, including a tusk-like upper incisor, upper cheek teeth, and postcranial elements, this species was reinterpreted as a proterotheriid of the genus ‘*Prothoatherium*’ Ameghino, 1902 (Cifelli and Guerrero Diaz, 1989). Soria (2001), in his comprehensive revision of Proterotheriidae, considered the genus ‘*Prothoatherium*’ to be invalid and referred its species to *Lambdaconus* (*L. lacerum*) and *Paramacrauchenia* (*Pa. scamnata* and *Pa. inexspectata*). ‘*Prothoatherium*’

(=*Neodolodus*) *colombianus* was not discussed in Soria (2001) because he considered *Neodolodus colombianus* a “condylarth” and therefore beyond the purview of his analysis. It is important to point out that this monograph represents a posthumous publication of Soria’s doctoral thesis, which was nearing completion when he suffered a tragic (and ultimately fatal) auto accident in January 1989 (Novas *et al.*, 1990). Since Cifelli and Guerrero Diaz (1989) was not published until later in 1989, Soria was unaware that *Neodolodus colombianus* had been referred to Proterotheriidae. Therefore, he did not include a taxonomic opinion on the matter in his thesis. Recently, Carrillo *et al.* (2018) referred ‘*Prothoatherium*’ (=*Neodolodus*) *colombianus* to *Lambdaconus* based on shared diagnostic features differing from *Paramacrauchenia* (the other genus to which some ‘*Prothoatherium*’ species were transferred by Soria (2001)), such as P4–M3 with a prominent metaconule, M3 with a small hypocone, and m1–3 lacking a paraconid. Villafañe et al. (2006) also referred to this species as *Lambdaconus colombianus* but did so without further explanation. In their discussion of the species of *Lambdaconus*, Schmidt et al. (2019) mentioned that the generic assignment of *Lambdaconus colombianus* required revision.

In our phylogenetic analysis (see below), *Neodolodus colombianus* is recovered as the sister taxon of *Protheosodon coniferus*, several nodes away from *Lambdaconus* spp. (which itself is not monophyletic; Fig. 10). As detailed in McGrath et al. (2020), the phylogenetic position of *Protheo. coniferus*, generally considered an ‘anisolambdid’ (Cifelli, 1983), should be treated with caution. Nevertheless, when *Protheo. coniferus* is excluded from the clade of ‘traditional’ proterotheriids (i.e.,

Proterotheriinae *sensu* Cifelli, 1983; clade X of McGrath et al., 2020), *N. colombianus* still does not group with *Lambdaconus* spp. (Fig. S14.2). Given the lack of phylogenetic support for a clade composed of *N. colombianus* and *Lambdaconus* spp. and the divergent morphology of *N. colombianus* compared to its close relatives (*e.g.*, small size, more bunodont dentition), *Neodolodus* warrants recognition as a distinct genus, as originally described.

RESULTS

Phylogenetic Analysis

The phylogenetic analysis resulted in 12 most-parsimonious trees of 351.775 steps trees with a consistency index of 0.369 and a retention index of 0.581. In the strict consensus tree (augmented version shown in Figure 10; unmodified version with Bremer supports shown in Figure S14.1), the two new taxa from Quebrada Honda are sister taxa that are in turn sister to a clade of *Mesolicaphrium sanalfonensis* and *Diplasiotherium* spp.

Proterotheriid and Macraucheniid Diversity

The overall trends of the proterotheriid minimum diversity and known diversity curves largely mirror each other (Fig. 11.1). Diversity remains rather consistent through the Paleogene with a small increase in the Vacan subage of the Casamayoran SALMA (mid Eocene). Peak proterotheriid diversity occurs in the

Santacrucian SALMA (early Miocene). The minimum required diversity curve generally shows a steady decline from this peak whereas the known diversity curve shows more drastic changes in the later Neogene. From the Itaboraian (early Eocene) to Chasicoan (early late Miocene) SALMAs, the minimum diversity curve is about five species higher than the known diversity curve. From the Huayquerian SALMA (late Miocene) to the Pleistocene, this gap shrinks.

The macraucheniid minimum diversity and known diversity curves do not match each other as closely as the proterotheriid curves. The Huayquerian has the highest known macraucheniid diversity of any SALMA (six), but the minimum required diversity curve peaks just prior to the Colhuehuapian SALMA. After macraucheniid diversity drops in the middle Miocene (Colloncuran–Mayoan SALMAs), the group experienced a second peak in the late Miocene (Chasicoan–Huayquerian SALMAs) according to the minimum diversity curve.

Proterotheriid and Macraucheniid Size

Proterotheriids increased in size through most of the Paleogene and generally maintained a consistent size range during the Neogene (Fig. 12.1). Most Neogene proterotheriids had m1 length of 10–15 mm. Notable exceptions include *Neodolodus colombianus* and *Picturotherium migueli*, which were considerably smaller than their contemporaries potentially related to their early divergence within the clade. *Diadiaphorus majusculus* and especially *Diplasiotherium robustum* were larger than most other proterotheriids, but their respective congeners, *Diadiaphorus caniadensis* and *Diplasiotherium pampa*, were within the normal Neogene proterotheriid size range—though toward the high end.

Early macraucheniids appear to follow a pattern similar to proterotheriids (Fig. 12.2), with increasing size through the Paleogene, though their first appearance is later, during the Mustersan SALMA (late Eocene). Through the Miocene, macraucheniids generally stayed within a m1 size range of ~17–25 mm. Also similar to proterotheriids, a small middle Miocene taxon, *Llullataruca shockeyi*, represents a long-surviving, early-diverging lineage. Unlike proterotheriids, macraucheniids greatly increased in size in the Pleistocene though the phylogeny implies that the lineage leading to these giant species must have diverged from *Promacrauchenia* in the late Miocene.

DISCUSSION

Phylogenetic Analysis

The two new proterotheriids from Quebrada Honda are recovered as sister taxa and form an exclusive clade with *Mesolicaphrium sanalfonensis*, *Diplasiotherium robustum*, and *Diplasiotherium pampa* (Fig. 10). As noted in McGrath et al. (2020), the position of *Diplasiotherium* spp. should be treated with caution because the two species referred to the genus are only known from lower dentitions and can only be scored for 28 of 92 characters (Soria, 2001; Schmidt et al., 2018). We recognize *O. riorosarioensis* and *O. akilachuta* as congeneric due to the morphological similarities described above.

Bolivian Proterotheriids

Olisanophus riorosarioensis and *O. akilachuta* are the first securely-identified proterotheriid species from Bolivia. Proterotheriid remains from the late Oligocene (Deseadan SALMA) Salla beds were referred by Hoffstetter (1977) to cf. *Deuterotherium* (=*Lambdaconus* per Soria, 2001) sp., though Marshall et al. (1983) only mentioned indeterminate proterotheriids from this locality. *Salladolodus deuterotherioides* Soria and Hoffstetter, 1983, also from Salla, is variously considered a proterotheriid (Shockey and Anaya, 2008) or didolodontid (Soria and Hoffstetter, 1983; Soria, 2001). This taxon is only known from a single specimen consisting of two upper molars, so its affinities will likely remain ambiguous until more material is recovered (see Gelfo, 2006). At present, proterotheriids from other Bolivian localities are only known from fragmentary, indeterminate remains (Villarroel and Marshall, 1989; Oiso, 1991).

Other Middle Miocene Proterotheriids

Proterotheriid diversity is poorly documented between the Santacrucian and Laventan SALMAs. *Anisolophus minusculus* is known from the southern Argentinian Collón Curá Formation (Pilcaniyeu Viejo area) as well as from the Santacrucian Santa Cruz Formation (Soria, 2001). Oiso (1991) referred a heavily worn mandible preserving Rm1–2 (GB Naz-007) to *Diadiaphorus* sp. from the possibly Colloncuran-age locality of Nazareno, Bolivia (Croft *et al.*, 2016). We disagree with this identification because GB Naz-007 is significantly smaller than *Diadiaphorus majusculus* and, due to wear, does not preserve any diagnostic morphology (Oiso, 1991: tab. 4; Soria, 2001: tab. 13). To our knowledge, proterotheriids have yet to be reported from Cerdas, Bolivia or Río Frias, Chile (Bondesio et al., 1980; Croft et al.,

2016). Marshall et al. (1983) listed *Diadiaphorus* as present during the Friasian SALMA, but the source of this statement is unclear. Carrillo et al. (2018) referred a specimen to *Lambdaconus* (=*Neodolodus*) cf. *L. colombianus* from the Castilletes Formation in northern Colombia dated to 15.1 Ma, coeval with Colloncuran SALMA faunas in Argentina and Chile. We agree with this identification (though we recognize it as *Neodolodus* cf. *N. colombianus*). No proterotheriids have yet been reported from El Petiso (Chubut Province, Argentina), a site that may pertain to the Laventan SALMA or postdate the Colloncuran and precede the Laventan (Villafañe et al., 2008; Pérez, 2010; Brandoni, 2014a).

Thoatheriopsis mendocensis may be middle Miocene in age. Villafañe et al. (2012) concluded that the type and only specimen originated from the Mariño Formation (Mendoza Province, Argentina), but they could not determine whether it came from the early Miocene Areniscas Entrecruzadas Member or the middle Miocene Estratos de Mariño Member.

With the discovery of *O. riorosarioensis* and *O. akilachuta* from Quebrada Honda, six proterotheriid species are now known from the Laventan SALMA (Fig. 11.1; Table 4). The other four taxa all occur at La Venta, Colombia (Cifelli and Guerrero, 1997), and two of these, *Mesolicaphrium sanalfonensis* and *Neodolodus colombianus*, were discussed previously. *Villarroelia totoyoi* is known from several localities at La Venta (Cifelli and Guerrero, 1997) and, in our analysis, is positioned as the sister taxon to a clade that includes many Santacrucian and later Neogene proterotheriids (Fig. 10). *Megadolodus molariformis* was originally described as a “condylarth,” but a reevaluation of its remains and the discovery of new material

revealed it to be a proterotheriid, though in its own subgroup, Megadolodine (McKenna, 1956; Cifelli and Villarroel, 1997). McGrath et al. (2020) recovered it as the earliest-diverging proterotheriid. A second megadolodine, *Bounodus enigmaticus*, was later described from the late Miocene Urumaco Formation, Venezuela (Carlini et al., 2006). Cifelli and Guerrero (1997) also reported an M2 from La Venta that resembles the Eocene proterotheriid *Anisolambda* that they believed represented a new taxon, but they chose not to name a new species based on a single tooth.

Tejada-Lara et al. (2015) reported multiple proterotheriid fossils from the Fitzcarrald local fauna, Peru but did not definitively identify any of them to genus. A distal tibia was referred to cf. *Tetramerorhinus* sp. based on its size and triangular astragalar facet. They also described a p1 of appropriate size for *M. sanalfonensis*, though this taxon's p1 is unknown, and a femur resembling that of *Tetramerorhinus* and *Villarroelia totoyoi*.

Paleoecological Implications of Olisanophus spp. at Quebrada Honda

Olisanophus riorosarioensis and *O. akilachuta* are similar in size (Table 5), degree of hypsodonty, and overall morphology (Figs. 8–9, S7–S12), and these similarities are reflected by their close phylogenetic relationship (Fig. 10). Although the coexistence of two such similar proterotheriids at Quebrada Honda may seem unusual, multiple species of closely related proterotheriids have also been recorded in the Santa Cruz Formation (Soria, 2001; McGrath et al., 2020). In contrast to Quebrada Honda, the four proterotheriids of the contemporaneous La Venta Fauna of Colombia (MacFadden et al., 1990; Flynn et al., 1997) display a variety of

morphologies. *Neodolodus colombianus* was small and had teeth with poorly developed lophs (Hoffstetter and Soria, 1986). *Megadolodus molariformis* was a large proterotheriid with thick-enameled, bunodont teeth (McKenna, 1956; Cifelli and Villarroel, 1997). *Villarroelia totoyoi* and *Mesolicaphrium sanalfonensis* were mid-sized proterotheriids whose teeth resembled those of other Miocene proterotheriids, including the *Olisanophus* spp. (Cifelli and Guerrero, 1997). This variation suggests that proterotheriids occupied a broader range of ecological niches at La Venta than at Quebrada Honda. *Neodolodus colombianus* and *Megadolodus molariformis* are very different from the Quebrada Honda proterotheriids in both size — *N. colombianus* being smaller and *Meg. molariformis* being larger (Table 4) — and in retaining many plesiomorphic features (Hoffstetter and Soria, 1986; Cifelli and Villarroel, 1997). They likely occupied ecological niches not present at Quebrada Honda given the absence of other mammals there with similar ecological adaptations.

Paleoenvironmental differences may be responsible for the lack of morphological and taxonomic diversity of Quebrada Honda proterotheriids compared to La Venta. La Venta corresponds to a tropical rainforest paleoenvironment (Guerrero, 1997; Kay and Madden, 1997a, b), whereas Quebrada Honda represents a less humid, wooded savannah ecosystem (Catena et al., 2017). Proterotheriids have been reconstructed as closed-habitat browsers (Ubilla et al., 2011; Cassini and Vizcaíno, 2012; Cassini, 2013; Corona et al., 2019b), so higher diversity in a tropical forest would be unsurprising. *Neodolodus colombianus* and *Meg. molariformis* are more brachydont than *Olisanophus* spp., perhaps restricting these taxa and their

close relatives to humid environments (Cifelli and Guerrero, 1997). Some authors have speculated that *Meg. molariformis* was a frugivore and perhaps a tropical forest endemic based on its brachydont molars with thick enamel (Cifelli and Villarroel, 1997; Kay and Madden, 1997b).

Evolutionary Trends

Proterotheriid Diversity—The most recent comprehensive review of proterotheriid diversity is that of Villafañe et al. (2006), though certain aspects of proterotheriid taxonomy and the temporal ranges of some taxa have changed since the publication of this work. Additionally, three new proterotheriid species have been named: *Olisanophus riorosarioensis* and *Olisanophus akilachuta* (both this work), and *Uruguayodon alius* Corona et al., 2019a. *Brachytherium cuspidatum* was recently re-validated, and *Lophogonodon gradatum* Ameghino, 1891, and *Lophogonodon paranensis* Ameghino, 1904, were considered to represent junior synonyms of *B. cuspidatum* by Schmidt (2015). *Neobrachytherium intermedium* and *Neobrachytherium morenoi* Rovereto, 1914, are now considered Montehermosan rather than Huayquerian in age based on stratigraphic reassessments of the Corral Quemado and Andalhualá formations (Reguero and Candela, 2011; Bonini et al., 2017). *Paramacrauchenia scamnata* was reported from Sierra Baguales, extending its temporal range to the Santacrucian (Bostelmann et al., 2013). *Thoatheriopsis mendocensis* is no longer considered Huayquerian in age and is treated as Laventan in age in this study (see Villafañe et al., 2012). Villafañe et al. (2006) also analyzed several taxa that we did not including several anisolambdine proterotheriids (=“anisolambdids”), (*Eolicaphrium primarium* Ameghino, 1902,

Guilielmofloweria plicata Ameghino, 1901, *Heteroglyphis dewoletzky* Roth, 1899, *Wainka tshotshe*, *Xesmodon langi* Roth, 1899, and *Xesmodon prolixus* Roth, 1899) that were not included here for reasons discussed in the methods section. Previous authors have disagreed on the position of *Diadiaphorus eversus* (Ameghino, 1898; Schmidt, 2015), placed in *Epitherium* by Soria (2001). In our opinion, the material assigned to this taxon is insufficient to confidently place it in any genus or include it in a phylogenetic analysis, so we omitted it from our diversity and body size analyses. *Epecuenia thoatherioides* is not sufficiently well-known to be included in the phylogenetic analysis (Soria, 2001), and since it is the only species referred to the genus, it cannot be easily allied with another taxon.

The minimum required diversity curve is consistently about five taxa higher than the known diversity curve from the Itaboraian through Huayquerian SALMAs, highlighting many gaps in the group's fossil record (Fig. 11.1). Three Eocene SALMAs, the Riochican, Mustersan, and Tinguiririan, include no named proterotheriid taxa, though undescribed or indeterminate proterotheriid remains from the Tinguiririca River Valley ([identified as an indaleciid which is a subgroup of Proterotheriidae per the definition of McGrath et al., 2020]; Tinguiririan SALMA; Wyss et al., 1994; Flynn et al., 2003; Croft et al., 2008), Barrancas Blancas (Tinguiririan SALMA; Dozo et al., 2014) and the La Barda locality ("Sapoan", pre-Vacan subage; Lorente, 2016; Krause et al., 2017) indicate that proterotheriids were present in southern South America at this time. The five Paleogene ghost lineages implied by the analysis are primarily due to *Paranisolambda prodromus*, which is the oldest proterotheriid (Itaboraian SALMA) but not one of the earliest-diverging ones

(Fig. 10; Cifelli, 1983). Several lineages (*e.g.*, *Paramacrauchenia* spp., *Lambdaconus* spp.) that diverged earlier than *P. prodromus* do not appear until the late Oligocene or early Miocene (Soria, 2001; Schmidt et al., 2019). These ghost lineages may be partially represented by some of the excluded “anisolambdids” (Villafañe et al., 2006). Discoveries of previously undocumented taxa and additional remains of “anisolambdids” are needed to fill this Paleogene gap.

Both the known diversity and minimum required diversity curves peak in the Santacrucian (Fig. 11.1), as in the study of Villafañe et al. (2006: fig. 1), but the minimum diversity curve indicates that there were many more than the 14 proterotheriids currently known from this interval. This fact is not surprising because all named Santacrucian proterotheriids come from southernmost South America (Santa Cruz province, Argentina, and Aysén and Magallanes regions, Chile; Soria, 2001; Bostelmann et al., 2013; McGrath et al. 2019). More northerly Santacrucian localities have yielded only indeterminate proterotheriid remains (*e.g.*, the Manantiales Basin in Argentina at ~33° S; López *et al.*, 2011) or none at all, as is the case at the Chilean localities of Chucal (~19° S; Croft et al., 2004), Laguna del Laja (~38°S; Flynn et al., 2008), and Lonquimay (~38°S; Solórzano et al., 2019). With the majority of South America unsampled, it is not hard to believe that at least five additional proterotheriid taxa should have existed at this time, perhaps many more considering the density of proterotheriid taxa in Patagonia.

Traditionally, two peaks in proterotheriid diversity were seen in the early and late Miocene (Soria, 2001; Villafañe et al., 2006; Ubilla et al., 2011; Schmidt, 2015; McGrath et al., 2020), but our analysis suggests that proterotheriids gradually

declined throughout the Miocene (Fig. 11.1). Villafañe et al. (2006) reported ten proterotheriids from the Huayquerian, nearly as many as in the Santacrucian (13 in their analysis), and these SALMAs represent two pronounced peaks in their analysis. Only six proterotheriids are now recognized from the Huayquerian SALMA, the same number as from the Laventan SALMA. Additionally, the minimum required diversity curve shows a more or less steady decline through the Miocene, save for two minor drops in the Colloncuran and Mayoan SALMAs. However, low sampling of these intervals likely drives this pattern (see Croft et al. (2018) and Prevosti and Forasiepi (2018) for a similar drop in Mayoan sparassodont diversity). Rather than a diversity 'trough,' the middle Miocene represents the beginning of the proterotheriids' steady decline, which continued through the Pleistocene.

Olisanophus riorosarioensis and *O. akilachuta* increase the number of known Laventan proterotheriids to six, equal to the Huayquerian (Fig. 11.1; Table 4). These species do not imply any additional ghost lineages given their close relationship with contemporaneous *Mesolicaphrium sanalfonensis.* This discovery shows that proterotheriids were thriving and speciating in low-latitude South America, further suggesting that many proterotheriid lineages remain undiscovered in the tropics.

Macraucheniid diversity—The macraucheniid minimum required diversity and known diversity curves show trends similar to the corresponding curves for proterotheriids except during the early Miocene (Fig. 11.2). According to the minimum diversity curve, macraucheniids were most diverse in the early Miocene, just prior to the Colhuehuapian. This early Miocene peak in the minimum required diversity curve is mainly caused by the five Santacrucian *Theosodon* species

included in this analysis, which may be an overestimate of true species diversity. Potential future synonymies among these *Theosodon* species could decrease this early Miocene peak and reveal the late Miocene (discussed below) to be the true pinnacle of macraucheniid diversity, in agreement with the group's known diversity.

Macraucheniids experienced a second diversity peak in the late Miocene (Fig. 11.2). Six macraucheniid species are known from the Huayquerian, the most of any SALMA (Table 4). Most of these come from the 'Conglomerado osífero' in the lower Ituzaingó Formation in northeast Argentina (Cione et al., 2000; Schmidt and Cerdeño, 2013; Brandoni, 2014b). However, the minimum required diversity curve indicates the true peak occurred slightly earlier, in the Chasicoan, because many Huayquerian taxa diverged prior to Chasicoan *Cullinia levis* Cabrera and Kraglievich, 1931 and *Paranauchenia hystata* Cabrera and Kraglievich, 1931 (Schmidt and Ferrero, 2014; McGrath et al., 2018).

Proterotheriid and macraucheniid diversity compared—Proterotheriids were consistently more diverse than macraucheniids until the Pliocene, but otherwise, these groups experienced largely similar trends in diversity (Fig. 11). After displaying relatively low diversity through most of the Paleogene, both clades diversified in the Deseadan. Both groups peaked in the early Miocene, though macraucheniids did so slightly earlier based on the minimum required diversity curves.

Although proterotheriid and macraucheniid diversity curves are broadly similar (Fig. 11), their evolutionary histories differ in several notable ways. Proterotheriids appear much earlier in the fossil record (Itaboraian) than macraucheniids (Mustersan), but the earliest proterotheriid, *Paranisolambda prodromus*, is not the

earliest-diverging proterotheriid; this implies that multiple proterotheriid lineages existed for much of the Paleogene, widening the difference between the early evolutionary histories of these groups. Proterotheriids and macraucheniids are grouped together within Lopholipterna (‘dentally advanced’ litopterns), though they are not sister taxa; rather, proterotheriids are sister to Macrauchenioidea, which includes both Macraucheniidae and Adianthidae (Cifelli, 1983). Since the oldest adianthids are Deseadan in age (Cifelli and Soria, 1983), either pre-Mustersan macrauchenioids remain undiscovered or the systematics of some early–middle Eocene litopterns requires reexamination.

Proterotheriids and macraucheniids declined noticeably after the Huayquerian (Fig. 11; Table 4). It is tempting to attribute this decline to competition from taxa dispersing from North American as part of the Great American Biotic Interchange (GABI), but most of these potential competitors first appear in South America after this decline began (camelids and equids in the late Pliocene, cervids and tapirids in the Pleistocene; Woodburne, 2010; Cione et al., 2015; Gasparini et al., 2017). Early late Miocene (Chasicoan SALMA?) peccaries and a gomphothere have been reported from western Amazonia (Campbell et al., 2000; Frailey and Campbell, 2012; Prothero et al., 2014) and could potentially have competed with proterotheriids and macraucheniids, but the ages of these remains are disputed (Alberdi et al., 2004; Dutra et al., 2017). Even if such ages are eventually substantiated, these groups are not recorded until the Pliocene and Pleistocene in more southern regions of South America, where the macraucheniid and proterotheriid decline is recorded (Reguero and Candela, 2011; Carrillo et al., 2015; Cione et al., 2015).

Although both groups declined after the Huayquerian, macraucheniids were more successful in the Pleistocene than proterotheriids (Fig. 11; Table 4); they were twice as diverse (four spp. vs. two spp.) and inhabited a much wider geographic range. Pleistocene macraucheniids are found throughout South America (Owen, 1838; Cartelle and Lessa, 1988; Tonni et al., 2009; Chávez Aponte et al., 2010), whereas contemporary proterotheriids are known exclusively from northern Argentina, Uruguay, and southeastern Brazil (Bond et al., 2001; Soria, 2001; Scherer et al., 2009; Ubilla et al., 2011; Corona et al., 2019a). This pattern suggests that macraucheniids were less affected than proterotheriids by competition with northern immigrants during the 'Interamerican Phase' of Cenozoic South America (*sensu* Goin et al., 2012) or that they had broader habitat tolerances.

Proterotheriid size—The smallest proterotheriids were the stratigraphically oldest taxa but not necessarily the earliest-diverging (Figs. 10, 12; Table 4). The earliest-diverging proterotheriids, the megadolodines (*i.e.*, *Megadolodus molariformis* + *Bounodus enigmaticus*) were as large or larger than their mid to late Miocene contemporaries, much larger than the stratigraphically oldest proterotheriids. With the caveat that the megadolodine m1 length-body mass relationship may differ from other proterotheriids because of their proportionately large molars (McKenna, 1956; Cifelli and Villarroel, 1997), they were undoubtedly larger than early Eocene proterotheriids based on postcranial remains that have been described for *Megadolodus*. These stratigraphically older taxa have traditionally been considered to be indaleciids or "anisolambdids" but are now considered to be proterotheriids based on the stem-based definition of the clade proposed by McGrath et al. (2020).

Of the five proterotheriid ghost lineages that span the late Eocene to late Oligocene, four show an increase in size. “Anisolambdids” that could not be placed in the phylogeny, such as *Wainka tshotshe* (*Carodnia* Zone) and *Lambdaconops porcus* (Vacan or Barrancan subage of Casamayoran SALMA), also roughly follow this pattern, though *Guilielmofloweria plicata* (Vacan or Barrancan subage of Casamayoran SALMA) is similar in size to the Deseadan *Protheosodon coniferus* (Soria, 2001). The fact that this increase in size follows a temporal rather than phylogenetic pattern strongly hints at a selective pressure for increased size over this interval. Among other South American groups, typotherian notoungulates, another group of small-bodied ungulates, did not significantly increase in body size during this interval (Reguero et al., 2010), whereas sparassodonts, sloths, and glyptodonts apparently increased in size during the Oligocene (Scillato-Yané, 1977).

After this Paleogene increase, proterotheriids generally maintained a constant body size from the Deseadan to the Pleistocene with little to no phylogenetic pattern (Fig. 12.1). *Diplasiotherium robustum*, *Diadiaphorus majusculus*, and *Meg. molariformis*, the largest proterotheriids, were not close relatives. The same is true for the smallest Neogene proterotheriids, *Neodolodus colombianus*, *Lambdaconus lacerum*, *Picturotherium migueli*, and *Paramacrauchenia scamnata*. The apparently random branching sequences shown in Figure 12.1 further attest that, relative to the variation seen within the group, size was not phylogenetically conserved in Neogene proterotheriids. Most Pliocene and Pleistocene proterotheriids were similar in size to their early Miocene relatives, suggesting that there was no selection for increased body size in Neogene proterotheriids.

Macraucheniid size—Macraucheniids continued to increase in size throughout their evolutionary history, and this size seems rather phylogenetically conserved, in contrast to proterotheriids (Fig. 12.2; Table 4). Starting with *Polymorphis* spp. Roth, 1899, which are the oldest and smallest macraucheniids, there is a shift to larger body size in Deseadan to Colhuehuapian species plus Laventan *Llullataruca shockeyi*. Along with *Theosodon*, these species traditionally comprised the 'Cramaucheniinae,' which is now considered paraphyletic (Schmidt and Ferrero, 2014; Forasiepi et al., 2016; McGrath et al., 2018). This 'grade' of macraucheniid evolution generally remained smaller than later-diverging macraucheniids, even in the geologically younger *L. shockeyi* (Fig. S6).

The next marked increase in macraucheniid body size occurred in *Theosodon*, and this size was generally maintained throughout the rest of the Miocene and Pliocene (Fig. 12.2). As a caveat, macraucheniid body mass may have increased over this interval even though it is not captured by m1 length. Using linear regression equations based on cranial and mandibular centroid size, the body mass of the late Miocene *Huayqueriana* Kraglievich, 1934 (~250 kg; Forasiepi et al., 2016) has been estimated to be roughly twice that of early Miocene *Theosodon garretorum* Scott, 1910, (~113 kg; Cassini et al., 2012), even though their m1 lengths are similar.

Late Pliocene and Pleistocene macraucheniids other than *Promacrauchenia yepesi* show another major size increase (Fig. 12.2; Table 4). This lineage of giant macraucheniids appears to have diverged from *Promacrauchenia* in the late middle Miocene, though this divergence date should be viewed cautiously due to the

uncertain taxonomy of *Promacrauchenia*. Macraucheniids were not the only giant mammals in Pleistocene South America; toxodonts, gomphotheres, sloths, and glyptodonts also attained masses > 1000 kg (Fariña et al., 1998; Croft, 2016). Pleistocene macraucheniids are hypothesized to have been mixed-feeders or browsers (Domingo et al., 2012; Varela and Fariña, 2015; Lobo et al., 2017), and their large size – coupled with their proportionately long neck – may have allowed them to feed on resources beyond the reach of many of their competitors such as hippidiform horses, camelids, and ground sloths (Melo França et al., 2015). Large size may have been a key factor that allowed macraucheniids to remain diverse and widespread after the GABI while proterotheriids became geographically restricted and decreased in diversity.

CONCLUSIONS

In this study, we describe two new species of proterotheriid, *Olisanophus riorosarioensis* (Figs. 8, S7) and *Olisanophus akilachuta* (Figs. 9, S8–S11), from the middle Miocene (Laventan SALMA) of Quebrada Honda, Bolivia. We also erect a new genus, *Mesolicaphrium*, to accommodate the roughly contemporaneous '*Prolicaphrium*' *sanalfonensis* from La Venta, Colombia. The two Quebrada Honda species are recovered as sister taxa within a larger clade that includes *Mesolicaphrium sanalfonensis* and *Diplasiotherium* spp. (Fig. 10). We also revalidate the monotypic genus *Neodolodus* for *Neodolodus colombianus* from La Venta.

Our analysis of proterotheriid and macraucheniid diversity and body size evolution in a phylogenetic context sheds new light on the paleobiology of these groups. Very few Paleogene proterotheriids are known (Table 4), but their phylogeny implies the existence of at least five lineages throughout this time (Fig. 11.1). Most of these ghost lineages appear to have increased in size over this time (Fig. 12.1) After a peak in the early Miocene (Santacrucian SALMA), proterotheriids steadily declined in diversity until the late Pleistocene. During this interval, proterotheriids remained within a certain size range and exhibited no discernable phylogenetic trends in body size.

Macraucheniids appear later in the fossil record than proterotheriids (Fig. 11.2; Table 4) and remained less diverse for much of their history. Similar to proterotheriids, macraucheniids peaked in diversity in the early Miocene (Colhuehuapian–Santacrucian SALMAs), but unlike proterotheriids, they experienced a second peak in the late Miocene (Chasicoan–Huayquerian SALMAs). In the Pleistocene, macraucheniids were rather diverse and widespread, in contrast to proterotheriids, suggesting that they were better able to adapt to climatic and/or biotic changes during that interval.

Acknowledgements

This manuscript was previously published in the journal *Ameghiniana* in 2020 with Federico Anaya and Darin Croft as co-authors.

We thank A. Carlini, P. Carlini, A. Catena, M. Ciancio, N. Drew. F. Mamani, O. Moeira, B. Saylor, B. Shockey, and E. Vilca for assistance in the field; A. Wyss,

C. Everett, B. Tiffney, and S. Porter for helpful discussions that improved the manuscript; the Universidad Autónoma Tomás Frías (Potosí, Bolivia) for support of field logistics; B. Barbieri for his initial prep work on the specimens; the American Museum of Natural History, Field Museum of Natural History, Museo Argentino de Ciencias Naturales “Bernardino Rivadavia”, Museo de La Plata, University of California Museum of Paleontology, and Yale Peabody Museum for access to their collections; R. Cifelli and the Oklahoma Museum of Natural History for providing study casts of specimens from La Venta; M. Crow for her initial descriptions and photographs of the specimens;A. Forasiepi, J. Gelfo, and one anonymous reviewer for constructive comments that improved the manuscript; D. Pol for editing the manuscript; and our home institutions for support of this research. Funding for this research was provided by the Tanya Atwater Global Field Travel Fund (to A. McGrath), the Lloyd and Mary Edwards Field Studies Fellowship (to A. McGrath), the American Museum of Natural History Richard Gilder Graduate School Collections Study Grant (to A. McGrath), the National Geographic Society Committee for Research and Exploration (NGS 8115-06 to D. Croft), and the National Science Foundation (EAR 0958733 and EAR 1423058 to D. Croft).

REFERENCES

Alberdi, M.T., J.L. Prado, and R. Salas. 2004. The Pleistocene Gomphotheriidae (Proboscidea) from Peru. Neues Jahrbuch Fur Geologie Und Palaontologie - Abhandlungen 231:423–452.

Ameghino, F. 1887. Enumeración sistemática de las especies de mamíferos fósiles

coleccionados por Carlos Ameghino en los terrenos eocenos de la Patagonia austral y depositados en el Museo de La Plata. Boletín Museo de La Pla. Boletín Museo de La Plata 5:445–469.

Ameghino, F. 1888. Lista de Las Especies de Mamíferos Fósiles Del Mioceno Superior de Monte-Hermoso, Hasta Ahora Conocidas. Buenos Aires, Argentina:, P. E. Coni.

Ameghino, F. 1889. Contribución al conocimiento de los mamíferos fósiles de la República Argentina. Actas de La Academia Nacional de Ciencias de Córdoba 6:1–1027.

Ameghino, F. 1891. Nuevos restos de mamíferos fósiles recogidos por Carlos Ameghino en el Eoceno inferior de la Patagonia austral. Especies nuevas: adiciones y corecciones. Revista Argentina de Historia Natural 1:289–328.

Ameghino, F. 1894. Ennumération synoptique des espéces de mammiféres fossilies des formations éocénes de Patagonie. Boletín de La Academia Nacional de Ciencias de Córdoba 13:259–445.

Ameghino, F. 1897. Mammiféres crétacés de l'Argentine (Deuxiéme contribution á la connaissance de la faune mammologique des couces á Pyrotherium). Boletín Del Instituto Geográfico Argentino 18:405–521.

Ameghino, F. 1899. Sinópsis Geológico-Paleontológica. Suplemento (Adiciones y Corecciones) 1. La Plata, Argentina:, .

Ameghino, F. 1901. Notices préliminaires sur des ongulés nouveaux des terrains crétacés de Patagonie. Boletín de La Academia Nacional de Ciencias de Córdoba 16:349–426.

Ameghino, F. 1902. Premiére contribution a la connaisance de la faune mammalogique des couches a Colpodon. Boletín de La Academia Nacional de Ciencias de Córdoba 17:71–138.

Ameghino, F. 1904. Nuevas especies de mamíferos Cretáceos y Terciarios de la República Argentina. Anales de La Sociedad Cientifica Argentina 57:327.

Bapst, D.W. 2012. paleotree: An R package for paleontological and phylogenetic analyses of evolution. Methods in Ecology and Evolution 3:803–807.

Bonaparte, J.F., and J. Morales. 1997. Un primitivo Notonychopidae (Litopterna) del Paleoceno inferior de Punta Peligro, Chubut, Argentina. Estudios Geológicos 274:263–274.

Bond, M., and M.G. Vucetich. 1983. *Indalecia grandensis* gen. et sp. nov. del Eoceno temprano del noroeste Argentino, tipo de una nueva subfamilia de los Adianthidae (Mammalia, Litopterna). Revista de La Asociación Geológica de Argentina 38:107–117.

Bond, M., D. Perea, M. Ubilla, and A.A. Tauber. 2001. *Neolicaphrium recens* Frenguelli, 1921, the only surviving Proterotheriidae (Litopterna, Mammalia) into

the South American Pleistocene. Palaeovertebrata 30:37–50.

Bondesio, P., J. Rabassa, R. Pascual, M.G. Vucetich, and G.J. Scillato-Yané. 1980. La Formación Collón-Curá de Pilcaniyeu Viejo y sus alrededores (Río Negro, República Argentino) su antigüedad y las condiciones ambientales segun su distribución, su litogenesis y sus vertebrados. Actas II Congreso Argentino de Paleontología y Bioestratigrafía y I Congreso Latinoamericano de Paleontología 85–99.

Bonini, R.A., S.M. Georgieff, and A.M. Candela. 2017. Stratigraphy, geochronology, and paleoenvironments of Miocene-Pliocene boundary of San Fernando, Belén (Catamarca, northwest of Argentina). Journal of South American Earth Sciences.

Bordas, A.F. 1936. Un nuevo mamífero del Colpodon de Gaiman (*Proheptaconus trelewense* gen et. sp. nov.). Physis 12:110–112.

Bostelmann, E. et al. 2013. Burdigalian deposits of the Santa Cruz Formation in the Sierra Baguales, Austral (Magallanes) Basin: age, depositional environment and vertebrate fossils. Andean Geology 40:458–489.

Brandoni, D. 2014a. "*Xyophorus*" sp. en el mioceno medio de Chubut: implicancias sistemáticas, biogeográficas ybiocronológicas del registro de un Nothrotheriinae en el neógeno de la Argentina. Ameghiniana 51:94–105.

Brandoni, D. 2014b. Los mamíferos continentales del 'Mesopotamiense' (Mioceno tardío) de Entre Ríos, Argentina. Asociación Paleontológica Argentina. Publicación Especial 14:179–191.

Burmeister, H. 1879. Description Physique de La République Argentine d'aprés Des Observations Porsonnelles et Étrangéres 3 (Animaux Vertébrés 1: Mammiféeres Vivants e Éteintes). Buenos Aires, Argentina:, P. E. Coni, .

Burmeister, H. 1885. Examen crítico de los mamíferos y reptiles fósiles denominados por D. Augusto Bravard y mencionados en su obra pecedente. Anales Del Museo Nacional de Buenos Aires 3:95–174.

Cabrera, A. 1939. Los géneros de la familia Typotheriidae. Physis 14:359–372.

Cabrera, A., and L. Kraglievich. 1931. Diagnosis previas de los ungulados fósiles de la Formación Arroyo Chasicó. Notas Del Museo de La Plata 1:107–113.

Campbell Jr., K.E., C.D. Frailey, and L.R. Pittman. 2000. The late Miocene gomphothere *Amahuacatherium peruvium* (Proboscidea: Gomphotheriidae) from Amazonian Peru: implications for the Great American Faunal Interchange. Boletín Del Instituto Geológico Minero y Metalúrgico. Serie D: Estudios Regionales 23:1–152.

Carlini, A.A., J.N. Gelfo, and R. Sánchez. 2006. A new Megadolodinae (Mammalia, Litopterna, Protherotheriidae) from the Urumaco Formation (late Miocene) of Venezuela. Journal of Systematic Palaeontology 4:279–284.

Carlini, A.A., D. Brandoni, R. Sánchez, and M.R. Sánchez-Villagra. 2018. A new Megatheriinae skull (Xenarthra, Tardigrada) from the Pliocene of northern Venezuela–implications for a giant sloth dispersal to Central and North America. Palaeontologia Electronica 21.2.16A:1–12.

Carrillo, J.D., A.M. Forasiepi, C. Jaramillo, and M.R. Sánchez-Villagra. 2015. Neotropical mammal diversity and the Great American Biotic Interchange: spatial and temporal variation in South America's fossil record. Frontiers in Genetics 5:1–11.

Carrillo, J.D. et al. 2018. The Neogene record of northern South American native ungulates. Smithsonian Contributions to Paleobiology 1–80.

Cartelle, C., and G. Lessa. 1988. Descriacao de um novo genero e especie de Macraucheniidae (Mammalia, Litopterna) do Pleistoceno do Brasil. Paula-Coutiana 3:3–26.

Cassini, G.H. 2013. Skull geometric morphometrics and paleoecology of Santacrucian (late early Miocene; Patagonia) native ungulates (Astrapotheria, Litopterna, and Notoungulata). Ameghiniana 50:193–216.

Catena, A.M., D.I. Hembree, B.Z. Saylor, F. Anaya, and D.A. Croft. 2017. Paleosol and ichnofossil evidence for significant Neotropical habitat variation during the late middle Miocene (Serravallian). Palaeogeography, Palaeoclimatology, Palaeoecology 487:381–398.

Chávez Aponte, E.O., I. Alfonzo-Hernández, and A. Agüero. 2010. Contribución preliminar a la caracterización paleoecológica de megamamíferos del Pleistoceno tardío de Venezuela. Resúmenes X Congreso Argentino de Paleontología y Bioestratigrafía y XII Congreso Latinoamericano de Paleontología 90–91.

Cifelli, R.L. 1983. The origin and affinities of the South American Condylarthra and early Tertiary Litopterna (Mammalia). American Museum Novitates 1–49.

Cifelli, R.L., and M.F. Soria. 1983. Systematics of the Adianthidae (Litopterna, Mammalia). American Museum Novitates 1–25.

Cifelli, R.L., and J. Guerrero Diaz. 1989. New remains of *Prothoatherium columbianus* (Litopterna, Mammalia) from the Miocene of Colombia. Journal of Vertebrate Paleontology 9:222–231.

Cifelli, R.L., and J. Guerrero. 1997. Litopterns; pp. 289–302 in R. F. Kay, R. H. Madden, R. L. Cifellii, and J. J. Flynn (eds.), Vertebrate Paleontology in the Neotropics: The Miocene Fauna of La Venta, Colombia. Smithsonian Institution Press, Washington, D.C., USA.

Cifelli, R.L., and C. Villarroel. 1997. Paleobiology and affinities of *Megadolodus*; pp. 265–288 in R. F. Kay, R. H. Madden, R. L. Cifellii, and J. J. Flynn (eds.), Vertebrate Paleontology in the Neotropics: The Miocene Fauna of La Venta, Colombia. Smithsonian Institution Press, Washington, D.C., USA.

Cione, A.L. et al. 2000. Miocene vertebrates from Entre Ríos province, eastern Argentina. El Neogeno de Argentina 14:191–237.

Cione, A.L., G.M. Gasparini, E. Soibelzon, L.H. Soibelzon, and E.P. Tonni. 2015. The Great American Biotic Interchange: A South American Perspective (J. Rabassa, G. Lohmann, J. Notholt, L.A. Mysak, and V. Unnithan (eds.). Dordrecht:, Springer Earth Systems Sciences, .

Corona, A., M. Ubilla, and D. Perea. 2019a. New records and diet reconstruction using dental microwear analysis for *Neolicaphrium recens* Frenguelli, 1921 (Litopterna, Proterotheriidae). Andean Geology 46:153–167.

Corona, A., D. Perea, and M. Ubilla. 2019b. A new genus of Proterotheriinae (Mammalia, Litopterna) from the Pleistocene of Uruguay. Journal of Vertebrate Paleontology 39:e1567523.

Croft, D.A. 2007. The middle Miocene (Laventan) Quebrada Honda fauna, southern Bolivia and a description of its notoungulates. Palaeontology 50:277–303.

Croft, D.A. 2016. Horned Armadillos and Rafting Monkeys: The Fascinating Fossil Mammals of South America. Bloomington, Indiana, USA:, Indiana University Press, 366 pp.

Croft, D.A., J.J. Flynn, and A.R. Wyss. 2004. Notoungulata and Litopterna of the early Miocene Chucal Fauna, northern Chile. Fieldiana Geology 1–52.

Croft, D.A., J.J. Flynn, and A.R. Wyss. 2008. The Tinguiririca fauna of Chile and the early stages of “modernization” of South American mammal faunas. Arquivos Do Museu Nacional, Rio de Janeiro 66:191–211.

Croft, D.A., J.M.H. Chick, and F. Anaya. 2011. New middle Miocene caviomorph rodents from Quebrada Honda, Bolivia. Journal of Mammalian Evolution 18:245–268.

Croft, D.A., J.N. Gelfo, and G.M. López. 2020. Splendid innovation: the extinct South American native ungulates. Annual Review of Earth and Planetary Sciences 48:259–290.

Croft, D.A., R.K. Engelman, T. Dolgushina, and G. Wesley. 2018. Diversity and disparity of sparassodonts (Metatheria) reveal non-analogue nature of ancient South American mammalian carnivore guilds. Proc. R. Soc. B 285.

Croft, D.A. et al. 2016. New mammal faunal data from Cerdas, Bolivia, a middle-latitude Neotropical site that chronicles the end of the Middle Miocene Climatic Optimum in South America. Journal of Vertebrate Paleontology 36.

Domingo, L., J.L. Prado, and M.T. Alberdi. 2012. The effect of paleoecology and paleobiogeography on stable isotopes of Quaternary mammals from South America. Quaternary Science Reviews 55:103–113.

Dozo, M.T., M.R. Ciancio, P. Bouza, and G. Martínez. 2014. Nueva asociación de mamíferos del Paleógeno en el este de la Patagonia (provincia de Chubut,

Argentina): Implicancias biocronológicas y paleobiogeográficas. Andean Geology 41:224–247.

Dunn, R.E. et al. 2013. A new chronology for middle Eocene-early Miocene South American Land Mammal Ages. Bulletin of the Geological Society of America 125:539–555.

Dutra, R.P. et al. 2017. Phylogenetic systematics of peccaries (Tayassuidae: Artiodactyla) and a classification of South American tayassuids. Journal of Mammalian Evolution 24: 345–358.

Engelman, R.K., and D.A. Croft. 2014. A new species of small-bodied sparassodont (Mammalia, Metatheria) from the middle Miocene locality of Quebrada Honda, Bolivia. Journal of Vertebrate Paleontology 34:672–688.

Engelman, R.K., F. Anaya, and D.A. Croft. 2017. New palaeothentid marsupials (Paucituberculata) from the middle Miocene of Quebrada Honda, Bolivia, and their implications for the palaeoecology, decline and extinction of the Palaeothentoidea. Journal of Systematic Palaeontology 15:787–820.

Fariña, R.A., S.F. Vizcaíno, and M.S. Bargo. 1998. Body mass estimations in Lujanian (late Pleistocene-early Holocene of South America) mammal megafauna. Mastozoologica Neotropical 5:87–108.

Flynn, J.J., and C.C. Swisher. 1995. Cenozoic South American Land Mammal Ages: correlation to global geochronologies. Geochronology Time Scales and Global Stratigraphic Correlation, SEPM Special Publication 54:317–333.

Flynn, J.J., J. Guerrero, and C.C. Swisher. 1997. Geochronology of the Honda Group; pp. 44–59 in R. F. Kay, R. H. Madden, R. L. Cifellii, and J. J. Flynn (eds.), Vertebrate Paleontology in the Neotropics: The Miocene Fauna of La Venta, Colombia. Smithsonian Institution Press, Washington, D.C., USA.

Flynn, J.J., A.R. Wyss, D.A. Croft, and R. Charrier. 2003. The Tinguiririca Fauna, Chile: biochronology, paleoecology, biogeography, and a new earliest Oligocene South American land mammal “age.” Palaeogeography, Palaeoclimatology, Palaeoecology 195:229–259.

Flynn, J.J. et al. 2008. Chronologic implications of new Miocene mammals from the Cura-Mallín and Trapa Trapa formations, Laguna del Laja area, south central Chile. Journal of South American Earth Sciences 26:412–423.

Forasiepi, A.M. et al. 2016. Exceptional skull of *Huayqueriana* (Mammalia, Litopterna, Macraucheniidae) from the late Miocene of Argentina: anatomy, systematics, and paleobiological implications. Bulletin of the American Museum of Natural History 1–76.

Frailey, C.D., and K.E. Campbell. 2012. Two new genera of peccaries (Mammalia, Artiodactyla, Tayassuidae) from upper Miocene deposits of the Amazon Basin. Journal of Paleontology 86:852–877.

Frenguelli, J. 1921. Sobre un proterotérido del Pampeano superior de Córdoba.

Actas de La Academia Nacional de Ciencias de Córdoba 7:7–23.

Gaudioso, P.J., G.M. Gasparini, R. Herbst, and R.M. Barquez. 2017. First record of the *Neolicaphrium recens* Frenguelli, 1921 (Mammalia, Litopterna) in the Pleistocene of Santiago del Estero province, Argentina. Papés Avulsos de Zoologia. Museu de Zología Da Universidade de Sao Paulo, Brasil 57:23–29.

Gelfo, J.N. 2006. Los Didolodontidae (Mammalia: Ungulatomorpha) del Terciario sudamericano. sistemática, origen y evolución. Universidad Nacional de La Plata, 464 pp.

Gelfo, J.N., G.M. López, and M. Lorente. 2016. Los ungulados arcaicos de América del Sur: “Condylarthra” y Litopterna. Contribuciones Científicas Del Museo Argentino de Ciencias Naturales “Bernardino Rivadavia” 6:285–291.

Goin, F.J. et al. 2012. Persistence of a Mesozoic, non-therian mammalian lineage (Gondwanatheria) in the mid-Paleogene of Patagonia. Naturwissenschaften 99:449–463.

Goloboff, P.A., and S.A. Catalano. 2016. TNT version 1.5, including a full implementation of phylogenetic morphometrics. Cladistics 32:221–238.

Goloboff, P.A., C.I. Mattoni, and A.S. Quinteros. 2006. Continuous characters analyzed as such. Cladistics 22:589–601.

Hoffstetter, R. 1976. Rongeurs caviomorphes de l’Oligocene de Bolivie. I. Introduction au Deseadien de Bolivie. Montpellier 7:1–14.

Hoffstetter, R. 1977. Un gisement de mammifères miocènes à Quebrada Honda (sud Bolivien). Comptes Rendus de l’Acadamie Des Sciences 284:127–129.

Hoffstetter, R., and M.F. Soria. 1986. *Neodolodus colombianus* gen. et sp. nov., un nouveau Condylarthre (Mammalia) dans le Miocene de Colombie. Comptes Rendus de l’Acadamie Des Sciences 303:1619–1622.

Hopkins, S.S.B. 2018. Estimation of body size in fossil mammals; pp. 7–22 in D.A. Croft, D.F. Su, and S.W. Simpson (eds.) Vertebrate Paleobiology and Paleoanthropology. Cham, Switzerland: Springer Geology.

Huxley, T. 1880. On the application of the laws of evolution to the arrangement of the Vertebrata, and more particularly of the Mammalia. Proceedings of the Zoological Society, London 43:649–662.

Kay, R.F., and R.H. Madden. 1997a. Mammals and rainfall: paleoecology of the middle Miocene at La Venta (Colombia, South America). Journal of Human Evolution 32:161–199.

Kay, R.F., and R.H. Madden. 1997b. Paleogeography and paleoecology; pp. 520–550 in R. F. Kay, R. H. Madden, R. L. Cifellii, and J. J. Flynn (eds.), Vertebrate Paleontology in the Neotropics: The Miocene Fauna of La Venta, Colombia. Smithsonian Institution Press, Washington, D.C., USA.

Kay, R.F., R.H. Madden, R.L. Cifelli, and J.J. Flynn. 1997. Vertebrate Paleontology in the Neotropics: The Miocene Fauna of La Venta, Colombia. Washington, D.C., USA:, Smithsonian Institution Press, .

Kraglievich, J.L. 1965. Speciation phyletique dans les rongeurs fossiles du genre *Eumysops* Ameghino (Echimyidae, Heteropsomyinae). Extrait de Mammalia 29:258–267.

Kraglievich, L. 1930. La Formacion Friaseana del Río Frias, Río Fénix, Laguna Blanca, etc., y su fauna de mamíferos. Physis 129–161.

Kraglievich, L. 1934. La antiguedad Pliocena de las faunas de Monte Hermoso y Chapadmalal, deducidas de su comparación con las que le precedieron y sucedieron. Montevideo, Uruguay, El Siglo Ilustrado, 136 pp.

Kramarz, A.G., and M. Bond. 2005. Los Litopterna (Mammalia) de la Formación Pinturas, Mioceno temprano-medio de Patagonia. Ameghiniana 42:611–625.

Krause, J.M. et al. 2017. New age constraints for early Paleogene strata of central Patagonia, Argentina: implications for the timing of South American Land Mammal Ages. Bulletin of the Geological Society of America 129:886–903.

Linnaeus, C. 1758. Systema Naturae per Regna Tri Naturae, 10th ed. Stockholm, Sweden, Laurentii Salvii.

Lobo, L.S., G. Lessa, C. Cartelle, and P.S.R. Romano. 2017. Dental eruption sequence and hypsodonty index of a Pleistocene macraucheniid from the Brazilian Intertropical Region. Journal of Paleontology 91:1083–1090.

López, G.M. et al. 2011. New Miocene mammal assemblages from Neogene Manantiales Basin, Cordillera Frontal, San Juan, Argentina pp. 211–226 in J.A. Salfity and R.A. Marquillas (eds.) Cenozoic Geology of the Central Andes of Argentina. Salta, Argentina, SCS Publisher.

Lorente, M. 2016. Isolated Litopterna postcranial remains from La Barda tuff (early Eocene), Paso del Sapo, Chubut, Argentina: proposed association with dental taxa and their implications. Ameghiniana 53:26–38.

MacFadden, B.J., and R.G. Wolff. 1981. Geological investigations of late Cenozoic vertebrate-bearing deposties in southern Bolivia. Anais, II Congreso Latino-Americano de Paleontología 765–778.

MacFadden, B.J. et al. 1990. Late Cenozoic paleomagnetism and chronology of Andean basins of Bolivia: evidence for possible oroclinal bending. Journal of Geology 98:541–555.

Marshall, L.G., R. Hoffstetter, and R. Pascual. 1983. Mammals and stratigraphy: geochronology of the continental mammal-bearing Tertiary of South America. Palaeovertebrata 13:1–93.

McGrath, A.J., F. Anaya, and D.A. Croft. 2018. Two new macraucheniids (Mammalia: Litopterna) from the late middle Miocene (Laventan South

American Land Mammal Age) of Quebrada Honda, Bolivia. Journal of Vertebrate Paleontology 38:e1461632.

McGrath, A.J., J.J. Flynn, and A.R. Wyss. 2020. Proterotheriids and macraucheniids (Litopterna: Mammalia) from the Pampa Castillo Fauna, Chile (early Miocene, Santacrucian SALMA) and a new phylogeny of Proterotheriidae. Journal of Systematic Palaeontology 18:717–738.

McKenna, M.C. 1956. Survival of primitive notoungulates and condylarths into the Miocene of Colombia. American Journal of Science 254:736–743.

Melo França, L. et al. 2015. Review of feeding ecology data of late Pleistocene mammalian herbivores from South America and discussions on niche differentiation. Earth-Science Reviews 140:158–165.

Ogg, J.G. 2012. Geomagnetic polarity time scale; pp. 85–114 in F.M. Gradstein, J.G. Ogg, M.D. Schmitz, and G.M. Ogg (eds.) The Geologic Time Scale 2012. Amsterdam, Netherlands, Elsevier Publishing.

Oiso, Y. 1991. New land mammal locality of middle Miocene (Colloncuran) age from Nazareno, southern Bolivia. Revista Técnica de YPBF 12:653–672.

Owen, R. 1838. Fossil Mammalia; pp. 81–111 in C. Darwin (ed.) The Zoology of the Voyage of the H.M.S. Beagle. London, UK:, Smith, Elder and Co.

Patterson, B., and R. Pascual. 1968. The fossil mammal fauna of South America. The Quarterly Review of Biology 43:409–451.

Paula Couto, C. 1952. Fossil mammals from the beginning of the Cenozoic in Brazil: Condylarthra, Litopterna, Xenungulata, and Astrapotheria. Bulletin of American Museum of Natural History 99:355–394.

Pérez, M.E. 2010. A new rodent (Cavioidea, Hystricognathi) from the middle Miocene of Patagonia, mandibular homologies, and the origin of the crown group Cavioidea *sensu stricto*. Journal of Vertebrate Paleontology 30:1848–1859.

Prevosti, F.J., and A.M. Forasiepi. 2018. Evolution of South American Mammalian Predators During the Cenozoic: Paleobiogeographic and Paleoenvironmental Contingencies. Cham, Switzerland, Springer Geology, .

Prothero, D.R., K.E. Campbell, B.L. Beatty, and C.D. Frailey. 2014. New late Miocene dromomerycine artiodactyl from the Amazon Basin: implications for interchange dynamics. Journal of Paleontology 88:434–443.

Pujos, F., G. De Iuliis, B.M. Quispe, and R.A. Flores. 2014. *Lakukullus anatisrostratus*, gen. et sp. nov., a new massive nothrotheriid sloth (Xenarthra, Pilosa) from the middle Miocene of Bolivia. Journal of Vertebrate Paleontology 34:1243–1248.

Reguero, M.A., and A.M. Candela. 2011. Late Cenozoic mammals from the Northwest of Argentina; pp. 411–426 in J.A. Salfity and R.A. Marquillas (eds.)

Cenozoic Geology of the Central Andes of Argentina. Salta, Argentina, SCS Publisher.

Reguero, M.A., A.M. Candela, and G.H. Cassini. 2010. Hypsodonty and body size in rodent-like notoungulates; pp. 258–367 in R.H. Madden, A.A. Carlini, M.G. Vucetich, and R.F. Kay (eds.) The Paleontology of Gran Barranca: Evolution and Environmental Change through the Middle Cenozoic of Patagonia. Cambridge, UK:, Cambridge University Press.

Roth, S. 1899. Aviso preliminar sobre mamíferos mesozóicos encontrados en Patagonia. Revista Del Museo de La Plata 9:381–388.

Rovereto, C. 1914. Los estratos araucanos y su fósiles. Anales Del Museo Nacional de Buenos Aires 25:1–250.

RStudioTeam. 2016. RStudio: integrated development for R. .

Scherer, C., V. Pitana, and A.M. Ribeiro. 2009. Proterotheriidae and Macraucheniidae (Litopterna, Mammalia) from the Pleistocene of Rio Grande do Sul State, Brazil. Revista Brasileira de Paleontologia 12:231–246.

Schindelin, J. et al. 2012. Fiji: an open-source platform for biological-image analysis. Nature Methods 9:676–682.

Schmidt, G.I. 2015. Actualización sistemática y filogenia de los Proterotheriidae (Mammalia, Litopterna) del “Mesopotamiense” (Mioceno tardío) de Entre Ríos, Argentina. Revista Brasileira de Paleontologia 18:521–546.

Schmidt, G.I., and E. Cerdeño. 2013. Los Ungulados Nativos (Litopterna y Notoungulata: Mammalia) del “Mesopotamiense” (Mioceno Tardío) de Entre Ríos, Argentina. El Neógeno de La Mesopotamia Agentina Asociación Paleontológica Argentina Publicación Especial 145–152.

Schmidt, G.I., and B.S. Ferrero. 2014. Taxonomic reinterpretation of *Theosodon hystatus* Cabrera and Kraglievich, 1931 (Litopterna, Macraucheniidae) and phylogenetic relationships of the family. Journal of Vertebrate Paleontology 34:1231–1238.

Schmidt, G.I., C.I. Montalvo, R. Sostillo, and E. Cerdeño. 2018. Proterotheriidae (Mammalia, Litopterna) from the Cerro Azul Formation (late Miocene), La Pampa Province, Argentina. Journal of South American Earth Sciences 83:165–177.

Schmidt, G.I., S.H. Del Pino, N.A. Muñoz, and M. Fernández. 2019. Litopterna (Mammalia) from the Santa Cruz Formation (early-middle Miocene) at the Río Santa Cruz, southern Argentina. Publicacion Electronica de La Asociacion Paleontologica Argentina 19:170–192.

Scillato-Yané, G.J. 1977. Sur quelques Glyptodontidae nouveaux (Mammalia, Edentata) du Déséadien (Oligocene inférieur) de Patagonie (Argentine). Bulletin Du Meséum National d’Histoire Naturelle, Paris, Série 3 64:249–262.

Scott, W.B. 1910. Mammalia of the Santa Cruz beds. Part I. Litopterna. Princeton University Expedition to Patagonia 7:1–156.

Shockey, B.J., and F. Anaya. 2008. Postcranial osteology of mammals from Salla, Bolivia (late Oligocene): form, function, and phylogenetic implications; pp. 135–167 in E.J. Sargis and M. Dagosto (eds.) Mammalian Evolutionary Morphology: A Tribute to Frederick S. Szalay. Springer Science.

Simpson, G.G. 1935. Descriptions of the oldest known South American mammals, from the Río Chico Formation. American Museum Novitates 1–26.

Simpson, G.G. 1948. The beginning of the age of mammals in South America, Part I. Introduction. Systematics: Marupialia, Edentata, Condylarthra, Litopterna, and Notioprogonia. Bulletin of American Museum of Natural History 91:1–232.

Simpson, G.G. 1980. Splendid Isolation: The Curious History of South Americna Mammals. New Haven, Connecticut, USA:, Yale University Press.

Solórzano, A., A. Encinas, R. Bobe, R. Maximiliano, and G. Carrasco. 2019. The early to late middle Miocene mammalian assemblages from the Cura-Mallín Formation, at Lonquimay, southern Central Andes, Chile (~38°S): biogeographical and paleoenvironmental implications Journal of South American Earth Sciences 96: 102319.

Soria, M.F. 1978. Una nueva y problematica forma de ungulado del Casamayorense. Actas Del Segundo Congreso Argentino Del Paleontologia y Bioestratigrafia y Primer Congreso Latinoamericano de Paleontologia 193–203.

Soria, M.F. 2001. Los Proterotheriidae (Litopterna, Mammalia), sistemática, origen y filogenia. Monografias Del Museo Argentino de Ciencias Naturales 1–171.

Soria, M.F., and R. Hoffstetter. 1983. Presence d'un condylarthre (*Salladolodus deuterotheriodes* gen. et sp. nov.) dans le Deseadien (Oligocene inferiuer) de Salla, Bolivie. Comptes Rendus de l'Acadamie Des Sciences 297:549–552.

Stirton, R.A. 1953. A new genus of interatheres from the Miocene of Colombia. California University Department of Geological Sciences B 29:265–347.

Takai, F., B.P. Arozqueta, T. Mizuno, A. Yoshida, and H. Kondo. 1984. On fossil mammals from the Tarija department, southern Bolivia. The Research Institute of Evolutionary Biology Publication No. 4 1–59.

Tejada-Lara, J. V. et al. 2015. Life in proto-Amazonia: middle Miocene mammals from the Fitzcarrald Arch (Peruvian Amazonia). Palaeontology 58:341–378.

Tomassini, R.L., C.I. Montalvo, C.M. Deschamps, and T. Manera. 2013. Biostratigraphy and biochronology of the Monte Hermoso formation (early Pliocene) at its type locality, Buenos Aires province, Argentina. Journal of South American Earth Sciences 48:31–42.

Tonni, E.P. et al. 2009. Preliminar correlation of the Pleistocene sequences of the Tarija valley (Bolivia) with the Pampean chronological standard. Quaternary

International 210:57–65.

Ubilla, M., D. Perea, M. Bond, and A. Rinderknecht. 2011. The first cranial remains of the Pleistocene proterotheriid *Neolicaphrium* Frenguelli, 1921 (Mammalia, Litopterna): a comparative approach. Journal of Vertebrate Paleontology 31:193–201.

Varela, L., and R.A. Fariña. 2015. Masseter moment arm as a dietary proxy in herbivorous ungulates. Journal of Zoology 296:295–304.

Villafañe, A.L., E. Ortiz-Jaureguizar, and M. Bond. 2006. Cambios en la riqueza taxonómica y en las tasas de primera y última aparición de los Proterotheriidae (Mammalia, Litopterna) durante el Cenozoico. Estudios Geológicos 62:155–166.

Villafañe, A.L., G.I. Schmidt, and E. Cerdeño. 2012. Consideraciones sistematicas y bioestratigraficas acerca de *Thoatheriopsis mendocensis* Soria, 2001 (Litopterna, Proterotheriidae). Ameghiniana 49:365–374.

Villafañe, A.L., M.E. Pérez, M.A. Abello, E. Bedatou, and M. Bond. 2008. Nueva localidad fosilífera del Mioceno medio en el noroeste de la provincia del Chubut. III Congreso Latinoamericano de Paleontología de Vertebrtebrados 265.

Villarroel, C., and L.G. Marshall. 1989. A new fossil land mammal locality of late Miocene (Huayquerian) Age from Muyu Huasi, southcentral Bolivia. Boletín Del Servicio Geológico de Bolivia, La Paz, Serie A 4:27–40.

Welker, F. et al. 2015. Ancient proteins resolve the evolutionary history of Darwin's South American ungulates. Nature 522:81–84.

Woodburne, M.O. 2010. The Great American Biotic Interchange: Dispersals, tectonics, climate, sea level and holding pens. Journal of Mammalian Evolution 17:245–264.

Woodburne, M.O. et al. 2014a. Revised timing of the South American early Paleogene land mammal ages. Journal of South American Earth Sciences 54:109–119.

Woodburne, M.O. et al. 2014b. Paleogene land mammal faunas of South America; a response to global climatic changes and indigenous floral diversity. Journal of Mammalian Evolution 21:1–73.

Wyss, A.R. et al. 1994. Paleogene mammals from the Andes of central Chile: A preliminary taxonomic, biostratigraphic, and geochronologic assessment. American Museum Novitates 1–31.

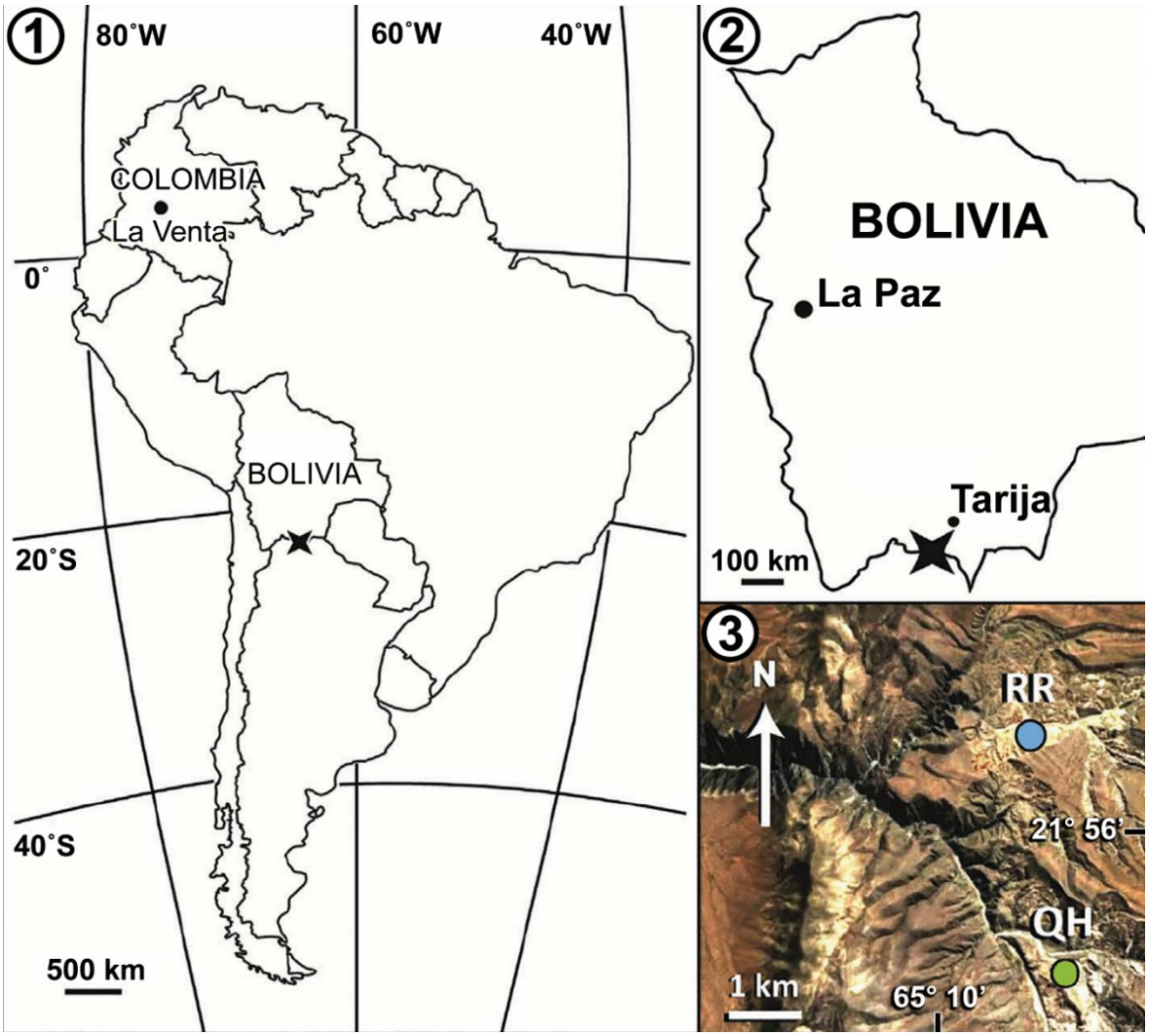

Figure 7: Locations of fossil localities mentioned in text, with Quebrada Honda indicated by a black star in **1** and **2**. Locations of Río Rosario (RR) and Quebrada Honda (QH) local areas indicated in **3**. Modified from Catena et al. (2017).

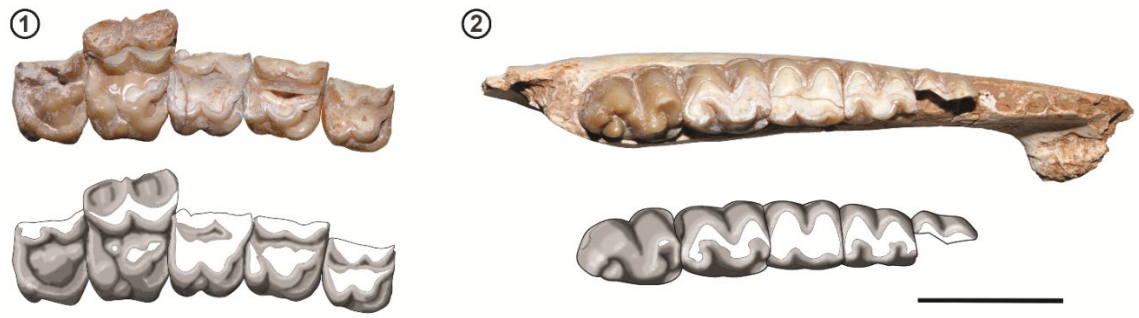

Figure 8: Photos (above) and illustrations (below) of the type specimen of *Olisanophus riorosarioensis* gen. et sp. nov. (UATF-V-001287) including **1**, partial RP3–M1, complete RM2, partial RM3; and **2**, left mandibular ramus preserving partial symphysis, roots of Lp1–2, partial Lp3, and complete Lp4–m3. In illustrations, white indicates exposed dentine. Scale bar= 2 cm.

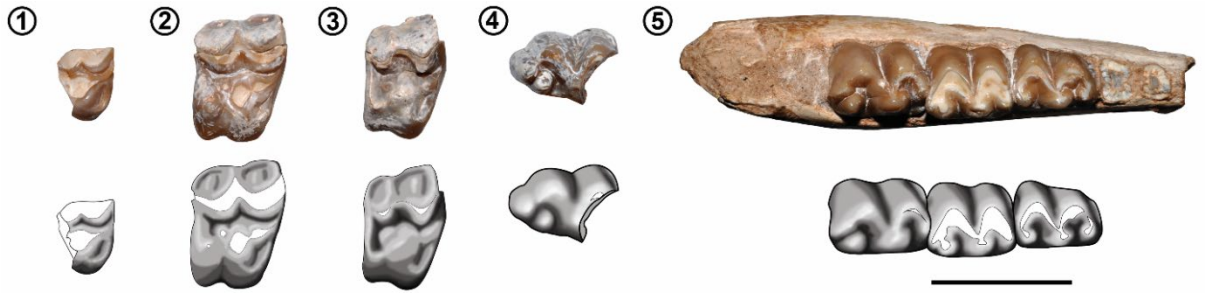

Figure 9: Photos (above) and illustrations (below) of *Olisanophus akilachuta* gen. et sp. nov. **1-4**, holotype (UATF-V-001780); **1**, partial RP3?; **2**, RM2; **3**, RM3; **4**, partial Lm3. **5**, referred specimen (UATF-V-001770), a left mandibular ramus preserving roots of Lp3 and complete Lp4–m2. In illustrations, white indicates exposed dentine. Scale bar= 2 cm.

Figure 10: Tree used for analyses of proterotheriid diversity and body size evolution. Bold lines represent each taxon's temporal range in megannum (Ma). Tree is modified version of strict consensus of 12 most-parsimonious trees of 351.775 steps each, with non-proterotheriid outgroups (*i.e.*, *Didolodus multicuspis* and *Protolipterna ellipsodontoides*) excluded. See unmodified version of this tree in Figure S14.1. *-species not included in the phylogenetic analysis due to incompleteness. ^-species scored together as *Anisolambda* spp. for phylogenetic analysis but treated separately for diversity and body size analyses. New taxa described in this study are in bold. Colored bands indicate time bins. Abbreviations: BAR, Barrancan; CHP, Chapadmalalan; CHS, Chasicoan; CLH, Colhuehuapian; CLL, Colloncuran; DES, Deseadan; HUA, Huayquerian; ITA, Itaboraian; LAV, Laventan; MAR, Marplatan; MAY, Mayoan; MON, Montehermosan; MUS, Mustersan; PLE, Pleistocene; RIO, Riochican; SAN, Santacrucian; TIN, Tinguiririan; VAC, Vacan.

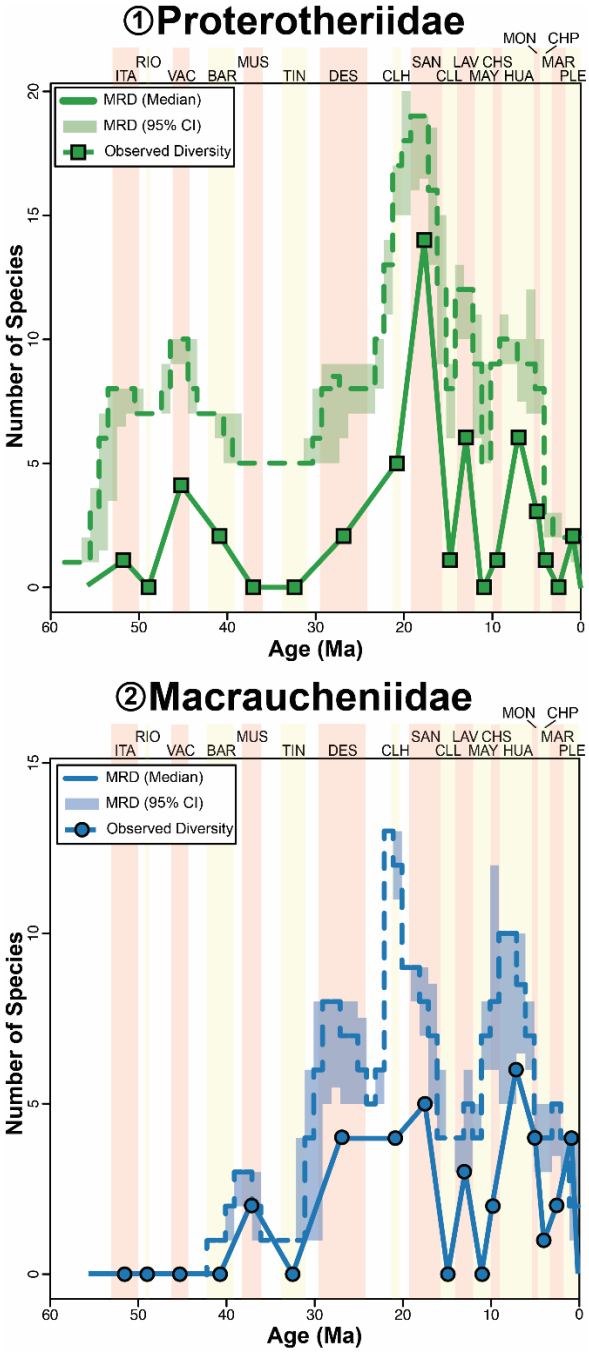

Figure 11: Diversity trends of **1**, Proterotheriidae and **2**, Macraucheniidae. Solid line indicates number of species recorded in each time bin which are indicated by colored bands (see Table 4). Dashed line represents the median minimum required diversity (MRD) and shaded area represents 95% confidence interval (CI) of the MRD based on 100 simulations. Abbreviations: BAR, Barrancan; CHP, Chapadmalalan; CHS, Chasicoan; CLH, Colhuehuapian; CLL, Colloncuran; DES, Deseadan; HUA, Huayquerian; ITA, Itaboraian; LAV, Laventan; MAR, Marplatan; MAY, Mayoan; MON, Montehermosan; MUS, Mustersan; PLE, Pleistocene; RIO, Riochican; SAN, Santacrucian; TIN, Tinguiririca n; VAC, Vacan.

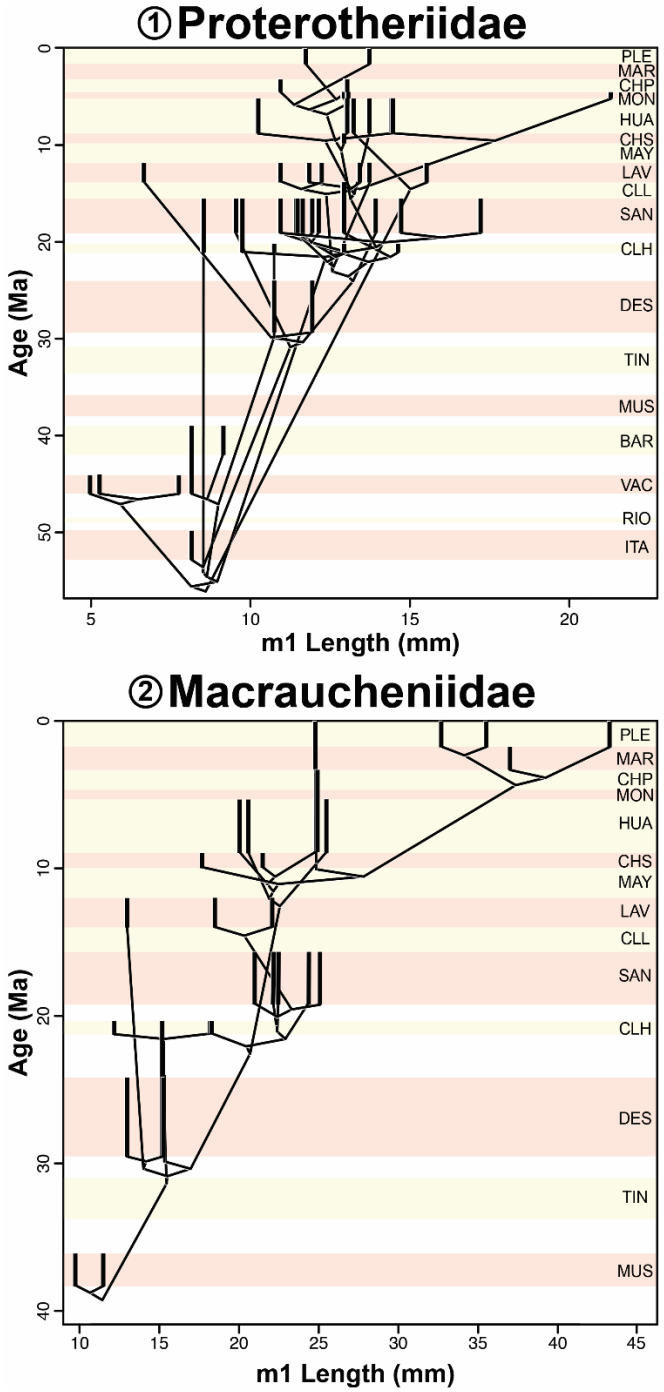

Figure 12: Phenograms showing evolution of mesiodistal m1 length (as proxy for body size) in **1**, Proterotheriidae and **2**, Macraucheniidae. Species' known temporal ranges represented by bold lines. Positions of nodes are reconstructed using maximum likelihood. Colored bands indicate time bins. Abbreviations: BAR, Barrancan; CHP, Chapadmalalan; CHS, Chasicoan; CLH, Colhuehuapian; CLL, Colloncuran; DES, Deseadan; HUA, Huayquerian; ITA, Itaboraian; LAV, Laventan; MAR, Marplatan; MAY, Mayoan; MON, Montehermosan; MUS, Mustersan; PLE, Pleistocene; RIO, Riochican; SAN, Santacrucian; TIN, Tinguiririan; VAC, Vacan.

Table 4: Temporal ranges and m1 sizes (in mm) of proterotheriids and macraucheniids. See Supplementary File 6 for methods used to estimate size of missing taxa, sources, and measurements of individual specimens. Abbreviations: PRO, Proterotheriidae; MAC, Macraucheniidae; BAR, Barrancan; CHP, Chapadmalalan; CHS, Chasicoan; CLH, Colhuehuapian; CLL, Colloncuran; DES, Deseadan; HUA, Huayquerian; ITA, Itaboraian; LAV, Laventan; MAR, Marplatan; MAY, Mayoan; MON, Montehermosan; MUS, Mustersan; PLE, Pleistocene; RIO, Riochican; SAN, Santacrucian; TIN, Tinguiririan; VAC, Vacan.

Taxon	**Clade**	**Range**	**m1 Length**
Paranisolambda prodromus	PRO	ITA	8.2
Adiantoides leali	PRO	VAC	5.3
Adiantoides magnus	PRO	VAC	7.8
Indalecia grandensis	PRO	VAC	5
Anisolambda amel	PRO	VAC-BAR	8.2
Anisolambda fissidens	PRO	BAR	9.2
Protheosodon coniferus	PRO	DES	12
Lambdaconus suinus	PRO	DES	10.8
Lambdaconus lacerum	PRO	CLH-SAN	8.5
Lambdaconus inaequifacies	PRO	CLH	10.8
Prolicaphrium specillatum	PRO	CLH	14.7
Paramacrauchenia scamnata	PRO	CLH-SAN	9.8
Paramacrauchenia inexspectata	PRO	CLH	13
Tetramerorhinus lucarius	PRO	SAN	11.7
Tetramerorhinus cingulatum	PRO	SAN	12.2
Tetramerorhinus mixtum	PRO	SAN	12
Tetramerorhinus prosistens	PRO	SAN	11.5
Tetramerorhinus fleaglei	PRO	SAN	11.5
Thoatherium minusculum	PRO	SAN	11
Diadiaphorus majusculus	PRO	SAN	17.3
Diadiaphorus caniadensis	PRO	SAN	14.8
Anisolophus australis	PRO	SAN	11
Anisolophus floweri	PRO	SAN	14
Anisolophus minusculus	PRO	SAN-CLL	13
Picturotherium migueli	PRO	SAN	9.6
Olisanophus riorosarioensis	PRO	LAV	11
Olisanophus akilachuta	PRO	LAV	12.3
Mesolicaphrium sanalfonensis	PRO	LAV	11.9
Villarroelia totoyoi	PRO	LAV	13.8
Neodolodus colombianus	PRO	LAV	6.7
Megadolodus molariformis	PRO	LAV	15.6
Thoatheriopsis mendocensis	PRO	LAV	13.5
Neobrachytherium ullumense	PRO	CHS	13

Neobrachytherium ameghinoi	PRO	HUA	14.5
Neobrachytherium intermedium	PRO	MON	13.1
Neobrachytherium morenoi	PRO	MON	13
Brachytherium cuspidatum	PRO	HUA	13.8
Proterotherium cervioides	PRO	HUA	10.3
Bounodus enigmaticus	PRO	HUA	13.3
Diplasiotherium pampa	PRO	HUA	14.5
Diplasiotherium robustum	PRO	MON	21.4
Eoauchenia primitiva	PRO	HUA-MON	13.1
Epitherium laternarium	PRO	MON	11
Neolicaphrium major	PRO	CHP	13.1
Neolicaphrium recens	PRO	PLE	11.8
Uruguayodon alius	PRO	PLE	13.8
Polymorphis lechei	MAC	MUS	9.75
Polymorphis alius	MAC	MUS	11.5
Coniopternium andinum	MAC	DES	15.3
Coniopternium primitivum	MAC	DES	13
Cramauchenia normalis	MAC	DES	15.2
Pternoconius polymorphoides	MAC	DES	15.3
Pternoconius tournoueri	MAC	CLH	18.3
Pternoconius bondi	MAC	CLH	12.2
Theosodon frenguellii	MAC	CLH	18.2
Theosodon fontanae	MAC	SAN	24.4
Theosodon garretorum	MAC	SAN	22.5
Theosodon gracilis	MAC	SAN	21
Theosodon lallemanti	MAC	SAN	22.2
Theosodon lydekkeri	MAC	SAN	25.1
Theosodon (La Venta)	MAC	LAV	22.1
Theosodon arozquetai	MAC	LAV	18.5
Llullataruca shockeyi	MAC	LAV	13
Cullinia levis	MAC	CHS	17.7
Paranauchenia hystata	MAC	CHS	21.5
Paranauchenia denticulata	MAC	HUA	24.8
Huayqueriana cristata	MAC	HUA	20.6
Oxyodontherium zeballosi	MAC	HUA	20.1
Scalabrinitherium bravardi	MAC	HUA	25.5
Promacrauchenia antiquua	MAC	HUA-MON	24.8
Promacrauchenia calchaquiorum	MAC	HUA-MON	24.8
Promacrauchenia kraglievichi	MAC	MON	24.8
Promacrauchenia chapadmalense	MAC	MON-CHP	24.8
Promacrauchenia yepesi	MAC	MAR-PLE	24.8
Windhausenia delacroixi	MAC	MAR	37
Macrauchenia patachonica	MAC	PLE	32.7

Macraucheniopsis ensenadensis	MAC	PLE	33.5
Xenorhinotherium bahiense	MAC	PLE	43.3

Table 5: Dental measurements of *Olisanophus riorosarioensis* and *Olisanophus akilachuta.* All measurements in mm. *indicates approximate measurement due to breakage. † indicates approximate measurement because tooth was not fully erupted. ‡ indicates measurements taken from Takai et al. (1984). MD, mesiodistal length; L, left; LL, labiolingual width R, right.

Taxon	Specimen	Tooth	MD	LL
Olisanophus riorosarioensis	UATF-V-001287	LP3	9.75*	—
		LP4	10.58*	—
		LM1	11.54*	—
		LM2	13.18	18.19
		LM3	10.96*	—
		RM3	11.21*	—
		Lp4	10.82	9.36
		Lm1	11	10.44
		Lm2	12.97	11.39
		Rm2	12.98*	11.01*
		Lm3	15.01†	11.2†
		Rm3	14.52†	11.13†
Olisanophus cf. *riorosarioensis*	RIEB-CM 423‡	Rp1–m3	68	—
Olisanophus akilachuta	UATF-V-001780	RM2	13.15	17.15
		LM3	11.03*	15.39
		RM3	11.63	16.32
		Lm3	—	10.86*
	UATF-V-001613	RM2	10.63	16.86
		RM3	10.57	15.17
	UATF-V-000967	RP4?	10.86*	—
	UATF-V-001770	Lp4	10.8	7.98
		Lm1	12.3	9.98
		Lm2	12.65	10.9

CHAPTER 3

CAVIOIDS, CHINCHILLOIDS, AND ERETHIZONTOIDS (RODENTIA, MAMMALIA) OF THE EARLY MIOCENE PAMPA CASTILLO FAUNA, CHILE

ABSTRACT

Caviomorph rodents became important components of South American faunas after their Eocene arrival from Africa. In this article, we describe the cavioid, chinchilloid, and erethizontid caviomorphs of the early Miocene Pampa Castillo fauna of southern Chile. This fauna's age and location make it key for resolving outstanding biostratigraphic questions concerning early Miocene Patagonian fossiliferous strata.

Each of the four major caviomorph clades ('superfamilies') is represented in the Pampa Castillo fauna, the members of three of which are detailed here: cavioids (3 genera and 3 species), chinchilloids (3 genera; 6 or 7 spp.), and erethizontids (2 genera; 2 spp.). We describe two new taxa, *Perimys* sp. nov.? (likely conspecific with a form first noted from the Pinturas Formation) and *Scleromys* sp. nov.?, neither of which we formally name given their fragmentary representation.

Abundant taxa such as *Neoreomys australis*, *Perimys erutus*, and *Prolagostomus pusillus*, corroborates previous work assigning the Pampa Castillo fauna to the Santacrucian South American Land Mammal "Age" (SALMA; inclusive of the 'Pinturan'). Several taxa, including *Eosteiromys*, *Perimys intermedius*, and *Perimys* sp. nov.?, are also found in the lower and middle Pinturas Formation (lmPF) but not 'core' Santacrucian faunas (from the Santa Cruz Formation [SCF] along the Río Santa Cruz and Atlantic coast), suggesting a distinctive resemblance between lmPF and Pampa Castillo rodents. Some authors consider the fauna from the lmPF

to form the basis of a ‘Pinturan’ SALMA or subage slightly older than that represented by core Santacrucian faunas, but this biochron has yet to be formally defined. The rodents of Pampa Castillo and their relative abundance suggest a paleoenvironment intermediate between the closed forests of the lmPF and the mosaic of open and closed habitats of the core Santacrucian faunas from the SCF.

KEYWORDS

Caviomorpha; Cavioidea; Chinchilloidea, Erethizontoidea; Miocene; Chile

INTRODUCTION

Prior to the Great American Biotic Interchange, South American Cenozoic terrestrial faunas were largely composed of endemic taxa (e.g., Simpson, 1940; Flynn et al., 2012; Croft, 2016) Caviomorph rodents first appear in South America in the middle Eocene, likely after rafting across the Atlantic Ocean from Africa (Rowe et al., 2010; Marivaux and Boivin, 2019). Initially, they diversified in low latitudes before dispersing southward (Antoine et al., 2012; Bertrand et al., 2012; Boivin et al., 2017). The four major clades ('superfamilies') of caviomorphs diverged from one another by the late Eocene or early Oligocene: Cavioidea (cavies, capybaras, agoutis, and kin), Chinchilloidea (chinchillas and kin), Erethizontoidea (porcupines), and Octodontoidea (spiny rats, tuco-tucos, degus, and kin) (Voloch et al., 2013; Boivin et al., 2019a). Members of the first three of these clades will be discussed herein, whereas the octodontoids of Pampa Castillo will be discussed in a subsequent paper. By the early Miocene, caviomorphs were diverse and abundant components of South American mammal communities (Vucetich et al., 2010; Candela et al., 2012; Arnal et al., 2019).

The early Miocene Santacrucian South American Land Mammal "Age" (SALMA) is likely the best understood pre-Quaternary interval in the Cenozoic of South America, but its precise duration and composition are disputed. Most Santacrucian SALMA localities are in Argentine Patagonia. These include the localities on which Ameghino (1889) originally based his 'Santacrucense,' which come from the Santa Cruz Formation (SCF) along the Río Santa Cruz (RSC; Fig.

13) in Santa Cruz Province, and span ~17.2–15.6 Ma (e.g., Barrancas Blancas, Segundas Barrancas Blancas, and Yaten Huageno; Cuitiño et al., 2016; Fernicola et al., 2019). The best-studied Santacrucian localities, sometimes referred to as the 'classic Santacrucian' localities, are from exposures of the SCF along the Atlantic Coast (Fig. 13; e.g., Monte León, Cerro Observatorio, and Killik Aike). They average slightly older (~17.8–16.2 Ma) than the RSC localities, but their faunas are nearly identical (Flynn and Swisher, 1995; Perkins et al., 2012; Trayler et al., 2020; Kay et al., 2021). For ease of reference, throughout this work we collectively term SCF localities and faunas from along the Río Santa Cruz, plus those from the Atlantic coast, as 'core Santacrucian' localities/faunas. The descriptor 'Santacrucian' alone will be used to refer to all faunas assigned to the Santacrucian SALMA.

Other Santacrucian faunas from the SCF in western Santa Cruz Province, such as Karaiken and Río Bote, seem to be slightly older than their eastern counterparts, are sometimes considered to represent a "Notohippidian stage" or "étage Notohippidien" within the Santacrucian SALMA (González Ruiz and Scillato-Yané, 2009; Fernicola et al., 2014; Cuitiño et al., 2016). At Lago Posadas, in the northwestern corner of Santa Cruz Province, SCF strata span a broad temporal range from ~18–14.2 Ma (Blisniuk et al., 2005; Cuitiño et al., 2015). Rodents from Pampa Castillo (Flynn et al., 2002a), a southern Chilean Santacrucian SALMA site recovered from strata that may correspond to the SCF, are described below. Santacrucian faunas also occur in the Pinturas Formation, which is divided into three stratigraphic sequences (upper, middle, and lower). The fauna of the upper sequence of the Pinturas Formation (uPF) is similar to those from localities bearing

core Santacrucian faunas, whereas the fauna of the lower and middle sequences of the Pinturas Formation (lmPF) comprises a mix of Colhuehuapian SALMA (also early Miocene, but slightly older) and Santacrucian taxa (Fig. 13); these lower sequences are also geochronologically older than localities bearing core Santacrucian faunas (Kramarz and Bellosi, 2005; Fleagle et al., 2012; Perkins et al., 2012). Faunal differences between the lmPF and core Santacrucian localities have long been recognized, leading some authors to recognize the fauna from the lmPF as a biostratigraphically distinct interval, the ‘Pinturan’, though this biochron has never been formalized (Castellanos, 1937; Kramarz and Bellosi, 2005; Kramarz and Bond, 2005; Kramarz et al., 2010; Dunn et al., 2013). The Upper Faunal Zone (UFZ) of the Trelew Member of the Sarmiento Formation at Gran Barranca was assigned to the ‘Pinturan’ interval by Kramarz et al. (2010; Fig. 13). It is unclear whether Santacrucian faunas from elsewhere in South America (e.g., those from Chucal and intervals from Laguna del Laja in Chile; Cerro Boleadoras Formation, Chinches Formation, and Mariño Formation at Divisadero Largo in Argentina, and Castilletes Formation in Colombia) might pertain to this ‘Pinturan’ interval, as they lack taxa that have been used to discriminate between ‘Pinturan’ and core Santacrucian faunas (Scillato-Yané and Carlini, 1998; Flynn et al., 2002b, 2008; Cerdeño and Vucetich, 2007; López et al., 2011; Carrillo et al., 2018; Solórzano et al., 2020).

The Pampa Castillo fauna can help resolve the confused chronology of Santacrucian faunas. The name of the mammal-bearing unit at Pampa Castillo is unsettled with different authors referring it to the Río Zeballos (Niemeyer, 1975), Santa Cruz (de la Cruz et al., 2004; Ugalde et al., 2015; Encinas et al., 2019),

Galera (Niemeyer et al., 1984; Flynn et al., 2002a), and Pampa Castillo (Scalabrino, 2009; Folguera et al., 2018) formations. Since this issue remains unresolved, we refer to this unit in this work as the Galera Formation to be consistent with our previous publications (Flynn et al., 2002a; McGrath et al., 2020). Pampa Castillo is located in southern Chile at a latitude (~47°S) equivalent to the northern Santa Cruz Province in Argentina (Fig. 13). Pampa Castillo, and exposures of the lmPF exposures in the upper Pinturas River valley are nearer to each other (~130 km) than either is to the core Santacrucian faunas (>350 km). Geochronological age estimates suggest that Pampa Castillo is also closer temporally to 'Pinturan' faunas than either is to core Santacrucian faunas. Folguera et al. (2018) reported a U/Pb date of 18.7 +/- 0.3 Ma from a reworked tuff directly below strata bearing the Pampa Castillo fauna. 'Pinturan' faunas of the lmPF and Upper Faunal Zone at Gran Barranca are ~19.0–17.9 Ma (Perkins et al., 2012; Dunn et al., 2013), whereas core Santacrucian faunas are ~17.5–15.6 Ma (Cuitiño et al., 2016; Trayler et al., 2020). Notably, fossiliferous strata between 19 and 17.5 Ma crop out at other SCF localities such as Río Bote, Karaiken and Lago Posadas, but these faunas are less-studied than their core Santacrucian counterparts along the RSC and Atlantic coast and/or past collections have lacked stratigraphic control (Fernicola et al., 2014; Cuitiño et al., 2015, 2016, 2019a). Pampa Castillo is closer geographically and in age to 'Pinturan' faunas than to core Santacrucian faunas but is not stratigraphically associated with either the lmPF (Pinturas Formation) or strata of the Upper Faunal Zone at Gran Barranca (Sarmiento Formation).

The Pampa Castillo fauna was first described by Flynn et al. (2002a), who provided an overview of the locality's geology, a composite taxonomic list of the fossil macroinvertebrates from underlying marine strata, a list and brief description of the fossil mammal fauna, and a detailed description of the palaeothentid marsupials. They assigned the mammalian fauna to the Santacrucian SALMA based on the presence of characteristic taxa such as *Nesodon* Owen, 1846, *Perimys* Ameghino, 1887a, and *Homalodotherium* Flower, 1873. McGrath et al. (2020) described the litopterns from Pampa Castillo, finding them consistent with assignment to the Santacrucian SALMA. In this work, we describe the cavioids, chinchilloids, and erethizontoids of Pampa Castillo and discuss their biochronologic and paleoenvironmental implications.

MATERIALS AND METHODS

Fossil rodents from Pampa Castillo were compared firsthand to related forms housed in the American Museum of Natural History and Yale Peabody Museum and described in the literature. Measurements were taken using Mitutoyo CD-8" digital calipers to the nearest 0.1 mm.

In the Systematic Paleontology section, "Referred Material" and "Locality and Horizon" refer to specimens from Pampa Castillo newly described in this contribution, whereas "Age and Distribution" refers to the full geographic and temporal range of the taxon.

We recognize that ‘Eocardiidae’ is a paraphyletic grade of cavioids, but we still employ this name as a useful shorthand for this non-monophyletic grouping of anatomically similar taxa (Pérez, 2010a; Pérez and Vucetich, 2012a; Boivin et al., 2019a).

Abbreviations

Anatomical—M/m: upper/lower molar; P/p: upper/lower premolar.

Institutional—SGOPV: Vertebrate Paleontology collections, Museo Nacional de Historia Natural, Santiago, Chile.

SYSTEMATIC PALEONTOLOGY

Mammalia Linnaeus, 1758

Eutheria Huxley, 1880

Rodentia Bowdich, 1821

Caviomorpha Wood, 1955

Cavioidea Fischer de Waldheim, 1817

Luantus Ameghino, 1899

Type species. *Luantus propheticus* Ameghino, 1899.

Included Species. The type species, *L. initialis* Ameghino, 1902*, L. toldensis* Kramarz, 2006*b, L. minor* Pérez et al., 2010, and *L. sompallwei* Solórzano et al., 2020.

Age and Distribution. Colhue-Huapi and Trelew members, Sarmiento Formation, Colhuehuapian SALMA, Chubut Province, Argentina; Galera Formation, Santacrucian SALMA, Aysén Region, Chile; Pinturas Formation, Santacrucian ('Pinturan') SALMA, Santa Cruz Province, Argentina; Tcm3 unit, Cura-Mallín Formation, Santacrucian? SALMA, Biobío Region, Chile.

Luantus minor Pérez et al., 2010

Figure 14A

Referred Material. SGOPV 2134, right m; SGOPV 2691, right p4–m2 (Fig. 14A); SGOPV 2697, left m1 or 2; SGOPV 2698, right p4?.

Locality and Horizon. Fossiliferous Interval 4 (SGOPV 2691, 2697, 2698) and Fossiliferous Interval 7 (SGOPV 2134); Galera Formation, Pampa Castillo, Chile.

Age and Distribution. Trelew Member, Sarmiento Formation, Colhuehuapian SALMA, Chubut Province, Argentina; Galera Formation, Santacrucian SALMA, Aysén Region, Chile.

Description. All Pampa Castillo specimens here referred to *Luantus minor* represent lower cheek teeth (Fig 2A; Table 6). They are bilobed, bear pointed protoconids and hypoconids, and are hypsodont (i.e., protohypsodont of Mones,

1982, but see Janis and Fortelius, 1988), being higher-crowned than *Luantus initialis* (Pérez et al., 2010). Enamel completely covers the lingual wall of the only specimen in which this region of the dentition is undamaged, SGOPV 2697.

SGOPV 2698 is likely a broken right p4, but damage makes its locus assignment uncertain. This tetralophodont tooth bears a wide, v-shaped hypoflexid and a convex posterolophid. SGOPV 2691 bears a moderately worn p4, the anterolophid of which is damaged (Fig. 14A). All three lingual flexids are open. The anterior wall of the v-shaped hypoflexid is slightly longer than its posterior counterpart. The posterolophid is straight and obliquely oriented. The m1–2 of SGOPV 2691 resemble one another save that m2 is larger and less-worn. The anterofossettid and mesofossettid are closed on both teeth. The metaflexid remains open in m1, but damage obscures this part of m2. These fossettids and the flexids are labiolingually elongate, except for the circular anterofossettid of m1. Both the anterior and posterior surfaces of the tooth are convex. Much like in p4, the walls of the molar hypoflexids are straight, though the hypoflexids of the molars are more symmetric. SGOPV 2697, representing either m1 or 2, is more heavily worn than the teeth of SGOPV 2691, as indicated by its completely closed metafossettid. The lingual border of this tooth curves labially opposite the mesofossettid.

Remarks. We refer these specimens to *Luantus* based on their rooted cheek teeth, persistent lingual fossettids, and presence of enamel covering the lingual surface of the lower molars, a combination of features distinguishing them from other early Miocene ‘eocardiids’ such as *Eocardia*, *Phanomys*, and *Schistomys* (Kramarz, 2006a; Pérez, 2010b; Pérez and Vucetich, 2012b). These teeth are also significantly

higher-crowned than the late Oligocene and early Miocene *Asteromys* and *Chubutomys* (Pérez et al., 2010, 2012; Pérez and Vucetich, 2012a). We assign these specimens to *L. minor* based on their degree of hypsodonty, enamel coverage, and size (Fig 2A; Table 6). The Colhuehuapian-aged *Luantus initialis* is much lower-crowned than other members of the genus (Pérez et al., 2010), including all specimens from Pampa Castillo, whereas *Luantus toldensis*, from the upper sequence of the Pinturas Formation, is more hypsodont than the specimens described herein (Kramarz, 2006a). The lower molars of *Luantus propheticus*, from the lower and middle Pinturas Formation and Upper Faunal Zone of the Sarmiento Formation, and *L. toldensis*, bear patches of exposed dentine on their lingual walls unlike specimens from Pampa Castillo (Kramarz, 2006a). Teeth of *Luantus initialis*, *L. propheticus*, and *L. toldensis* are all larger than the *Luantus* specimens recovered from Pampa Castillo (Kramarz, 2006a; Pérez, 2010b; Pérez et al., 2010). *Luantus* specimens from Pampa Castillo match *L. minor* in all respects, including size.

Luantus minor was previously reported only from the Colhuehuapian-aged Trelew Member of the Sarmiento Formation at Bryn Gwyn in northeastern Chubut Province, Argentina (Pérez et al., 2010). The occurrence of *L. minor* at Pampa Castillo, and absence of *L. propheticus* and *L. toldensis,* is surprising given the absence of *L. minor* and abundance of *L. propheticus* and *L. toldensis* at the geographically proximal and temporally similar Pinturas Formation (Kramarz, 2006a; Fig. 13).

Eocardia Ameghino, 1887c

Type Species. *Eocardia montana* Ameghino, 1887c.

Included Species. The type species, *Eoc. fissa* Ameghino, 1891b, *Eoc. excavata* Ameghino, 1891b, *Eoc. robusta* Vucetich, 1984, and *Eoc. robertoi* Vucetich, 1984. We follow the taxonomy of Pérez (2010a) for this genus.

Age and Distribution. Galera Formation, Santacrucian SALMA, Aysén Region, Chile; Santa Cruz Formation, Santacrucian SALMA, Santa Cruz Province, Argentina; Chinches Formation; Santacrucian SALMA, San Juan Province, Argentina; Collón Curá Formation, Colloncuran SALMA, Chubut, Neuquén, and Río Negro provinces, Argentina.

cf. *Eocardia excavata* Ameghino, 1891b

Figure 14B–D

Eocardia perforata Flynn et al., 2002a: 289 (*partim*), table 1.

Referred Material. SGOPV 2133 left M1–2; SGOPV 2690 left m1–2; SGOPV 2692 right M3 (Fig. 14B); SGOPV 2693 left M1 or 2; SGOPV 2694 right M2 (Fig. 14C); and SGOPV 2696 right M1 (Fig. 14D).

Locality and Horizon. Fossiliferous Interval 7, Galera Formation, Pampa Castillo, Aysén Region, Chile.

Age and Distribution. Chinches Formation; Santacrucian SALMA, San Juan Province, Argentina; Galera Formation, Santacrucian SALMA, Aysén Region, Chile; Santa Cruz Formation, Santacrucian SALMA, Santa Cruz Province, Argentina.

Description. Save for SGOPV 2133, all referred specimens were recovered in close proximity, include no overlapping elements, and are similar in size, indicating they may represent a single individual (Fig 2B–D). In the upper molars of SGOPV 2133, 2693, 2694, and 2696, the anterior and posterior walls of the lobes are slightly convex, with their pointed apices directed lingually. No labial fossettes are present. The labial walls of these teeth lack enamel and bear a slight sulcus opposite the hypoflexus. The hypoflexus extends nearly to the labial edge of the tooth, and its walls are essentially straight. At its apex, the hypoflexus turns slightly posteriorly. Cementum occurs inside the hypoflexus. SGOPV 2692, an M3, is similar to the more anterior molars, except that its posterior lobe extends posteriorly (Fig. 14B). This lobe also projects slightly lingually and nearly reaches the labiolingual midpoint of the tooth. Additionally, the apex of the posterior lobe points posteriorly. The apex of the anterior lobe is damaged.

SGOPV 2690 consists of two poorly preserved lower molariforms in a mandibular fragment. We presume these teeth represent the left m1–2 but are not certain. These teeth are bilobed, lack enamel lingually, and contain cementum within hypoflexids that nearly reach the labial wall.

Remarks. We assign these specimens to cf. *Eocardia excavata*. The lack of labial fossettes, slightly convex anterior and posterior edges, pointed molar lobes, and deeply penetrating hypoflexi/ids rule out assignment to the cavioids *Chubutomys leucoreios* Pérez et al., 2010, *Luantus*, and *Phanomys* Ameghino, 1887b (Fig. 14B–D; Kramarz 2006b; Pérez 2010; Pérez et al. 2010; Pérez and Vucetich 2012a). We further rule out *Eocardia fissa*, *Eoc. montana*, *Eoc. robertoi*, *Eoc. robusta*, *Matiamys*

elegans Vucetich, 1984, and *Schistomys erro* Ameghino, 1887b, based on the posterior lobe of M3 being less extended in SGOPV 2692 than in these other taxa (Vucetich, 1984; Pérez, 2010a; McGrath, personal obs.). Apart from *Eoc. fissa* and *Sch. erro*, teeth of these species also are larger than the specimens described here (Table 6). This material most likely pertains to *Eocardia excavata* or *Schistomys rollinsii* Scott, 1905, both of which resemble these Pampa Castillo specimens in their similarly developed M3 posterior lobes and absence of enamel on the antero- and postero-labial corners and labial walls of their upper molars (Pérez, 2010b). These taxa are best distinguished from one another by their premolars. *Eocardia excavata* (and other species of *Eocardia*) have a unilobed P4 and bilobed p4, whereas the reverse is true of *Sch. rollinsii* (and *Sch. erro*) (Scott, 1905; Pérez, 2010b). The thinner, more gently convex molar lobes of these teeth more closely match *Eoc. excavata* than *Sch. rollinsii*, but we cannot rule out assignment to *Sch. rollinsii* without knowing the premolar morphology.

Eocardia excavata has previously been reported from various localities in the Santa Cruz Formation in eastern and central Santa Cruz Province but not from western localities such as Lago Posadas, Karaiken, and Sierra Baguales, which are geographically closer to Pampa Castillo (Fig. 13; Scott 1905; Pérez 2010; Bostelmann et al. 2013; Arnal et al. 2019; Cuitiño et al. 2019a). *Eocardia excavata* has also been recovered at Las Hornillas in the Chinches Formation of west-central Argentina (San Juan Province; López et al., 2011). If our tentative assignment is correct, this and the specimen noted below are the first documented occurrences of any species of *Eocardia* outside Argentina.

cf. *Eocardia* sp.

Figure 14E

Eocardia perforata Flynn et al., 2002a: 289 (*partim*), table 1.

Referred Material. SGOPV 2695, partial left m2 and left m3 in mandibular fragment (Fig. 14E).

Locality and Horizon. Fossiliferous Interval 7, Galera Formation, Pampa Castillo, Chile.

Description. SGOPV 2695 consists of a mandibular fragment in which unerupted parts of two cheek teeth are visible (Fig. 14E). The teeth appear to be euhypsodont (i.e., ever-growing), given that they are fairly large and have a simplified coronal morphology similar to *Eocardia*. The complete tooth represents m3, as evidenced by the wide, shallow flexid on its posterior lobe, which is slightly longer and wider than the anterior lobe. This tooth bears a thin layer of enamel labially.

Remarks. The lower cheek teeth of SGOPV 2695 approximately match in size their counterparts in material from elsewhere assigned to *Schistomys* and *Eocardia* (Table 6), the two euhypsodont ‘eocardiid’ genera known from the early Miocene of Patagonia (Scott, 1905; Pérez, 2010b). It cannot be determined which of these genera SGOPV 2695 represents, as premolars are generally necessary to distinguish them. However, SGOPV 2695 is smaller than nearly all known specimens of *Sch. erro* and *Sch. rollinsii,* favoring assignment to cf. *Eocardia* sp. Of

the known *Eocardia* species, SGOPV 2695 falls within the size range of *Eoc. excavata* and *Eoc. fissa.*

Dasyproctidae Smith, 1842

Neoreomys Ameghino, 1887a

Type Species. *Neoreomys australis* Ameghino, 1887a.

Included Species. The type species, *N. pinturensis* Kramarz, 2006b, and possibly '*N.*' *huilensis* Fields, 1957.

Age and Distribution. Chinches Formation, Santacrucian SALMA, San Juan Province, Argentina; Chucal Formation, Santacrucian SALMA, Arica y Parinacota Region, Chile; Galera Formation, Santacrucian SALMA, Aysén Region, Chile; Pinturas Formation, Santacrucian ('Pinturan') SALMA, Santa Cruz Province, Argentina; Santa Cruz Formation, Santacrucian SALMA, Santa Cruz Province, Argentina; Colhue-Huapi Member, Sarmiento Formation, Santacrucian ('Pinturan') SALMA, Chubut Province, Argentina; Cura-Mallín Formation, Santacrucian? SALMA, Biobío Region, Chile; Collón Curá Formation, Colloncuran SALMA, Chubut, Neuquén, and Río Negro provinces, Argentina; Río Mayo or Pedregoso Formation, Mayoan SALMA, Santa Cruz or Chubut Province, Argentina; La Victoria Formation, Laventan SALMA, Huila Department, Colombia.

Neoreomys australis Ameghino, 1887a

Locality and Horizon. Fossiliferous Intervals E-0, E-2, 4, 5, 7, and 8, Pampa Castillo, Galera Formation, Aysén Region, Chile.

Age and Distribution. Chinches Formation, Santacrucian SALMA, San Juan Province, Argentina; Galera Formation, Santacrucian SALMA, Aysén Region, Chile; Pinturas Formation, Santacrucian ('Pinturan') SALMA, Santa Cruz Province, Argentina; Santa Cruz Formation, Santacrucian SALMA, Santa Cruz Province, Argentina; Collón Curá Formation, Colloncuran SALMA, Chubut, Neuquén, and Río Negro provinces, Argentina.

Description. A full specimen inventory and detailed description of *N. australis* from Pampa Castillo, including an analysis of ontogenetic changes in occlusal morphology, is the subject of another, ongoing project. Summary remarks are presented here in order to preliminarily review all of the cavioids from this fauna. Measurements of these specimens are not reported in Tables 6 or 7 or Supplementary Information 1.

Remarks. *Neoreomys australis* is known from the Santa Cruz and Pinturas formations (Ameghino, 1887c; Scott, 1905; Kramarz, 2006b; Arnal et al., 2019). Material from the Chinches and Collón Curá formations, which crop out in more northerly Patagonia, is referred to *Neoreomys* cf. *N. australis* (Vucetich et al., 1993; López et al., 2011). In the past, a variety of *Neoreomys* species were recognized (Ameghino, 1887c; Scott, 1905), but most contemporary authors follow Fields (1957) in recognizing *N. australis* as the sole species represented in the Santa Cruz Formation (Kramarz, 2006b; Croft, 2013; Arnal et al., 2019). *Neoreomys pinturensis* is known from the lower sequence of the Pinturas Formation, where it co-occurs with

N. australis, and the Upper Faunal Zone of the Sarmiento Formation at Gran Barranca (Kramarz and Bellosi, 2005; Kramarz, 2006b; Kramarz et al., 2010). Two non-Patagonian taxa include '*Neoreomys*' *huilensis* (Fields, 1957) from the middle Miocene of La Venta, Colombia, though this taxon's assignment to *Neoreomys* is questionable (Walton, 1997), and an undescribed taxon from the Cura-Mallín Formation of central Chile (Flynn et al., 2008).

Neoreomys australis is the most abundantly recovered fossil mammal from Pampa Castillo, comprising more than half of all specimens recovered and including a nearly complete skull (Flynn et al., 2002a, fig. 6A). It is also the most abundant rodent in the Santa Cruz Formation (Scott, 1905; Croft, 2013; Arnal et al., 2019; Zurita-Altamirano et al., 2019) but is much less abundant in the Pinturas Formation (Kramarz and Bellosi, 2005; Kramarz, 2006b). Even if the number of specimens of *N. australis* and *N. pinturensis* are combined, they do not dominate the fauna of the Pinturas Formation to the degree that *N. australis* does at Pampa Castillo or localities in the Santa Cruz Formation.

Chinchilloidea Bennett, 1833

Neoepiblemidae Kraglievich, 1926

Perimys Ameghino, 1887a

Type Species. *Perimys erutus* Ameghino, 1887a.

Included Species. The type species, *Per. onustus* Ameghino, 1887a, *Per. dissimilis* Ameghino, 1902, *Per. incavatus* Ameghino, 1902, *Per. intermedius* Kramarz, 2002, and *Perimys* sp. nov.? Kramarz, 2002.

Age and Distribution. Colhue-Huapi and Trelew members, Sarmiento Formation, Colhuehuapian SALMA, Chubut Province, Argentina; Pinturas Formation, Santacrucian ('Pinturan') SALMA, Santa Cruz Province, Argentina; Galera Formation, Santacrucian SALMA, Aysén Region, Chile; Santa Cruz Formation, Santacrucian SALMA, Santa Cruz Province, Argentina.

Affinities. *Perimys* is generally considered a member of the extinct chinchilloid subgroup Neoepiblemidae; per Rasia and Candela (2018), Neoepiblemidae includes the early Miocene, medium-sized *Perimys* and *Doryperimys* Kramarz et al., 2015, and the late Miocene gigantic rodents *Phoberomys* Kraglievich, 1926, and *Neoepiblema* Ameghino, 1889. Most phylogenetic analyses place *Perimys* as the earliest diverging neoepiblemid (Rasia and Candela, 2018; Busker et al., 2019; Kerber and Sánchez-Villagra, 2019; Rasia et al., 2021). Boivin et al. (2019a), the only study to include *Perimys* in an analysis of all caviomorphs, recovered it as a stem-cavioid. Other studies presumed a priori that *Perimys* is a chinchilloid, only including one or two non-chinchilloids as outgroups and not testing chinchilloid monophyly.

General Description. Here we summarize features shared by species referred to *Perimys*. The differences between these species are detailed subsequently. The cheek teeth of *Perimys* are hypselodont. When freshly erupted, they consist of four lophs/ids that quickly merge into two such structures, though M3 becomes

trilophodont (Boivin et al., 2019b; Rasia and Candela, 2019a). Unlike most caviomorphs, the P4 opens labially with a wide flexus (likely the mesoflexus), the apex of which projects posteriorly. The M1 and 2 are bilophodont; their hypoflexi open lingually and are wider than those of *Prolagostomus* and *Pliolagostomus*. The anterior loph is composed of the anteroloph and protocone, while the posterior one includes the mesolophule, metaloph, hypocone, and posteroloph. The mesolophule and hypocone make up the central loph on the trilophodont M3, while the metaloph and posteroloph comprise the posterior loph. The lower cheek teeth are generally quite similar, being bilophodont with anterolabially opening hypoflexids. Teeth generally increase in size posteriorly within the toothrow. Currently recognized species of *Perimys* are distinguished by the borders of their hypoflexi/ids, the distribution of enamel around their teeth, and the presence of 'columns' (i.e., stylids or cuspules) on the labial surfaces of upper molars and lingual surfaces of lower molars.

Remarks. Among other early Miocene chinchilloid caviomorphs, *Perimys* most closely resembles the neoepiblemid *Doryperimys olsacheri* Kramarz et al., 2015, and the chinchillids *Prolagostomus* and *Pliolagostomus*. The labially opening P4 is the clearest distinction between *Perimys* and chinchillids (Arnal et al., 2019; Rasia and Candela, 2019b). The third loph of M3 reaches the lingual edge of the tooth in species of *Perimys* but not in chinchillids. The lophs/ids and hypoflexi/ids are generally broader in *Perimys* than in *Prolagostomus* and *Pliolagostomus*. *Perimys* mostly notably differs from *Doryperimys* of the Cerro Bandera Formation (most likely

Colhuehuapian SALMA) in the more rounded ends of its lower molar lophids. A suite of additional distinguishing features are detailed by Kramarz et al. (2015).

Perimys erutus Ameghino, 1887a

Figure 15A

Perimys procerus Flynn et al., 2002a: 289, table 1.

Perimys scalaris Flynn et al., 2002a: 289, table 1.

Referred Material. SGOPV 2294, left p4; SGOPV 2361, partial skull with complete upper dentition (Flynn et al., 2002a, fig. 6B; identified as *Perimys* '*procerus*' therein); SGOPV 2386, left p4–m1; SGOPV 2391, right p4; SGOPV 2616, right P4–M1; SGOPV 2617, right m2–3; SGOPV 2618, right M1 or 2; SGOPV 2619, left P4–M2 (Fig. 15A) and left m2–3; SGOPV 2620, right m1 or 2; SGOPV 2621, right M1 or 2; SGOPV 2622, left M1 or 2; SGOPV 2623, right p4–m1; SGOPV 2624, left M1–3; SGOPV 2625, right P4; SGOPV 2626, left M1 or 2; SGOPV 2627, left M3; SGOPV 2628, right M3; SGOPV 2629, right M1–2; SGOPV 2630, right lower molar; SGOPV 2631, right p4; SGOPV 2632, left M3; SGOPV 2633, right M1 or 2; SGOPV 2634, left p4 in mandibular fragment with incisor root; SGOPV 2635, right M3; SGOPV 2636, right m3; SGOPV 2637, right P4; SGOPV 2638, left M1 or 2; SGOPV 2639, left p4 in mandibular fragment with incisor root; SGOPV 2640, right p4 in mandibular fragment with incisor root; SGOPV 2641, right m1 or 2; SGOPV 2642, left M1 or 2; SGOPV 2643, right m1 or 2; SGOPV 2644, right M1 or 2; SGOPV 2672, right P4; SGOPV 2722, right m1 or 2.

Locality and Horizon. Fossiliferous Interval E-0 (SGOPV 2386, 2618, 2627, 2628, 2631, 2632, 2633, 2634, 2635, 2636, 2637, 2638, 2639, 2640, 2672, 2722), Fossiliferous Interval 1A (SGOPV 2361), Fossiliferous Interval E-2 (SGOPV 2616), Fossiliferous Interval 4 (SGOPV 2617, 2617, 2621, 2623, 2624, 2625, 2629, 2630), Fossiliferous Interval 7 (SGOPV 2641, 2642, 2643, 2644), Glyptodont Glen (SGOPV 2294, 2620, 2626), and unknown fossiliferous interval (SGOPV 2391, 2622), Galera Formation, Pampa Castillo, Chile.

Age and Distribution. Pinturas Formation, Santacrucian ('Pinturan') SALMA, Santa Cruz Province, Argentina; Galera Formation, Santacrucian SALMA, Aysén Region, Chile; Santa Cruz Formation, Santacrucian SALMA, Santa Cruz Province, Argentina.

Description. Specimens of *Per. erutus* from Pampa Castillo resemble those from other sites. *Perimys erutus,* the smallest-bodied species of *Perimys* (Tables 6–7), is distinguished from other members of the genus by the following dental characters. The hypoflexi/ids of M1–3 and p4–m3 have straight or nearly straight borders (Fig. 15A). Enamel surfaces on M1–3 labially, and p4–m3 lingually, usually complete or lacking only a narrow vertical band. M1–2 usually bear 'pillars' opposite the anterior loph on the labial surface. The m3 is the only lower tooth that possesses a small lingual flexid.

Remarks. *Perimys erutus* is one of the most abundant rodents recovered from Pampa Castillo, trailing only *Perimys onustus* and *Neoreomys australis* in the number of specimens identified (Supplementary File 9). It occurs throughout the stratigraphic section, but most abundantly in the lowest fossiliferous horizon,

Fossiliferous Interval E-0. This taxon is also known from throughout the Santa Cruz Formation and from the upper sequence of the Pinturas Formation (Ameghino, 1887c; Scott, 1905; Kramarz, 2002; Arnal et al., 2019). Two of the five *Perimys* species recognized from Pampa Castillo by Flynn et al. (2002a), *Perimys* '*scalaris*' and *Perimys* '*procerus*,' were identified as junior synonyms of *Per. erutus* by Kramarz (2002).

Perimys onustus Ameghino, 1887a

Figure 15B–D

Perimys perpinguis Flynn et al., 2002a: 289, table 1.

Perimys impactus Flynn et al., 2002a: 289 (*partim*), table 1.

Perimys onustus Flynn et al., 2002a: 289 (*partim*), table 1.

Referred Material. SGOPV 2014, right p4–m2 and left m2; SGOPV 2030; left m3; SGOPV 2045, left P4–M3, right P4–M2, and partial right M3; SGOPV 2056, left m1 or 2; SGOPV 2060, left P4–M3, right P4, and right M1 or 2; SGOPV 2080, lower incisors and fragments of right p4–m3; SGOPV 2101, left p4–m1; SGOPV 2273, right p4–m1 and partial right m2–3 (Fig. 15D); SGOPV 2378, left m1 or 2; SGOPV 2421, right P4; SGOPV 2655, right P4; SGOPV 2656, right M3; SGOPV 2657, left P4; SGOPV 2658, left M3; SGOPV 2659, right M1 or 2; SGOPV 2660, right M1 or 2; SGOPV 2661, left P4–M2 (Fig. 15C); SGOPV 2662, left M3 (Fig. 15B); SGOPV 2663, partial right P4; SGOPV 2664, right M1 or 2; SGOPV 2665, left m1 or 2;

SGOPV 2666, right p4; SGOPV 2667, right m1 or 2; SGOPV 2668, left p4; SGOPV 2669, left m1 or 2; SGOPV 2670, left m3?; SGOPV 2671, left m1 or 2; SGOPV 2673, right M1 or 2; SGOPV 2674, right m1 or 2; SGOPV 2675, right m2–3; SGOPV 2676, right lower molar; SGOPV 2677, left lower molar; SGOPV 2678, right M3; SGOPV 2680, right P4; SGOPV 2681, right P4; SGOPV 2683, right P4–M2; SGOPV 2684, left m1 or 2; SGOPV 2685, m1 or 2; SGOPV 2687, left M1 or 2.

Locality and Horizon. Fossiliferous Interval E-0 (SGOPV 2421, 2673) Fossiliferous Interval E-2 (SGOPV 2101, 2675), Fossiliferous Interval 2 (SGOPV 2014), Fossiliferous Interval 3 (SGOPV 2030), Fossiliferous Interval 4 (SGOPV 2045, 2056, 2060, 2273, 2661, 2662, 2663, 2664, 2671, 2674, 2681, 2682), Fossiliferous Interval 5 (SGOPV 2080, 2665, 2687), Fossiliferous Interval 6-7 (SGOPV 2655, 2656, 2657, 2658, 2659, 2660), Fossiliferous Interval 7 (SGOPV 2121, 2378, 2666, 2667, 2668, 2669, 2670, 2677, 2678, 2680), Glyptodont Glen (SGOPV 2676), and unknown fossiliferous interval (SGOPV 2683), Galera Formation, Pampa Castillo, Chile.

Age and Distribution. Galera Formation, Santacrucian SALMA, Aysén Region, Chile; Santa Cruz Formation, Santacrucian SALMA, Santa Cruz Province, Argentina.

Description. Specimens of *Perimys onustus* from Pampa Castillo closely match those reported from the Santa Cruz Formation. This taxon is the largest-bodied species of *Perimys*, though little worn teeth fall within the size range exhibited by other *Perimys* species (Tables 6–7). The edges of the hypoflexi/ids of *Per. onustus* are often sinuous (Fig. 15B–D). Enamel on the labial surfaces of M1–3 and the lingual surfaces of p4–m3 is usually complete or missing a narrow vertical band.

M1–3 bear labial flexi, and p4–m3 bear lingual flexids (becoming more pronounced posteriorly). The upper molars are characterized by the anterolabial 'pillars' mentioned previously.

Remarks. *Perimys onustus* is the most commonly preserved species of *Perimys* in the Pampa Castillo fauna, slightly more abundant than *Per. erutus* (Supplementary File 9). After *Neoreomys australis*, *Per. onustus*, the second-most commonly recovered species at Pampa Castillo, occurs throughout the section. This is the first detailed description of material assigned to *Per. onustus* outside of the Santa Cruz Formation of Argentina (Scott, 1905; Croft, 2013; Arnal et al., 2019). Flynn et al. (2002a) reported *Per. onustus* from Pampa Castillo, as well as two species synonymized with it in an unpublished PhD dissertation (Kramarz, 2001), *Perimys* '*impactus*' and *Perimys* '*perpinguis*.'

Perimys intermedius Kramarz, 2002

Figure 15E

Perimys onustus Flynn et al., 2002a: 289 (*partim*), table 1.

Referred Material. SGOPV 2281, left p4–m1; SGOPV 2299, right m3; SGOPV 2645, right M3; SGOPV 2651, right P4–M1; SGOPV 2652, right m1–3 (Fig. 15E); SGOPV 2653, partial right M3; SGOPV 2654, right m1–2.

Locality and Horizon. Fossiliferous Interval E-0 (SGOPV 2299), Fossiliferous Interval 4 (SGOPV 2651, 2652, 2653), Fossiliferous Interval 4abc (SGOPV 2281),

and Fossiliferous Interval 7 (SGOPV 2645, 2654), Galera Formation, Pampa Castillo, Aysén Region, Chile.

Age and Distribution. Pinturas Formation, Santacrucian ('Pinturan') SALMA, Santa Cruz Province, Argentina; Galera Formation, Santacrucian SALMA, Aysén Region, Chile.

Description. As its name suggests, *Perimys intermedius* is intermediate in size between *Per. erutus* and *Per. onustus* (Tables 6–7; Kramarz 2002). The molar hypoflexi/id borders are straight, unlike in *Per. onustus* (Fig. 15E). *Per. intermedius* is most obviously distinguished from other species of the genus by the lack of enamel on the lingual faces of its lower molars and the labial faces of M1–2 (the labial wall of M3 in *Per. intermedius* generally bears enamel but in a narrower band than other species). The upper molars of *Per. intermedius* lack labial flexi, while p4–m2 lack lingual flexids. Specimens from Pampa Castillo here assigned to *Per. intermedius* are closely similar to those from the Pinturas Formation described by Kramarz (2002).

Remarks. *Perimys intermedius* is the least abundant of the four *Perimys* species at Pampa Castillo (Supplementary File 9). Of the four specimens whose precise provenance is known, three were recovered low in the section (Fossiliferous Interval E-0), and one high (Fossiliferous Interval 7). Besides Pampa Castillo, *Per. intermedius* has only been identified in the lower and middle sequences of the Pinturas Formation (lmPF), where it is the most abundant species of *Perimys* (Kramarz, 2002).

Perimys sp. nov.? Kramarz, 2002

Figure 15F

Perimys sp. Kramarz, 2002: 175–176.

Perimys impactus Flynn et al., 2002a: 289 (*partim*), table 1.

Referred Material. SGOPV 2267, right m2–3 (Fig. 15F); SGOPV 2285, right M1 or 2; SGOPV 2401, right m3; SGOPV 2431, right m3; SGOPV 2646, SGOPV 2647, right m1–2; SGOPV 2648, right m1 or 2; SGOPV 2649, left m1 or 2; SGOPV 2650, right m2–3; SGOPV 2679, left M1 or 2; SGOPV 2684, left m1 or 2; SGOPV 2686, left p4–m1.

Locality and Horizon. Fossiliferous Interval E-0 (SGOPV 2285, 2401, 2650), Fossiliferous Interval E-2 (SGOPV 2267, 2686), Fossiliferous Interval 4 (SGOPV 2646, 2647, 2648, 2649, 2684), and Fossiliferous Interval 7 (SGOPV 2431, 2679), Galera Formation, Pampa Castillo, Aysén Region, Chile.

Age and Distribution. Galera Formation, Santacrucian SALMA, Aysén Region, Chile; Pinturas Formation, Santacrucian (‘Pinturan’) SALMA, Santa Cruz Province, Argentina.

Description. These specimens from Pampa Castillo are similar in size (Tables 6–7) and morphology to the unnamed new species of *Perimys* from the Pinturas Formation mentioned by Kramarz (2002) and differ from other *Perimys* species in several respects. The labial edges of the upper molars are marked by narrow band

of enamel, and a narrow band of enamel occurs on the lingual surface of the lower molars unlike *Per. intermedius.* The edges of the hypoflexi/ids are straight in these specimens unlike *Per. onustus* (Fig. 15F).

Remarks. Owing to their poor match to described species, Kramarz (2002) assigned four distinctive specimens from the Pinturas Formation to *Perimys* sp. but declined to recognize a new species given the limited and fragmentary sample. The specimens from Pampa Castillo here assigned to *Perimys* sp. nov.? match Kramarz's (2002) description. *Perimys* sp. nov.? is distinguished from other members of the genus by a unique combination of features that are seen individually in other species (size, sinuosity of lophs, and enamel distribution). Unfortunately, our material is equally unsatisfactory for diagnosing a new species. In view of this, and being unable to directly examine the material described by Kramarz (2002), we similarly opt against naming a new taxon at this time.

Perimys sp. nov.? is the third most abundant species of *Perimys* at Pampa Castillo, after *Per. onustus* and *Per. erutus* (Supplementary File 9). In the Pinturas Formation, it is also the third most abundant, although it is far less common than *Per. intermedius* and *Per. erutus* (Kramarz, 2002).

Chinchillidae Bennett, 1833

Lagostominae Wiegmann, 1835

Prolagostomus Ameghino, 1887a

Type species. *Prolagostomus pusillus* Ameghino, 1887a.

Included Species. The type species, *Pro. obliquidens* Scott, 1905, *Pro. rosendoi* Vucetich, 1984, and *Prolagostomus.* sp. nov. Kramarz, 2002.

Age and Distribution. Pinturas Formation, Santacrucian ('Pinturan') SALMA, Santa Cruz Province, Argentina; Cerro Boleadoras Formation, Santacrucian SALMA, Neuquén Province, Argentina; Galera Formation, Santacrucian SALMA, Aysén Region, Chile; Santa Cruz Formation, Santacrucian SALMA, Santa Cruz Province, Argentina; Cura-Mallín Formation, Santacrucian? SALMA, Biobío Region, Chile; Collón Curá Formation, Colloncuran SALMA, Chubut, Neuquén, and Río Negro provinces, Argentina; Río Frías Formation, Colloncuran SALMA, Aysén Region, Chile, and Chubut Province, Argentina; unnamed formation (Quebrada Honda), Laventan SALMA, Tarija Department, Bolivia.

Prolagostomus pusillus Ameghino 1887a

Figure 15G–I

Pliolagostomus notatus Flynn et al., 2002a: 289, table 1.

Prolagostomus divisus Flynn et al., 2002a: 289, table 1.

Prolagostomus profluens Flynn et al., 2002a: 289, table 1.

Prolagostomus pusilus (sic) Flynn et al., 2002a: 289, table 1.

Referred Material. SGOPV 2427, left M1 or 2; SGOPV 2599, partial right P4–M2; SGOPV 2600, left lower molariform; SGOPV 2601, left lower molariform; SGOPV

2602, left p4 with root of left lower incisor (Fig. 15I); SGOPV 2603, partial left P4–M1; SGOPV 2604, left p4; SGOPV 2605, right lower molariform; SGOPV 2606, left p4 with root of left lower incisor; SGOPV 2607, right P4–M1 (Fig. 15G); SGOPV 2608, right M2–M3 (Fig. 15H); SGOPV 2609, partial left M1 or 2?; SGOPV 2610, partial left P4–M1; SGOPV 2611, right p4 and root of right lower incisor; SGOPV 2612, left lower molariform; SGOPV 2613, right p4; SGOPV 2614, left p4; SGOPV 2615, right p4.

Locality and Horizon. Fossiliferous Interval E-2 (SGOPV 2612), Fossiliferous Interval 4 (SGOPV 2613), Fossiliferous Interval 6-7 (SGOPV 2427, 2607, 2608, 2609, 2610, 2611), and Fossiliferous Interval 7 (SGOPV 2599, 2600, 2601, 2602, 2603, 2604, 2605, 2606, 2614, 2615), Galera Formation, Pampa Castillo, Chile.

Age and Distribution. Galera Formation, Santacrucian SALMA, Aysén Region, Chile; Santa Cruz Formation, Santacrucian SALMA, Santa Cruz Province, Argentina; Cura-Mallín Formation, Santacrucian? SALMA, Biobío Region, Chile; Collón Curá Formation, Colloncuran SALMA, Chubut, Neuquén, and Río Negro provinces, Argentina; Río Frías Formation, Colloncuran SALMA, Aysén Region, Chile, and Chubut Province, Argentina.

Description. The cheek teeth of *Pro. pusillus* are hypselodont with two simple laminae, except M3, which has three laminae. Although broadly similar to *Perimys*, the laminae and hypoflexi/ids of *Pro. pusillus* are much narrower anteroposteriorly. Moreover, the hypoflexus P4 of *Pro. pusillus* opens lingually, like M1–3, differing from *Perimys* (where the laminae of P4 open labially). The hypoflexi of P4–M3 are oriented transversely and filled with cementum. The molars of *Pro. pusillus* differ

from those of *Pliolagostomus* in the former's slightly more convex anterior and posterior borders. Additionally, the anterior lophs (anteroloph, per Rasia and Candela 2019a) of the upper molars project further labially than the posterior lophs in *Pro. pusillus*, whereas they extend equally far in *Pliolagostomus*. The anterior and lingual faces of the lower molars have a smooth transition in *Pro. pusillus*, whereas in *Pliolagostomus* the interface is more angular.

Lower molars of the Colloncuran-aged *Pro. rosendoi* are unknown (Vucetich, 1984), and the lower molars of a possibly new *Prolagostomus* species from the Pinturas Formation are indistinguishable from those of *Pro. pusillus* (Fig. 15I; Kramarz, 2002; Rasia, 2016). We assign these lower molar specimens from the Pampa Castillo fauna to *Pro. Pusillus,* however, because it is the most parsimonious conclusion given their morphological match with *Pro. pusillus* and the presence of upper teeth only referable to *Pro. pusillus* in the same stratigraphic level.

Remarks. In an unpublished PhD thesis, Rasia (2016) recognized two, or possibly three, *Prolagostomus* species from the Santacrucian SALMA, many fewer than previous authors (e.g., Ameghino, 1887a; Scott, 1905), by synonymizing most previously recognized species with the type, *Pro. pusillus*. *Prolagostomus obliquidens* was left valid, but one of the authors of this study (AJM) was unable to locate the type and sole specimen of *Pro. obliquidens* in the collections of the Yale Peabody Museum. Rasia (2016) concurred with Kramarz (2002) that the *Prolagostomus* specimens from the Pinturas Formation seem distinct from all known species but cautioned that better quality specimens were needed to verify this hypothesis.

Prolagostomus pusillus is common at Pampa Castillo, its abundance trailing only that of *N. australis*, *Per. onustus*, *Per. erutus*, and *Perimys* sp. nov.? among rodents (Supplementary File 9). *Prolagostomus pusillus,* previously reported from the Santa Cruz, Río Frías, and Collón Curá formations and the Honda Group (Bolivia) (Ameghino, 1887c; Scott, 1905; Vucetich, 1984; Bamba and Croft, 2015; Rasia, 2016), is likely the only species of the genus recorded at Pampa Castillo.

Dinomyidae Alston, 1876

Scleromys Ameghino, 1887a

Type Species. *Scleromys angustus* Ameghino, 1887a.

Included Species. The type species, *Scl. osbornianus* Ameghino, 1894, *Scl. quadrangulatus* Kramarz, 2006a, and *Scl. praecursor* Boivin et al., 2017b. Note: Although "*Scleromys*" *colombianus* Fields, 1957 and "*Scleromys*" *schurmanni* Stehlin, 1940 from northern South America appear more closely related to the extant Dinomyidae than to fossil species of *Scleromys* from Patagonia, they have not yet been formally reassigned to another taxon (Patterson and Wood, 1982; Walton, 1997; Kramarz et al., 2013). As they are clearly distinct from *Scleromys* sensu stricto, they will not be considered here.

Age and Distribution. Chambira Formation, Deseadan SALMA, Peru; Pinturas Formation, Santacrucian ('Pinturan') SALMA, Santa Cruz Province, Argentina; Galera Formation, Santacrucian SALMA, Aysén Region, Chile; Santa Cruz Formation, Santacrucian SALMA, Santa Cruz Province, Argentina; Cura-Mallín

Formation, Santacrucian? SALMA, Biobío Region, Chile; Chinches Formation, Santacrucian SALMA, San Juan Province, Argentina.

Scleromys quadrangulatus Kramarz, 2006a

Figure 15J–K

Scleromys sp. Flynn et al., 2002a: 289 (*partim*), table 1.

Referred Material. SGOPV 2699, roots of left p4 and complete left m1–2 (Fig. 15K); SGOPV 2700, complete right p4 (Fig. 15J) and partial right m1–2; SGOPV 2701, left m1 or 2; SGOPV 2702, left p4; SGOPV 2703, left m1 or 2.

Locality and Horizon. Fossiliferous Interval 4 (SGOPV 2699, 2700, 2702, 2703) and unknown fossiliferous interval (SGOPV 2701), Galera Formation, Pampa Castillo, Aysén Region, Chile.

Age and Distribution. Pinturas Formation, Santacrucian ('Pinturan') SALMA, Santa Cruz Province, Argentina; Galera Formation, Santacrucian SALMA, Aysén Region, Chile.

Description. Two specimens, SGOPV 2700 and SGOPV 2702, preserve the p4 of *Scl. quadrangulatus*. Although p4 of SGOPV 2700 is slightly longer anteroposteriorly than that of SGOPV 2702, these teeth are otherwise remarkably similar (Table 6). Metalophulid I is straight and transversely oriented in both (Fig. 15J). The posterolophid of p4 in SGOPV 2700 is straighter and more transverse than in SGOPV 2702, but this difference likely reflects the latter specimen's lesser wear, as

evidenced by its open anteroflexid. The m1 and m2 of *Scl. quadrangulatus* closely resemble one another; both are preserved in SGOPV 2699 and SGOPV 2700 (Fig. 15J–K). SGOPV 2703, an isolated tooth, thus may represent either tooth position. As on p4, the metalophulid I of m1 and m2 are straight and transversely oriented. In the m1–2 of SGOPV 2703, and the m1 of SGOPV 2699, the anterofossettid is completely separated from the mesoflexid/fossettid by the neomesolophid, but in m1–2 of SGOPV 2701 and the m2 of SGOPV 2699, the neomesolophid does not join metalophulid I, so the fossettids are merged. The anterolabial corners of m1 and m2 of SGOPV 2700 are damaged, so their details are unknown.

Remarks. We assign these specimens to *Scleromys quadrangulatus* based on the diagnostic straight, transverse metalophulid I. This is the only known record of *Scl. Quadrangulatus* apart from the lower and middle part of the Pinturas Formation (Kramarz, 2006b). *Scleromys angustus* and *Scleromys osbornianus* are known from the Santa Cruz Formation (Ameghino, 1887c; Scott, 1905; Arnal et al., 2019), and the latter species also occurs in the upper Pinturas Formation (Kramarz, 2006b). A fourth species, *Scleromys praecursor*, has been reported from the late Oligocene (Deseadan SALMA) of Contamana, Peru (Boivin et al., 2017).

Scleromys sp. nov.?

Figure 15L–M

Scleromys sp. Flynn et al., 2002a: 289 (*partim*), table 1.

Referred Material. SGOPV 2704, right lower molar.

Locality and Horizon. Fossiliferous Interval 4, Galera Formation, Pampa Castillo, Aysén Region, Chile.

Description. SGOPV 2704 likely represents a right lower molar (Fig. 15L). It is approximately the same size as the Pampa Castillo specimens assigned to *Scl. quadrangulatus* (Table 6). The metaflexid and hypoflexid are merged, and the mesofossettid is hourglass-shaped. No trace of the anterofossettid is preserved. The posterior border of the metaflexid-hypoflexid is irregular rather than smoothly curved or sinuous. The posterolophid is broad and smoothly convex. The anteroloph, in contrast, is straight and extends anterolingually from the protoconid. The hypoconid extends further labially than the protoconid. The most notable aspect of this tooth is its lack of enamel around its posterolingual corner (Fig 3M).

Remarks. SGOPV 2704 differs from other species of *Scleromys* in its lack of enamel on the posterolabial corner of the lower molar (Fig. 15L). Enamel is discontinuous on the cheek teeth of some late-diverging dinomyids (Rinderknecht et al., 2011; Kerber et al., 2018), but this feature has not been reported in Santacrucian or Laventan species of *Scleromys* or "*Scleromys*" (Scott, 1905; Fields, 1957; Walton, 1997; Kramarz, 2006b; Cerdeño and Vucetich, 2007). This enamel band has smooth borders and a constant width from crown to root, which suggests that its absence from the posterolabial corner is not a preservational artifact. We conservatively refer this specimen to *Scleromys* sp. nov.? since the only available material is a single tooth.

Erethizontoidea Bonaparte, 1845

Erethizontidae Bonaparte, 1845

Eosteiromys Ameghino, 1902

Type Species. *Eosteiromys homogenidens* Ameghino, 1902.

Included Species. The type species, *Eos. annectens* Ameghino, 1899, and *Eos. segregatus* Ameghino, 1902.

Age and Distribution. Colhue-Huapi Member, Sarmiento Formation, Colhuehuapian and Santacrucian ('Pinturan') SALMAs, Chubut Province, Argentina; Cerro Bandera Formation, Colhuehuapian(?) SALMA, Neuquén Province, Argentina; Galera Formation, Santacrucian SALMA, Aysén Region, Chile; Pinturas Formation, Santacrucian ('Pinturan') SALMA, Santa Cruz Province, Argentina.

Eosteiromys cf. *Eos. annectens* Ameghino, 1899

Figure 16A

Steiromys new sp. Flynn et al., 2002a: 289, table 1.

Referred Material. SGOPV 2157, right mandibular fragment with roots of the incisor and p4, and complete m1–2 (Fig. 16A); SGOPV 2688, partial right (d?)p4; SGOPV 2752, left dp4.

Locality and Horizon. Fossiliferous Interval E-0 (SGOPV 2157, 2688) and unknown level (SGOPV 2752), Galera Formation, Pampa Castillo, Aysén Region, Chile.

Age and Distribution. Galera Formation, Santacrucian SALMA, Aysén Region, Chile; Pinturas Formation, Santacrucian (‘Pinturan’) SALMA, Santa Cruz Province, Argentina.

Description. SGOPV 2157 preserves the root of the lower right incisor. This incisor seems slightly labiolingually flattened (although the specimen may be slightly deformed), but it is still convex labially (externally/ventrally), and slightly thicker labiolingually than wide mesiodistally.

The crown of (d?)p4 of SGOPV 2157 is obliterated (Fig. 16A), whereas SGOPV 2688 represents a heavily worn partial (d?)p4. SGOPV 2688 is tetralophodont and bears a small spur within the anterofossettid, likely representing a neolophid (Candela, 2002; Boivin and Marivaux, 2020). The neomesolophid splits before reaching the lingual edge of the dp4, to meet the metaconid and mesostylid, producing a small fossettid. The mesolophid is small and weakly joined to the mesostylid. The hypolophid and posterolophid are both obliquely oriented, and the posterolophid is strongly curved. SGOPV 2752 also represents a dp4 but is much better preserved. It is pentalophodont; the mesostylid does not fully connect with the ectolophid, and there is a small structure suggestive of a neolophid within the anterofossettid.

SGOPV 2157 preserves m1 and m2, both of which are brachydont and tetralophodont (Fig. 16A; Table 6). The anterofossettids and metafossettids are closed, whereas the mesoflexids and hypoflexids remain open. All three lingual flexids/fossettids are approximately equal in width. In m1, the anterofossettid, mesoflexid, and metafossettid extend approximately the same distance labially, but

in m2, the anterofossettid extends farther than the other two fossettids. Metalophulid I on both teeth is straight and transversely oriented, whereas the neomesolophid and hypolophid are somewhat sinuous. The posterolophid curves gently to join the hypoconid. Particularly in m2, the anterior arm of the hypoconid, separating the hypoflexid and metafossettid, is thinner than the other lophids suggesting that these features were united in an earlier stage in wear.

Remarks. We regard SGOPV 2157 as assignable to a species of *Eosteiromys* based on its tetralophodont molars, unlike *Branisamyopsis* Candela, 2003, which is pentalophodont. Additionally, the incisor in this specimen is transversely narrow, with a slightly convex labial (external) face, unlike in *Steiromys* Ameghino, 1887a, which has much broader (mesiodistally) incisors with flatter faces. Among named *Eosteiromys* species, SGOPV 2157 bears closest resemblance to *Eos. annectens* Kramarz, 2004. The weak connection between the hypoconid and hypolophid distinguishes this taxon from *Eosteiromys homogenidens*. Although SGOPV 2157 is smaller than all specimens of *Eos. annectens* from the Pinturas Formation (Kramarz, 2004), this difference is slight (~0.5 mm). In an unpublished PhD thesis, Candela (2000) described a species smaller than *Eos. annectens* from the Colhuehuapian of Gran Barranca that also has a weak connection between the hypoconid and hypolophid (Kramarz, 2004; Vucetich et al., 2010). Unfortunately, we were unable to study this material firsthand to compare it to SGOPV 2157 directly.

We also refer SGOPV 2688 and 2752 to *Eosteiromys* cf. *Eos. annectens*. The p4s and dp4s of *Steiromys* and *Branisamyopsis* are hexalophodont, while those of *Hypsosteiromys* Patterson, 1958 are tetralophodont (Candela, 2002, 2003). The

morphology of SGOPV 2752 closely matches that of *Eos. annectens* (Kramarz, 2004), including its incomplete mesolophid and slight neolophid. The identification of SGOPV 2688 is much more tenuous due to its high degree of wear, but its size (larger than contemporaneous octodontoids), and known presence of *Eos.* cf. *Eos. annectens* in the fauna lead us to assign it to this taxon.

Eosteiromys species are known from Colhuehuapian and 'Pinturan' localities throughout Patagonia (Kramarz, 2004; Kramarz et al., 2005, 2010; Vucetich et al., 2010). *Eosteiromys annectens*, to which we provisionally refer the specimens from Pampa Castillo, was previously reported only from the lower and middle sequences of the Pinturas Formation (Kramarz and Bellosi, 2005).

Steiromys Ameghino, 1887a

Type Species. *Steiromys detentus* Ameghino, 1887a.

Included Species. The type species, *St. duplicatus* Ameghino, 1887a, and *St. principalis* Ameghino, 1899.

Age and Distribution. Galera Formation, Santacrucian SALMA, Aysén Region, Chile; Pinturas Formation, Santacrucian ('Pinturan') SALMA, Santa Cruz Province, Argentina; Santa Cruz Formation, Santacrucian SALMA, Santa Cruz Province, Argentina.

Steiromys sp.

Figure 16B–C

Steiromys duplicatus Flynn et al., 2002a: 289, table 1.

Referred Material. SGOPV 2190, partial left M1 or M2 (Fig. 16B); SGOPV 2689, right m3 (Fig. 16C).

Locality and Horizon. Fossiliferous Interval E-0 (SGOPV 2689) and Fossiliferous Interval 7 (SGOPV 2190), Galera Formation, Pampa Castillo, Aysén Region, Chile.

Description. SGOPV 2190 is a little-worn brachydont upper molar that is missing the posterolabial corner (Fig. 16B; Table 7). The anteroloph is labiolingually oriented until it joins the protocone, which itself has an arm that projects posterolingually. The parafossette, enclosed labially, is continuous with the hypoflexus, but a small, low crest connecting the protocone and protoloph indicates that these features would become separated after additional wear. The protoloph and mesolophule parallel one another, and the mesoflexus is open. The hypocone is large and pointed.

The tetralophodont SGOPV 2689, a right m3, is low-crowned, bears thick enamel bands around its perimeter, and is notably larger than the lower molars assigned to *Eosteiromys* cf. *Eos. annectens* (Fig 4C; Table 6). Metalophulid I is straight and angled slightly anterolingually. The posterior arm of the protoconid, angled posterolingually, barely reaches the entolophid despite the specimen's advanced wear stage. The hypolophid is labiolingually oriented and straight, whereas the posterolophid is curved. The anterofossettid, the anteroposteriorly widest of the lingual fossettids, broadens lingually. The metafossettid is the next widest lingual fossettid, and the mesofossettid is the narrowest. All three lingual

fossettids are very shallow. The hypoflexid, which points directly lingually, is constricted at its labial edge by the protoconid and hypoconid.

Neither specimen preserves sufficient diagnostic morphology to assign it to one of the three recognized species of this genus.

Remarks. These specimens are lower crowned than *Hypsosteiromys* (Candela and Vucetich, 2002) and notably larger than *Eosteiromys* (Tables 6–7; Kramarz 2004). The flexi of SGOPV 2190 are deep and wide, unlike those of *Branisamyopsis* (Fig. 16B; Kramarz 2004). SGOPV 2689 is tetralophodont (Fig. 16C), distinguishing it from *Branisamyopsis* and *Hypsosteiromys* (Candela and Vucetich, 2002; Candela, 2003).

Steiromys is a common rodent in faunas in the Santa Cruz and Pinturas formations (e.g., Scott 1905; Kramarz 2004; Croft, 2013; Arnal et al. 2019). *Steiromys detentus* and *St. principalis* are known exclusively from the Santa Cruz and Pinturas formations, respectively, whereas *St. duplicatus* has been recovered from both.

DISCUSSION

Pampa Castillo Compared to Other Santacrucian Rodent Faunas

Cavioids—The cavioid assemblage from Pampa Castillo is largely what would be expected of a Santacrucian SALMA fauna, with the exception of *Luantus minor*.

Eocardia (Fig. 14B–E) is fairly common in Santa Cruz Formation (SCF) faunas (Fig. 17; Scott, 1905; Candela et al., 2012; Arnal et al., 2019) but absent from the Pinturas Formation (Kramarz, 2006a). *Luantus minor* (Fig. 14A) was previously known only from the Colhuehuapian-aged fauna at Bryn Gwyn, which is both older and approximately 800 km north of the core Santacrucian faunas (Fig. 13; Pérez et al., 2010). *Luantus* is abundant in the Pinturas Formation, where it is represented by two species (*L. propheticus* in lower-middle Pinturas Formation [lmPF] and *L. toldensis* in the upper Pinturas Formation), neither of which occurs at Pampa Castillo. Other 'eocardiids' such as *Phanomys* and *Schistomys* are known from the Santa Cruz and Pinturas formations (Scott, 1905; Kramarz, 2006a; Bostelmann et al., 2013; Cuitiño et al., 2019a; Pérez et al., 2019) but have yet to be identified from Pampa Castillo, though the presence of *Schistomys* cannot be ruled out completely due to the lack of diagnostic premolars in specimens assigned to *Eocardia* (Fig. 14B–E). Overall, 'eocardiids' are fairly uncommon at Pampa Castillo compared to other early Miocene Patagonian faunas (Fig. 17).

Neoreomys australis is the most common rodent (and mammal) at Pampa Castillo, a pattern seen in many SCF faunas (Fig 5; Scott, 1905; Candela et al., 2012; Pérez et al., 2019). Two species are known from the lmPF, *N. australis* and *Neoreomys pinturensis*, with the latter being more abundant in levels where they co-occur (Kramarz, 2006b). Although *Neoreomys* is common in the lmPF, it forms a smaller fraction of the fauna than *N. australis* does at Pampa Castillo and many SCF localities (Fig. 17).

Cavioids provide mixed evidence for Pampa Castillo's broader temporal affinities. The presence of *Luantus* seemingly indicates affinities with lmPF and Colhuehuapian faunas, but the presence of *Eocardia* and the absence of *N. pinturensis* seem to show a closer relationship with SCF faunas.

Chinchilloids—The chinchilloid community supports the Pampa Castillo fauna's referral to the Santacrucian SALMA. All four *Perimys* species, including the yet unnamed *Perimys* sp. nov.? originally reported from the lmPF (Kramarz, 2002), that have been reported from Santacrucian localities elsewhere also are found at Pampa Castillo. Pampa Castillo is the only locality where all four co-occur, however; there does not appear to be any stratigraphic pattern to these species' relative abundance at Pampa Castillo. Two of these species, *Per. intermedius* and *Perimys* sp. nov.?, were previously known only from the lmPF and upper Pinturas Formation, respectively (Fig. 15E–F; Kramarz, 2002). *Perimys onustus* (Fig. 15B–D) was previously known only from the SCF, whereas *Per. erutus* (Fig. 15A) was known from the SCF and Pinturas Formation (Scott, 1905; Kramarz, 2002; Arnal et al., 2019). *Prolagostomus pusillus* is the only chinchillid identified from Pampa Castillo and is common throughout the SCF (Fig. 15G–I; Rasia, 2016). Kramarz (2002) recognized a probable new species of *Prolagostomus* from the lmPF and upper Pinturas Formation which we did not recover at Pampa Castillo. *Pliolagostomus*, a chinchillid known from core Santacrucian faunas of the SCF, is absent at Pampa Castillo. *Scleromys* is common throughout Santacrucian assemblages, but the taxon from Pampa Castillo, *Scl. quadrangulatus*, was previously known only from the lmPF

(Fig. 15J–K; Scott, 1905; Kramarz, 2002; Arnal et al., 2019). A single tooth (SGOPV 2704; Fig. 15L–M) may represent a new species of *Scleromys*.

Chinchilloids point to a close association of Pampa Castillo and the lmPF. Three taxa, *Per. intermedius*, *Perimys* sp. nov., and *Scl. quadrangulatus*, are known exclusively from these two faunas. The absence of *Pliolagostomus*, *Scl. angustus*, and *Scl. osbornianus* at both Pampa Castillo and lmPF also support this relationship, as these taxa are common in core Santacrucian coastal SCF and RSC faunas (Fig. 17). An important contrast between the rodent faunas from Pampa Castillo and the lmPF is that all *Prolagostomus* specimens from the Pinturas Formation have been assigned to a probable new species (Kramarz, 2002), while all specimens from Pampa Castillo pertain to *Pro. pusillus,* a widespread Santacrucian–Laventan SALMA species.

Erethizontoids—Although uncommon, the erethizontids from Pampa Castillo (Fig. 17) are typical of Santacrucian assemblages. *Eosteiromys annectens*, to which we provisionally assign two specimens (Fig. 16A), was previously known only from the lmPF (Kramarz, 2004). *Eosteiromys* is otherwise known from the Colhuehuapian SALMA, though *Eosteiromys homogenidens* has been provisionally recorded in the lmPF as well (Kramarz et al., 2005; Vucetich et al., 2010). *Steiromys* is common throughout Santacrucian assemblages. Both *St. detentus* and *St. duplicatus* occur in SCF deposits (Scott, 1905; Candela et al., 2012; Arnal et al., 2019). *Steiromys principalis* is only known from the lmPF, where *St. duplicatus* is also known (Kramarz, 2004). Unfortunately, the two *Steiromys* specimens identified from Pampa Castillo are inadequate for species-level identification (Fig. 16B–C). The single

erethizontid genus known from other Santacrucian faunas not represented at Pampa Castillo is *Branisamyopsis*, which is also apparently absent from the SCF. *Branisamyopsis praesigmoides* Kramarz, 2004, is known from the lmPF, but the genus is also known from the Colhuehuapian and Colloncuran SALMAs (Candela, 2003).

The presence of *Eosteiromys* at Pampa Castillo suggests affinities with the lmPF, although the absence of *Branisamyopsis*, as in the SCF, argues against this. *Steiromys* is common in most Santacrucian assemblages, so its presence at Pampa Castillo is of limited biogeographic significance.

Paleoenvironmental Implications

The fossil rodents of Pampa Castillo are indicative of a forested paleoenvironment including some open areas. Erethizontids are considered forest-dwellers due to their brachydont dentition, an inference based on extant species and, at least for *Steiromys*, scansorial-arboreal specializations of their skeleton (Kramarz and Bellosi, 2005; Candela et al., 2012; Muñoz et al., 2019). Erethizontids are not abundant at Pampa Castillo. High-crowned (hypsodont) and particularly ever-growing (hypselodont or euhypsodont) cheek teeth in rodents and ungulates are widely considered indicative of grazing habits and/or open environments (Williams and Kay, 2001; Mendoza and Palmqvist, 2008; Kaiser et al., 2013; Ma et al., 2017). Several hypselodont rodents (*Prolagostomus*, *Perimys*, and *Eocardia*) occur at Pampa Castillo. *Perimys*, the most common hypselodont genus (Fig. 17),

has been interpreted as a digger based on its forelimb anatomy (Muñoz et al., 2019), and thus its hypselodonty may reflect abrasive subterranean food sources like roots and tubers rather than open habitats. *Eocardia*, however, has a cursorially adapted skeleton, likely reflecting the presence of some open paleohabitats at Pampa Castillo (Candela et al., 2012; Muñoz et al., 2019). Modern chinchillids favor open habitats, but the locomotory and dietary preferences of *Prolagostomus* have never been analyzed in their own right. The most abundant rodent at Pampa Castillo, *Neoreomys australis*, has been interpreted as ambulatory with running and possibly swimming capabilities, and a diet similar to, but slightly harder and more abrasive than, modern dasyproctids (agoutis), again suggesting a closed or somewhat closed forest habitat (Candela et al., 2012; Muñoz et al., 2019). The octodontoid caviomorphs of Pampa Castillo are not described here, but the majority of specimens are brachydont suggesting a closed habitat.

Pampa Castillo appears to record a paleoenvironment intermediate between those of fossiliferous localities of the eastern Santa Cruz Formation (SCF), and those of the lower to middle sequences of the Pinturas Formation (lmPF). Fossil vertebrate-based, sedimentological, and paleobotanical studies focusing on core Santacrucian localities have reconstructed the paleoenvironment as a mosaic of open and closed habitats on a coastal floodplain with a seasonal subtropical paleoclimate (Brea et al., 2012; Kay et al., 2012; Raigemborn et al., 2015, 2018a, 2018b; Cuitiño et al., 2019a, 2019b; Catena and Croft, 2020; Kay et al., 2021). Arnal et al. (2019) summarized the taxonomic composition and abundance of rodents at different RSC sites, where *Neoreomys australis* is the most abundant rodent.

However, it is not as dominant there as at Pampa Castillo, given the nearly equal abundance of *Neoreomys*, *Eocardia,* and *Prolagostomus* in RSC faunas versus the clear dominance of *Neoreomys* at Pampa Castillo (Fig. 17). The most abundant octodontoids at RSC sites (*Spaniomys*, *Stichomys*) are hypsodont, unlike those present at Pampa Castillo. As mentioned, the cursorial *Eocardia* is very abundant at RSC, and the morphologically similar *Schistomys* is also present. Erethizontids are represented solely by *Steiromys* spp. in RSC faunas (and throughout the SCF).

The fossil fauna of the lmPF suggests that it records a more humid paleoenvironment than at Pampa Castillo (Kramarz and Bellosi, 2005; Novo and Fleagle, 2015). The paleopedological, sedimentological, and ichnofossil record suggest semi-arid conditions (Bown and Larriestra, 1990; Genise and Bown, 1994). Kramarz and Bellosi (2005) reconciled this contradiction by suggesting that while is the fossil fauna was composed primarily of taxa that inhabited the area during relatively humid times, the sedimentological record is dominated by processes operating during drier intervals. Accordingly, the lmPF rodent community may be seen as having inhabited a relatively humid paleoenvironment, despite seemingly conflicting lithological indicators. Erethizontids are generally considered indicators of forested paleohabitats due to their brachydont dentitions, arboreal adaptations, and the habits of extant taxa (Candela and Picasso, 2008; Candela et al., 2012; Kay et al., 2012). They are more diverse (3 genera; 5 species) and abundant in the lmPF than at Pampa Castillo (Kramarz, 2004). Additionally, no hypselodont ‘eocardiids’ are present in the lmPF (Kramarz, 2006a), unlike at Pampa Castillo. *Neoreomys australis*, the most abundant rodent at Pampa Castillo, is found in the lmPF, but a

lower-crowned species, *Neoreomys pinturensis*, is also present in the lmPF, suggesting a more closed habitat there than at Pampa Castillo (Kramarz, 2006b). Chinchilloids of the lmPF (*Per. intermedius*, *Scl. quadrangulatus*, and *Prolagostomus* sp. nov.) are not paleoenvironmentally informative, as these taxa have not been linked to any particular habitat type through their dietary or locomotory adaptations (Kramarz, 2002; Kramarz and Bellosi, 2005).

Biochronological Implications of Pampa Castillo Cavioids, Chinchilloids and Erethizontids

Together, cavioids, chinchilloids, and erethizontoids support temporal correlation of the Pampa Castillo fauna to other assemblages from the Santacrucian SALMA, but a more precise assignment is challenging. There are resemblances to, but also differences from, the rodent faunas from both core Santacrucian and 'Pinturan' (the lower to middle Pinturas Formation [lmPF] and UFZ at the Gran Barranca) faunal assemblages. The Pinturas Formation was first recognized as bearing a fauna distinct from and more 'primitive' than Santacrucian assemblages by Ameghino (1906) which he termed the Astrapothericulense after the astrapothere *Astrapothericulus* Ameghino, 1902. This distinction was endorsed by Frenguelli (1931) and Castellanos (1937), who referred to the fauna as the 'Pinturense,' but was subsequently disregarded by most researchers (e.g., Wood and Patterson, 1959; Marshall et al., 1983; Flynn and Swisher, 1995). Thorough description of Pinturas Formation rodents more recently (e.g., Kramarz 2001, 2002, 2004) led Kramarz and Bellosi (2005) to refer to the rodent community of the lower and middle sequences of the Pinturas Formation (lmPF) as the 'Pinturan' association. Since

then, various authors have used the term ‘Pinturan’ to refer to this fauna from the lmPF as a whole as well as to the hypothesized biochronologic interval that would be typified by it (e.g., Flynn et al., 2008; Kramarz et al., 2010; Dunn et al., 2013; Solórzano et al., 2020). Though ‘Pinturan’ and Astrapothericulense (or Astrapothericulan) refer to similar assemblages, the former name is preferable. Ameghino (1906) coined Astrapothericulense based on fossil collections made without precise stratigraphic control, likely including fossils from all levels of Pinturas Formation, whereas ‘Pinturan’ is restricted to faunas from the lower and middle sequences (Kramarz and Bellosi, 2005).

It may be that taxonomic differences between core Santacrucian and ‘Pinturan’ faunas are more reflective of differences in paleoenvironment than age distinctions. The Pampa Castillo rodent fauna represents an assemblage that appears to be taxonomically and paleoenvironmentally intermediate between the lmPF and core Santacrucian faunas. More detailed analyses of the taxonomic composition and geochronological age of other elements of the Pampa Castillo fauna may shed additional light on its correlation with and affinities to other faunas within the Santacrucian SALMA. Better characterizing faunal similarities between the Pinturas Formation of Argentina and the Galera Formation/Pampa Castillo fauna would help justify formally recognizing ‘Pinturan’ as a distinct SALMA or a ‘subage’ of the Santacrucian.

CONCLUSIONS

Each of the three major clades (‘superfamilies’) of caviomorphs described in this article is represented by multiple taxa. Cavioids are represented by three genera and three species (Fig. 14), including the most abundant taxon in the Pampa Castillo fauna, *Neoreomys australis* (Fig. 17). Chinchilloids are represented by three genera and six or seven species. Pampa Castillo is the only fauna where four species of *Perimys* co-occur (Fig. 15A–F). SGOPV 2542 (Fig. 15L–M) may represent a new species of *Scleromys* that is not named (Fig. 15J–K). Erethizontids, although rare, are represented by two genera (Fig. 16).

Caviomorphs of the Pampa Castillo fauna suggest a paleoenvironment intermediate between the open and closed mosaic habitat of the core Santacrucian faunas of the Santa Cruz Formation along the Río Santa Cruz and Atlantic coast and the closed forest of the lower and middle sequences of the Pinturas Formation (lmPF). Hypselodont, cursorial ‘eocardiids’ such as *Eocardia*, indicators of open habitats in modern ecosystems, are present in the Pampa Castillo fauna but are less diverse and abundant than in core Santacrucian faunas (Fig. 17). Erethizontids, presumed to have been somewhat arboreal and therefore indicative of closed paleohabitats, are more diverse and abundant in the lmPF than at Pampa Castillo.

The cavioid, chinchilloid, and erethizontid rodents of Pampa Castillo support its assignment to the Santacrucian SALMA, in agreement with previous work (Flynn et al., 2002a; McGrath et al., 2020). We also agree with the earlier observation by Chick et al. (2010) that the Pampa Castillo rodent community shares certain similarities to that of the lmPF which some authors recognize as the characteristic

fauna of a distinct but as yet not formalized biochronologic interval, the ‘Pinturan.’ Additional taxonomic and geochronologic work is needed, however, to more clearly assess whether the Pampa Castillo fauna supports or refutes the existence of a distinct ‘Pinturan’ biochron.

Acknowledgements

We are grateful to the following institutions for providing access to their collections: American Museum of Natural History and Yale Peabody Museum for providing access to their collections for comparison purposes. We thank the Eppley Foundation for Scientific Research and the American Museum of Natural History for funding the field work in Chile, and Rutgers University and The Field Museum for supporting JF’s participation. We thank Greg Buckley, René Burgos, Roger Carpenter, Mark Norell, Michael Novacek, Paul Raty, Paul Sereno, Carlos de Smet, Cruz Vargas, and members and friends of the de Smet family, for assistance in the field. Jeanne Kelly and Jane Shumsky of the American Museum of Natural History expertly prepared the specimens.

REFERENCES

Alston, E.R. 1876. On the classification of the order Glires. Proceedings of the Zoological Society of London 44:61–98.

Ameghino, F. 1887a. Observaciones generales sobre el orden de mamíferos extinguidos sudamericanos llamados toxodontes (Toxodontia) y sinopsis de los

géneros y especies hasta ahora conocidos. Anales Del Museo de La Plata Entrega es:1–66.

Ameghino, F. 1887b. Apuntes preliminares sobre algunos mamíferos extinguidos del yacimiento de Monte Hermoso. Boletín Museo de La Plata 1:3–20.

Ameghino, F. 1887c. Enumeración sistemática de las Ameghino, F. 1887. Enumeración sistemática de las especies de mamíferos fósiles coleccionados por Carlos Ameghino en los terrenos eocenos de la Patagonia austral y depositados en el Museo de La Plata. Boletín Museo de La Pla. Boletín Museo de La Plata 5:445–469.

Ameghino, F. 1889. Contribución al conocimiento de los mamíferos fósiles de la República Argentina. Actas de La Academia Nacional de Ciencias de Córdoba 6:1–1027.

Ameghino, F. 1891. Caracteres diagnósticas de cincuenta epécias nuevas de mamíferos fósiles argentinos. Revista Argentina de Historia Natural 1:129–167.

Ameghino, F. 1894. Ennumération synoptique des espéces de mammiféres fossilies des formations éocénes de Patagonie. Boletín de La Academia Nacional de Ciencias de Córdoba 13:259–445.

Ameghino, F. 1899. Sinópsis Geológico-Paleontológica. Suplemento (Adiciones y Corecciones) 1. La Plata, Argentina:, .

Ameghino, F. 1902. Premiére contribution a la connaisance de la faune mammalogique des couches a Colpodon. Boletín de La Academia Nacional de Ciencias de Córdoba 17:71–138.

Ameghino, F. 1906. Les formations sédimentaires du Crétacé Supérieur et du Tertiaire de Patagonie avec un parallelé entre leurs faunes mammalogiques et celles de l’ancien continent. Anales Del Museo Nacional de Buenos Aires (Tercera Serie) 8:1–568.

Antoine, P.-O. et al. 2012. Middle Eocene rodents from Peruvian Amazonia reveal the pattern and timing of caviomorph origins and biogeography. Proceedings of the Royal Society B: Biological Sciences 279:1319–1326.

Arnal, M., M.E. Pérez, and C.M. Deschamps. 2019. Revision of the Miocene caviomorph rodents from the Río Santa Cruz. Publicación Electrónica de La Asociación Paleontológica Argentina 19:193–229.

Bamba, K., and D.A. Croft. 2015. A reassessment of the middle Miocene lagostomine chinchillids (Rodentia) of Quebrada Honda, Bolivia. Society of Vertebrate Paleontology Annual Meeting 84.

Bennett, E.T. 1833. On the family Chinchillidae, and on a new genus referrible to it. Proceedings of the Zoological Society of London 1:35.64.

Bertrand, O.C., J.J. Flynn, D.A. Croft, and A.R. Wyss. 2012. Two new taxa (Caviomorpha, Rodentia) from the early Oligocene Tinguiririca fauna (Chile).

American Museum Novitates 1–36.

Blisniuk, P.M., L.A. Stern, C.P. Chamberlain, B.D. Idleman, and P.K. Zeitler. 2005. Climatic and ecologic changes during Miocene surface uplift in the southern Patagonian Andes. Earth and Planetary Science Letters 230:125–142.

Boivin, M., and L. Marivaux. 2020. Dental homologies and evolutionary transformations in Caviomorpha (Hystricognathi, Rodentia): new data from the Paleogene of Peruvian Amazonia. Historical Biology 32:528–554.

Boivin, M., L. Marivaux, and P.-O. Antoine. 2019a. L'apport du registre paléogéne d'Amazonie sur la diversification initiale des Caviomorpha (Hystricognathi, Rodentia): implications phylogénétiques, macroéevolutives et paléobiogéographiques. Geodiversitas 41:143–245.

Boivin, M., P.O. Antoine, A. Benites-Palomino, L. Marivaux, and R. Salas-Gismondi. 2019b. A new record of a giant neoepiblemid rodent from Peruvian Amazonia and an overview of lower tooth dental homologies among chinchilloids. Acta Palaeontologica Polonica 64:627–642.

Boivin, M. et al. 2017. Late middle Eocene caviomorph rodents from Contamana, Peruvian Amazonia. Palaeontologia Electronica 20.1:1–50.

Bonaparte, C.L. 1845. Catalogo Methodico Dei Mammiferi Europei. Milan:, Luigi Di Giacomo Pirola, .

Bostelmann, E. et al. 2013. Burdigalian deposits of the Santa Cruz Formation in the Sierra Baguales, Austral (Magallanes) Basin: age, depositional environment and vertebrate fossils. Andean Geology 40:458–489.

Bowdich, T.E. 1821. An Analysis of the Natural Classifications of Mammalia: For the Use of Students and Travelers. Paris, France:, J. Smith.

Bown, T.M., and C.N. Larriestra. 1990. Sedimentary paleoenvironments of fossil platyrrhine localities, Miocene Pinturas Formation, Santa Cruz Province, Argentina. Journal of Human Evolution 19:87–119.

Brea, M., A.F. Zucol, and A. Iglesias. 2012. Fossil plant studies from late Early Miocene of the Santa Cruz Formation: paleoecology and paleoclimatology at the passive margin of Patagonia, Argentina; pp. 104–129 in S.F. Vizcaíno, R.F. Kay, and M.S. Bargo (eds.) Early Miocene Paleobiology in Patagonia: High-Latitude Paleocommunities of the Santa Cruz Formation. Cambridge, UK:, Cambridge University Press.

Busker, F., M.E. Pérez, and M.T. Dozo. 2019. A new chinchilloid (Rodentia, Hystricognathi) from the early Miocene of the localities of Bryn Gwyn and Gran Barranca (Patagonia, Argentina). Comptes Rendus Palevol 18:525–540.

Candela, A.M. 2000. Los Erethizontidae (Rodentia, Hystricognathi) fósiles de Argentina. Sistemática e historia evolutiva y biogeográfica. Universidad de La Plata, 357 pp.

Candela, A.M. 2002. Lower deciduous tooth homologies in Erethizontidae (Rodentia, Hystricognathi): evolutionary significance. Acta Palaeontologica Polonica 47:717–723.

Candela, A.M. 2003. A new porcupine (Rodentia, Hystricognathi, Erethizontidae) from the early and middle Miocene of Patagonia. Ameghiniana 40:483–494.

Candela, A.M., and M.G. Vucetich. 2002. *Hypsosteiromys* (Rodentia, Hystricognathi) from the early Miocene of Patagonia (Argentina), the only Erethizontidae with a tendency to hypsodonty. Geobios 35:153–161.

Candela, A.M., and M.B.J. Picasso. 2008. Functional anatomy of the limbs of Erethizontidae (Rodentia, Caviomorpha): indicators of locomotor behavior in Miocene porcupines. Journal of Morphology 269:552–593.

Candela, A.M., L.L. Rasia, and M.E. Pérez. 2012. Paleobiology of Santacrucian caviomorph rodents: a morphofunctional approach; pp. 287–305 in S.F. Vizcaíno, R.F. Kay, and M.S. Bargo (eds.) Early Miocene Paleobiology in Patagonia: High-Latitude Paleocommunities of the Santa Cruz Formation. Cambridge, UK, Cambridge University Press.

Carrillo, J.D. et al. 2018. The Neogene record of northern South American native ungulates. Smithsonian Contributions to Paleobiology 1–80.

Castellanos, A. 1937. Ameghino y la antiguedad del hombre sudamericano. Asociación Cultural de Conferencias de Rosario, Ciclo de Caracter General 2:47–192.

Catena, A.M., and D.A. Croft. 2020. What are the best modern analogs for ancient South American mammal communities? Evidence from ecological diversity analysis (EDA). Palaeontologia Electronica 23:1–36.

Cerdeño, E., and M.G. Vucetich. 2007. The first rodent from the Mariño Formation (Miocene) at Divisadero Largo (Mendoza, Argentina) and its biochronological implications. Andean Geology 34:199–207.

Chick, J., D.A. Croft, H.E. Dodson, J.J. Flynn, and A.R. Wyss. 2010. The early Miocene rodent fauna of Pampa Castillo, Chile. Society of Vertebrate Paleontology Annual Meeting, Program and Abstracts Book 71A-72A.

Croft, D.A. 2013. What constitutes a fossil mammal community in the early Miocene Santa Cruz Formation? Journal of Vertebrate Paleontology 33:37–41.

Croft, D.A. 2016. Horned Armadillos and Rafting Monkeys: The Fascinating Fossil Mammals of South America. Bloomington, Indiana, USA:, Indiana University Press, 366 pp..

Cuitiño, J.I., R. Ventura Santos, P.J. Alonso Muruaga, and R.A. Scasso. 2015. Sr-stratigraphy and sedimentary evolution of early Miocene marine foreland deposits in the northern Austral (Magallanes) Basin, Argentina. Andean Geology 43:364–385.

Cuitiño, J.I., S.F. Vizcaíno, M.S. Bargo, and I. Aramendía. 2019a. Sedimentology and fossil vertebrates of the Santa Cruz Formation (early Miocene) in Lago Posadas, southwestern Patagonia, Argentina. Andean Geology 46:383–420.

Cuitiño, J.I., J.C. Fernicola, M.S. Raigemborn, and V. Krapovickas. 2019b. Stratigraphy and depositional environments of the Santa Cruz Formation (early-middle Miocene) along the Río Santa Cruz, southern Patagonia, Argentina. Publicación Electrónica de La Asociación Paleontológica Argentina 19:14–33.

Cuitiño, J.I. et al. 2016. U-Pb geochronology of the Santa Cruz Formation (early Miocene) at the Río Bote and Río Santa Cruz (southernmost Patagonia, Argentina): implications for the correlation of fossil vertebrate localities. Journal of South American Earth Sciences 70:198–210.

Dunn, R.E. et al. 2013. A new chronology for middle Eocene-early Miocene South American Land Mammal Ages. Bulletin of the Geological Society of America 125:539–555.

Encinas, A. et al. 2019. Cenozoic basin evolution of the central Patagonian Andes: evidence from geochronology, stratigraphy, and geochemistry. Geoscience Frontiers 10:1139–1165.

Fernicola, J.C., J.I. Cuitiño, S.F. Vizcaíno, M.S. Bargo, and R.F. Kay. 2014. Fossil localities of the Santa Cruz Formation (early Miocene, Patagonia, Argentina) prospected by Carlos Ameghino in 1887 revisited and the location of the Notohippidian. Journal of South American Earth Sciences 52:94–107.

Fernicola, J.C., S.F. Vizcaíno, M.S. Bargo, R.F. Kay, and J.I. Cuitiño. 2019. Analysis of the early–middle Miocene mammal associations at the Río Santa Cruz (Patagonia, Argentina). Publicación Electrónica de La Asociación Paleontológica Argentina 19:239–259.

Fields, R.W. 1957. Hystricomorph rodents from the late Miocene of Colombia, South America. University of California Publications in Geological Science 32:207–403.

Fischer de Waldheim, G. 1817. Adversaria zoologica. Mémoires de La Société Impériale Des Naturalistes de Moscou 5:357–428.

Fleagle, J.G. et al. 2012. Absolute and relative ages of fossil localities in the Santa Cruz and Pinturas Formations; pp. 41–58 in S.F. Vizcaíno, R.F. Kay, and M.S. Bargo (eds.) Early Miocene Paleobiology in Patagonia: High-Latitude Paleocommunities of the Santa Cruz Formation. Cambridge, UK, Cambridge University Press.

Flower, W.H. 1873. On a newly discovered extinct mammal from Patagonia (*Homalodotherium cunninghami*). Proceedings of the Royal Society of London 21:383.

Flynn, J.J., and C.C. Swisher. 1995. Cenozoic South American Land Mammal Ages: correlation to global geochronologies. Geochronology Time Scales and Global

Stratigraphic Correlation, SEPM Special Publication 54:317–333.

Flynn, J.J., R. Charrier, D.A. Croft, and A.R. Wyss. 2012. Cenozoic Andean faunas: shedding new light on South American mammal evolution, biogeography, environments, and tectonics; pp. 51–75 in B.D. Patterson and L.P. Costa (eds.) Bones, Clones and Biomes: The History and Geography of Recent Neotropical Mammals. Chicago, Illinois, USA:, University of Chicago Press.

Flynn, J.J., D.A. Croft, R. Charrier, G. Hérail, and A.R. Wyss. 2002a. The first Cenozoic mammal fauna from the Chilean Altiplano. Journal of Vertebrate Paleontology 22:200–206.

Flynn, J.J. et al. 2002b. A new fossil mammal assemblage from the southern Chilean Andes: implications for geology, geochronology, and tectonics. Journal of South American Earth Sciences 15:285–302.

Flynn, J.J. et al. 2008. Chronologic implications of new Miocene mammals from the Cura-Mallín and Trapa Trapa formations, Laguna del Laja area, south central Chile. Journal of South American Earth Sciences 26:412–423.

Folguera, A., A. Encinas, A. Echaurren, G. Gianni, and D. Orts. 2018. Constraints on the Neogene growth of the central Patagonian Andes at the latitude of the Chile triple junction (45–47° S) using U/Pb geochronology in synorogenic strata. Tectonophysics 744:134–154.

Frenguelli, J. 1931. Nomenclatura estratigrafica patagonica. Anales de La Sociedad Cientifica de Santa Fe 3:1–115.

Genise, J.F., and T.M. Bown. 1994. New Miocene scarabeid and hymenopterous nests and early Miocene (Santacrucian) paleoenvironments, Patagonian Argentina. Ichnos 3:107–117.

González Ruiz, L.R., and G.J. Scillato-Yané. 2009. A new Stegotheriini (Mammalia, Xenarthra, Dasypodidae) from the “Notohippidian” (early Miocene) of Patagonia, Argentina. Neues Jahrbuch Fur Geologie Und Palaontologie - Abhandlungen 252:81–90.

Huxley, T. 1880. On the application of the laws of evolution to the arrangement of the Vertebrata, and more particularly of the Mammalia. Proceedings of the Zoological Society, London 43:649–662.

Janis, C.M., and M. Fortelius. 1988. On the means whereby mammals achieve increased functional durability of their dentition, with special reference to limiting factors. Biological Reviews 63:197–230.

Kaiser, T.M. et al. 2013. Hypsodonty and tooth facet development in relation to diet and habitat in herbivorous ungulates: implications for understanding tooth wear. Mammal Review 43:34–46.

Kay, R.F., S.F. Vizcaíno, and M.S. Bargo. 2012. A review of the paleoenvironment and paleoecology of the Miocene Santa Cruz Formation; pp. 331–364 in S.F. Vizcaíno, R.F. Kay, and M.S. Bargo (eds.) Early Miocene Paleobiology in

Patagonia: High-Latitude Paleocommunities of the Santa Cruz Formation. Cambridge, UK, Cambridge University Press.

Kay, R.F., S.F. Vizcaíno, M.S. Bargo, J.P. Spradley, and J.I. Cuitiño. 2021. Paleoenvironments and paleoecology of the Santa Cruz Formation (early-middle Miocene) along the Río Santa Cruz, Patagonia (Argentina). Journal of South American Earth Sciences 109:103296.

Kerber, L., and M.R. Sánchez-Villagra. 2019. Morphology of the middle ear ossicles in the rodent *Perimys* (Neoepiblemidae) and a comprehensive anatomical and morphometric study of the phylogenetic transformations of these structures in caviomorphs. Journal of Mammalian Evolution 26:407–422.

Kerber, L. et al. 2018. A new rodent (Caviomorpha: Dinomyidae) from the upper Miocene of southwestern Brazilian Amazonia. Historical Biology 30:985–993.

Kraglievich, L. 1926. Los grandes roedores terciarios de la Argentina y sus relaciones con ciertos géneros pleistocenos de las Antillas. Anales Del Museo Nacional de Buenos Aires 34:121–135.

Kramarz, A.G. 2001. Estudio de la fauna do roedores de la Formación Pinturas, Mioceno medio-inferior de la Provincia de Santa Cruz. Universidad de Buenos Aires, 300 pp.

Kramarz, A.G. 2002. Roedores chinchilloideos (Hystricognathi) de la Formación Pinturas, Mioceno temporano-medio de la provincia de Santa Cruz, Argentina. Revista Del Museo Argentino de Ciencias Naturales Bernardino Rivadavia 4:167–180.

Kramarz, A. 2004. Octodontoids and erethizontoids (Rodentia, Hystricognathi) from the Pinturas Formation, early–middle Miocene of Patagonia, Argentina. Ameghiniana 41:199–216.

Kramarz, A.G. 2006a. Eocardiids (Rodentia, Hystricognathi) from the Pinturas Formation, late early Miocene of Patagonia, Argentina. Journal of Vertebrate Paleontology 26:770–778.

Kramarz, A.G. 2006b. *Neoreomys* and *Scleromys* (Rodentia, Hystricognathi) from the Pinturas Formation, late early Miocene of Patagonia, Argentina. Revista Del Museo Argentino de Ciencias Naturales, Nueva Serie 8:53–62.

Kramarz, A.G., and E.S. Bellosi. 2005. Hystricognath rodents from the Pinturas Formation, early-middle Miocene of Patagonia, biostratigraphic and paleoenvironmental implications. Journal of South American Earth Sciences 18:199–212.

Kramarz, A.G., and M. Bond. 2005. Los Litopterna (Mammalia) de la Formación Pinturas, Mioceno temprano-medio de Patagonia. Ameghiniana 42:611–625.

Kramarz, A., A.C. Garrido, A.M. Forasiepi, M. Bond, and C.P. Tambussi. 2005. Estratigrafía y vertebrados (Aves y Mammalia) de la Formación Cerro Bandera, Mioceno temprano de la Provincia del Neuquén, Argentina. Revista Geológica

de Chile 32:273–291.

Kramarz, A.G., M.G. Vucetich, and M. Arnal. 2013. A new early Miocene chinchilloid hystricognath rodent; an approach to the understanding of the early chinchillid dental evolution. Journal of Mammalian Evolution 20:249–261.

Kramarz, A.G., M. Bond, and M. Arnal. 2015. Systematic description of three new mammals (Notoungulata and Rodentia) from the early Miocene Cerro Bandera Formation, northern Patagonia, Argentina. Ameghiniana 52:585–597.

Kramarz, A.G. et al. 2010. A new mammal fauna at the top of the Gran Barranca sequence and its biochronological significance; *In* R.H. Madden, A.A. Carlini, M.G. Vucetich, and R.F. Kayeds.(editors) (editors) The Paleontology of Gran Barranca: Evolution and Environmental Change through the Middle Cenozoic of Patagonia.: 260–273 Cambridge, UK:, Cambridge University Press.

de la Cruz, R., D. Welkner, M. Suárez, and D. Quiroz. 2004. Geología del area Oriental de la Hojas Cochrane y Villa O'Higgins, Región Aisén del General Carlos Ibáñez del Campo. Carta Geológica de Chile 57.

Linnaeus, C. 1758. Systema Naturae per Regna Tri Naturae, 10th ed. Stockholm, Sweden:, Laurentii Salvii.

López, G.M. et al. 2011. New Miocene mammal assemblages from Neogene Manantiales Basin, Cordillera Frontal, San Juan, Argentina; pp. 211–226 in J.A. Salfity and R.A. Marquillas (eds.) Cenozoic Geology of the Central Andes of Argentina. Salta, Argentina, SCS Publisher.

Ma, H., D. Ge, G. Shenbrot, J. Pisano, and Q. Yang. 2017. Hypsodonty of Dipodidae (Rodentia) in correlation with diet preferences and habitats. Journal of Mammalian Evolution 24:485–494.

Marivaux, L., and M. Boivin. 2019. Emergence of hystricognathous rodents: Palaeogene fossil record, phylogeny, dental evolution and historical biogeography. Zoological Journal of the Linnean Society 187:929–964.

Marshall, L.G., R. Hoffstetter, and R. Pascual. 1983. Mammals and stratigraphy: geochronology of the continental mammal-bearing Tertiary of South America. Palaeovertebrata 13:1–93.

McGrath, A.J., J.J. Flynn, and A.R. Wyss. 2020. Proterotheriids and macraucheniids (Litopterna: Mammalia) from the Pampa Castillo Fauna, Chile (early Miocene, Santacrucian SALMA) and a new phylogeny of Proterotheriidae. Journal of Systematic Palaeontology 18:717–738.

Mendoza, M., and P. Palmqvist. 2008. Hypsodonty in ungulates: an adaptation for grass consumption or for foraging in open habitat? Journal of Zoology 274:134–142.

Mones, A. 1982. An equivocal nomenclature: What means hypsodonty? Paläontologische Zeitschrift 56:107–111.

Muñoz, N.A., N. Toledo, A.M. Candela, and S.F. Vizcaíno. 2019. Functional morphology of the forelimb of early Miocene caviomorph rodents from Patagonia. Lethaia 52:91–106.

Niemeyer, J., R.F. Skarmeta, and W. Espinosa. 1984. Hojas Peninsula de Taitao y Puerto Aysen Servicio Nacional de Geológica y Mineria. Carta Geológica de Chile 80.

Niemeyer, R.H. 1975. Geología de la región comprendida entre el Lago General Carrera y el Río Chacabuco, Aisén. Universidad de Chile, 309 pp.

Novo, N.M., and J.G. Fleagle. 2015. New specimens of platyrrhine primates from Patagonia (Pinturas Formation, early Miocene). Ameghiniana 52:367–372.

Owen, R. 1846. Notices of some fossil Mammalia of South America. British Association for the Advancement of Science Report 1846, Transaction of the Sections 16:65–67.

Patterson, B. 1958. A new genus of erethizontid rodents from the Colhuehuapian of Patagonia. Breviora 92:1–4.

Patterson, B., and A.E. Wood. 1982. Rodents from the Deseadan Oligocene of Bolivia and the relationships of the Caviomorpha. Bulletin of the Museum of Comparative Zoology 149:371–543.

Pérez, M.E. 2010a. A new rodent (Cavioidea, Hystricognathi) from the middle Miocene of Patagonia, mandibular homologies, and the origin of the crown group Cavioidea *sensu stricto*. Journal of Vertebrate Paleontology 30:1848–1859.

Pérez, M.E. 2010b. Sistemática, ecología y bioestratigrafía de Eocardiidae (Rodentia, Hystricognathi, Cavioidea) del Mioceno temprano y medio de Patagonia. Universidad Nacional de La Plata, 373 pp.

Pérez, M.E., and M.G. Vucetich. 2012a. *Asteromys punctus* Ameghino (Rodentia, Hystricognathi, Cavioidea) from the late Oligocene of Patagonia (Argentina) and the early evolution of Cavioidea *sensu stricto*. Ameghiniana 49:118–125.

Pérez, M.E., and M.G. Vucetich. 2012b. A revision of the fossil genus Phanomys Ameghino, 1887 (Rodentia, Hystricognathi, Cavioidea) from the early Miocene of Patagonia (Argentina) and the acquisition of euhypsodonty in Cavioidea sensu stricto. Paläontologische Zeitschrift 86:187–204.

Pérez, M.E., M.G. Vucetich, and A.G. Kramarz. 2010. The first Eocardiidae (Rodentia) in the Colhuehuapian (early Miocene) of Bryn Gwyn (northern Chubut, Argentina) and the early evolution of the peculiar cavioid rodents. Journal of Vertebrate Paleontology 30:528–534.

Pérez, M.E., M. Krause, and M.G. Vucetich. 2012. A new species of *Chubutomys* (Rodentia, Hystricognathi) from the late Oligocene of Patagonia and its implications on the early evolutionary history of Cavioidea. Geobios 45:573–580.

Pérez, M.E. et al. 2019. New caviomorph rodents from the late Oligocene of Salla, Bolivia: taxonomic, chronological, and biogeographic implications for the Deseadan faunas of South America. Journal of Systematic Palaeontology 17:821–847.

Perkins, M.E. et al. 2012. Tephrochronology of the Miocene Santa Cruz and Pinturas Formations, Argentina; pp. 23–40 in S.F. Vizcaíno, R.F. Kay, and M.S. Bargo (eds.) Early Miocene paleobiology in Patagonia: High-Latitude Paleocommunities of the Santa Cruz Formation. Cambridge, UK, Cambridge University Press.

Raigemborn, M.S. et al. 2015. Paleoenvironmental reconstruction of the coastal Monte Léon and Santa Cruz formations (early Miocene) at Rincón del Buque, southern Patagonia: a revisited locality. Journal of South American Earth Sciences 60:31–55.

Raigemborn, M.S. et al. 2018a. Multiproxy studies of early Miocene pedogenic calcretes in the Santa Cruz Formation of southern Patagonia, Argentina indicate the existence of a temperate warm vegetation adapted to a fluctuating water table. Palaeogeography, Palaeoclimatology, Palaeoecology 500:1–23.

Raigemborn, M.S. et al. 2018b. Paleosols and related soil-biota of the early Miocene Santa Cruz Formation (Austral-Magallanes Basin, Argentina): a multidisciplinary approach to reconstructing ancient terrestrial ecosystems. Latin American Journal of Sedimentology and Basin Analysis 25:117–148.

Rasia, L.L. 2016. Los Chinchillidae (Rodentia, Caviomorpha) fósiles de la República Argentina: sistemática, historia evolutiva y biogeográfica, significado bioestratigráfico y paleoambiental. Universidad Nacional de La Plata, 381 pp.

Rasia, L.L., and A.M. Candela. 2018. Reappraisal of the giant caviomorph rodent *Phoberomys burmeisteri* (Ameghino, 1886) from the late Miocene of northeastern Argentina, and the phylogeny and diversity of Neoepiblemidae. Historical Biology 30:486–495.

Rasia, L.L., and A.M. Candela. 2019a. Upper molar morphology, homologies and evolutionary patterns of chinchilloid rodents (Mammalia, Caviomorpha). Journal of Anatomy 234:50–65.

Rasia, L.L., and A.M. Candela. 2019b. *Prolagostomus amplus* Ameghino is a junior synonym of the Patagonian rodent *Pliolagostomus notatus* Ameghino (Chinchillidae; early Miocene, Santa Cruz Formation). Ameghiniana 56:72–77.

Rasia, L.L., A.M. Candela, and C. Cañón. 2021. Comprehensive total evidence phylogeny of chinchillids (Rodentia, Caviomorpha): cheek teeth anatomy and evolution. Journal of Anatomy.

Rinderknecht, A., E. Bostelmann, and M. Ubilla. 2011. New genus of giant Dinomyidae (Rodentia: Hystricognathi: Caviomorpha) from the late Miocene of Uruguay. Journal of Mammalogy 92:169–178.

Rowe, D.L., K.A. Dunn, R.M. Adkins, and R.L. Honeycutt. 2010. Molecular clocks keep dispersal hypotheses afloat: evidence for trans-Atlantic rafting by rodents. Journal of Biogeography 37:305–324.

Scalabrino, B. 2009. Déformation d'un continent audessus d'une dorsale océanique active en subduction. Université Montpellier, 388 pp.

Scillato-Yané, G.J., and A.A. Carlini. 1998. Nuevos Xenarthra del Friasense (Mioceno medio) de Argentina. Studia Geologica Salmanticensia 34:43–67.

Scott, W.B. 1905. Mammalia of the Santa Cruz Beds. Part III. Glires; pp. 384–499 in Reports of the Princeton Expedition to Patagonia. Princeton, NJ, USA, Princeton University Press.

Simpson, G.G. 1940. Review of the mammal-bearing Tertiary of South America. Proceedings of the American Philosophical Society 83:649–709.

Smith, C.H. 1842. Mammalia. Introduction to mammals; pp. 75–313 in W. Jardine (ed.) The Naturalist's Library. London, UK:, Chatto and Windus.

Solórzano, A. et al. 2020. Late early Miocene caviomorph rodents from Laguna del Laja (~37° S), Cura-Mallín Formation, south-central Chile. Journal of South American Earth Sciences 102:102658.

Stehlin, H.G. 1940. Ein nager aus dem Miocene von Colombien. Eclogae Geologicae Helvetiae 32:179–283.

Trayler, R.B. et al. 2020. An improved approach to age-modeling in deep time: implications for the Santa Cruz Formation, Argentina. Geological Society of America Bulletin 132:233–244.

Ugalde, R., E. Bostelmann, K.E. Buldrini, and J.L. Oyarzún. 2015. Lithofacies, architecture, and depositional environments of the Santa Cruz Formation in Chilean Patagonia. Congreso Geológico Chileno 816–820.

Voloch, C.M., J.F. Vilela, L. Loss-Oliveira, and C.G. Schrago. 2013. Phylogeny and chronology of the major lineages of New World hystricognath rodents: insights on the biogeography of the Eocene/Oligocene arrival of mammals in South America. BMC Research Notes 6:43–46.

Vucetich, M.G. 1984. Los roedores de la edad Friasense (Mioceno medio) de Patagonia. Revista Del Museo de La Plata 8:47–126.

Vucetich, M.G., M.M. Mazzoni, and U.F.J. Pardiñas. 1993. Los roedores de la Formación Collón Cura (Mioceno Medio), y la Ignimbrita Pilcaniyeu. Cañadón del Tordillo, Neuquén. Ameghiniana 30:361–381.

Vucetich, M.G., A.G. Kramarz, and A.M. Candela. 2010. Colhuehuapian rodents from Gran Barranca and other Patagonian localities: the state of the art; pp. 206–219 in R.H. Madden, A.A. Carlini, M.G. Vucetich, and R.F. Kay (eds.) The Paleontology of Gran Barranca: Evolution and Environmental Change through the Middle Cenozoic of Patagonia. Cambridge, UK:, Cambridge University

Press.

Walton, A.H. 1997. Rodents; pp. 392–402 in R.F. Kay, R.H. Madden, R.L. Cifellii, and J.J. Flynn (eds.) Vertebrate Paleontology in the Neotropics: The Miocene Fauna of La Venta, Colombia. Washington, D.C., USA, Smithsonian Institution Press.

Wiegmann, A.F.A. 1835. Bericht über die fortschritte der zoologie im Jahre 1834. Achiv Für Naturgeschichte 1:255–348.

Williams, S.H., and R.F. Kay. 2001. A comparative test of adaptive explanations for hypsodonty in ungulates and rodents. Journal of Mammalian Evolution 8:207–229.

Wood, A.E. 1955. A revised classification of the rodents. Journal of Mammalogy 36:165–187.

Wood, A.E., and B. Patterson. 1959. The rodents of the Deseadan Oligocene of Patagonia and the beginnings of South American rodent evolution. Bulletin of the Museum of Comparative Zoology 120:281–428.

Zurita-Altamirano, D. et al. 2019. The Allemann collection from the Santa Cruz Formation (late early Miocene), Argentina, in Zurich, Switzerland. Swiss Journal of Paleontology 138:259–275.

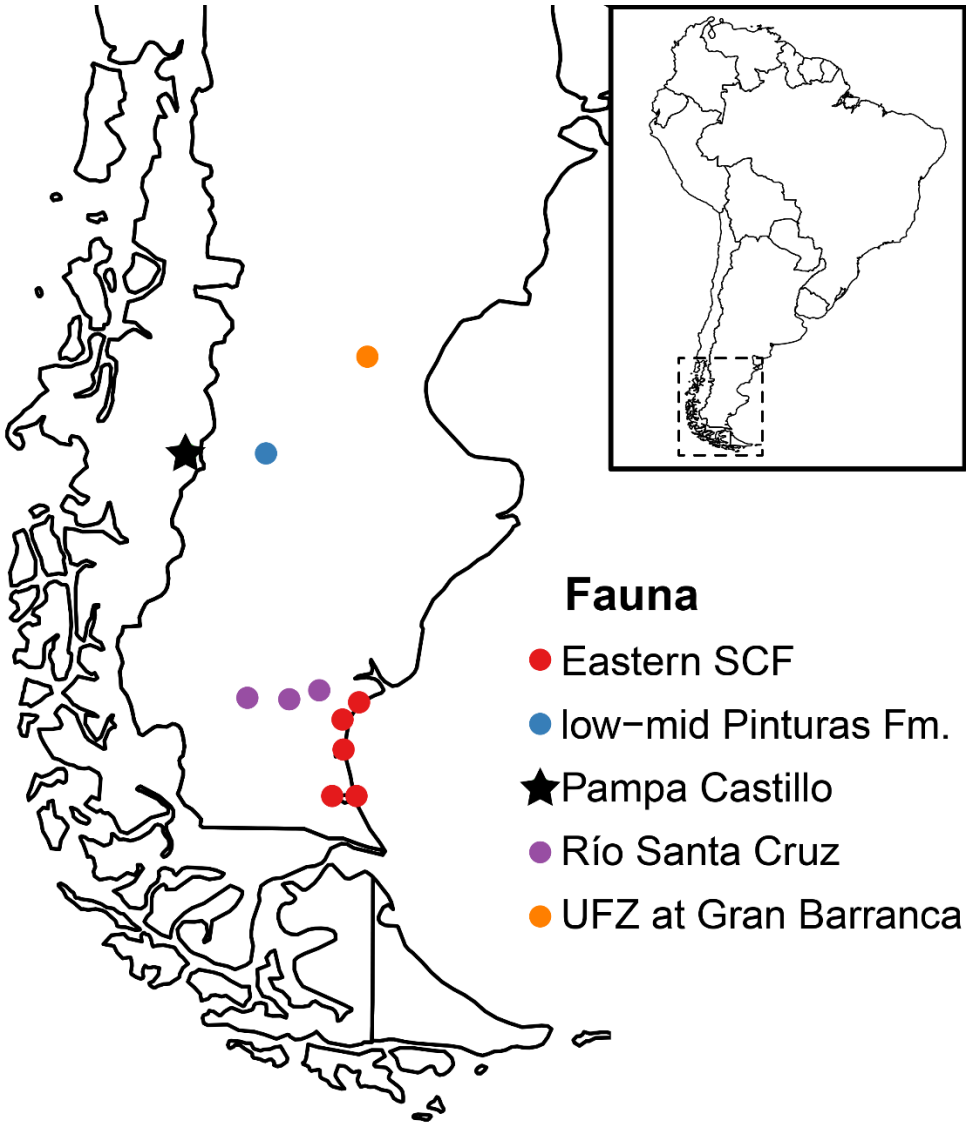

Figure 13: Map showing location of Pampa Castillo and other localities mentioned in the text. Abbreviations: Fm., Formation; SCF, Santa Cruz Formation; UFZ, Upper Faunal Zone.

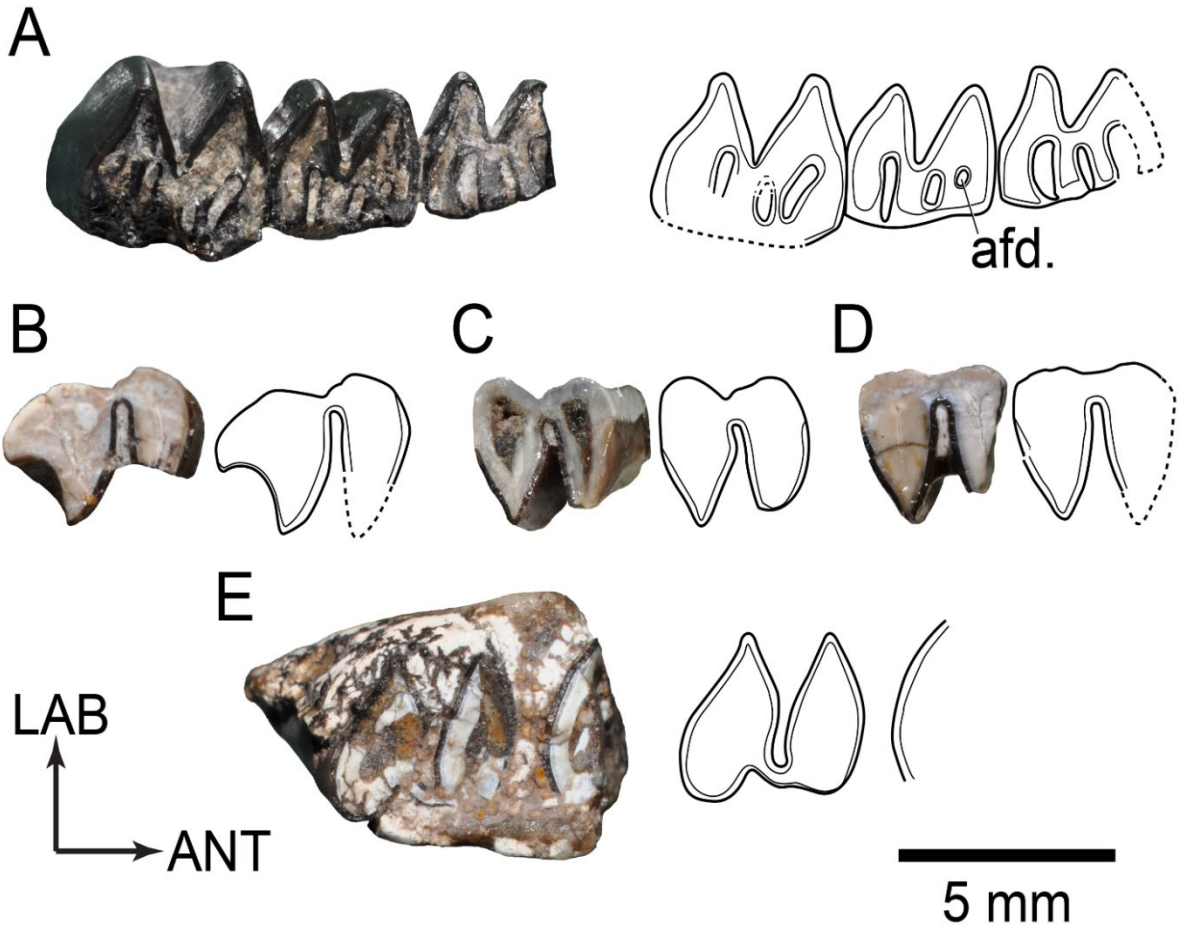

Figure 14: Cavioids from Pampa Castillo. **A,** *Luantus minor* (SGOPV 2691) partial right p4–m2 (reversed). *Eocardia* cf. *excavata*, **B**, (SGOPV 2692) right M3; **C,** (SGOPV 2694) right M2; **D,** (SGOPV 2696) right M1. **E,** cf. *Eocardia* sp. (SGOPV 2695) roots of partial left m2–3 in mandibular fragment. Dotted line represents presumed structure of partial tooth. Labial is up and anterior is right. Scale bar is 5 mm. Abbreviation: afd., anterofossettid.

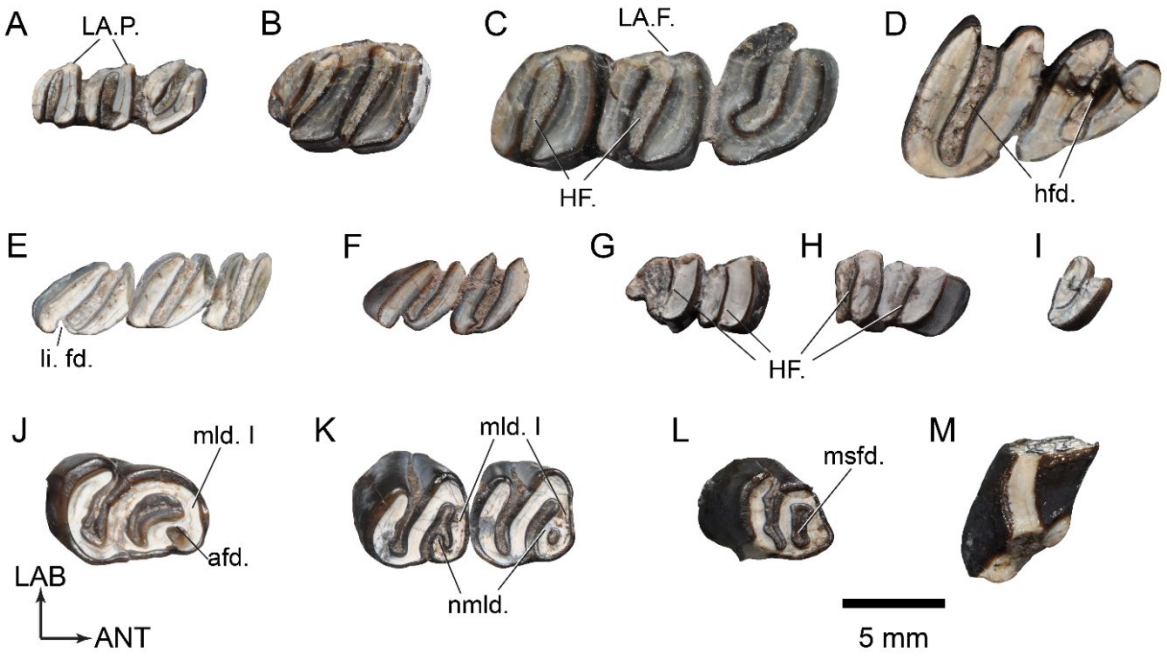

Figure 15: Chinchilloids from Pampa Castillo. **A,** *Perimys erutus* (SGOPV 2619) left P4–M2 (reversed). *Perimys onustus*, **B,** (SGOPV 2662) left M3 (reversed); **C,** (SGOPV 2661) left P4–M2 (reversed); and **D,** (SGOPV 2273) right p4–m1 (reversed). **E,** *Perimys intermedius* (SGOPV 2652) right m1–3 (reversed). **F,** *Perimys* sp. nov.? (SGOPV 2267) right m2–3 (reversed). *Prolagostomus pusillus*, **G,** (SGOPV 2607) right M2–M3; and **H,** (SGOPV 2608) right P4–M1. **I,** *Prolagostomus* cf. *pusillus* (SGOPV 2602) left p4. *Scleromys quadrangulatus*, **J,** (SGOPV 2700) right p4 (reversed); and **K,** (SGOPV 2699) left m1–2. *Scleromys* sp. nov.? anterior is right. Scale bar is 5 mm. Abbreviations: afd., anterofossettid; HF., hypoflexus; hfd., hypoflexid; LA.F., labial flexus; LA.P., labial pillar; li. fd., lingual flexid; mld I, metalophulid I; msfd., mesofossettid; nmld, neomesolophulid.

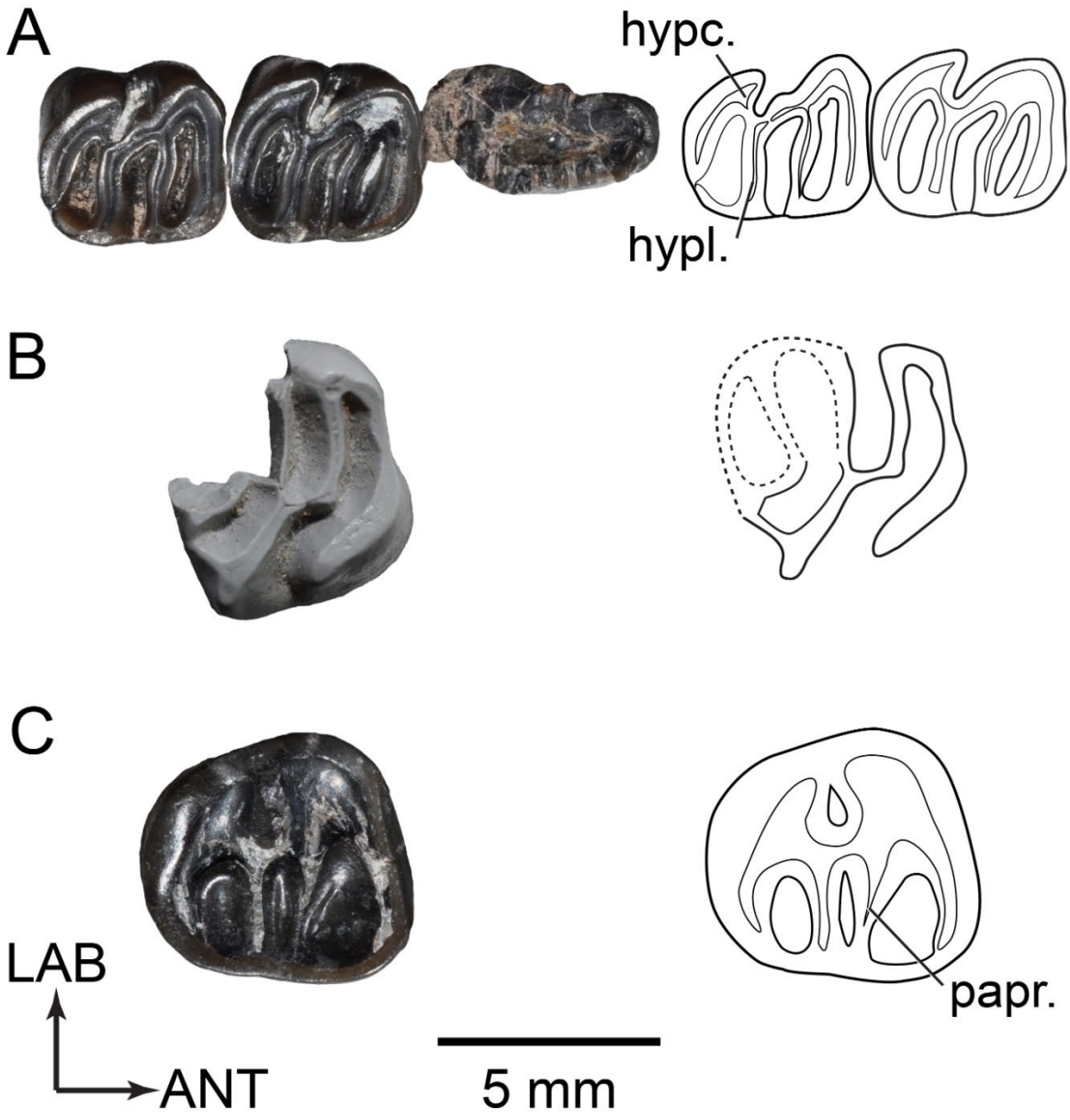

Figure 16: Erethizontids from Pampa Castillo. **A**, *Eosteiromys* cf. *annectens* (SGOPV 2157) root of right p4 and right m1–2 (reversed); and *Steiromys* sp. **B**, (SGOPV 2190 [cast]) partial left M1 or 2 (reversed); and **C**, (SGOPV 2689) right M3 (reversed). Dotted line represents presumed structure of partial tooth. Labial is up and anterior is right. Scale bar is 5 mm. Abbreviations: hypc., hypoconid; hypl., hypolophid; papr., posterior arm of protoconid.

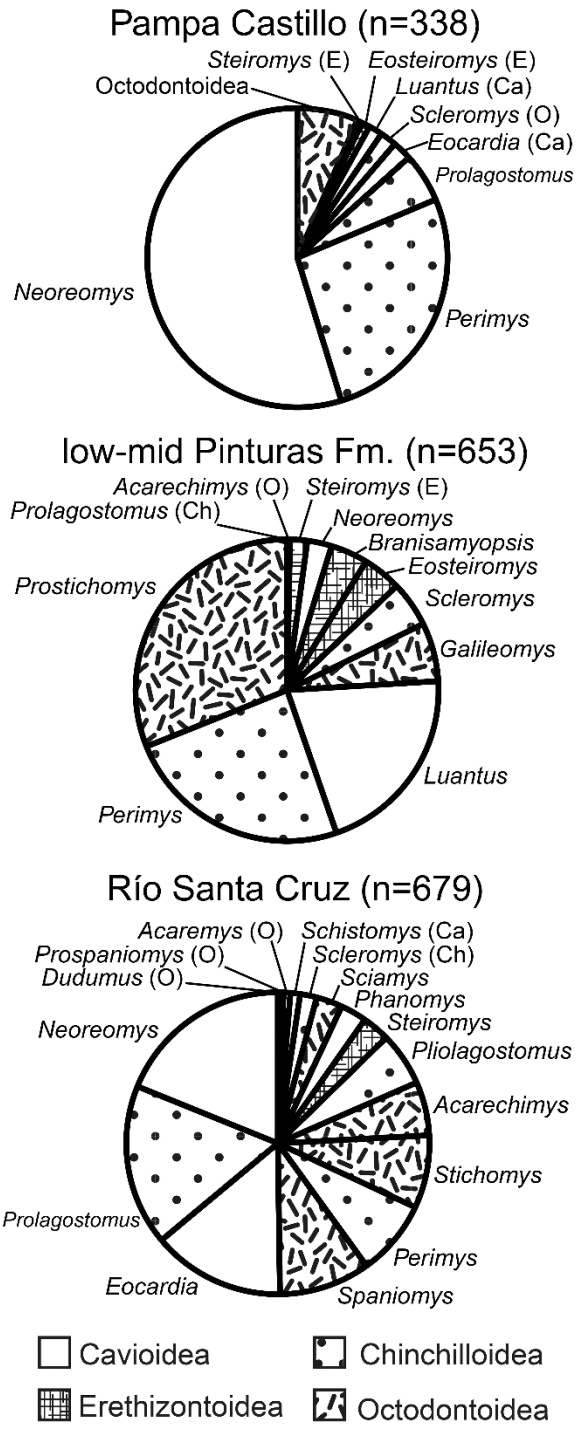

Figure 17: Relative abundance of rodent genera at Pampa Castillo, lower and middle sequences of the Pinturas Formation, and Río Santa Cruz. Wedges filled according to 'superfamily' or labeled with Ca (Cavioidea), Ch (Chinchilloidea), E (Erethizontoidea), and O (Octodontoidea) if too narrow to view fill. References: Pampa Castillo: this study. Low-mid Pinturas Formation: Kramarz (2001, 2002, 2004, 2006a, b). Río Santa Cruz: Arnal et al. (2019).

Table 6: Summary statistics of lower tooth measurements of Pampa Castillo cavioids, chinchilloids, and erethizontoids. See Supplementary File 9 for measurements of individual specimens. Measurements reported in mm.

Taxon		**p4**		**m1**		**m2**		**m1 or 2**		**m3**	
		AP	**LL**	**AP**	**LL**	**AP**	**LL**	**AP**	**LL**	**AP**	**LL**
Luantus minor	N	0	1	1	1	1	1	2	2	0	0
	MEAN	—	2.9	3.6	3.3	4.3	3.8	3.0	2.9	—	—
	MAX	—	2.9	3.6	3.3	4.3	3.8	3.5	3.6	—	—
	MIN	—	2.9	3.6	3.3	4.3	3.8	2.5	2.1	—	—
Eocardia cf. *E. excavata*	N	0	0	1	1	0	1	0	0	0	0
	MEAN	—	—	3.2	3.1	—	3.3	—	—	—	—
	MAX	—	—	3.2	3.1	—	3.3	—	—	—	—
	MIN	—	—	3.2	3.1	—	3.3	—	—	—	—
cf. *Eocardia* sp.	N	0	0	0	0	0	0	0	0	1	1
	MEAN	—	—	—	—	—	—	—	—	4.5	4.2
	MAX	—	—	—	—	—	—	—	—	—	—
	MIN	—	—	—	—	—	—	—	—	—	—
Perimys erutus	N	7	7	2	2	2	2	3	3	2	2
	MEAN	3.1	3.3	3.6	3.4	3.6	3.8	3.3	3.4	3.4	3.4
	MAX	4.0	3.7	3.6	3.6	3.8	3.8	3.6	3.6	3.5	3.5
	MIN	2.3	3.0	3.5	3.2	3.3	3.7	3.1	3.3	3.2	3.3
Perimys onustus	N	5	5	4	4	4	4	9	9	1	1
	MEAN	5.8	6.0	5.5	5.7	5.5	5.9	5.6	6.1	5.8	7.1
	MAX	7.3	6.8	6.5	6.9	6.2	6.7	7.7	7.1	—	—
	MIN	4.6	4.7	3.9	4.1	3.7	3.7	4.3	5.2	—	—
Perimys intermedius	N	1	1	2	2	1	1	0	0	2	2
	MEAN	3.8	3.5	3.7	3.6	3.9	3.5	—	—	5.0	4.3
	MAX	—	—	3.7	3.7	—	—	—	—	5.0	5.2
	MIN	—	—	3.7	3.5	—	—	—	—	4.9	3.3
Perimys sp. nov.?	N	1	1	1	3	3	3	4	4	3	3
	MEAN	4.4	3.7	3.7	4.1	3.9	4.0	4.1	4.4	4.5	4.1
	MAX	—	—	—	4.8	4.8	4.5	4.6	4.9	4.9	4.5
	MIN	—	—	—	3.3	3.1	3.3	3.4	3.9	3.8	3.6
Prolagostomus pusillus	N	6	6	0	0	0	0	4	4	0	0
	MEAN	3.3	3.2	—	—	—	—	3.1	3.6	—	—
	MAX	4.3	3.8	—	—	—	—	3.5	4.0	—	—
	MIN	2.6	2.6	—	—	—	—	2.5	3.3	—	—
Scleromys quadrangulatus	N	2	2	1	1	2	2	2	2	0	0
	MEAN	6.2	4.8	4.8	4.4	4.9	4.7	4.9	4.6	—	—
	MAX	6.6	4.9	—	—	4.9	4.9	5.2	5.1	—	—
	MIN	5.7	4.6	—	—	4.8	4.5	4.5	4.0	—	—
	N	0	0	0	0	0	0	1	1	0	0

Scleromys sp. nov.?	MEAN	—	—	—	—	—	—	4.8	4.6	—	—
	MAX	—	—	—	—	—	—	—	—	—	—
	MIN	—	—	—	—	—	—	—	—	—	—
Eosteiromys cf. *E. annectens*	N	2	2	1	1	1	1	0	0	0	0
	MEAN	6.2	3.3	4.5	4.0	4.8	4.0	—	—	—	—
	MAX	7.1	3.5	—	—	—	—	—	—	—	—
	MIN	5.3	3.0	—	—	—	—	—	—	—	—
Steiromys sp.	N	0	0	0	0	0	0	0	0	1	1
	MEAN	—	—	—	—	—	—	—	—	6.1	5.9
	MAX	—	—	—	—	—	—	—	—	—	—
	MIN	—	—	—	—	—	—	—	—	—	—

Table 7: Summary statistics of upper tooth measurements of Pampa Castillo cavioids, chinchilloids, and erethizontoids. See Supplementary File 9 for measurements of individual specimens. Measurements reported in mm.

Taxon		**P4**		**M1**		**M2**		**M1 or 2**		**M3**	
		AP	**LL**	**AP**	**LL**	**AP**	**LL**	**AP**	**LL**	**AP**	**LL**
Eocardia cf. *E. excavata*	N	0	0	2	2	2	2	1	1	1	1
	MEAN	—	—	3.4	3.1	3.6	3.4	3.3	3.1	4.6	3.7
	MAX	—	—	3.4	3.2	3.9	3.5	—	—	—	—
	MIN	—	—	3.3	3	3.2	3.3	—	—	—	—
Perimys erutus	N	4	4	3	3	3	3	9	9	5	5
	MEAN	2.9	4.0	2.7	3.6	2.7	3.5	2.61	3.7	4.5	3.24
	MAX	3.5	4.5	2.9	3.8	3	4	3.2	4.1	5	3.6
	MIN	2.4	3.2	2.4	3.4	2.4	3.1	2.3	3.3	3.9	2.8
Perimys onustus	N	7	9	4	4	3	4	5	5	4	4
	MEAN	5.0	6.5	4.5	5.9	4.5	5.7	4.4	5.8	7.5	5.6
	MAX	5.6	7.6	5	6.1	4.7	5.8	4.6	6.2	8.9	6
	MIN	4.2	4.9	4.1	5.6	4.3	5.6	4.3	5.4	6.1	5.4
Perimys intermedius	N	1	1	1	1	0	0	0	0	0	2
	MEAN	3.2	3.9	2.9	3.9	—	—	—	—	—	4.05
	MAX	—	—	—	—	—	—	—	—	—	4.1
	MIN	—	—	—	—	—	—	—	—	—	4
Perimys sp. nov.?	N	0	0	0	0	0	0	2	2	0	0
	MEAN	—	—	—	—	—	—	3.3	5.1	—	—
	MAX	—	—	—	—	—	—	3.3	5.4	—	—
	MIN	—	—	—	—	—	—	3.3	4.8	—	—
Prolagostomus pusillus	N	3	3	3	4	1	1	1	1	1	1
	MEAN	3.0	3.4	3.0	3.78	2.4	3.6	2	2.7	3.5	3.3
	MAX	3.1	3.8	3.2	4	—	—	—	—	—	—
	MIN	2.9	3.1	2.5	3.6	—	—	—	—	—	—
Steiromys sp.	N	0	0	0	0	1	1	0	0	0	0
	MEAN	—	—	—	—	6.4	6.1	—	—	—	—
	MAX	—	—	—	—	—	—	—	—	—	—
	MIN	—	—	—	—	—	—	—	—	—	—

CHAPTER 4

OCTODONTOIDS (RODENTIA, MAMMALIA) FROM PAMPA CASTILLO, CHILE, AND HOW RODENTS INFORM EARLY MIOCENE SOUTH AMERICAN BIOCHRONOLOGY

ABSTRACT

By the early Miocene, caviomorph rodents were diverse and abundant components of South American mammal communities. In this work, we describe the octodontoid caviomorphs of Pampa Castillo, an early Miocene site from the Galera Formation in southern Chile (Aysén Region). Six genera and eight species of octodontoids are present, three of which are new. *Dudumus* sp. nov. and *Caviocricetus* sp. nov. are members of genera better-known from older strata. The third new species, *Prostichomys* sp. nov., we refrained from naming because it is only represented by a single tooth. The other octodontoids support the referral of Pampa Castillo to the Santacrucian SALMA, in agreement with previous studies.

We conducted faunal similarity analyses using hierarchical clustering with the Jaccard and Simpson similarity indexes on eleven early to middle Miocene Patagonian rodent faunas to resolve outstanding biochronologic questions around this interval. Faunas generally clustered according to the three South American Land Mammal Ages (SALMAs) to which they were previously assigned: Colhuehuapian, Santacrucian, and post-Santacrucian (Friasian/Colloncuran). The Pinturan is a proposed biochronologic interval between the Colhuehuapian and Santacrucian SALMAs that is based on the faunas of the lower and middle sequences of the Pinturas Formation and Upper Faunal Zone at Gran Barranca. Pampa Castillo clustered with these Pinturan faunas when genera were used as the taxonomic unit, but it clustered with the faunas on which the Santacrucian SALMA is based, from outcrops of the Santa Cruz Formation along the Atlantic coast and Río Santa Cruz,

when species were used. This conflict demonstrates that the Pampa Castillo fauna is intergradational between the Pinturan and ‘typical’ Santacrucian faunas. Geochronologic data show that some Pinturan sites overlap temporally with faunas that clustered with the ‘typical’ Santacrucian faunas in our analyses (Pampa Castillo and upper sequence of the Pinturas Formation) or qualitatively resemble them (Notohippidian). These lines of evidence suggest that the Pinturan is not a valid biochronologic interval, and that the differences between it and the ‘typical’ Santacrucian faunas are likely attributable to geographic or paleoenvironmental, rather than temporal, differences.

KEYWORDS

Caviomorphs, Miocene, octodontoids, SALMA, Chile, biochronology.

INTRODUCTION

For the majority of the Cenozoic, South American mammal faunas consisted of endemic taxa (Cione et al. 2015; Croft 2016). Caviomorph rodents were one of these endemic groups after their arrival from across the Atlantic in the middle Eocene (Rowe et al. 2010; Boivin et al. 2017). Caviomorphs initially appeared in low latitudes where they split into four main lineages (i.e., 'superfamilies'): Cavioidea, Chinchilloidea, Erethizontoidea, and Octodontoidea (Boivin et al. 2019). By the late Oligocene, caviomorphs had dispersed southward and were diverse and abundant components of Patagonian fossil faunas (Vucetich et al. 2010b, 2015). Octodontoidea, the group primarily discussed herein, today consists of degus, tuco-tucos, spiny rats, hutias, and other small to mid-sized rodents, and numerous fossil species are also known (Upham and Patterson 2012; Arnal and Vucetich 2015a).

Biochronology, a temporal scheme based on the succession of fossil organisms, is a useful framework for interpreting biological evolution and inferring the ages of geologic strata that lack absolute dates (i.e., ones based on radiometric or paleomagnetic methods). Mammals are the primary group used for terrestrial Cenozoic biochronology, since their remains usually constitute the bulk of fossils recovered from such sites, and 'land mammal age' systems have been established for North America, Africa, East Asia, and South America (Marshall et al. 1983; Flynn et al. 1984; Flynn and Swisher 1995; Qiu et al. 2013; Van Couvering and Delson 2020). The South American Land Mammal Age (SALMA) scheme covers much of the Cenozoic, though many Paleogene gaps remain (Flynn and Swisher 1995; Dunn

et al. 2013; Woodburne et al. 2014). Rodents are a particularly useful group for biochronology because of their abundance and rapid evolution relative to larger-bodied mammals.

The South American fossil record of the early Miocene is dominated by Patagonian faunas (Madden et al. 2010; Vizcaíno et al. 2012b; Croft 2016). The earliest Miocene faunas from the continent are assigned to the Colhuehuapian SALMA. Colhuehuapian localities are most common in Chubut and Neuquén provinces, Argentina (Fig. 18) and date to ~21–20 Ma (Table 8; Kramarz et al. 2005; Ré et al. 2010; Dunn et al. 2013). Faunas of the next youngest SALMA, the Santacrucian, occur mainly in Santa Cruz Province, Argentina, and adjacent Chile (Flynn et al. 2002; Kramarz and Bellosi 2005; Vizcaíno et al. 2012a). Santacrucian faunas from exposures of the Santa Cruz Formation (SCF) along the Atlantic coast (Sa-SC-AC) and Río Santa Cruz (Sa-SC-RSC) are among the best-studied Neogene fossil mammal strata in South America and span ~17.8–15.63 Ma (Table 8; Vizcaíno et al. 2012b; Croft 2016; Cuitiño et al. 2016). Historically, two other biochronologic intervals have been proposed to span the gap between the Colhuehuapian and Santacrucian SALMAs: the Notohippidian and the Pinturan. The Notohippidian is based on SCF deposits in southwestern Santa Cruz Province (Fernicola et al. 2014), and was first recognized by Ameghino (1900-02). The Pinturan is based on faunas from the Pinturas and Sarmiento formations in northern Santa Cruz and southern Chubut provinces, Argentina (Kramarz and Bellosi 2005; Kramarz et al. 2010). Both ‘ages’ were recognized as bearing more ‘primitive’ mammal communities than the Santacrucian faunas of the Sa-SC-RSC and Sa-SC-

AC. There is debate whether these units represent regional variants of the Santacrucian SALMA, ‘sub-ages’ of the Santacrucian SALMA, or distinct SALMAs, though this last option has only been suggested for the Pinturan (Marshall et al. 1983; Flynn and Swisher 1995; Kramarz et al. 2010). Recent geochronologic work in Santa Cruz province and adjacent regions has advanced our understanding of the absolute (i.e., numerical) ages of these faunas (e.g., Perkins et al. 2012; Dunn et al. 2013; Cuitiño et al. 2016, 2019b). This improved geochronologic framework provides an opportunity to assess whether the taxonomic differences between ‘Pinturan’ and Sa-SC-RSC and Sa-SC-AC faunas are due to temporal or paleoenvironmental/geographical differences between the strata from which they derive.

The site of Pampa Castillo in southern Chile has yielded an early Miocene fossil mammal fauna that is relevant to the debate regarding early Miocene South American biochronology due to its location. It is positioned further north than Sa-SC-RSC and Sa-SC-AC localities, almost directly west of the upper Río Pinturas valley, the site of the best known ‘Pinturan’ fauna, the lower and middle sequences of the Pinturas Formation (Sa-lmP; Fig. 18). The Pampa Castillo fauna was first reported by Flynn et al. (2002b), who assigned it to the Santacrucian SALMA. These authors assigned the mammal-bearing strata to the Galera Formation, which we follow herein, whereas others attribute them to the Santa Cruz Formation (de la Cruz et al. 2004; Ugalde et al. 2015). Given Pampa Castillo’s relative geographic proximity to the Sa-lmP and its possible stratigraphic relationship with Sa-SC-RSC and Sa-SC-AC faunas, it is an important site for uncovering the relationships among these

faunas. Chick et al. (2010) re-examined the rodents of Pampa Castillo and noted that several taxa were shared with the Sa-lmP. McGrath et al. (2020) described Pampa Castillo's litopterns and recognized one taxon previously known only from the Sa-lmP (*Picturotherium*) and another exclusive to the SCF (*Thoatherium*). These studies suggest that Pampa Castillo is key to understanding early Miocene biochronology in this region of South America.

Herein we describe Pampa Castillo octodontoids. We combine data about this octodontoid assemblage with that from cavioids, chinchilloids, and erethizontoids described in Chapter 3 and analyze the Pampa Castillo rodent community along with ten other early to middle Miocene rodent communities (Table 8) and use hierarchical clustering methods to assess their relative similarities. Combined with geochronologic data, this analysis sheds light on the biochronology of early and middle Miocene South American mammal faunas.

GEOLOGICAL SETTING

More detailed accounts of the geology of Pampa Castillo is provided elsewhere Frassinetti and Covacevich (1999) and Flynn et al. (2002b) contain more detailed accounts of the geology of Pampa Castillo, but a brief summary is provided here. These Andean fossiliferous localities lie at ~1,350 m elevation on a ~4.5 km^2 promontory that projects above the treeline in the Aysén Region of southern Chile (~47° S, 72.5° W; Fig. 18) between Lago General Carrera (=Lago Buenos Aires) and

Lago Cochrane (=Lago Pueyrredón), north of the Río Chacabuco. The mammal-bearing strata have been variously assigned to the Río Zeballos (Niemeyer 1975), Santa Cruz (de la Cruz et al. 2004; Ugalde et al. 2015; Encinas et al. 2019), Galera (Niemeyer et al. 1984; Flynn et al. 2002b), and Pampa Castillo (Scalabrino 2009; Folguera et al. 2018) formations. Consistent with previous paleontological works on this site (Flynn et al. 2002b; McGrath et al. 2020), we refer to these strata as the Galera Formation.

Folguera et al. (2018) reported a U/Pb date of 18.7 +/- 0.3 Ma from a reworked tuff ~10 m above the contact between the 'Pampa Castillo' (=Galera) Formation and the conformably underlying Guadal Formation at Meseta Guadal. Encinas et al. (2019) reported a maximum depositional age of ~19.8 +/- 0.4 Ma (based on detrital zircons) for a sandstone at the top of the Guadal Formation at Pampa Castillo.

BIOCHRONOLOGICAL CONTEXT

In this paper, we analyze rodent communities from the early and middle Miocene that span the Colhuehuapian, Santacrucian, and Colloncuran/Friasian/Mayoan/Laventan SALMAs. Generally, these first two SALMAs are referred to as 'early Miocene' and the others as 'middle Miocene.' There is a significant temporal gap between the Colhuehuapian and the preceding SALMA, the Deseadan (late Oligocene; Flynn and Swisher 1995; Dunn et al. 2013). The gap

between the Colhuehuapian and Santacrucian SALMAs is smaller. Two biochronologic intervals, the Pinturan and Notohippidian, are purported to bridge this Colhuehuapian-Santacrucian gap or represent the oldest part of the Santacrucian SALMA (Kramarz et al. 2010; Bostelmann et al. 2013; Dunn et al. 2013). The Santacrucian SALMA and the SALMA immediately following it do not seem to have any temporal gap and possibly even overlap (Cuitiño et al. 2016). The name applied to this post-Santacrucian biochronologic interval is debated. After the Santacrucian (which ends ~15.6 Ma; Cuitiño et al. 2016), the next-oldest SALMA that is near-universally recognized is the Chasicoan SALMA which begins ~10.0 Ma (Flynn and Swisher 1995). Four SALMAs have been proposed for the intervening interval: Colloncuran, Friasian, Laventan, and Mayoan. Unfortunately, the type faunas of these proposed SALMAs are poorly understood, not well-constrained geochronologically, and/or represent geographically distant regions. Resolving this issue is beyond the scope of this work, but see Bucher et al. (2021) for a more detailed discussion of middle Miocene SALMAs.

Colhuehuapian SALMA

The Colhuehuapian is the oldest Miocene SALMA. Dated Colhuehuapian faunas range from 21.0–20.1 Ma (Dunn et al. 2013). The most extensively studied Colhuehuapian faunas come from the lower faunal zone of the Colhue-Huapi Member of the Sarmiento Formation at Gran Barranca (Cp-GB-LFZ) and the Trelew Member of the Sarmiento Formation at Bryn Gwyn (Cp-BG; Vucetich et al. 2010a). Both localities are in Chubut Province, southern Argentina (Fig. 18).

The mammalian fauna of the Cerro Bandera Formation, which crops out in Neuquén Province, Argentina (Fig.1), is usually referred to the Colhuehuapian SALMA, but the presence of taxa shared with older (Deseadan SALMA) faunas casts doubt on this idea (Kramarz et al. 2005, 2015).

Santacrucian SALMA

The Santacrucian SALMA is likely the most extensively studied pre-Quaternary age in South American paleontology. Ameghino (1889) originally based his “Santacrucense” on fossils from Santa Cruz Formation localities along the Río Santa Cruz (Sa-SC-RSC) in Santa Cruz Province, Argentina (Fig. 18). These deposits have received renewed attention in the last two decades, including geochronologic analyses that have constrained these faunas to ~17.22–15.63 Ma (Cuitiño et al. 2016; Fernicola et al. 2019b). Between the time of Ameghino and this recent resurgence in interest in the Sa-SC-RSC, most expeditions to the SCF sampled exposures along the Atlantic coast (Sa-SC-AC) of Santa Cruz province (Vizcaíno et al. 2012a). Marshall et al. (1983) considered the Sa-SC-AC locality of Monte León to be the type locality of the Santacrucian SALMA. Sa-SC-AC localities range in age from ~17.8–16.2 Ma, considerably overlapping with those of the Sa-SC-RSC (Fleagle et al. 2012; Trayler et al. 2020). These two faunas are taxonomically similar and geographically proximate (Fig. 18; Fernicola et al. 2019b).

Ameghino (1900-02) recognized a fauna from the SCF at Karaiken and along the Río Bote in western Santa Cruz Province, that was more ‘primitive’ than that of the Sa-SC-RSC and Sa-SC-AC. He referred this fauna to a new interval, the *étage Notohippidéen* (Notohippidian stage), which was older than the *étage*

Santacruzienne (Santacrucian stage) described from the Sa-SC-RSC and Sa-SC-AC (Fig. 18; Fernicola et al. 2014). Later, Marshall and Pascual (1977) reported an additional Notohippidian locality at Cerro Centinela (also from the SCF) and recognized that Karaiken contained strata containing Notohippidian and 'typical' Santacrucian strata. Unfortunately, Ameghino (1900-02) did not provide the precise stratigraphic provenance of his Notohippidian fossils, so it is impossible to know which came from 'Notohippidian' versus 'Santacrucian' levels at Karaiken (Cuitiño et al. 2016). Strata bearing Notohippidian faunas at Karaiken and Río Bote range from ~18.85–18.00 Ma in age (Fleagle et al. 2012; Perkins et al. 2012; Cuitiño et al. 2016).

Other fossiliferous SCF outcrops also occur south of Lago Posadas (=Lago Pueyrredón) in northwestern Santa Cruz Province, but they have produced many fewer fossils than those of the Sa-SC-RSC or Sa-SC-AC, and are particularly poor in rodents (4 genera, 1 identified to species-level; Cuitiño et al. 2019b). The fossil-bearing strata are older (~18.15–16.45 Ma) than the Sa-SC-AC and Sa-SC-RSC faunas (Cuitiño et al. 2019b). Sierra Baguales in southern Chile is an SCF locality that has been interpreted to represent a post-Colhuehuapian, pre-Santacrucian interval based on its faunal content and maximum age (from detrital zircons near the base of the SCF) of 18.23 +/- 0.26 Ma (Bostelmann et al. 2013). Only two rodent taxa have been reported from this fauna, so it could not be included in our analysis.

Patagonian Santacrucian faunas have also been reported from the Pinturas Formation (Fig. 18). Ameghino (1906) recognized this assemblage as being more 'primitive' than what was known from the Sa-SC-RSC and Sa-SC-AC and referred to

the faunal interval as the '*Astrapothericulense*' (Astrapothericulan). Importantly, Ameghino (1906) indicated no subdivisions of the Pinturas Formation, so one must assume that his Astrapothericulan fauna included taxa from all levels. Frenguelli (1931) and Castellanos (1937) supported the notion of a distinct Astrapothericulan fauna ('*Pinturense*' according to Castellanos 1937). However, the concept of the Astrapothericulan/Pinturan as a distinct age was disregarded by most later authors (e.g., Wood and Patterson 1959; Marshall et al. 1983; Flynn and Swisher 1995). Revisions of the Pinturas Formation rodent assemblage in the early 2000s (Kramarz 2001a, 2002, 2004) led Kramarz and Bellosi (2005) to distinguish the fauna of the lower and middle sequences (Sa-lmP) from that of the upper sequence (Sa-uP). The Sa-uP rodent assemblage was noted to resemble those of the Sa-SC-RSC and Sa-SC-AC, whereas that of the Sa-lmP contained a mix of 'typical' Santacrucian taxa (i.e., from the Sa-SC-RSC and Sa-SC-AC), those of Colhuehuapian age, and endemic taxa. Kramarz and Bellosi (2005) termed the Sa-lmP rodents the 'Pinturan association.' Subsequent description of proterotheriid litopterns (Kramarz and Bond 2005) and microbiotheriid marsupials (Chornogubsky and Kramarz 2012) from the Pinturas Formation documented this same faunal pattern. With the discovery of a second 'Pinturan' fauna at Gran Barranca (see below), some authors began to recognize the Pinturan as a 'subage' of the Santacrucian SALMA or a full SALMA, but this distinction has not been formalized. A tuff within the lower sequence of the Pinturas Formation at Estancia El Carmen has been dated at ~17.99 +/- 0.02 Ma (Perkins et al. 2012). One other Sa-lmP locality, Portezuelo Sumich Norte, has an absolute age associated with it. Above the fossiliferous strata at this locality lie

mature paleosols, an unconformity, then a tephra dated to 16.9 Ma (Bown and Larriestra 1990; Fleagle et al. 2012). Therefore, the strata containing the Sa-lmP fauna are likely well-older than 16.9 Ma. Precise age estimates from Sa-uP strata are lacking, but Fleagle et al. (2012) pointed out several discrepancies between the faunal evidence and what can be inferred about the ages of certain localities. Estancia El Carmen, in the Río Pinturas Valley, has produced Sa-lmP and Sa-uP rodent assemblages and includes the 17.99 Ma tuff mentioned previously within the lower sequence. The Pinturas Formation also crops out further south at places like Gobernador Gregores and La Cañada, which have exclusively produced Sa-uP faunas (Kramarz and Bellosi 2005). However, a tephra from a nearby site, La Cañada West, has been dated to ~18 Ma (Fleagle et al. 2012). Additionally, although Kramarz and Bellosi (2005) assigned the Pinturas Formation strata at Gobernador Gregores to the upper sequence based on its rodent community, Bown and Fleagle (1993) believed they corresponded to the lower sequence based on lithology. If the lithologic correlation is correct, this would imply that the Gobernador Gregores locality is ~17.8 Ma (Fleagle et al. 2012). Regardless, the ages and stratigraphic relationships of localities bearing Sa-uP faunas are tentative.

The Upper Faunal Zone of the Colhue-Huapi Member of the Sarmiento Formation at Gran Barranca (Sa-GB-UFZ) has produced what may be a second exemplar of a Pinturan fauna (Kramarz et al. 2010). The discovery of a ‘Pinturan’ fauna outside of the Pinturas Formation led Kramarz et al. (2013) to argue that the Pinturan represents a valid biochronologic interval rather than a distinctive local

fauna. Dunn et al. (2013) constrained the Sa-GB-UFZ to 19.04–18.62 Ma, older than the ‘Pinturan’ strata of the Sa-lmP.

Post-Santacrucian (Middle Miocene) Faunas

Cañadón de Tordillo (Cc-CT) is a fossil locality from the Collón Curá Formation Vucetich et al. (1993) used the Cc-CT rodent assemblage to define the Colloncuran SALMA *s.s.* (as part of a Santacrucian-Friasian *s.s.*-Colloncuran *s.s.*-Mayoan sequence). Madden et al. (1997) reported an age of 15.7 Ma for the Pilcaniyeu Ignimbrite, which lies between the two fossil-bearing layers at Cc-CT (Vucetich et al. 1993). Bucher et al. (2021) reported several fossiliferous localities of the Collón Curá Formation in the Paso del Sapo Basin in Chubut Province, Argentina. They recognized distinct upper and lower sections of this unit. The lower section, occurring at the Cruces Infinitos and Los Yeguarizos (Cc-CILY) localities, was more fossiliferous than the upper and spanned 14.86–12.75 Ma (Table 8). Bucher et al. (2021) noted that the Cc-CILY fauna resembles Colloncuran s.s. faunas but also differs in some respects. Other fossiliferous outcrops of the Collón Curá Formation are known (e.g., El Petiso and Cerro Zeballos; Pérez 2010; Pérez and Vucetich 2011; Brandoni et al. 2017; Vera et al. 2019), but none of them individually has produced a sufficient number of rodent taxa to be included in this analysis.

Several rodent-bearing fossil localities have been historically referred to the Río Frías Formation including Alto Río Cisnes (the type locality of the Friasian SALMA), Río Huemules, Río Fénix, and Laguna Blanca (Marshall et al. 1983; Vucetich 1984). Unfortunately, we could not include any of these assemblages in our

analysis. The exact stratigraphic provenance of fossils from these localities is uncertain, and changes to the categorization of the relevant strata mean that the fossils from any one site could come from multiple stratigraphic units (see González Ruiz et al. 2017). More recent collections from Alto Río Cisnes may permit this biochronologically significant fauna to be better-characterized in the near future (Bostelmann et al. 2012). We restricted our sample to Patagonian rodent communities, so the faunas of La Venta (Colombia) and Quebrada Honda (Bolivia), which are referred to the Laventan SALMA, were not included despite their diverse rodent communities (Walton 1997; Croft et al. 2011).

MATERIAL AND METHODS

The octodontoids of Pampa Castillo were compared to specimens housed in the American Museum of Natural History and Yale Peabody Museum and to their close relatives described in the literature. Measurements were taken using Mitutoyo CD-8” digital calipers. We follow the dental terminology of Boivin and Marivaux (2020).

Faunal Similarity Analysis

We compared eleven early–middle Miocene Patagonian rodent faunas (Table 8; Supplementary File 10) using the Jaccard and Simpson similarity indexes (i.e., coefficients), both of which are used to calculate the similarity of two given communities. Both indices are calculated using the number of shared taxa as the

numerator. The denominator of the Jaccard index is the total number of taxa found in both communities, whereas the denominator of the Simpson similarity index is the number of taxa found in the less speciose of the two (Jaccard 1912; Simpson 1943). This difference makes the Jaccard index more sensitive to differences in overall taxon richness (Raup and Crick 1979). The Simpson similarity coefficient was calculated using the fossil package v. 0.4.0 (Vavrek 2011) for R v. 4.0.2 (R Core Team 2020). Both indices were analyzed identically after being calculated.

We conducted pairwise comparisons of every combination of faunas producing a matrix of similarity scores, which was then transformed into a distance matrix (1-similarity matrix). Next, we performed hierarchical cluster analysis on the distance matrix using the hclust command in the stats R package (R Core Team 2020) with the unweighted pair-group arithmetic mean method (UPGMA; method="average"). We performed analyses using both species and genus occurrence data, as well as with all provisionally occurring taxa (i.e., those reported in the literature as cf. or ?) included and excluded. This resulted in eight total analyses. Taxa reported as distinct, but not formally named, in the literature (i.e., as 'GENUS sp. nov.') were counted as distinct species. We processed all data in R with the help of the tidyverse v. 1.3.0 (Wickham et al. 2019) and ggdendro v. 0.1-20 (de Vries and Ripley 2016) packages.

Institutional Abbreviations

SGOPV, Vertebrate Paleontology collections, Museo Nacional de Historia Natural, Santiago, Chile.

SYSTEMATIC PALEONTOLOGY

Mammalia Linnaeus, 1758

Eutheria Huxley, 1880

Rodentia Bowdich, 1821

Caviomorpha Wood, 1955

Pan-Octodontoidea Arnal and Vucetich, 2015a

Acarechimys Patterson in Kraglievich, 1965

Type Species. *Acarechimys minutus* Ameghino, 1887a.

Included Species. The type, *Acarechimys constans* Ameghino, 1887a, *Acarechimys minutissimus* Ameghino, 1887a, *Acarechimys gracilis* Ameghino, 1891a, and *Acarechimys leucotheae* Vucetich et al., 2015.

Stratigraphic & Geographic Range. Sarmiento Formation, Deseadan–Colhuehuapian SALMAs, Chubut Province, Argentina; Pinturas Formation, Santacrucian ('Pinturan') SALMA, Santa Cruz Province, Argentina; Santa Cruz Formation, Santacrucian SALMA, Santa Cruz Province, Argentina; Galera Formation, Santacrucian SALMA, Aysén Region, Chile; Chucal Formation, Santacrucian SALMA, Arica y Parinacota Region, Chile; Curá Mallín Formation, Santacrucian SALMA?, Biobío Region, Chile; Collón Curá Formation, Chubut,

Neuquén, and Río Negro provinces, Colloncuran SALMA, Argentina; Villavieja Formation, Laventan SALMA, Colombia; unnamed formation (Quebrada Honda), Laventan SALMA, Tarija Department, Bolivia; unnamed formation (Fitzcarrald Arch), Laventan SALMA, Peru; Pebas Formation, late? Miocene, Peru.

Acarechimys minutus Ameghino 1887a

Figure 19A

2002 *Acarechimys* new sp. Flynn, Novacek, Dodson, et al., table 1 [*partim*].

Material. SGOPV 2131, left m1; SGOPV 2136, right m1–2; SGOPV 2367, left dp4–m3 (Fig. 19A).

Description. Only lower dentitions of *A. minutus* have been recovered from Pampa Castillo. The teeth are brachydont. SGOPV 2367 is the only specimen that preserves dp4, but the crown preserves little occlusal morphology (Fig. 19A). In dp4, the posterior arm of the protoconid (=metalophulid II of Arnal et al. 2017) does not reach the metaconid and ends approximately halfway labiolingually across the tooth. The remaining lower molars are trilophodont. As seen in SGOPV 2367 (Fig. 19A), the lingual cuspids are broader than the cristids and clearly distinct from them. In all molars, metalophulid I and the hypolophid are straight and transverse, whereas the posterolophid is curved and anteriorly concave. The metaflexid closes to form a metafossettid before the merged anteroflexid/mesoflexid in all molars. The two lingual cuspids, the protoconid and hypoconid, are fairly pointed and border a wide hypoflexid with an apex that points posterolabially. An accessory cuspid is present

slightly posterior and lingual to the metaconid in the m1 in all specimens and in the m2 of SGOPV 2367 (Fig. 19A). The m1s also have a small projection off of the ectolophid that, following Boivin and Marivaux (2020), we interpret as the posterior arm of the protoconid. Both structures are reduced in m2 and absent in m3.

SGOPV 2367 preserves most of the horizontal ramus of the mandible. No mental foramen is present. The notch for the insertion of the masseter muscle pars infraorbitalis reaches the dp4-m1 border at its anterior-most extent. The incisor root is damaged but is mediolaterally compressed in cross-section.

Remarks. We assign these specimens to *A. minutus* for several reasons. They fall within the size range of this species, slightly larger than *A. minutissimus* and smaller than *A. constans* and *A. gracilis* (Table 9; Arnal et al. 2017; table 1). The patterns of accessory cuspid presence and protoconid posterior arm development also matches those of *A. minutus*. The laterally compressed incisor, lack of mental foramen, and the position of masseter insertion also matches *A. minutus*.

Locality and Horizon. Fossiliferous Interval 7 (SGOPV 2131, 2136) and Bangles Quarry (SGOPV 2365, 2367), Pampa Castillo, Galera Formation, Aysén Region, Chile.

Age and Distribution. Santa Cruz Formation, Santacrucian SALMA, Santa Cruz Province, Argentina; Galera Formation, Santacrucian SALMA, Aysén Region, Chile; Collón Curá Formation, Colloncuran SALMA, Neuquén Province, Argentina; Honda Group (Quebrada Honda), Laventan SALMA, Tarija Department, Bolivia.

Acarechimys cf. *minutissimus* Ameghino, 1887a

Figure 19B

2002 *Acarechimys* cf. *A. minutus* Flynn, Novacek, Dodson, et al., table 1.

Material. SGOPV 2191, left dp4.

Description. Although damaged, most of the crown morphology of SGOPV 2191, a left dp4, remains discernable. This tooth exhibits little wear; the hypoflexid and metaflexid are continuous, and the mesolophid ends short of the ectolophid. The posterior arm of the protoconid is small and barely extends into the anterofossettid. The hypolophid extends lingually from the ectolophid and meets the entoconid at an angle, resulting in a 'kinked' appearance to this lophid. Lingually, the posterolophid is oriented labiolingually; labially, it bends abruptly anteriorly to meet the pointed hypoconid.

Remarks. SGOPV 2191 is smaller than *A. constans* and *A. gracilis* and within the size ranges of *A. minutus* and *A. minutissimus* (Table 9; Arnal et al. 2017; table 1). We refer it to *A.* cf. *minutissimus* because the mesolophid is well-developed, unlike that of *A. minutus.* The ectolophid and protoconid are unconnected in SGOPV 2191. This morphology is also seen in another small *Acarechimys* species, *A. leucotheae*, from the late Oligocene (Deseadan SALMA) of Patagonia; however, the ectolophid appears less labiolingually oriented than in *A. leucotheae* (Vucetich et al. 2015). Given that this specimen consists of an isolated dp4 that is also within the size range of *A. minutus*, a taxon we also recognize from Pampa Castillo, we provisionally assign SGOPV 2191 to *A.* cf. *minutissimus.*

Locality and Horizon. Fossiliferous Interval E-0 W, Pampa Castillo, Galera Formation, Chile.

Age and Distribution. Pinturas Formation, Santacrucian (‘Pinturan’) SALMA, Argentina; Santa Cruz Formation, Santacrucian SALMA, Argentina; Galera Formation, Santacrucian SALMA, Chile; Collón Curá Formation, Colloncuran SALMA, Argentina; Villavieja Formation, Laventan SALMA, Colombia.

Acarechimys constans Ameghino, 1887a

Figure 19C–D

2002 *Acarechimys* new sp. Flynn, Novacek, Dodson, et al., table 1 [*partim*].

Material. SGOPV 2135, right m2–3; SGOPV 2137, left dp4–m2; SGOPV 2138, right dp4–m1; SGOPV 2139, right m1–2; SGOPV 2143, left m1; SGOPV 2198, partial left m1 with complete left m2–3; SGOPV 2199, left dp4–m1; SGOPV 2362, left dp4–m1; SGOPV 2705, left dp4–m2 (Fig. 19D); SGOPV 2707, partial left DP4 and complete left M1 (Fig. 19C).

Description. SGOPV 2707 preserves the only upper teeth of *Acarechimys constans* recovered from Pampa Castillo, a partial left dP4 and a complete left M1 (Fig. 19C; Table 10). Both teeth are brachydont. The posterolabial part of dP4 is absent, but otherwise the tooth is complete. The anteroloph and protoloph are straight, parallel, and joined together to enclose a labiolingually elongate parafossette. The protocone and hypocone surround a U-shaped hypoflexus that opens directly lingually. The

preserved portion of the posteroloph is straight. M1 bears four labial crests (Fig. 19C). The anteroloph, protoloph, and mesolophule are straight and transverse; the fourth crest, a merged metaloph and posteroloph, is slightly anteriorly concave. The anteroloph is thinner than the protoloph and does extend as far labially as the paracone. The parafossette and metafossette are enclosed, with the latter being much shallower and nearly obliterated. In the anterolingual corner, the M1 protocone forms an obtuse angle with the anteroloph, and the enamel on its anterior and lingual edges is very thick. The protocone has a posterolingual spur that results in an oblique hypoflexus. The hypocone is smaller than the protocone and more pointed in occlusal view. This cusp forms a slight angle with the posteroloph, making the posterior edge of M1 somewhat sinuous.

Several specimens preserve the lower dentition of *A. constans* with SGOPV 2705 being shown in Figure 19D. The dp4 is pentalophodont, with both the mesolophid and posterior arm of the protoconid reaching the metaconid. Among specimens that preserve dp4, SGOPV 2705 is the only one in which there is a structure extending posterolingually from the metaconid, which we interpret as a mesostylid. As in *A. minutus*, the hypolophid is straight and transverse, whereas the posterolophid is strongly curved. The lower molars of *A. constans* are broadly similar to those of *A. minutus* but differ in several respects. They bear an accessory cuspid within the anteroflexid + mesoflexid of m1 (Fig. 19D). In m1, this accessory cuspid is not associated/fused with metalophulid I. The posterior arm of the protoconid extends further lingually in *A. constans* and merges with the accessory cuspid after moderate wear, giving the tooth a tetralophodont appearance. Neither the accessory

cuspid or extended posterior arm of the protoconid are present in m2 or m3 (SGOPV 2198), making them truly trilophodont.

SGOPV 2362 preserves the horizontal ramus of the mandible. A mental foramen is present, and the anterior end of notch for the insertion of the masseter pars infraorbitalis is below the anterior half of m1. The lower incisor of this specimen is slender and more circular in cross-section than that of *A. minutus*.

Remarks. We assign these specimens to *A. constans* based on their occlusal morphology, but their size is also in agreement with Arnal et al. (2017)'s description of this taxon, as they are slightly larger than *A. minutus* (Table 9). The presence of accessory cuspids in m1 only and a well-developed mesolophid in dp4 most clearly distinguish these specimens from *A. minutus*. The mandibular morphology described herein also fits with the observations of Arnal et al. (2017).

Locality and Horizon. Fossiliferous Interval E-0 W (SGOPV 2198, 2199, 2707), Fossiliferous Interval 7 (SGOPV 2135, 2137, 2138, 2139, 2143, 2705), and Bangles Quarry (SGOPV 2362), Pampa Castillo, Galera Formation, Chile.

Age and Distribution. Santa Cruz Formation, Santacrucian SALMA, Santa Cruz Province, Argentina; Galera Formation, Santacrucian SALMA, Aysén Region, Chile.

Remarks. Acarechimys is well-recorded in the fossil record, having been found in late Oligocene to middle Miocene (Deseadan–Laventan SALMAs) deposits throughout South America (Arnal et al. 2017). Historically, *Acarechimys* was placed in the Echimyidae or Acaremyidae (Scott 1905; Wood and Patterson 1959; Patterson and Wood 1982; Vucetich et al. 1993), but recent studies have

contradicted these views. Various phylogenetic analyses have recovered *Acarechimys* as a stem octodontoid (Arnal et al. 2014, 2017; Arnal and Vucetich 2015a, b; Candela 2016) or an abrocomid (Verzi et al. 2014). Arnal et al. (2017) recovered the five *Acarechimys* species they recognized as a monophyletic group. The analysis of Verzi et al. (2017) recovered three species as members of Abrocomidae (including the type, *A. minutus*) and two as members of Octodontidae. These authors proposed a new (monotypic) genus to accommodate *A. constans*, *Ameghinomys* Verzi et al. 2017, and recognized a new species, *Acarechimys pascuali* Verzi et al. 2017, based on several specimens previously assigned to *A. constans*. We follow the taxonomy of Arnal et al. (2017) here and recognize *A. constans* as a species of *Acarechimys*.

In Patagonia, four of the five *Acarechimys* species recognized by Arnal et al. (2017) occur in early Miocene and younger strata; the fifth, *A. leucotheae,* is exclusive to the late Oligocene of Chubut Province, Argentina (Vucetich et al. 2015). *Acarechimys constans* has been previously reported only from exposures of the Santa Cruz Formation along the Río Santa Cruz and Atlantic coast (Arnal et al. 2017, 2019). The temporal and geographic ranges of *A. minutus* are broader encompassing the SCF and younger deposits of the Collón Cura Formation in Patagonia (Colloncuran SALMA) and possibly the Laventan locality of Quebrada Honda in southern Bolivia, though this latter record may represent a yet unnamed species (Croft et al. 2011; Arnal et al. 2017). *Acarechimys minutissimus* is the most wide-ranging species of its genus being found Santacrucian–Laventan SALMAs and from Patagonia to Colombia (Walton 1997; Arnal et al. 2017). Previous Chilean

Acarechimys records include *Acarechimys* sp. nov. from Santacrucian levels of the Cura-Mallín Formation at Laguna del Laja in south-central Chile (Flynn et al. 2008) and *Acarechimys* sp. from the Santacrucian Chucal Fauna in northern Chile (Croft et al. 2007).

Dudumus Arnal et al., 2014

Type Species. *Dudumus ruigomezi* Arnal et al., 2014.

Included Species. The type, *Dudumus* sp. nov. 1 Arnal et al., 2019, and *Dudumus* sp. nov. 2 (this study).

Diagnosis (Emended from Arnal et al. 2014). Small octodontoid approximately the size of *Acarechimys* and *Acaremys murinus* and smaller than *Sciamys*, *Plesiacarechimys*, and *Prospaniomys*. DP4/dp4 retained throughout life. Lower and upper molariforms low-crowned and terraced to a lesser degree than in *Caviocricetus*. Cusps/ids well differentiated from crests/cristids. The dp4 with metalophulid I separated from the metaconid in little-worn specimens and a spur projecting posterolingually from the posterior wall of metalophulid I, between the protoconid and anteroconid. Lower molars with large lingual cusps and second transverse cristid longer in m2 than in m1 and m3, as in *Prospaniomys priscus*. Dental morphology of upper cheek teeth similar to *Caviocricetus*, with anteroposterior diameter longer than transverse diameter. Paracone conspicuously higher than the rest of the tooth and larger than mesostyle. Mesolophule present,

longer, and higher than in *Caviocricetus*. As for anteroloph, mesolophule does not reach labial edge of upper molars.

Age and Distribution. Trelew Member, Sarmiento Formation, Colhuehuapian SALMA, Chubut Province, Argentina; Santa Cruz Formation, Santacrucian SALMA, Santa Cruz Province, Argentina; Galera Formation, Santacrucian SALMA, Aysén Region, Chile.

Dudumus sp. nov. 2

Figure 20A–B

Holotype*.* SGOPV 2140, maxillary fragment bearing left M1–2 (Fig. 20A–B).

Diagnosis. Similar in overall size and hypsodonty to *D. ruigomezi.* Differs from this taxon in having more anteroposteriorly elongate upper molars. Posteroloph more strongly curved than in *D. ruigomezi*. Hypocone less lingually offset from protocone than in *D. ruigomezi*.

Description. The type and only specimen of *Dudumus* sp. nov. 2 consists of a small maxillary fragment with two molariforms that we interpret as M1–2 (Fig. 20A–B). These teeth cannot represent P4/DP4–M1 because a partial molariform alveolus is present anterior to them. They also cannot represent M2–3 because these two teeth closely resemble each other (except for differing levels of wear), and the M3 of *D. ruigomezi* and closely related octodontoids (e.g., *Acarechimys*, *Acaremys*,

Caviocricetus) differs considerably from M2 (Vucetich and Verzi 1996; Arnal et al. 2014, 2017; Arnal and Vucetich 2015*b*).

M1 of SGOPV 2140 is longer anteroposteriorly than wide labiolingually (Table 10). It is 'terraced,' with the labial cusps, particularly the paracone, rising higher than the other portions of the tooth (Fig. 20B). This is an unusual morphology in octodontoids that was first reported in *Caviocricetus lucasi* and later in *D. ruigomezi* and *Acarechimys* (Vucetich and Verzi 1996; Arnal et al. 2014, 2017). The tooth is tetralophodont (Fig. 20A). The mesoflexus is wider than the paraflexus, but its labial borders are at a similar distance from the occlusal surface, which implies that they would close with a similar degree of wear. The anteroloph does not reach the labial border of the tooth. The anteroloph is thinner than the other crests and forms an obtuse angle with the protocone. The protoloph is of variable thickness and connects to the paracone. The third transverse crest is fairly straight, unlike in some specimens *D. ruigomezi* (Arnal et al. 2014). It is difficult to assess the homologies of the third transverse crest when it is complete as in *Dudumus* sp. nov. 2, but when it is incomplete, as in the DP4 of *D. ruigomezi*, the weaker connection of this crest to the mesostyle suggests that it corresponds to the mesolophule (Boivin and Marivaux 2020). The mesolophule and protoloph diverge in *Dudumus* sp. nov. 2, so the mesoflexus is wider at its labial end. In *D. ruigomezi*, these crests are roughly parallel, so the mesoflexus is more U-shaped than V-shaped in occlusal view. M2 is nearly identical to M1 except for exhibiting less wear. One possible difference is the shape of the anteroloph, which does not form a noticeable angle where it meets the protocone. However, wear may still be responsible for this difference.

Remarks. We recognize *Dudumus* sp. nov. 2 as distinct from *D. ruigomezi*, the type and previously only known species of *Dudumus*, based on its anteroposteriorly longer upper molars and differing upper molar crests (Fig. 20A–B; Table 10). *Dudumus ruigomezi* is known only from outcrops of the Trelew Member of the Sarmiento Formation at Bryn Gwyn (Cp-BG) in eastern Chubut Province, Argentina (Fig. 18; Arnal et al. 2014). Cp-BG fauna has been referred to the Colhuehuapian SALMA, making it older than the Santacrucian fauna of Pampa Castillo (Flynn et al. 2002b).

Arnal et al. (2019) reported a probable new species of *Dudumus* (which is referred to here as *Dudumus* sp. nov. 1) based on a single specimen preserving M1–2 that was collected from outcrops of the Santa Cruz Formation along the Río Santa Cruz. They stated that this taxon differs from *D. ruigomezi* and *Caviocricetus lucasi* in the proportions of its teeth. We do not believe that the specimen described herein represents the same species as *Dudumus* sp. nov. 1 because of its smaller size and several morphological differences (M. Arnal pers. comm. [2020]). *Dudumus* is generally recovered as a stem-octodontoid (Arnal et al. 2014; Arnal and Vucetich 2015a, b; Busker and Dozo 2019; Boivin et al. 2019a).

Vucetich and Verzi (1996) suggested that the fourth crest of the upper molariforms of *C. lucasi* is composed of both the posteroloph and metaloph because this crest is formed by distinct labial (metaloph) and lingual (posteroloph) portions in little-worn specimens. Boivin and Marivaux (2020) identified the main posterolabial cusp in octodontoids as a mesostyle rather than a metacone (as interpreted by most previous authors), which suggests that the metaloph of *C. lucasi* represents the

metaloph and metacone. The incomplete fusion of the labial part of this fourth crest to the posterolabial cusp corroborates this view. Arnal et al. (2014) observed the same morphology in *D. ruigomezi*, and it is also seen in the M2 of *Dudumus* sp. nov. 2. Previous authors have not identified this morphology in other tetralophodont stem-octodontoids, but constrictions in the fourth crest in little-worn molars of *Acarechimys* (Arnal et al. 2017: figs. 4.2, 5.2), *Prospaniomys* (Arnal et al. 2019: fig. 2.17), and *Prostichomys bowni* (Kramarz 2001: fig. 2) suggest that it may be more widespread.

Age and Distribution. Galera Formation, Santacrucian SALMA, Aysén Region, Chile.

Caviocricetus Vucetich and Verzi, 1996

Type Species. *Caviocricetus lucasi* Vucetich and Verzi, 1996.

Included Species. The type and *Caviocricetus* sp. nov.

Diagnosis (Emended from Vucetich and Verzi 1996*)*. Small, brachydont octodontoid, similar in size to *Acarechimys minutus*, *Acarechimys minutissimus*, and *Dudumus ruigomezi*. The dp4 with a ‘v’-shaped anterior border. Terraced molariforms with paracone and mesostyle and meta- and entoconid higher than the rest of the tooth except in highly worn teeth. Terracing more extreme than in *Dudumus* and *Acarechimys* Lower molars trilophodont with an independent ‘knob’ within anteroflexid + mesoflexid that protrudes less than lophids. Anteroflexid + mesoflexid wider anteroposteriorly than in *Acarechimys*. Upper molars tetralophodont and anteroposterior diameter greater than labiolingual. Anteroloph

much shorter labiolingually than protoloph. Third transverse crest, likely the mesolophule, labiolingually shorter than protoloph.

Age and Distribution. Trelew Member, Sarmiento Formation, Colhuehuapian SALMA, Chubut Province, Argentina; Cerro Bandera Formation, Colhuehuapian? SALMA, Neuquén Province, Argentina; Galera Formation, Santacrucian SALMA, Aysén Region, Chile.

Caviocricetus sp. nov.

Figure 20C–D

Holotype. SGOPV 2194, maxillary fragment bearing right DP4–M1.

Diagnosis. Smaller than the type species, *C. lucasi*. Anteroloph of M1 better developed and more transversely oriented than in *C. lucasi*. Protocone wider than in *C. lucasi* and producing a narrower hypoflexus, similar to other octodontoids.

Description. SGOPV 2194 consists of a maxillary fragment bearing moderately worn right DP4–M1 (Fig. 20C; Table 10). The teeth are low-crowned, tetralophodont, and terraced (i.e., the labial cusps are higher than the lingual cusps; Fig. 20D). This terracing is more extreme than in *Dudumus* spp. (Fig. 20B; Arnal et al. 2014) and *Acarechimys* spp. (Arnal et al. 2017). The anteroloph of DP4 is short and connects to the protocone with no obvious angle or inflection point between them. This crest curves toward the paracone but would not join it to enclose the parafossette until heavily worn. The protoloph is straight and obliquely oriented (anterolabially-

posterolingually). The paracone is notably broader and higher than the protoloph. The fairly straight third transverse crest joins the mesostyle to enclose the posterofossette. The fourth transverse crest varies in thickness; its posterior border protrudes sharply near its labiolingual midpoint (approximating a triangle), while the anterior border (posterior border of the posterofossette) is smoothly curved. The likely homologies of this crest are discussed below. The hypocone and protocone are triangular, with their apexes pointed slightly posteriorly. The apex of the hypoflexus is also angular and opens posterolabially. Its posterior wall is much longer than its anterior one.

M1 broadly resembles DP4 except for its lesser degree of wear. The anteroloph is longer and more labiolingually oriented than that of DP4 (Fig. 20C). It forms a marked angle where it meets the protocone. The protocone of M1 is wider than that of DP4 as well as M1–2 of the type species, *C. lucasi* (Vucetich and Verzi 1996). This wide protocone likely contributes to the narrower hypoflexus of *Caviocricetus* sp. nov. compared to *C. lucasi.* The paracone is more labial than the mesostyle, so that the protoloph is longer in this tooth than in DP4. The lingual half of the third transverse crest of M1 is labiolingually oriented, but its labial end is directed more posteriorly to meet the mesostyle and enclose the posterofossette. Following Boivin and Marivaux (2020), we interpret the lack of an intimate connection between this crest and the mesostyle as indicating that it is formed entirely by the mesolophule (i.e., the mesoloph is absent). The fourth transverse crest appears to be comprised of multiple parts, as in *Dudumus* sp. nov. 2 (Fig. 20A). The lingual portion that extend from the hypocone likely represents the

posteroloph, whereas the labial portion corresponds to the metaloph or metaloph + metacone.

Remarks. SGOPV 2194 is the type and only specimen of *Caviocricetus* sp. nov. (Fig. 20C–D). Two other small, tetralophodont octodontoids are known from Pampa Castillo: *Acarechimys minutissimus* and *Dudumus* sp. nov. 2. *Caviocricetus* sp. nov. differs from them in several respects. *Dudumus* sp. nov. 2 is ~40% larger, with less terraced molariforms and a straighter third transverse crest (Fig. 20; Table 10). The DP4–M1 of *Caviocricetus* sp. nov. are relatively longer than those of *A. minutissimus*, the paraflexus remains open longer, the labial flexi/fossettes are shorter and broader, and the protocone is slimmer (Arnal et al. 2017).

Caviocricetus was previously only known from the type species, *C. lucasi*. This species was originally discovered in Cp-BG that have produced a Colhuehuapian fauna (Vucetich and Verzi 1996; Vucetich et al. 2010a). Kramarz et al. (2005) later reported *C. lucasi* from the Cerro Bandera Formation (Cp-CB) at Sierra Portezuelo Norte. Phylogenetic analyses generally recover *Caviocricetus* as a stem-octodontoid (Arnal and Vucetich 2015a, b; Arnal et al. 2017; Boivin et al. 2019; Busker and Dozo 2019), but in some analyses, it is a member of Abrocomidae (Verzi et al. 2017) or Octodontinae (Verzi et al. 2014).

Locality and Horizon. Fossiliferous Interval E-0 W, Pampa Castillo, Galera Formation, Aysén Region, Chile.

Age and Distribution. Galera Formation, Santacrucian SALMA, Aysén Region, Chile.

Echimyidae Gray, 1825

Spaniomys Ameghino, 1887a

Type Species. *Spaniomys riparius* Ameghino, 1887a.

Included Species. The type, *Spaniomys modestus* Ameghino, 1887a, and *Spaniomys biplicatus* Ameghino, 1894.

Age and Distribution. Galera Formation, Santacrucian SALMA, Aysén Region, Chile; Pinturas Formation, Santacrucian SALMA, Santa Cruz Province, Argentina; Santa Cruz Formation, Santacrucian SALMA, Santa Cruz Province, Argentina.

Spaniomys cf. *riparius* Ameghino, 1887a

Figure 21

2002 *Spaniomys riparius* Flynn, Novacek, Dodson, et al., table 1.

Material. SGOPV 2128, right p4 (Fig. 21B); SGOPV 2129, right m1 or 2 (Fig. 21C); SGOPV 2130, right m3 (Fig. 21D); SGOPV 2132, left M1 or 2 (Fig. 21A).

Description. The lone upper molar of *S.* cf. *riparius* in our sample, SGOPV 2132, represents M1 or M2 (Fig. 21A). This tooth is tetralophodont, and the labial cuspids are not easily distinguished from the lophs. The anteroloph is damaged, and the protoloph is quite broad and transverse. The third transverse crest connects to the posteroloph producing a distinctive morphology in the posterior portion of this tooth

that resembles a “Y”. Following Boivin and Marivaux (2020), we interpret this crest as the mesoloph. Labial of its junction with the mesoloph, the posteroloph bows outward and becomes anteriorly concave.

Three lower teeth of *S.* cf. *riparius* have been recovered from Pampa Castillo. The dp4 is tetralophodont (Fig. 21B). Metalophulid I is broad and transverse, but the other three lophids are thinner and slightly anteriorly concave. The protoconid and hypoconid are broad, triangular, and point labially. They delineate a broad hypoflexid that is transversely oriented. The m1 or 2 (SGOPV 2129) broadly resembles dp4 except for several differences (Fig. 21C): it is labiolingually wider than dp4 (Table 9); the anterior border of metalophulid I is straight rather than curved; and the protoconid is notably larger than the hypoconid, making the hypoflexid points slightly more anteriorly. M3 is trilophodont (Fig. 21D). Its lophids are more strongly curved than those of dp4 or m1 or 2.

Remarks. Ameghino (1887a, 1894) recognized three species of *Spaniomys*, but the genus is in need of revision, precluding us from assigning the specimens described here to any of these species with confidence (Kramarz 2004; Arnal et al. 2019). Arnal et al. (2019) assigned some of their *Spaniomys* specimens from the Santa Cruz Formation to *S. riparius* based on size but referred most to *Spaniomys* sp. We assign the specimens described herein to *S.* cf. *riparius* primarily because they are larger than *S. modestus*, based on the range provided by Kramarz (2004; Tables 9–10).

Spaniomys occurs throughout the Santa Cruz Formation (Ameghino 1887a; Scott 1905; Arnal et al. 2019) as well as the upper sequence of the Pinturas

Formation (Kramarz 2004). The phylogenetic position of *Spaniomys* within Octodontoidea has varied among recent studies, which have found it to be a member of Abrocomidae (Verzi et al. 2014, 2017; Candela 2016) or Echimyidae (Arnal et al. 2017; Boivin et al. 2019) or part of an unresolved polytomy within crown Octodontoidea (Arnal and Vucetich 2015a).

Locality and Horizon. Fossiliferous Interval E-0, Pampa Castillo, Galera Formation, Aysén Region, Chile.

Acaremyidae Wood, 1949

Acaremys Ameghino, 1887a

Type Species. *Acaremys murinus* Ameghino, 1887a.

Included Species. The type, *Acaremys major* Scott, 1905, and *Acaremys messor* Ameghino, 1889.

Age and Distribution. Trelew and Colhué-Huapi members, Sarmiento Formation, Colhuehuapian SALMA, Chubut Province, Argentina; Pinturas Formation, Santacrucian ('Pinturan') SALMA, Santa Cruz Province, Argentina; Santa Cruz Formation, Santacrucian SALMA, Santa Cruz Province, Argentina; Galera Formation, Santacrucian SALMA, Aysén Region, Chile.

Acaremys sp. Ameghino, 1887a

Figure 22A

Material. SGOPV 2365, maxillary fragment with right DP4–M1.

Description. SGOPV 2365 is part of a right maxilla preserving the anterior part of the zygomatic arch and DP4–M1 (Fig. 22A). Unlike many octodontoids, species of *Acaremys* replace their deciduous premolars (Arnal and Vucetich 2015b). Nevertheless, we identify the more anterior tooth of SGOPV 2365 as DP4 because it is less worn than M1 and its morphology matches previously descriptions of this tooth (Arnal and Vucetich 2015b). M1 is not fully erupted, but DP4 is slightly higher crowned than the corresponding tooth of *Acarechimys.* The DP4 is anteroposteriorly longer than it is wide (Table 10). The anteroloph is long and curved and reaches the labial edge of the tooth. The protoloph is straight and points slightly toward the anterolabial corner. The paraflexus is open but would have closed before the mesoflexus based on its shallower labial end. The third transverse crest is parallel to the protoloph and is fused to the mesostylid. The posterofossette appears to have closed early in ontogeny due to the thickness its labial border. The fourth crest, likely composed of the metaloph and posteroloph, is even more strongly curved than the anteroloph. The protocone and hypocone are small and triangular. They border a shallow hypoflexus that opens posteriorly and does not extend very far labially.

The coronal morphology of M1 is partially obscured by DP4, which overlaps it (Fig. 22A), but it is tetralophodont, and its labiolingual and anteroposterior dimensions are subequal unlike the anteroposteriorly elongate DP4. The para- and posterofossettes are already enclosed, even with the complete lack of wear. The protoloph and third transverse crest diverge slightly so that the mesoflexus widens labially. In other respects, M1 is similar to DP4.

Remarks. We assign SGOPV 2365 to *Acaremys* sp. based on its size and morphology (Fig. 22A). *Galileomys* has somewhat terraced molars that are much wider labiolingually than long (Vucetich and Kramarz 2003; Kramarz 2004) The DP4 of *Sciamys* is very different than that of SGOPV 2365, and the upper molar hypoflexi of this taxon penetrate further labially than in SGOPV 2365 (Arnal et al. 2019). The upper molars of *Pseudoacaremys kramarzi* have a protocone that is more labial than the hypocone, which we do not observe in SGOPV 2365 (Arnal and Vucetich 2015b). The para- and posterofossettes of *'Acaremys*' *preminutus* are much broader labiolingually than those of SGOPV 2365 (Arnal and Vucetich 2015b), precluding referral to this taxon. Arnal and Vucetich (2015b) recognized three species of *Acaremys*. The dental morphology of SGOPV 2365 resembles the type and best-known species, *A. murinus*, but we cannot confidently assign the specimen to this species because of its smaller size than the specimens reported by Arnal and Vucetich (2015b: table 2; Table 10) and the fact that *A. messor* and '*A.*' *tricarinatus* are known exclusively from lower molars. However, one *Acaremys* species, *A. major* can be ruled out, because it is much larger than SGOPV 2365. Despite the small size of SGOPV 2365. *A. murinus* is still closer in size to this specimen than all other morphologically similar species. However, this size difference and our lack of ability to directly compare SGOPV 2365 to several *Acaremys* spp. and '*A.*' *tricarinatus* precludes us from assigning it beyond the genus level.

Locality and Horizon. Bangles Quarry, Pampa Castillo, Galera Formation, Aysén Region, Chile.

cf. *Acaremys* sp.

Figure 22B

Material. SGOPV 2343, right P4–M1 and partial M2–3 (Fig. 22B); SGOPV 2363, partial palate with partial left P4–M1, complete left M2, complete right P4, and partial right M1.

Description. SGOPV 2343 and SGOPV 2363 both include parts of the upper dentition and are heavily worn. The M2–3 of SGOPV 2343 still preserve para- and posterofossettes (Fig. 22B), but these features are obliterated in SGOPV 2363. The teeth are significantly wider labiolingually than long (Table 10). P4 is tetralophodont in most acaremyids, but the third transverse crest is poorly developed and merges with the fourth crest early in ontogeny (Vucetich and Kramarz 2003; Arnal and Vucetich 2015b). That is the case in the P4 of SGOPV 2343, which appears trilophodont, with the mesoflexus penetrating further lingually than the paraflexus. Only the roots of M1 are present in SGOPV 2363. In SGOPV 2343, the anteroloph of M1 forms a largely straight anterior border that curves to meet the paracone. The mesoflexus and hypoflexus are narrower than in P4 and have straight borders. As on DP4, the mure extends approximately halfway across the occlusal surface of the M1. The posterior half of M1 is broader than in P4, making the anterior and posterior halves of the former tooth more symmetrical. The M2 parafossette of SGOPV 2343 is small and subcircular (Fig. 22B). The paracone projects slightly further labially than the mesostyle. The apex of the hypoflexus points anterolabially. Only the labial half of M3 is preserved in SGOPV 2343. The parafossette is elongate labiolingually. The mesoflexus is slightly wider than in M2 but is bordered labially by a similarly

pointed paracone and metacone. As in M2, the paracone is more labial than the mesostylid, but this difference is more pronounced in M3.

Remarks. The identities of SGOPV 2343 and SGOPV 2363 are difficult to determine due to their highly worn state. We believe they pertain to an acaremyid because the teeth are labiolingually elongate and the morphology of P4 compares favorably. The portion of P4 anterior to the mure is much broader anteroposteriorly than the portion posterior to the mure. The P4s of acaremyids like *Acaremys*, *Galileomys*, and *Sciamys* either lack or have reduced third transverse crests (Vucetich and Kramarz 2003; Arnal and Vucetich 2015b). In worn specimens, where the mesoflexus is the only remaining labial flexus/fossette, this arrangement produces a morphology like that seen in the P4 of SGOPV 2343 and 2363.

Unfortunately, the heavily worn nature of these specimens precludes us from confidently assigning them to an acaremyid genus, but we can rule out several taxa. The P4 of *Platypittamys* lacks a hypoflexus, and *Pseudoacaremys* retains its DP4, unlike these specimens (Wood 1949; Arnal and Vucetich 2015b). *Acaremys*, *Galileomys*, and *Sciamys* are all of approximately the same size and known from the Santacrucian SALMA (inclusive of the 'Pinturan') (Scott 1905; Kramarz 2004; Arnal and Vucetich 2015b). The features used to distinguish these taxa are not present in SGOPV 2343 and 2363 or have been obliterated by wear. We refer these two specimens to cf. *Acaremys* sp. because SGOPV 2365 (Fig. 22A) confirms the presence of *Acaremys* at Pampa Castillo.

Locality and Horizon. Fossiliferous Interval E-0, Pampa Castillo, Galera Formation, Aysén Region, Chile.

Adelphomyidae Patterson and Pascual, 1968

Prostichomys Kramarz, 2001

Type Species. *Prostichomys bowni* Kramarz, 2001.

Included Species. The type and *Prostichomys* sp. nov.

Age and Distribution. Pinturas Formation, Santacrucian ('Pinturan') SALMA, Santa Cruz Province, Argentina; Galera Formation, Santacrucian SALMA, Aysén Region, Chile; Curá-Mallín Formation, Santacrucian SALMA, Biobío Region, Chile.

Prostichomys sp. nov.

Figure 23

Material. SGOPV 2706, left m1 or 2.

Description. SGOPV 2706 is a relatively high-crowned tetralophodont m1 or m2 that is slightly larger than its counterpart in *P. bowni* (Table 9; Kramarz 2001). It most notably differs from *P. bowni* and all other early Miocene octodontoids in having a metalophulid I that does not connect to the protoconid, leaving the anteroflexid open on the anterior edge of the tooth (Fig. 23). This opening remains despite the closure of the lingual opening of the anteroflexid and metaflexid. The metaconid is smoothly curved, resulting in a rounded anterolingual corner of the tooth. A bulge extends anteriorly from the second transverse cristid into the anteroflexid. This bulge would likely fuse with metalophulid I with additional wear,

splitting the anteroflexid/fossettid in two, as in *Platypittamys* (Wood 1949). The second transverse cristid barely reaches the lingual edge of the tooth and is oriented obliquely, with its the lingual end positioned more posteriorly than its labial end. The hypolophid is straight, and there is no swelling for the entoconid is apparent. The posterolophid curves to meet the entoconid, enclosing the metafossettid. The mesofossettid is narrower but deeper than the other lingual flexids/fossettids, and its apex points anterolabially. The hypoconid and protoconid are both triangular and project directly labially. As a result, the hypoflexid is very wide and opens labially.

Remarks. SGOPV 2706 is a fairly high-crowned, tetralophodont lower molar. The hypolophid and posterolophid are relatively straight, broad, and consistent in width (Fig. 23). The metaflexid and anteroflexid close early in ontogeny (at least lingually). This combination of features precludes assignment to most Oligocene–Miocene octodontoid genera. Many erethizontoid lower molars are tetralophodont, but this tooth is too small and high-crowned to pertain to this clade (Table 9; Candela and Vucetich 2002; Candela 2003; Kramarz 2004). The two species that most resemble SGOPV 2706 are two adelphomyids, *Prostichomys bowni* and *Xylechimys obliquus*, both of which represent the only named species of their respective genera. *Prostichomys bowni* resembles SGOPV 2706 more than *X. obliquus* does in crown height, its well-developed posterolophid, and its broad proto- and hypoconids (Kramarz 2001). However, the unusual anteroflexid morphology of SGOPV 2706 is much more similar to what is seen in *X. obliquus* (Patterson and Pascual 1968). Thus, SGOPV 2706 bears features of both genera, but we favor assignment to *Prostichomys.* The second transverse cristid (likely the posterior arm of the

protoconid) reaches the metaconid in SGOPV 2706, a condition more similar to that of *P. bowni* than *X. obliquus.* The metaflexid of *Xylechimys* appears that it will close very late in ontogeny if at all, whereas the metafossettid is nearly enclosed in SGOPV 2706 (Fig. 23). Although the anteroflexid does not open anteriorly in *P. bowni*, the protoconid and metalophulid I are weakly connected, suggesting that they may be separate in newly erupted teeth (Kramarz 2001: fig. 1). Although we base our assignment of SGOPV 2706 on morphology, it is also worth noting that *X. obliquus* is known from the late Oligocene (Deseadan SALMA; Wood 1949), whereas *P. bowni* has been found in 'Pinturan' faunas of the Pinturas and Sarmiento formations (Santacrucian SALMA; Kramarz 2001; Kramarz et al. 2010). Therefore, *P. bowni* is closer in age to the strata from which SGOPV 2706 originates at Pampa Castillo. SGOPV 2706 is clearly morphologically distinct from *P. bowni*, so we recognize it as a new species, but we refrain from erecting a new taxon based on a single molar of uncertain locus.

Prostichomys bowni is the most abundant rodent in the lower and middle sequences of the Pinturas Formation, ranging from ~38–65% of rodent specimens across all localities (Kramarz and Bellosi 2005: fig. 6). *Prostichomys* is rare at Pampa Castillo; SGOPV 2706 as the only recognized specimen out of 338 total rodent specimens. Flynn et al. (2008) mentioned two new species of *Prostichomys* from Santacrucian levels of the Cura-Mallín Formation in central Chile that have not yet been described. *Prostichomys* is traditionally recognized as an adelphomyine echimyid along with *Adelphomys*, *Deseadomys*, *Paradelphomys*, *Quebradahondomys*, *Ricardomys*, *Stichomys*, and *Xylechimys* (Patterson and

Pascual 1968; Walton 1997; Kramarz 2001; Croft et al. 2011; Verzi et al. 2016). However, Boivin et al. (2019) recovered this clade outside of crown-Octodontoidea and raised it to 'family rank' with the name Adelphomyidae.

Locality and Horizon. Fossiliferous Interval E-0 E, Pampa Castillo, Galera Formation, Aysén Region, Chile.

RESULTS

The octodontoid assemblage from Pampa Castillo consists of six genera and eight species, including three new species: *Caviocricetus* sp. nov., *Dudumus* sp. nov. 2, and *Prostichomys* sp. nov. Although we feel confident that *Prostichomys* sp. nov. represents a new taxon, we do not want to erect a new taxon based on a single molar. This work represents the first formal description of *Acaremys*, *Caviocricetus*, *Dudumus*, *Prostichomys*, and *Spaniomys* from Chile.

In seven of the eight analyses, the three faunas traditionally recognized as Colhuehuapian, Cp-GB-LFZ, Cp-CB, and Cp-BG, formed a cluster (Table 8; Figs. 24, S15–S16). The lone exception was the genus-level analysis excluding provisional taxa using the Jaccard index where the Cerro Bandera Formation (Cp-CB) was recovered outside of the group encompassing all other faunas (Fig. S15A). In the seven analyses where they do form a cluster, Cp-GB-LFZ and Cp-BG are recovered as more similar to each other than the Cp-CB. This cluster was recovered outside of the cluster comprised of all other faunas in all analyses.

The two faunas assigned to post-Santacrucian SALMAs, Cc-CILY and Cc-CT, clustered together in all eight analyses.

The relationships of the faunas traditionally assigned to the Santacrucian SALMA varied across the eight analyses. Sa-SC-AC and Sa-SC-RSC formed an exclusive pair in all eight analyses. The Sa-uP was the next most-similar fauna to this pair in seven of eight analyses with the species-level analysis including provisional taxa using the Jaccard index as the one exception (Fig. 24B). The Sa-lmP and Sa-GB-UFZ are recovered as an exclusive cluster or with only Pampa Castillo separating them in seven of eight analyses. In the genus-level analysis without provisional taxa using the Jaccard index (Fig. S15A), Sa-GB-UFZ plotted outside the cluster including the five other Santacrucian faunas. The position of Pampa Castillo differed depending on whether genera or species were the taxonomic unit of interest. In the genus-level analyses, Pampa Castillo was recovered in the Sa-lmP + Sa-GB-UFZ cluster (Fig. 24A, S15A, S16A, S16C), the two faunas most often recognized as ‘Pinturan’ (Table 8). Which of these two faunas was recovered as most similar to Pampa Castillo depended on whether the Jaccard (Sa-lmP + Pampa Castillo) or Simpson similarity index (Sa-GB-UFZ + Pampa Castillo) was used. Conversely, in the four species-level analyses, Pampa Castillo was recovered as more similar to the Sa-SC-RSC+Sa-SC-AC pair (Figs. 24B, S15B, S16B, S16D). In one of these four analyses, when provisional taxa were included using the Jaccard index (Fig. 24B), Pampa Castillo was recovered as more similar to this pair than the Sa-uP was. The six faunas traditionally assigned to the Santacrucian SALMA (inclusive of the Pinturan) formed an exclusive cluster in six of

eight analyses. However, in the two species-level analyses using the Simpson similarity index, the Sa-lmP+Sa+GB-UFZ pairing plotted outside of a cluster that included the other four Santacrucian faunas and the two post-Santacrucian faunas (Fig. S16B, S16D).

DISCUSSION

Pampa Castillo Octodontoids

The octodontoid assemblage at Pampa Castillo is fairly diverse with six genera and, likely, eight species (seven if SGOPV 2191 represents *A. minutus* or *A. constans* rather than *A. minutissimus*). There is no clear stratigraphic pattern in taxon presence or abundance among the various fossiliferous levels at Pampa Castillo. Three species are newly described in this work one of which, *Prostichomys* sp. nov., we decline to name because it is represented by a single lower molariform (Fig. 23). The only named species of *Prostichomys*, *P. bowni*, comes from the Pinturas Formation and Sa-GB-UFZ (Kramarz 2001; Kramarz et al. 2010). Flynn et al. (2008) reported two new species of *Prostichomys* from the Cura-Mallín Formation at Laguna del Laja, but we do not believe that either represents the same species as the one described in this article. *Caviocricetus* sp. nov. is the second recognized species of its genus (Fig. 20C–D). The type species, *C. lucasi*, is known from Cp-BG and Cp-CB faunas that are assigned to the Colhuehuapian SALMA (Vucetich and Verzi 1996; Kramarz et al. 2005), so *Caviocricetus* sp. nov. represents a geographic

(Fig. 18) and temporal expansion of the range of this genus. *Dudumus* sp. nov. 2 is also the second named species of its genus (Fig. 20A–B). Arnal *et al.* (2019) reported a new species of *Dudumus* from Sa-SC-RSC, but we do not believe it is conspecific with *Dudumus* sp. nov. 2 based on published information and additional details provided by the lead author (M. Arnal, pers. comm. [2020]). The type species of *Dudumus*, *D. ruigomezi*, is found at Cp-BG (Arnal et al. 2014); like *Caviocricetus* sp. nov., *Dudumus* sp. nov. 2 represents a genus at Pampa Castillo previously known only from the Colhuehuapian SALMA.

The other octodontoids of Pampa Castillo are all species typical of other Santacrucian faunas. *Acarechimys minutus* and *A. minutissimus* have wide temporal and geographic ranges including various SCF sites and, in the case of *A. minutissimus*, Pinturas Formation localities (Fig. 19A–B; Arnal et al. 2017). *Acarechimys constans* was previously only known from the Santa Cruz Formation (Fig. 19C–D). *Spaniomys riparius* is known exclusively from the SCF, but *S. modestus* is known from both the Santa Cruz and Pinturas formations (Fig. 21; Kramarz 2004; Arnal et al. 2019). The systematics of this genus require revision, so the biogeographic and biostratigraphic significance of the individual species remains uncertain. *Acaremys* is a common component of Colhuehuapian and Santacrucian faunas of the Sarmiento, Pinturas, and Santa Cruz formations (Fig. 22; Arnal and Vucetich 2015b).

Relationships of Early to Middle Miocene Patagonian Faunas

In general, faunas cluster according to their previously assigned SALMA designations (Figs. 24, S15–S16). The Santacrucian and post-Santacrucian faunas

are more similar to each other than either is to those referred to the Colhuehuapian. Age differences likely account for this pattern. The youngest Santacrucian deposits at Sa-SC-RSC temporally overlap Cc-CT, whereas there is a ~1.5-million-year gap between the youngest Colhuehuapian (Cp-GB-LFZ) and oldest Santacrucian (Sa-GB-UFZ) deposits (Table 8). However, in six of eight analyses, the Santacrucian faunas, which span ~3.4 million years, form a cluster to the exclusion of the Colhuehuapian or post-Santacrucian faunas (Figs. 24, S15, S16A, S16C). At either end of this range, these Santacrucian faunas are closer in age to some Colhuehuapian or post-Santacrucian faunas than to some Santacrucian faunas. Therefore, age is not the sole driver of the clustering patterns.

Colhuehuapian Faunas—The Colhuehuapian SALMA is represented by three faunas in this analysis, although the referral of Cp-CB to this SALMA is uncertain. Cp-GB-LFZ and Cp-BG plot together in all eight analyses. The Cp-CB falls just outside of this pair in seven analyses and on a branch separate from all other faunas in one analysis (Fig. S15A). This fauna was originally referred to the Colhuehuapian SALMA, but the subsequent discovery of taxa not otherwise known after the Deseadan SALMA (late Oligocene) like *Cephalomys*, *Leucokephalos*, and Archaeohyracidae has cast doubt on this assignment (Kramarz et al. 2015). Our analysis included no definitively pre-Colhuehuapian faunas, so it cannot inform this debate. Nonetheless, the Cp-CB plots with the Colhuehuapian faunas of Cp-GB-LFZ and Cp-BG in seven of eight analyses, highlighting the many similarities among them.

Post-Santacrucian Faunas—The two post-Santacrucian faunas in this analysis cluster together in all eight analyses. As mentioned previously, Cc-CT temporally overlaps the youngest Santacrucian deposits at Sa-SC-RSC (Table 8). The Cc-CILY fauna is at least ~0.8 myr and perhaps up to ~3.1 myr younger than Cc-CT. The fact that these two faunas group with one another to the exclusion of Santacrucian faunas demonstrates a clear distinction between Santacrucian and post-Santacrucian rodent communities. It is worth noting that Cc-CT lies ~1,100 km north of the Sa-SC-RSC and ~730 km north of the Sa-lmP, the northernmost Santacrucian fauna in this analysis (Fig. 18). Cc-CT and Cc-CILY are only ~250 km apart. Therefore, we cannot rule out the idea that geography plays some role in the clustering pattern we observe here. Better characterization of lower-latitude rodent communities of Santacrucian age, such as Laguna del Laja, Chucal, or Divisadero Largo, will help disentangle the influences of geography and age (Flynn et al. 2002a, 2008; Cerdeño and Vucetich 2007).

Santacrucian Faunas—The remaining faunas in our analysis are typically assigned to the Santacrucian SALMA if one includes the ‘Pinturan’ faunas of the Sa-lmP and Sa-GB-UFZ. Sa-SC-RSC and Sa-SC-AC have been recognized as being very similar taxonomically , paleoenvironmentally, and in age (Fleagle et al. 2012; Cuitiño et al. 2016, 2019a; Fernicola et al. 2019a, b). They are also geographically close and at a similar latitude (Fig. 18). In concordance with these interpretations and proximity, these two faunas are recovered as the most similar pair of faunas in all analyses. The cluster analyses also support the division of the Pinturas Formation fossil assemblage into distinct lower-middle (Sa-lmP) and upper (Sa-uP) faunas. The

Sa-uP is recovered as the immediate outgroup to the Sa-SC-RSC+Sa-SC-AC pair in seven of eight analyses in agreement with Kramarz and Bellosi (2005)'s assertion that the Sa-uP rodent assemblage resembles that of the Sa-SC-RSC and Sa-SC-AC. Conversely, the Sa-lmP forms its own cluster with Sa-GB-UFZ and/or Pampa Castillo, depending on the specific analysis.

The Sa-GB-UFZ and Sa-lmP, the two faunas most often cited as representing the 'Pinturan' interval, are closely associated in three of the four analyses (Kramarz et al. 2010; Dunn et al. 2013). In the only analysis in which they are not associated, the genus-level analysis excluding provisional taxa using the Jaccard index (Fig. S15A), Sa-GB-UFZ falls outside the cluster of all other Santacrucian faunas. We believe this result is anomalous, reflecting that Sa-GB-UFZ is the least speciose fauna in our analysis and, therefore, has fewer opportunities to share taxa with other faunas (Table 8). This idea is supported by the recovery of Sa-GB-UFZ as most similar to Pampa Castillo (and then Sa-lmP) in the same analysis using the Simpson similarity index, which uses the number of taxa in the less rich of the two faunas being analyzed rather than the sum of taxa to calculate their similarity (Raup and Crick 1979). The similarity of the Sa-lmP and Sa-GB-UFZ is demonstrated by the presence of three taxa, *Neoreomys pinturensis*, *Prostichomys bowni*, and *Luantus propheticus*, found exclusively in these two faunas (Kramarz and Bellosi 2005; Kramarz et al. 2010). The similarity of these faunas despite age differences (Table 8) and distinct stratigraphic provenances (Pinturas and Sarmiento formations) supports the idea that the 'Pinturan' fauna was widespread and persisted for a significant amount of time.

Interestingly, Pampa Castillo's position in the faunal clustering analyses varies between the genus- and species-level analyses. These differences are noteworthy, as Pampa Castillo is well-nested in each cluster. In the genus-level analyses, Pampa Castillo is recovered as most similar to the Sa-lmP using the Jaccard index and most similar to the Sa-GB-UFZ using the Simpson similarity index (Figs. 24A, 15A, S16A, S16C). Based on these analyses, Pampa Castillo appears to represent a Pinturan fauna. Conversely, in the species-level analyses, Pampa Castillo is closer to the Sa-SC-RSC and Sa-SC-AC, in a cluster distinct from that Sa-lmP and Sa-GB-UFZ within the broader Santacrucian cluster (Fig. 24B, S15B, S16B, S16D). In the Pampa Castillo fauna, certain taxa are known from fragmentary remains that preclude their assignment to species-level (e.g., *Steiromys* sp. and *Acaremys* sp.). *Steiromys principalis* is known exclusively from the Sa-lmP, and *Steiromys detentus* is known exclusively from the Sa-SC-AC and Sa-SC-RSC (Kramarz 2004; Arnal et al. 2019). The third species, *Steiromys duplicatus* is known from both. Recognition of one of the two stratigraphically restricted species at Pampa Castillo would shed light on the true affinities of the fauna. However, even if all records of fragmentary taxa from Pampa Castillo (and other Santacrucian localities) were positively identified to species-level, the Pampa Castillo still records taxa that are known from Sa-SC-RSC+Sa-SC-AC, but not Sa-lmP+Sa-GB-UFZ localities, and vice versa. *Spaniomys riparius*, *Perimys onustus*, *Acarechimys constans*, and *Eocardia* are all found in Sa-SC-RSC and Sa-SC-AC but not Sa-lmP or Sa-GB-UFZ (Supplementary File 10). However, the reverse is true of *Prostichomys*, *Perimys intermedius*, and *Eosteiromys*. The Pampa Castillo rodent

community clearly preserves elements of both the Sa-SC-RSC+Sa-SC-AC and Sa-lmP+Sa-GB-UFZ faunas. The fact that Pampa Castillo shares more genera with the Sa-lmP-UFZFB and more species with the Sa-SC-RSC+Sa-SC-AC may be significant but may also be coincidental. The recognition of two taxa as members of different genera or merely different species is a matter of degree rather than reflecting anything concrete about their time since divergence or paleoecological differences. Therefore, we will not draw any biochronologic or paleoenvironmental conclusions based on the genus- versus species-level similarity patterns. We merely treat the genus- and species-level patterns as differing results coming from different, though not independent, sources of data.

Pinturan: SALMA, Sub-Age or Local Fauna?

Pinturan: Faunal Content and Age—Kramarz and Bellosi (2005) recognized the rodent assemblage of the Sa-lmP as the ‘Pinturan association’ and suggested that this fauna was slightly older than the ‘typical’ Santacrucian faunas of the Sa-SC-RSC and Sa-SC-AC. The subsequent discovery of a second Pinturan fauna, Sa-GB-UFZ, demonstrated that this assemblage occurs outside of the geographically and stratigraphically limited area of the Sa-lmP (i.e., valley of the Río Pinturas; Kramarz et al. 2010). Several species are found in both the Pinturan and Sa-SC-RSC+Sa-SC-AC, such as *Neoreomys australis* and *Steiromys duplicatus* (Kramarz 2004, 2006a; Arnal et al. 2019). Other Pinturan taxa, such as *Eosteiromys* and *Branisamyopsis*, are shared with older Colhuehuapian but not Sa-SC-RSC+Sa-SC-AC faunas. Some species, such as *P. bowni*, *Luantus propheticus*, and *Steiromys principalis*, are exclusive to Pinturan faunas (Kramarz 2004, 2006b). Some of these

Pinturan ‘endemics’ have been interpreted as representing earlier ‘evolutionary stages’ than their Sa-SC-RSC+Sa-SC-AC counterparts. For example, the ‘eocardiid’ *L. propheticus* has rooted cheek teeth, whereas they are ever-growing in *Eocardia* spp. and ‘eocardiids’ closer to crown Cavioidea *s.s.* (Kramarz 2006b; Pérez and Vucetich 2012). Similarly, Neoreomys *pinturensis* from Sa-lmP has lower-crowned cheek teeth than *N. australis*, which is abundant at Sa-SC-RSC+Sa-SC-AC localities (Kramarz 2006a; Croft 2013; Arnal et al. 2019). Detailed descriptions of Sa-lmP proterotheriids (Kramarz and Bond 2005) and microbiotheriids (Chornogubsky and Kramarz 2012) show a comparable mixture of Sa-SC-AC+Sa-SC-RSC and Colhuehuapian taxa. Platyrrhine primates from these faunas have also received considerable attention, but no genera are shared between Pinturan and Sa-SC-RSC+Sa-SC-AC faunas (Kay et al. 2012; Novo and Fleagle 2015).

The Pinturan fauna differs from the Sa-SC-RSC+Sa-SC-AC faunas in taxon abundance as well as identity. Too few fossils are known from the Sa-GB-UFZ for reliable abundance data, but the Sa-lmP is much better-sampled (Kramarz et al. 2010). Erethizontids and primates are much more numerous and diverse in the Sa-lmP than in the Sa-SC-RSC+Sa-SC-AC faunas (Kramarz 2004; Novo and Fleagle 2015). Chinchillids are nearly absent in the Sa-lmP, represented by a single, as yet-unnamed species of *Prolagostomus* (Kramarz 2002). Conversely, *Prolagostomus* and its close relative *Pliolagostomus* are quite common at Sa-SC-RSC and less common, but still more than in the Sa-lmP, at Sa-SC-AC sites (Croft 2013; Arnal et al. 2019; Rasia and Candela 2019). These abundance differences suggest that Sa-lmP and Sa-SC-RSC+Sa-SC-AC faunas record different paleoenvironments. Fossil

erethizontids and primates are generally believed to have been arboreal given the habits of their extant relatives and analyses of the fossils themselves (Youlatos and Meldrum 2011; Candela et al. 2012; Kay et al. 2012). The higher abundance and diversity of these clades in the Sa-lmP compared to Sa-SC-RSC+Sa-SC-AC faunas suggests that the former inhabited a more closed, forested paleoenvironment.

Dated units are lacking at many Sa-lmP localities, however, where present, geochronological data show that Pinturan faunas are slightly older than those of the Sa-SC-RSC and Sa-SC-AC. Thus, the 17.99 Ma tuff at Estancia El Carmen is the best guidepost for this fauna's age (Table 8; Perkins et al. 2012). Strata bearing the Sa-GB-UFZ are better constrained and older (19.04–18.62 Ma) than those of the Sa-lmP (Dunn et al. 2013). The oldest strata bearing Sa-SC-AC fossils are estimated to be ~17.8 Ma (Perkins et al. 2012; Cuitiño et al. 2016).

Notohippidian: History, Faunal Content, and Age—The resolution of the Pinturan question is intertwined with the other proposed pre-Santacrucian biochronologic interval, the Notohippidian. Ameghino (1900-02) identified the fossil fauna coming from the SCF at Karaiken in southwestern Santa Cruz Province as representing a distinct, earlier interval than the fauna of the Sa-SC-RSC and Sa-SC-AC that he termed the Notohippidian (Appendix 2). Fernicola et al. (2014) determined that fossils collected from the SCF along the Río Bote must have been included in this original Notohippidian definition despite not being mentioned by Ameghino (1900-02). Marshall and Pascual (1977) found a third SCF locality with a Notohippidian fauna at Cerro Centinela. They also found that two fossiliferous horizons occur at Karaiken, a lower Notohippidian layer and an upper layer that produced an

assemblage resembling Sa-SC-RSC and Sa-SC-AC faunas. Ameghino (1900-02) did not report the precise stratigraphic provenance of his fossils, so about it is uncertain which of his 'Notohippidian' fossils were actually collected from this lower horizon. The only fossils that unquestionably represent the Notohippidian fauna are those from Río Bote and Cerro Centinela, where no upper 'Santacrucian' levels have been identified. Fernicola et al. (2014: table 1) were able to deduce which taxa must come from Río Bote because they were named by Florentino Ameghino (1887, 1889) prior to his brother Carlos' (Florentino's primary collector) first visit to Karaiken in 1889. Unfortunately, the combined rodent assemblage of Río Bote and Cerro Centinela is insufficiently diverse to be included in our faunal similarity analysis (Appendix 2).

However, the age of the Notohippidian fauna is still relevant to answering the Pinturan question, and its rodent community can at least be qualitatively compared to that of other Santacrucian faunas. Cuitiño et al. (2016) constrained the age of the Notohippidian faunas to 18.85–18.00 Ma. They noted that this interval overlaps that estimated for Pinturan faunas (19.04–~17.99 Ma) and predates deposits containing Sa-SC-RSC and Sa-SC-AC faunas (~17.8–15.63 Ma; Table 8). In contrast, the Notohippidian fauna is qualitatively more similar to the Sa-SC-RSC and Sa-SC-AC than the Sa-lmP, despite its greater temporal affinity with the latter (Appendix 2). *Schistomys erro*, *Adelphomys*, and *Perimys erutus* are present at verified Notohippidian localities (i.e., Río Bote and/or Cerro Centinela) as well as Sa-SC-RSC+Sa-SC-AC faunas but are absent from the Sa-lmP (Appendix 2; Kramarz and Bellosi 2005; Arnal et al. 2019). Ameghino (1900-02)'s list of 'Notohippidian' rodents

includes additional species shared with Sa-SC-RSC+Sa-SC-AC faunas. Although this list includes taxa from the 'typical' Santacrucian level at Karaiken, some likely do originate from the lower Notohippidian horizon. Such shared species include *Eocardia montana*, *Sciamys principalis*, and *Acaremys murinus* (Appendix 2). Differences between the Notohippidian and Pinturan faunas must be attributed to geographic or paleoenvironmental differences given that they nearly completely overlap temporally (Cuitiño et al. 2016). Therefore, the Notohippidian fauna's (qualitatively) closer taxonomic connection to the Sa-SC-RSC and Sa-SC-AC casts doubt on the validity of both it and the Pinturan as valid biochronologic intervals.

Pampa Castillo and the Pinturan—According to our genus-level analyses, Pampa Castillo should be considered a Pinturan fauna (Figs. 24A, S15A, S16A, S16C). Species-level analyses, however, suggest that Pampa Castillo is more similar to the Sa-SC-RSC and Sa-SC-AC (Figs. 24B, S15B, S16B, S16D). Though the age of the Pampa Castillo fauna is poorly constrained, the ~18.7 Ma tuff near the base of the Galera Formation at Pampa Castillo suggests that it could be older than the Sa-SC-RSC and Sa-SC-AC faunas and contemporaneous with Pinturan and Notohippidian faunas (Table 8; Folguera et al. 2018). The stratigraphic section at Pampa Castillo shows no indication of hosting distinct lower and upper faunal associations as the Pinturas Formation does. For example, the lowest fossil horizon at Pampa Castillo, Fossiliferous Interval E-0, includes species shared with Sa-SC-RSC and Sa-SC-AC rather than Pinturan faunas (*A. constans* and *S.* cf. *riparius*). This is particularly noteworthy considering that Pampa Castillo is geographically much closer to the

Pinturan faunas of the Sa-lmP and Sa-GB-UFZ than to the Sa-SC-RSC and Sa-SC-AC (Fig. 18).

Pampa Castillo shows a conflicting faunal pattern rather than one that clearly aligns it with Pinturan or Sa-SC-RSC+Sa-SC-AC faunas (Fig. 24). Pampa Castillo's rodent assemblage represents an intergradation of those of 'distinct' Pinturan and Sa-SC-RSC+Sa-SC-AC faunas. As in Sa-SC-RSC+Sa-SC-AC faunas, *N. australis*, *P. erutus*, and *Prolagostomus pusillus* are abundant at Pampa Castillo (Croft 2013; Arnal et al. 2019), but as in Pinturan faunas, *Eosteiromys*, *Prostichomys*, and *Perimys intermedius* are also present (Kramarz and Bellosi 2005). The proterotheriid litopterns of Pampa Castillo also demonstrate this intergradation, with the cooccurrence of *Picturotherium* (Sa-lmP) and *Thoatherium* (Sa-SC-RSC+Sa-SC-AC) (Soria 2001; Kramarz and Bond 2005; McGrath et al. 2020). Further geochronologic and paleoenvironmental analyses would shed light on what additional similarities Pampa Castillo shares with Pinturan versus Sa-SC-RSC+Sa-SC-AC faunas, but ultimately, knowing the exact pattern of these temporal, paleoenvironmental, and stratigraphic connections is not needed to appreciate Pampa Castillo's significance. The existence of Pampa Castillo that is clearly intergradational between the 'typical' Santacrucian faunas of the Sa-SC-RSC and Sa-SC-AC and the 'Pinturan' faunas of the Sa-lmP and Sa-GB-UFZ demonstrates that these two faunas represent two conditions of a continually varying assemblage of taxa rather than exemplars of two distinct assemblages. Therefore, the 'Pinturan' should not be considered a distinct biochronologic interval from the Santacrucian SALMA, but rather, a different sort of Santacrucian assemblage recording the fauna of a different paleoenvironment.

Geography of Santacrucian Localities—Some authors skeptical of the validity of a Pinturan interval have referred to it as a "Santacrucian local fauna" (Wood and Patterson 1959, p. 367), but this characterization seems inaccurate. Pampa Castillo represents the third example of a fauna with Pinturan-like taxa, so the Pinturan cannot be dismissed as a peculiar fossil association restricted to the upper Río Pinturas valley. Given their more northerly and geographically widespread distribution, it is possible that contemporaneous mammal communities across South America were more like Pampa Castillo, Sa-lmP, and Sa-GB-UFZ than Sa-SC-RSC and Sa-SC-AC. Pampa Castillo and Sa-GB-UFZ are ~320 km apart, and Sa-GB-UFZ lies nearly two latitudinal degrees north of Pampa Castillo and Sa-lmP localities. Sa-SC-RSC and Sa-SC-AC localities are comparatively much closer to each other (Fig. 18). These faunas, and the Notohippidian and Sa-uP faunas, are found at higher latitudes than Pampa Castillo and the Pinturan faunas (Fernicola et al. 2014). Some authors have noted that two non-Patagonian early Miocene faunas resemble the Pinturan fauna. The Tcm3 level of the Cura-Mallín Formation at Laguna del Laja is roughly contemporaneous with the Santacrucian SALMA (Flynn et al. 2008). This unit contains a mixture of Pinturan and Sa-SC-RSC+Sa-SC-AC taxa (e.g., *Luantus*, *Prostichomys*, and *Phanomys*; Flynn et al. 2008; Solórzano et al. 2020). No rodents have been described to species-level from the Santacrucian-aged faunas of Chucal (northern Chile; Flynn et al. 2002a) or the Castilletes Formation (Venezuela; Carrillo et al. 2018). Further study of Santacrucian-aged faunas from middle and low-latitudes will enable a better understanding of the

relative roles of age, geography, and paleoenvironment in shaping faunas of this age throughout the entire continent.

CONCLUSIONS

The octodontoid community at Pampa Castillo is diverse, with six genera and eight species represented. We identify and describe three new species. *Dudumus* sp. nov. will be the first named Santacrucian species of this genus (Fig. 20A–B), though a different, unnamed new species from the Sa-SC-RSC was previously reported Arnal *et al.* (2019). Similarly, *Caviocricetus* sp. nov. is the first Santacrucian example of its genus (Fig. 20C–D). Both genera were previously known from Colhuehuapian faunas. *Prostichomys* sp. nov.is clearly distinct from the type and only known species of its genus*, P. bowni*, but we decline to formally name it as it is represented by a single lower molariform (Fig. 23). The previously described species from Pampa Castillo support the referral of this fauna to Pampa Castillo in agreement with previous assessments (Flynn et al. 2002b; McGrath et al. 2020).

In the faunal similarity analyses, faunas generally clustered according to their previously assigned SALMAs: Colhuehuapian, Santacrucian (inclusive of the Pinturan), and post-Santacrucian (Friasian, Colloncuran, and/or Mayoan; Figs. 24, S15–S16). The two Pinturan faunas, Sa-lmP and Sa-GB-UFZ, generally clustered together. Pampa Castillo clustered with the Pinturan faunas when genera were used

as the taxonomic unit of interest and with the Sa-SC-RSC+Sa-SC-AC (on which the Santacrucian SALMA is based) in the species-level analyses.

Pinturan faunas do not appear to represent a distinctive biochronologic interval. Pampa Castillo's differing position in the genus- and species-level analyses shows that it contains elements of both Pinturan and the 'typical' Santacrucian faunas of the Sa-SC-RSC and Sa-SC-AC (Figs. 24, S15–S16). The intergradational nature of the rodent community of Pampa Castillo demonstrates that Pinturan and 'typical' Santacrucian faunas are not always distinct; they can be intermixed. The Sa-lmP and Sa-GB-UFZ are indeed older than the Sa-SC-RSC and Sa-SC-AC, supporting the possibility of a biochronologic separation, but the ages of the Notohippidian, Pampa Castillo, and Sa-uP faunas muddy this chronology, though the ages of these latter two faunas are poorly constrained (Table 8). The contemporaneity of Sa-lmP+Sa-GB-UFZ, the Sa-SC-RSC+Sa-SC-AC-like Notohippidian fauna, and the "mixed" Pampa Castillo fauna suggests that the faunal differences among them are geographic and/or paleoenvironmental rather than temporal. Given that all of these faunas come from the southern latitudes of South America, further study of early Miocene faunas from other regions is needed to better characterize how this interval of South American mammal evolution looked across the continent and determine if the definition of the Santacrucian SALMA must become more inclusive.

Acknowledgements

We are grateful to the following institutions for providing access to their collections: American Museum of Natural History and Yale Peabody Museum for

providing access to their collections for comparison purposes. We would like to thank the Eppley Foundation for Scientific Research and the American Museum of Natural History for funding the field work in Chile. We thank Greg Buckley, René Burgos, Roger Carpenter, Paul Raty, Paul Sereno, Carlos de Smet, Cruz Vargas, and members and friends of the de Smet family for their assistance in the field. Jeanne Kelly and Jane Shumsky of the American Museum of Natural History prepared the specimens. We would like to thank Michelle Arnal for helpful conversations that improved the manuscript and sharing unpublished data.

REFERENCES

Ameghino, F. 1887. 1887. Enumeración sistemática de las especies de mamíferos fósiles coleccionados por Carlos Ameghino en los terrenos eocenos de la Patagonia austral y depositados en el Museo de La Plata. Boletín Museo de La Pla. Boletín Museo de La Plata 5:445–469.

Ameghino, F. 1889. Contribución al conocimiento de los mamíferos fósiles de la República Argentina. Actas de La Academia Nacional de Ciencias de Córdoba 6:1–1027.

Ameghino, F. 1891. Nuevos restos de mamíferos fósiles recogidos por Carlos Ameghino en el Eoceno inferior de la Patagonia austral. Especies nuevas: adiciones y corecciones. Revista Argentina de Historia Natural 1:289–328.

Ameghino, F. 1894. Ennumération synoptique des espéces de mammiféres fossilies des formations éocénes de Patagonie. Boletín de La Academia Nacional de Ciencias de Córdoba 13:259–445.

Ameghino, F. 1906. Les formations sédimentaires du Crétacé Supérieur et du Tertiaire de Patagonie avec un parallelé entre leurs faunes mammalogiques et celles de l'ancien continent. Anales Del Museo Nacional de Buenos Aires (Tercera Serie) 8:1–568.

Ameghino, F. 1900-02. L'age des formations sédimentaires de Patagonie. Anales de La Sociedad Cientifica Argentina 50, 51, 54:109–130, 145–165, 209–229, 20–

39, 65–91, 189-197,.

Arnal, M., and M. G. Vucetich. 2015a. Main radiation events in Pan-Octodontoidea (Rodentia, Caviomorpha). Zoological Journal of the Linnean Society 175:587–606.

Arnal, M., and M. G. Vucetich. 2015b. Revision of the fossil rodent *Acaremys* Ameghino, 1887 (Hystrocognathi, Octodontoidea, Acaremyidae) from the Miocene of Patagonia (Argentina) and the description of a new acaremyid. Historical Biology 27:42–59.

Arnal, M., M. E. Pérez, and C. M. Deschamps. 2019. Revision of the Miocene caviomorph rodents from the Río Santa Cruz. Publicación Electrónica de La Asociación Paleontológica Argentina 19:193–229.

Arnal, M., A. G. Kramarz, M. G. Vucetich, and E. C. Vieytes. 2014. A new early Miocene octodontoid rodent (Hystricognathi, Caviomorpha) from Patagonia (Argentina) and a reassessment of the early evolution of Octodontoidea. Journal of Vertebrate Paleontology 34:397–406.

Arnal, M., M. G. Vucetich, D. A. Croft, M. S. Bargo, J. C. Fernicola, and S. F. Vizcaíno. 2017. Systematic revision and evolutionary history of *Acarechimys* Patterson in Kraglievich, 1965 (Rodentia, Caviomorpha, Octodontoidea. Ameghiniana 54:307–330.

Boivin, M., and L. Marivaux. 2020. Dental homologies and evolutionary transformations in Caviomorpha (Hystricognathi, Rodentia): new data from the Paleogene of Peruvian Amazonia. Historical Biology 32:528–554.

Boivin, M., L. Marivaux, A. M. Candela, M. J. Orliac, F. Pujos, R. Salas-Gismondi, J. V. Tejada-Lara, and P.-O. Antoine. 2017. Late middle Eocene caviomorph rodents from Contamana, Peruvian Amazonia. Palaeontologia Electronica 20.1:1–50.

Boivin, M., L. Marivaux, and P.-O. Antoine. 2019. L'apport du registre paléogéne d'Amazonie sur la diversification initiale des Caviomorpha (Hystricognathi, Rodentia): implications phylogénétiques, macroéevolutives et paléobiogéographiques. Geodiversitas 41:143–245.

Bostelmann, E., J. P. Le Roux, A. Vásquez, N. M. Gutiérrez, J. L. Oyarzún, C. Carreño, T. Torres, R. Otero, A. Llanos, C. M. Fanning, and F. Hervé. 2013. Burdigalian deposits of the Santa Cruz Formation in the Sierra Baguales, Austral (Magallanes) Basin: age, depositional environment and vertebrate fossils. Andean Geology 40:458–489.

Bostelmann, J. E., R. Bobe, G. Carrasco, B. V. Alloway, P. Santi-Malnis, A. Mancuso, B. Agüero, Z. Alemseged, and Y. Godoy. 2012. The Alto Río Cisnes fossil fauna (Río Frías Formation, early middle Miocene, Friasian SALMA): a keystone and paradigmatic vertebrate assemblage of the South American fossil record. Abriendo Ventanas Al Pasado: III Simposio Paleontología En Chile 42–45.

Bowdich, T. E. 1821. An Analysis of the Natural Classifications of Mammalia: For the Use of Students and Travelers. J. Smith, Paris, France, 180 pp.

Bown, T. M., and C. N. Larriestra. 1990. Sedimentary paleoenvironments of fossil platyrrhine localities, Miocene Pinturas Formation, Santa Cruz Province, Argentina. Journal of Human Evolution 19:87–119.

Bown, T. M., and J. G. Fleagle. 1993. Systematics, biostratigraphy, and dental evolution of the Palaeothentidae, later Oligocene to early-middle Miocene (Deseadan-Santacrucian) caenolestoid marsupials of South America. Journal of Paleontology 67:1–76.

Brandoni, D., L. González Ruiz, A. Reato, and G. Martin. 2017. Chronological implications of the nothrotheriid '*Xyophorus*' (Mammalia, Xenarthra) from the Collón Curá Formation (Miocene of Patagonia, Argentina). Historical Biology 2963:1–9.

Bucher, J., M. E. Pérez, L. R. González Ruiz, L. D'Elía, and A. Bilmes. 2021. New middle Miocene (Langhian-Serravallian) vertebrate localities in northwestern Patagonia, Argentina: a contribution to high latitude south american land mammal ages sequence. Journal of South American Earth Sciences 107:103024.

Busker, F., and M. T. Dozo. 2019. Rediscovering a forgotten rodent of Patagonia and its phylogenetic implications. Journal of Systematic Palaeontology 17:759–773.

Candela, A. M. 2003. A new porcupine (Rodentia, Hystricognathi, Erethizontidae) from the early and middle Miocene of Patagonia. Ameghiniana 40:483–494.

Candela, A. M. 2016. Analyzing the impact of conflictive dental characters on the phylogeny of octodontoid rodents. Acta Palaeontologica Polonica 61:455–468.

Candela, A. M., and M. G. Vucetich. 2002. *Hypsosteiromys* (Rodentia, Hystricognathi) from the early Miocene of Patagonia (Argentina), the only Erethizontidae with a tendency to hypsodonty. Geobios 35:153–161.

Candela, A. M., L. L. Rasia, and M. E. Pérez. 2012. Paleobiology of Santacrucian caviomorph rodents: a morphofunctional approach; pp. 287–305 in S. F. Vizcaíno, R. F. Kay, and M. S. Bargo (eds.), Early Miocene Paleobiology in Patagonia: High-Latitude Paleocommunities of the Santa Cruz Formation. Cambridge University Press, Cambridge, UK.

Carrillo, J. D., E. Amson, C. Jaramillo, R. Sánchez, L. Quiroz, and C. Cuartas. 2018. The Neogene record of northern South American native ungulates. Smithsonian Contributions to Paleobiology 1–80.

Castellanos, A. 1937. Ameghino y la antiguedad del hombre sudamericano. Asociación Cultural de Conferencias de Rosario, Ciclo de Caracter General 2:47–192.

Cerdeño, E., and M. G. Vucetich. 2007. The first rodent from the Mariño Formation

(Miocene) at Divisadero Largo (Mendoza, Argentina) and its biochronological implications. Andean Geology 34:199–207.

Chick, J., D. A. Croft, H. E. Dodson, J. J. Flynn, and A. R. Wyss. 2010. The early Miocene rodent fauna of Pampa Castillo, Chile. Society of Vertebrate Paleontology Annual Meeting, Program and Abstracts Book 71A-72A.

Chornogubsky, L., and A. G. Kramarz. 2012. Nuevos hallazgos de Microbiotheriidae (Mammalia, Marsupialia) en la Formación Pinturas (Mioceno temprano, Argentina). Ameghiniana 49:442–450.

Cione, A. L., G. M. Gasparini, E. Soibelzon, L. H. Soibelzon, and E. P. Tonni. 2015. The Great American Biotic Interchange: A South American Perspective (J. Rabassa, G. Lohmann, J. Notholt, L. A. Mysak, and V. Unnithan (eds.). Springer Earth Systems Sciences, Dordrecht, 97 pp.

Van Couvering, J. A., and E. Delson. 2020. African Land Mammal Ages. Journal of Vertebrate Paleontology 40:e1803340.

Croft, D. A. 2013. What constitutes a fossil mammal community in the early Miocene Santa Cruz Formation? Journal of Vertebrate Paleontology 33:37–41.

Croft, D. A. 2016. Horned Armadillos and Rafting Monkeys: The Fascinating Fossil Mammals of South America. Indiana University Press, Bloomington, Indiana, USA, 304 pp.

Croft, D. A., J. J. Flynn, and A. R. Wyss. 2007. A new basal glyptodontid and other Xenarthra of the early Miocene Chucal Fauna, northern Chile. Journal of Vertebrate Paleontology 27:781–797.

Croft, D. A., J. M. H. Chick, and F. Anaya. 2011. New middle Miocene caviomorph rodents from Quebrada Honda, Bolivia. Journal of Mammalian Evolution 18:245–268.

Cuitiño, J. I., J. C. Fernicola, M. S. Raigemborn, and V. Krapovickas. 2019a. Stratigraphy and depositional environments of the Santa Cruz Formation (early-middle Miocene) along the Río Santa Cruz, southern Patagonia, Argentina. Publicación Electrónica de La Asociación Paleontológica Argentina 19:14–33.

Cuitiño, J. I., S. F. Vizcaíno, M. S. Bargo, and I. Aramendía. 2019b. Sedimentology and fossil vertebrates of the Santa Cruz Formation (early Miocene) in Lago Posadas, southwestern Patagonia, Argentina. Andean Geology 46:383–420.

Cuitiño, J. I., J. C. Fernicola, M. J. Kohn, R. Trayler, M. Naipauer, M. S. Bargo, R. F. Kay, and S. F. Vizcaíno. 2016. U-Pb geochronology of the Santa Cruz Formation (early Miocene) at the Río Bote and Río Santa Cruz (southernmost Patagonia, Argentina): implications for the correlation of fossil vertebrate localities. Journal of South American Earth Sciences 70:198–210.

Dunn, R. E., R. H. Madden, M. J. Kohn, M. D. Schmitz, C. A. E. Strömberg, A. A. Carlini, G. H. Ré, and J. Crowley. 2013. A new chronology for middle Eocene-early Miocene South American Land Mammal Ages. Bulletin of the Geological

Society of America 125:539–555.

Encinas, A., A. Folguera, R. Riffo, P. Molina, L. Fernández Paz, V. D. Litvak, D. A. Colwyn, V. A. Valencia, and M. Carrasco. 2019. Cenozoic basin evolution of the central Patagonian Andes: evidence from geochronology, stratigraphy, and geochemistry. Geoscience Frontiers 10:1139–1165.

Fernicola, J. C., J. I. Cuitiño, S. F. Vizcaíno, M. S. Bargo, and R. F. Kay. 2014. Fossil localities of the Santa Cruz Formation (early Miocene, Patagonia, Argentina) prospected by Carlos Ameghino in 1887 revisited and the location of the Notohippidian. Journal of South American Earth Sciences 52:94–107.

Fernicola, J., M. S. Bargo, S. F. Vizcaino, and R. F. Kay. 2019a. Historical background for a revision of the paleontology of the Santa Cruz Formation (early-middle Miocene) along the Río Santa Cruz, Patagonia, Argentina. Publicación Electrónica de La Asociación Paleontológica Argentina 19:1–13.

Fernicola, J. C., S. F. Vizcaíno, M. S. Bargo, R. F. Kay, and J. I. Cuitiño. 2019b. Analysis of the early-middle Miocene mammal associations at the Río Santa Cruz (Patagonia, Argentina). Publicacion Electronica de La Asociacion Paleontologica Argentina 19:239–259.

Fleagle, J. G., M. E. Perkins, M. T. Heizler, A. a. Tauber, B. Nash, T. M. Bown, M. T. Dozo, and M. F. Tejedor. 2012. Absolute and relative ages of fossil localities in the Santa Cruz and Pinturas Formations; pp. 41–58 in S. F. Vizcaíno, R. F. Kay, and M. S. Bargo (eds.), Early Miocene Paleobiology in Patagonia: High-Latitude Paleocommunities of the Santa Cruz Formation. Cambridge University Press, Cambridge, UK.

Flynn, J. J., and C. C. Swisher. 1995. Cenozoic South American Land Mammal Ages: correlation to global geochronologies. Geochronology Time Scales and Global Stratigraphic Correlation, SEPM Special Publication 54:317–333.

Flynn, J. J., B. J. MacFadden, and M. C. McKenna. 1984. Land-mammal ages, faunal heterochrony, and temporal resolution in Cenozoic terrestrial sequences. Journal of Geology 92:687–705.

Flynn, J. J., D. A. Croft, R. Charrier, G. Hérail, and A. R. Wyss. 2002a. The first Cenozoic mammal fauna from the Chilean Altiplano. Journal of Vertebrate Paleontology 22:200–206.

Flynn, J. J., M. J. Novacek, H. E. Dodson, D. Frassinetti, M. C. McKenna, M. A. Norell, K. E. Sears, C. C. Swisher, and A. R. Wyss. 2002b. A new fossil mammal assemblage from the southern Chilean Andes: implications for geology, geochronology, and tectonics. Journal of South American Earth Sciences 15:285–302.

Flynn, J. J., R. Charrier, D. A. Croft, P. B. Gans, T. M. Herriott, J. A. Wertheim, and A. R. Wyss. 2008. Chronologic implications of new Miocene mammals from the Cura-Mallín and Trapa Trapa formations, Laguna del Laja area, south central Chile. Journal of South American Earth Sciences 26:412–423.

Folguera, A., A. Encinas, A. Echaurren, G. Gianni, and D. Orts. 2018. Constraints on the Neogene growth of the central Patagonian Andes at the latitude of the Chile triple junction (45–47° S) using U/Pb geochronology in synorogenic strata. Tectonophysics 744:134–154.

Frassinetti, D., and V. Covacevich. 1999. Invertebrados fósiles marinos de la Formación Guadal (Oligoceno superior-Mioceno inferior) en Pampa Castillo, Región de Aisén, Chile. Servicio Nacional de Geología y Minería 51:1–96.

Frenguelli, J. 1931. Nomenclatura estratigrafica patagonica. Anales de La Sociedad Cientifica de Santa Fe 3:1–115.

González Ruiz, L. R., A. Reato, M. Cano, and O. Martínez. 2017. Old and new specimens of a poorly known glyptodont from the Miocene of Patagonia and their biochronological implications. Acta Palaeontologica Polonica 62:181–194.

Gray, J. E. 1825. Outline of an attempt at the disposition of the Mammalia into tribes and families with a list of the genera apparently appertaining to each tribe. Annals of Philosophy 10:337–344.

Huxley, T. 1880. On the application of the laws of evolution to the arrangement of the Vertebrata, and more particularly of the Mammalia. Proceedings of the Zoological Society, London 43:649–662.

Jaccard, P. 1912. The distribution of the flora in the Alpine zone. New Phytologist 11:37–50.

Kay, R. F., J. M. G. Perry, M. Malinzak, K. L. Allen, C. Kirk, J. M. Plavcan, and J. G. Fleagle. 2012. Paleobiology of Santacrucian primates; pp. 306–330 in S. F. Vizcaíno, R. F. Kay, and M. S. Bargo (eds.), Early Miocene Paleobiology in Patagonia: High-Latitude Paleocommunities of the Santa Cruz Formation. Cambridge University Press, Cambridge, UK.

Kraglievich, J. L. 1965. Speciation phyletique dans les rongeurs fossiles du genre *Eumysops* Ameghino (Echimyidae, Heteropsomyinae). Extrait de Mammalia 29:258–267.

Kramarz, A. G. 2001. *Prostichomys bowni* un nuevo roedor Adelphomyinae (Hystricognathi, Echimyidae) del Mioceno medio–inferior de Patagonia, Argentina. Ameghiniana 38:163–168.

Kramarz, A. G. 2002. Roedores chinchilloideos (Hystricognathi) de la Formación Pinturas, Mioceno temporano-medio de la provincia de Santa Cruz, Argentina. Revista Del Museo Argentino de Ciencias Naturales Bernardino Rivadavia 4:167–180.

Kramarz, A. 2004. Octodontoids and erethizontoids (Rodentia, Hystricognathi) from the Pinturas Formation, early–middle Miocene of Patagonia, Argentina. Ameghiniana 41:199–216.

Kramarz, A. G. 2006a. Eocardiids (Rodentia, Hystricognathi) from the Pinturas Formation, late early Miocene of Patagonia, Argentina. Journal of Vertebrate

Paleontology 26:770–778.

Kramarz, A. G. 2006b. *Neoreomys* and *Scleromys* (Rodentia, Hystricognathi) from the Pinturas Formation, late early Miocene of Patagonia, Argentina. Revista Del Museo Argentino de Ciencias Naturales, Nueva Serie 8:53–62.

Kramarz, A. G., and E. S. Bellosi. 2005. Hystricognath rodents from the Pinturas Formation, early-middle Miocene of Patagonia, biostratigraphic and paleoenvironmental implications. Journal of South American Earth Sciences 18:199–212.

Kramarz, A. G., and M. Bond. 2005. Los Litopterna (Mammalia) de la Formación Pinturas, Mioceno temprano-medio de Patagonia. Ameghiniana 42:611–625.

Kramarz, A., A. C. Garrido, A. M. Forasiepi, M. Bond, and C. P. Tambussi. 2005. Estratigrafía y vertebrados (Aves y Mammalia) de la Formación Cerro Bandera, Mioceno Temprano de la Provincia del Neuquén, Argentina. Revista Geológica de Chile 32:273–291.

Kramarz, A. G., M. G. Vucetich, A. A. Carlini, M. R. Ciancio, M. A. Abello, C. M. Deschamps, and J. N. Gelfo. 2010. A new mammal fauna at the top of the Gran Barranca sequence and its biochronological significance; pp. 260–273 in R. H. Madden, A. A. Carlini, M. G. Vucetich, and R. F. Kay (eds.), The Paleontology of Gran Barranca: Evolution and Environmental Change through the Middle Cenozoic of Patagonia. Cambridge University Press, Cambridge, UK.

Kramarz, A. G., M. Bond, and M. Arnal. 2015. Systematic description of three new mammals (Notoungulata and Rodentia) from the early Miocene Cerro Bandera Formation, northern Patagonia, Argentina. Ameghiniana 52:585–597.

de la Cruz, R., D. Welkner, M. Suárez, and D. Quiroz. 2004. Geología del area Oriental de la Hojas Cochrane y Villa O'Higgins, Región Aisén del General Carlos Ibáñez del Campo. Carta Geológica de Chile 57.

Linnaeus, C. 1758. Systema Naturae per Regna Tri Naturae, 10th ed. Laurentii Salvii, Stockholm, Sweden, 824 pp.

Madden, R. H., J. Guerrero, R. F. Kay, J. J. Flynn, C. C. Swisher, and A. H. Walton. 1997. The Laventan Stage and Age; pp. 499–519 in R. F. Kay, R. H. Madden, R. L. Cifelli, and J. J. Flynn (eds.), Vertebrate Paleontology in the Neotropics: The Miocene Fauna of La Venta, Colombia. Smithsonian Institution Press, Washington, D.C., USA.

Madden, R. H., A. A. Carlini, M. G. Vucetich, and R. F. Kay 2010. The Paleontology of Gran Barranca. Cambridge University Press, Cambridge, UK, 448 pp.

Marshall, L. G., and R. Pascual. 1977. Nuevos marsupiales Caenolestidae del "Piso Notohipedense" (SW de Santa Cruz) de Ameghino, sus aportaciones a la cronología y evolución de las comunidades de mamíferos sudamericanos. Publicaciones Del Museo Municipal de Ciencias Naturales de Mar Del Plata "Lorenzo Scaglia" 2:91–122.

Marshall, L. G., R. Hoffstetter, and R. Pascual. 1983. Mammals and stratigraphy: geochronology of the continental mammal-bearing Tertiary of South America. Palaeovertebrata 13:1–93.

McGrath, A. J., J. J. Flynn, and A. R. Wyss. 2020. Proterotheriids and macraucheniids (Litopterna: Mammalia) from the Pampa Castillo Fauna, Chile (early Miocene, Santacrucian SALMA) and a new phylogeny of Proterotheriidae. Journal of Systematic Palaeontology 18:717–738.

Niemeyer, J., R. F. Skarmeta, and W. Espinosa. 1984. Hojas Peninsula de Taitao y Puerto Aysen Servicio Nacional de Geológica y Mineria. Carta Geológica de Chile 80.

Niemeyer, R. H. 1975. Geología de la región comprendida entre el Lago General Carrera y el Río Chacabuco, Aisén. Universidad de Chile, 309 pp.

Novo, N. M., and J. G. Fleagle. 2015. New specimens of platyrrhine primates from Patagonia (Pinturas Formation, early Miocene). Ameghiniana 52:367–372.

Patterson, B., and R. Pascual. 1968. New echimyid rodents from the Oligocene of Patagonia, and a synopsis of the family. Bulletin of the Museum of Comparative Zoology.

Patterson, B., and A. E. Wood. 1982. Rodents from the Deseadan Oligocene of Bolivia and the relationships of the Caviomorpha. Bulletin of the Museum of Comparative Zoology 149:371–543.

Pérez, M. E. 2010. A new rodent (Cavioidea, Hystricognathi) from the middle Miocene of Patagonia, mandibular homologies, and the origin of the crown group Cavioidea sensu stricto. Journal of Vertebrate Paleontology 30:1848–1859.

Pérez, M. E., and M. G. Vucetich. 2011. A new extinct genus of Cavioidea (Rodentia, Hystricognathi) from the Miocene of Patagonia (Argentina) and the evolution of cavioid mandibular morphology. Journal of Mammalian Evolution 18:163–183.

Pérez, M. E., and M. G. Vucetich. 2012. A revision of the fossil genus *Phanomys* Ameghino, 1887 (Rodentia, Hystricognathi, Cavioidea) from the early Miocene of Patagonia (Argentina) and the acquisition of euhypsodonty in Cavioidea sensu stricto. Paläontologische Zeitschrift 86:187–204.

Perkins, M. E., J. G. Fleagle, M. T. Heizler, B. Nash, T. M. Brown, A. A. Tauber, and M. T. Dozo. 2012. Tephrochronology of the Miocene Santa Cruz and Pinturas Formations, Argentina; pp. 23–40 in S. F. Vizcaíno, R. F. Kay, and M. S. Bargo (eds.), Early Miocene paleobiology in Patagonia: High-Latitude Paleocommunities of the Santa Cruz Formation. Cambridge University Press, Cambridge, UK.

Qiu, Z.-X., Z.-D. Qiu, T. Deng, C.-K. Li, Z.-Q. Zhang, B.-Y. Wang, and X. Wang. 2013. Neogene land mammal stages/ages of China: toward the goal to

establish an Asian land mammal stage/age scheme; pp. 29–90 in X. Wang, L. Flynn, and M. Fortelius (eds.), Fossil Mammals of Asia. Columbia University Press, New York, New York, USA.

R Core Team. 2020. R: a language and environment for statistical computing. .

Rasia, L. L., and A. M. Candela. 2019. *Prolagostomus amplus* Ameghino is a junior synonym of the Patagonian rodent *Pliolagostomus notatus* Ameghino (Chinchillidae; early Miocene, Santa Cruz Formation). Ameghiniana 56:72–77.

Raup, D. M., and R. E. Crick. 1979. Measurement of faunal similarity in paleontology. Journal of Paleontology 53:1213–1227.

Ré, G. H., E. S. Bellosi, M. T. Heizler, J. F. Vilas, R. H. Madden, A. A. Carlini, R. F. Kay, and M. G. Vucetich. 2010. A geochronology for the Sarmiento Formation at Gran Barranca; pp. 46–58 in R. H. Madden, A. A. Carlini, M. G. Vucetich, and R. F. Kay (eds.), The Paleontology of Gran Barranca: Evolution and Environmental Change through the Middle Cenozoic of Patagonia. Cambridge University Press, Cambridge, UK.

Rowe, D. L., K. A. Dunn, R. M. Adkins, and R. L. Honeycutt. 2010. Molecular clocks keep dispersal hypotheses afloat: evidence for trans-Atlantic rafting by rodents. Journal of Biogeography 37:305–324.

Scalabrino, B. 2009. Déformation d'un continent audessus d'une dorsale océanique active en subduction. Université Montpellier, 388 pp.

Scott, W. B. 1905. Mammalia of the Santa Cruz Beds. Part III. Glires; pp. 384–499 in Reports of the Princeton Expedition to Patagonia. Princeton University Press, Princeton.

Simpson, G. G. 1943. Mammals and the nature of continents. American Journal of Science 241:1–31.

Solórzano, A., A. Encinas, A. Kramarz, G. Carrasco, G. Montoya-Sanhueza, and R. Bobe. 2020. Late early Miocene caviomorph rodents from Laguna del Laja (~37° S), Cura-Mallín Formation, south-central Chile. Journal of South American Earth Sciences 102:102658.

Soria, M. F. 2001. Los Proterotheriidae (Litopterna, Mammalia), sistemática, origen y filogenia. Monografias Del Museo Argentino de Ciencias Naturales 1–171.

Trayler, R. B., M. D. Schmitz, J. I. Cuitiño, M. J. Kohn, M. S. Bargo, R. F. Kay, C. A. E. Strömberg, and S. F. Vizcaíno. 2020. An improved approach to age-modeling in deep time: implications for the Santa Cruz Formation, Argentina. Geological Society of America Bulletin 132:233–244.

Ugalde, R., E. Bostelmann, K. E. Buldrini, and J. L. Oyarzún. 2015. Lithofacies, architecture, and depositional environments of the Santa Cruz Formation in Chilean Patagonia. Congreso Geológico Chileno 816–820.

Upham, N. S., and B. D. Patterson. 2012. Diversification and biogeography of the

Neotropical caviomorph lineage Octodontoidea (Rodentia: Hystricognathi). Molecular Phylogenetics and Evolution 63:417–429.

Vavrek, M. J. 2011. fossil: palaeoecological and palaeogeographical analysis tools. Palaeontologia Electronica 14:1T.

Vera, B., L. González Ruiz, N. Novo, G. Martin, A. Reato, and M. F. Tejedor. 2019. The Interatheriinae (Mammalia, Notoungulata) of the Friasian *sensu stricto* and Mayoan (middle to late Miocene), and the fossils from Cerro Zeballos, Patagonia, Argentina. Journal of Systematic Palaeontology 17:1143–1163.

Verzi, D. H., A. I. Olivares, and C. C. Morgan. 2014. Phylogeny and evolutionary patterns of South American octodontoid rodents. Acta Palaeontologica Polonica 59:757–769.

Verzi, D. H., A. I. Olivares, and C. C. Morgan. 2017. Systematics and evolutionary significance of the small Abrocomidae from the early Miocene of southern South America. Historical Biology 29:411–422.

Verzi, D. H., A. I. Olivares, C. C. Morgan, and A. Álvarez. 2016. Contrasting phylogenetic and diversity patterns in octodontoid rodents and a new definition of the family Abrocomidae. Journal of Mammalian Evolution 23:93–115.

Vizcaíno, S. F., M. S. Bargo, and R. F. Kay. 2012a. Background for a paleoecological study of the Santa Cruz Formation (late Early Miocene) on the Atlantic Coast of Patagonia; pp. 1–22 in S. F. Vizcaíno, R. F. Kay, and M. S. Bargo (eds.), Early Miocene Paleobiology in Patagonia: High-Latitude Paleocommunities of the Santa Cruz Formation. Cambridge University Press, Cambridge, UK.

Vizcaíno, S. F., R. F. Kay, and M. S. Bargo 2012b. Early Miocene Paleobiology in Patagonia: High-Latitude Paleocommunities of the Santa Cruz Formation Cambridge University Press, Cambridge, UK, 369 pp.

de Vries, A., and B. D. Ripley. 2016. ggdendro: create dendrograms and tree diagrams using “ggplot2.” .

Vucetich, M. G. 1984. Los roedores de la edad Friasense (Mioceno medio) de Patagonia. Revista Del Museo de La Plata 8:47–126.

Vucetich, M. G., and D. H. Verzi. 1996. A peculiar octodontoid (Rodentia, Caviomorpha) with terraced molars from the lower Miocene of Patagonia (Argentina). Journal of Vertebrate Paleontology 16:297–302.

Vucetich, M. G., and A. G. Kramarz. 2003. New Miocene rodents from Patagonia (Argentina) and their bearing on the early radiation of the octodontoids (Hystricognathi). Journal of Vertebrate Paleontology 23:435–444.

Vucetich, M. G., M. M. Mazzoni, and U. F. J. Pardiñas. 1993. Los roedores de la Formación Collón Cura (Mioceno Medio), y la Ignimbrita Pilcaniyeu. Cañadón del Tordillo, Neuquén. Ameghiniana 30:361–381.

Vucetich, M. G., A. G. Kramarz, and A. M. Candela. 2010a. Colhuehuapian rodents from Gran Barranca and other Patagonian localities: the state of the art; pp. 206–219 in R. H. Madden, A. A. Carlini, M. G. Vucetich, and R. F. Kay (eds.), The Paleontology of Gran Barranca: Evolution and Environmental Change through the Middle Cenozoic of Patagonia. Cambridge University Press, Cambridge, UK.

Vucetich, M. G., E. C. Vieytes, M. E. Pérez, and A. A. Carlini. 2010b. The rodents from La Cantera and the early evolution of caviomorphs in South America; pp. 193–205 in R. H. Madden, A. A. Carlini, M. G. Vucetich, and R. F. Kay (eds.), The Paleontology of Gran Barranca: Evolution and Environmental Change through the Middle Cenozoic of Patagonia. Cambridge University Press, Cambridge, UK.

Vucetich, M. G., M. T. Dozo, M. Arnal, and M. E. Pérez. 2015. New rodents (Mammalia) from the late Oligocene of Cabeza Blanca (Chubut) and the first rodent radiation in Patagonia. Historical Biology 27:236–257.

Walton, A. H. 1997. Rodents; pp. 392–409 in R. F. Kay, R. H. Madden, R. L. Cifellii, and J. J. Flynn (eds.), Vertebrate Paleontology in the Neotropics: The Miocene Fauna of La Venta, Colombia. Smithsonian Institution Press, Washington, D.C., USA.

Wickham, H., et al. 2019. Welcome to the tidyverse. Journal of Open Source Software 4:1686.

Wood, A. E. 1949. A new Oligocene rodent genus from Patagonia. American Museum Novitates 1435:1–54.

Wood, A. E. 1955. A revised classification of the rodents. Journal of Mammalogy 36:165–187.

Wood, A. E., and B. Patterson. 1959. The rodents of the Deseadan Oligocene of Patagonia and the beginnings of South American rodent evolution. Bulletin of the Museum of Comparative Zoology 120:281–428.

Woodburne, M. O., F. J. Goin, M. S. Raigemborn, M. Heizler, J. N. Gelfo, and E. V. Oliveira. 2014. Revised timing of the South American early Paleogene land mammal ages. Journal of South American Earth Sciences 54:109–119.

Youlatos, D., and J. Meldrum. 2011. Locomotor diversification in New World monkeys: Running, climbing, or clawing along evolutionary branches. Anatomical Record 294:1991–2012.

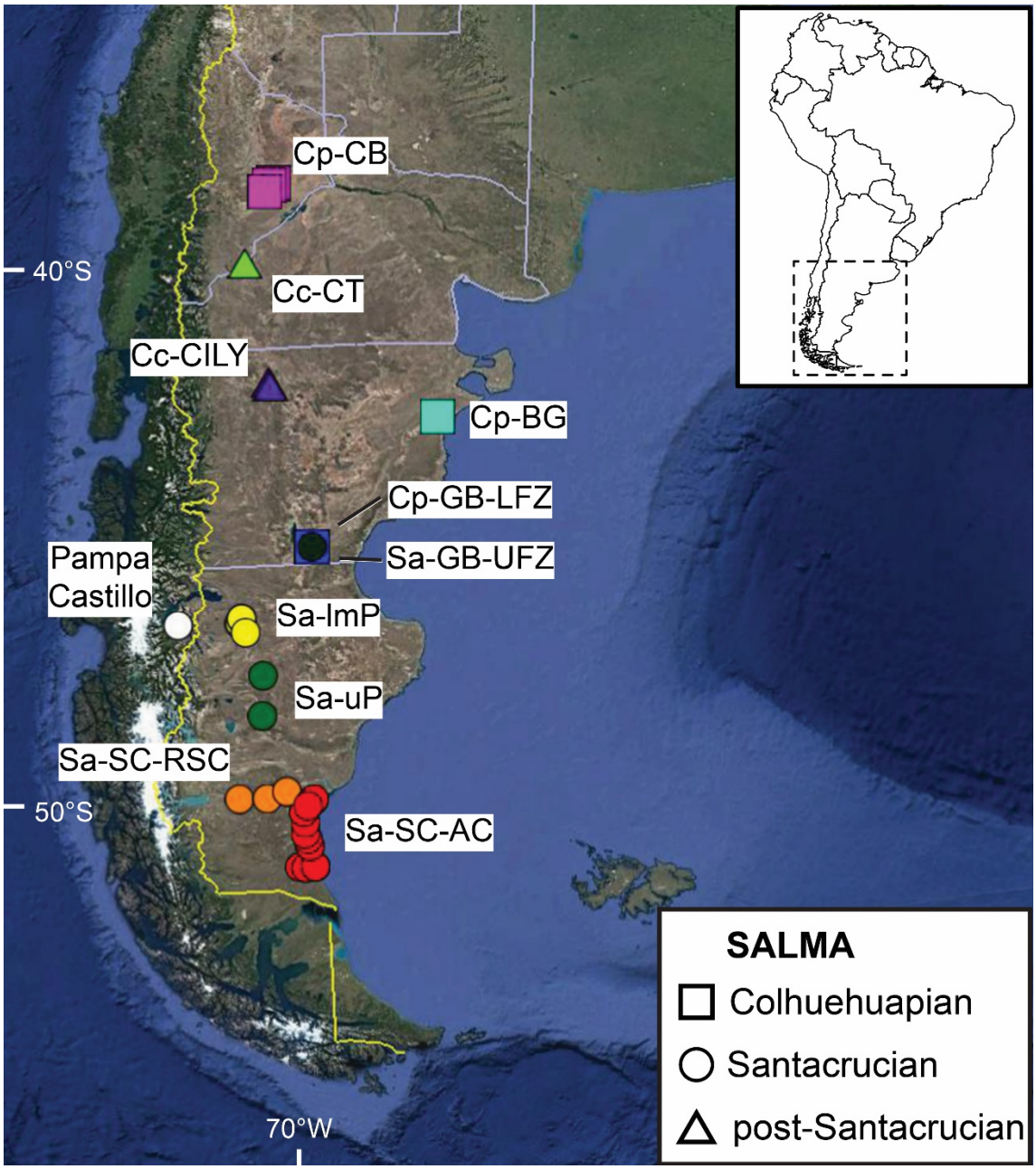

Figure 18: Map of Pampa Castillo and other faunas used in faunal similarity analysis. Some faunas consist of multiple localities. Point shape is determined by SALMA, and color determined by fauna. **Abbreviations:** Cc-CILY, Cruces Infinitos and Los Yeguarizos; Cc-CT, Cañadón de Tordillo; Cp-BG, Bryn Gwyn; Cp-CB, Cerro Bandera Formation; Cp-GB-LFZ, lower faunal zone of Colhue-Huapi Member of Sarmiento Formation at Gran Barranca; Sa-GB-UFZ, upper faunal zone of Colhue-Huapi Member of Sarmiento Formation at Gran Barranca; Sa-lmP, lower and middle sequences of Pinturas Formation; Sa-SC-AC, Santa Cruz Formation along Atlantic coast; Sa-SC-RSC, Santa Cruz Formation along Río Santa Cruz; Sa-uP, upper sequence of Pinturas Formation.

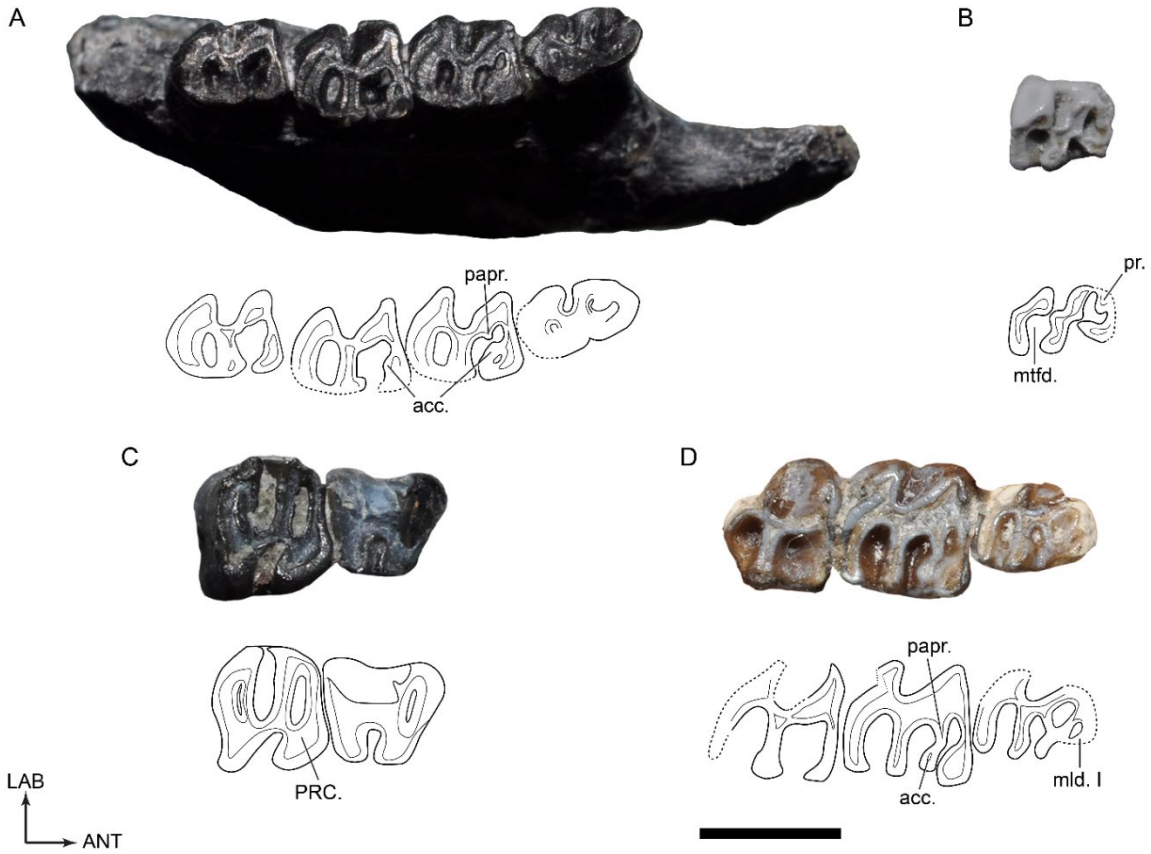

Figure 19: Photos and line drawings of *Acarechimys* from Pampa Castillo. **A.** *A. minutus*, SGOPV 2367, mandible with left dp4–m3. **B.** *A.* cf. *minutissimus*, SGOPV 2191 (cast), left dp4. **C–D.** *A. constans*, **C.** SGOPV 2707, left DP4–M1 (reversed); **D.** SGOPV 2705, left dp4–m2. **Abbreviations:** acc, accessory cuspid; ANT, anterior; LAB, labial; mld I, metalophulid I; mtfd, metaflexid; papr, posterior arm of the protoconid; pr, protoconid; PRC, protocone. Dashed line indicates reconstructed outline of tooth. Scale bar = 2 mm.

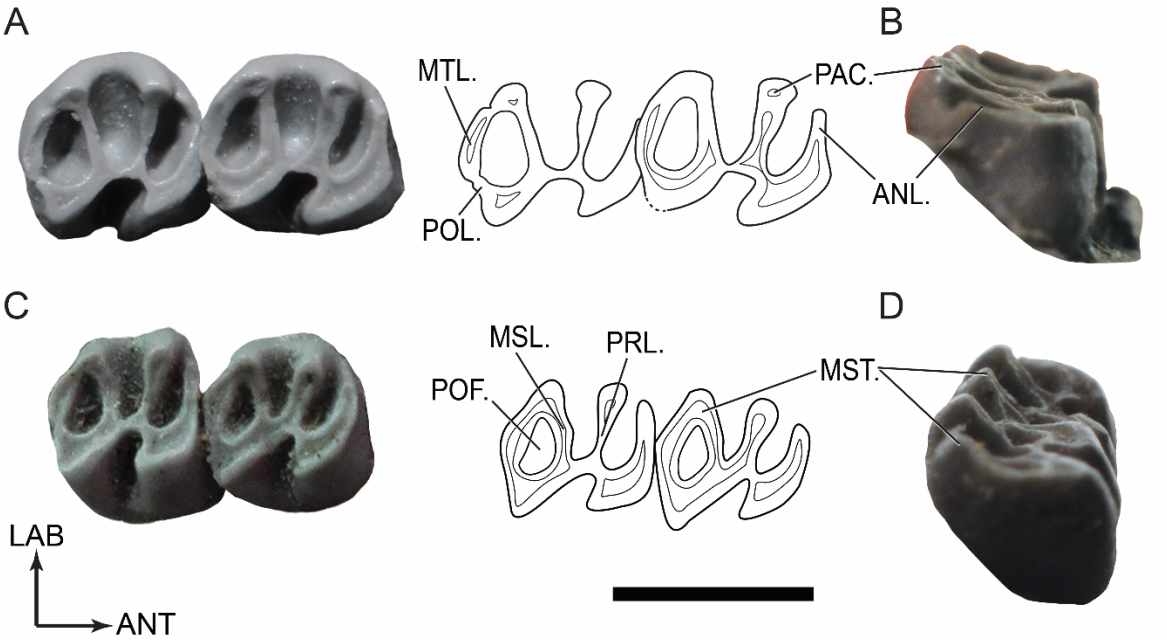

Figure 20: Photos and line drawings of new octodontoid taxa from Pampa Castillo. *Dudumus* sp. nov. 2., SGOPV 2140 (cast of type), left M1–2 in **A.** occlusal (reversed) and **B.** anterior view. *Caviocricetus* sp. nov., SGOPV 2194 (cast of type), right DP4–M1 in **C.** occlusal and **D.** posterior view. **Abbreviations:** ANL, anteroloph; ANT, anterior; LAB, labial; MSL, mesolophule; MST, mesostyle; MTL, metaloph; PAC, paracone; POL, posteroloph; POF, posterofossette; PRL, protoloph. Scale bar = 2 mm.

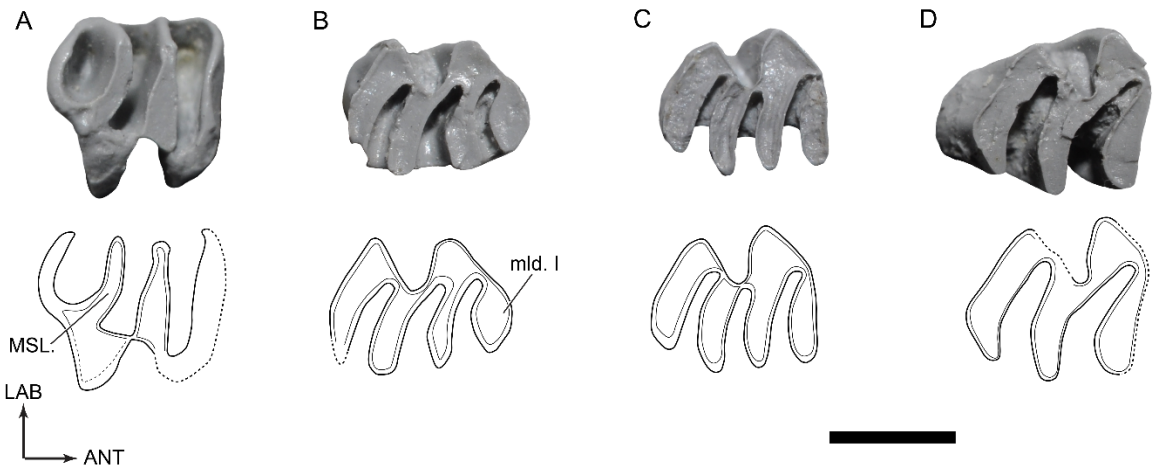

Figure 21: Photos and line drawings of *Spaniomys* cf. *riparius* (all casts) from Pampa Castillo. **A.** SGOPV 2132, left M1 or 2 (reversed); **B.** SGOPV 2128, right p4 (reversed); **C.** SGOPV 2129, right m1 or 2 (reversed); **D.** SGOPV 2130, right m3 (reversed). **Abbreviations:** ANT, anterior; LAB, labial; MSL, mesoloph; mld I, metalophulid I. Dashed line indicates reconstructed outline of tooth. Scale bar = 2 mm.

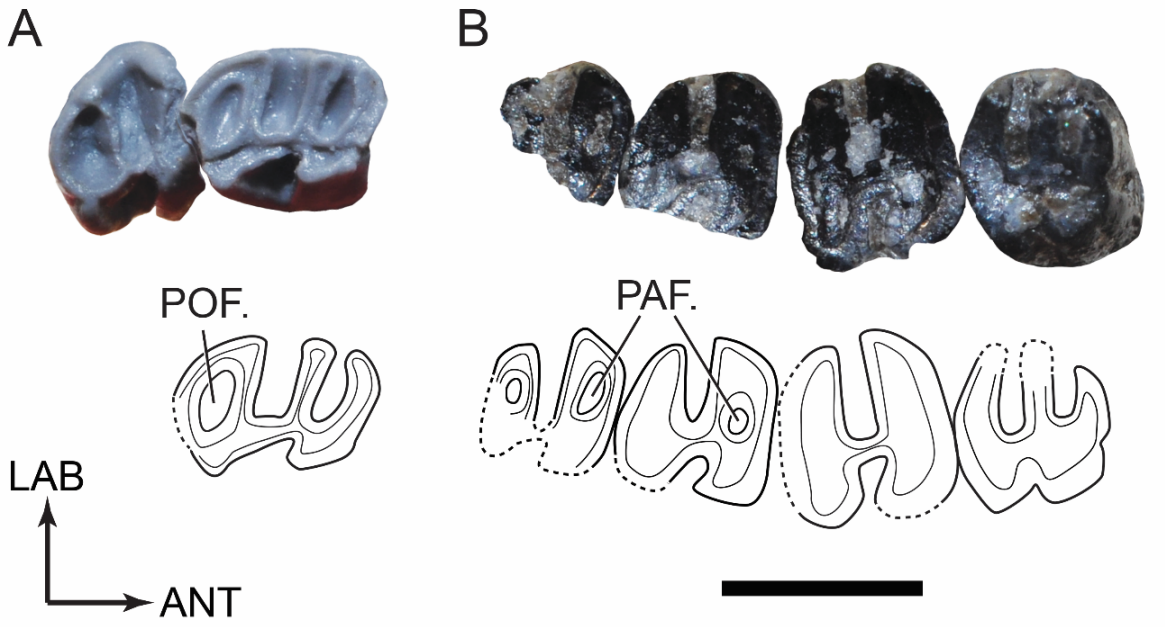

Figure 22: Photos and line drawings of *Acaremys* from Pampa Castillo. **A.** *Acaremys* sp., SGOPV 2365 (cast), right DP4–M1. **B.** cf. *Acaremys* sp., SGOPV 2343, right P4–M3. **Abbreviations:** ANT, anterior; LAB, labial; PAF, parafossette; POF, posterofossette. Dashed line indicates reconstructed outline of tooth. Scale bar = 2 mm.

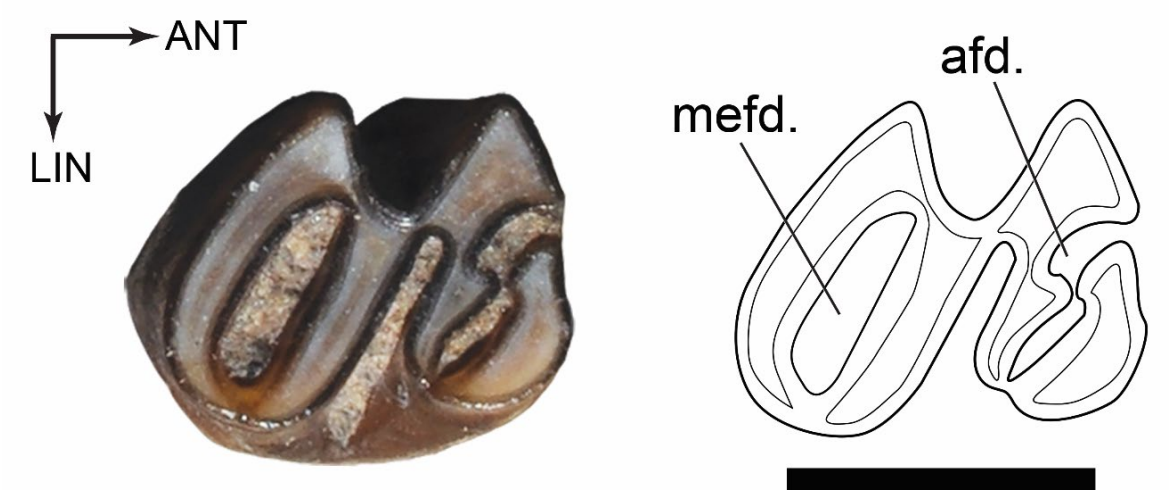

Figure 23: Photo and line drawing of *Prostichomys* sp. nov., SGOPV 2706, left m1 or 2. **Abbreviations:** afd, anterofossettid; ANT, anterior; LIN, lingual; mefd, metafossettid. Scale bar = 2 mm.

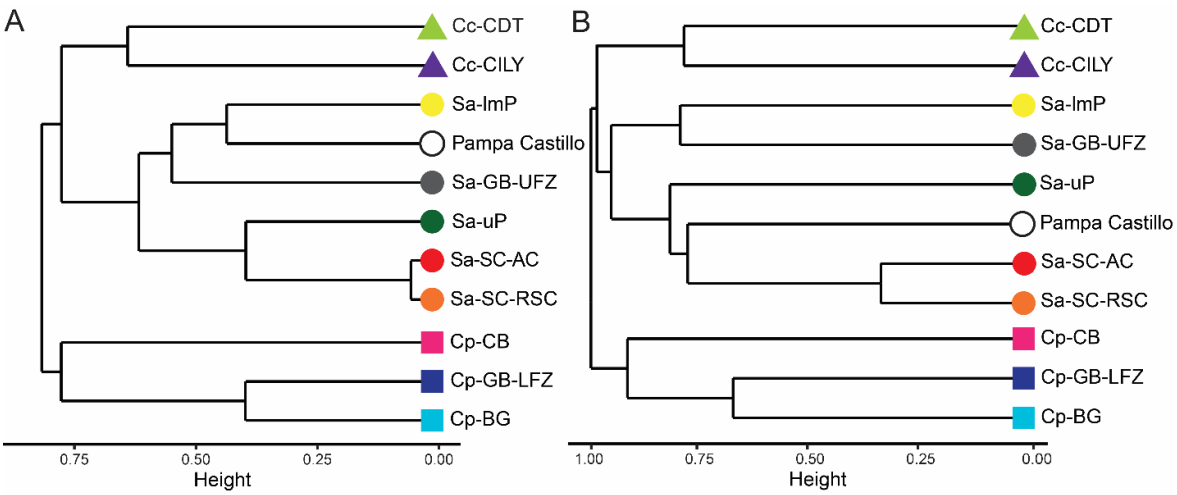

Figure 7: Results of hierarchical clustering analysis using Jaccard index on Miocene Patagonian rodent communities with provisionally recognized taxa includedusing **A.** genera and **B.** species. Colors and shapes of fauna symbols as in Figure 18. **Abbreviations:** Cc-CILY, Cruces Infinitos and Los Yeguarizos; Cc-CT, Cañadón de Tordillo; Cp-BG, Bryn Gwyn; Cp-CB, Cerro Bandera Formation; Cp-GB-LFZ, lower faunal zone of Colhue-Huapi Member of Sarmiento Formation at Gran Barranca; Sa-GB-UFZ, upper faunal zone of Colhue-Huapi Member of Sarmiento Formation at Gran Barranca; Sa-lmP, lower and middle sequences of Pinturas Formation; Sa-SC-AC, Santa Cruz Formation along Atlantic coast; Sa-SC-RSC, Santa Cruz Formation along Río Santa Cruz; Sa-uP, upper sequence of Pinturas Formation.

Table 8. Rodent taxon counts and ages of faunas used in faunal similarity analysis. There are no published absolute dates for the fossil mammal-bearing strata at Bryn Gwyn or the Cerro Bandera Formation. **Abbreviations:** Cc-CILY, Cruces Infinitos and Los Yeguarizos; Cc-CT, Cañadón de Tordillo; Cp-BG, Colhuehuapian levels of Bryn Gwyn; Cp-CB, Cerro Bandera Fm.; Cp-GB-LFZ, Lower Faunal Zone of Colhue-Huapi Member at Gran Barranca; Fm., Formation; Mem., Member; NP, non-provisionally recognized taxa; Pint., Pinturan; Sa-GB-UFZ, Upper Faunal Zone of Colhue-Huapi Member at Gran Barranca; Sa-lmP, lower and middle sequences of Pinturas Fm., Sa-uP, upper sequence of Pinturas Fm; Sa-SC-AC, Exposures of Santa Cruz Fm. along Atlantic coast; Sa-SC-RSC, Exposures of Santa Cruz Fm. along Río Santa Cruz. **References:** [1]Bucher *et al.* (2021); [2]Madden *et al.* (1997); [3]Dunn *et al.* (2013); [4]Folguera *et al.* (2018); [5]Fleagle *et al.* (2012); [6]Perkins *et al.* (2012); [7]Cuitiño *et al.* (2016).

Fauna	# Gen. (# NP)	# Spp. (# NP)	Age (Ma)	Stratigraphy	SALMA
Cc-CILY	8 (8)	5 (5)	14.86–12.75[1]	Collón Curá Fm.	Colloncuran?
Cc-CT	9 (7)	6 (6)	~15.7[2]	Pilcaniyeu Mem.–Collón Curá Fm.	Colloncuran
Cp-BG	17 (16)	19 (18)	—	Trelew Mem.–Sarmiento Fm.	Colhuehuapian
Cp-CB	9 (8)	8 (8)	—	Cerro Bandera Fm.	Colhuehuapian?
Cp-GB-LFZ	16 (16)	25 (25)	21.0–20.5[3]	Colhue-Huapi Mem.–Sarmiento Fm.	Colhuehuapian
Pampa Castillo	14 (14)	18 (15)	<18.7[4]	Galera Fm.	Santacrucian
Sa-GB-UFZ	6 (5)	3 (3)	19.04–18.62[3]	Colhue-Huapi Mem.–Sarmiento Fm.	Santacrucian (Pint.)
Sa-lmP	12 (12)	14 (14)	~17.99[5]	Pinturas Fm.	Santacrucian (Pint.)
Sa-uP	11 (11)	11 (11)	~17.8?[5]	Pinturas Fm.	Santacrucian
Sa-SC-AC	16 (16)	29 (29)	~17.8–16.2[6]	Santa Cruz Fm.	Santacrucian
Sa-SC-RSC	17 (17)	31 (31)	~17.22–15.63[7]	Santa Cruz Fm.	Santacrucian

Table 9. Lower tooth measurements of Pampa Castillo octodontoids. All measurements reported in mm. * indicates that measurement is approximate due to moderate damage. — indicates that tooth is present but cannot be measured due to extensive damage.

Taxon	**Spec. #**	**dp4**		**m1**		**m2**		**m1 or 2**		**m3**	
		AP	**LL**	**AP**	**LL**	**AP**	**LL**	**AP**	**LL**	**AP**	**LL**
Acarechimys minutus	SGOPV 2131							1.9	1.6		
	SGOPV 2136	—	—	1.6	1.4	1.6	1.5				
	SGOPV 2367	1.7	1.0	1.7	1.3	1.8	1.4			1.7	1.2
Acarechimys cf. *minutissimus*	SGOPV 2191	1.5	1.0								
Acarechimys constans	SGOPV 2135					2.0	1.7			—	—
	SGOPV 2137	1.8	1.1	1.7	1.5	1.7	1.4*				
	SGOPV 2138	2.1	1.5	2.0	1.7						
	SGOPV 2139	—	—	2.1	1.7	1.9	1.8				
	SGOPV 2143			2.0	1.8						
	SGOPV 2198			1.8	1.6	2.1	1.9				
	SGOPV 2199	2.0	1.4	1.9	1.6						
	SGOPV 2362	2.5	1.6	2.2	1.5						
	SGOPV 2705	1.8*	1.3*	1.9*	1.8*	—	1.8				
	SGOPV 2707										
Spaniomys cf. *riparius*	SGOPV 2128	3.0	2.1								
	SGOPV 2129							2.7	2.2		
	SGOPV 2130									3.1	2.7
Prostichomys sp. nov.	SGOPV 2706							2.9	2.4		

Table 10. Upper tooth measurements of Pampa Castillo octodontoids. All measurements reported in mm. * indicates that measurement is approximate due to moderate damage. — indicates that tooth is present but cannot be measured due to extensive damage. ^{D} indicates that measurement is of DP4. If left and right teeth are present, measurements are reported as left/right.

Taxon	**Spec. #**	**P4**		**M1**		**M2**		**M1 or 2**		**M3**	
		AP	**LL**	**AP**	**LL**	**AP**	**LL**	**AP**	**LL**	**AP**	**LL**
Acarechimys constans	SGOPV 2707	—^{D}	—^{D}	1.7	1.9						
Spaniomys cf. *riparius*	SGOPV 2132							2.7	2.3*		
Dudumus sp. nov. 2	SGOPV 2140			1.9	1.5	1.8	1.3				
Caviocricetus sp. nov.	SGOPV 2194	1.4^{D}	1.0^{D}	1.3	1.1						
Acaremys murinus	SGOPV 2365	2.0^{D}	1.3^{D}	—	—						
cf. *Acaremys*	SGOPV 2343	1.7	1.9	1.5	1.7						
	SGOPV 2363	1.7/ 1.9	2.0*/ 1.9*	— /—	— /—	1.8/	2.4/				

CHAPTER 5

SYSTEMATIC AND ECOMORPHOLOGICAL UTILITY OF SOUTH AMERICAN NATIVE UNGULATE (NOTOUNUGLATA & LITOPTERNA) TARSALS FROM THE EARLY MIOCENE SANTA CRUZ FORMATION

ABSTRACT

Morphology of the astragalus and calcaneus, the two proximal tarsal (ankle) bones, both commonly recovered as fossils, correlates with locomotory style and habitat. I analyzed the tarsal morphology of 11 genera of South American native ungulates (SANUs) from the early Miocene Santa Cruz Formation in southern Argentina to address three questions: 1. Can SANU tarsals be identified to lower-order taxa? 2. Are linear measurements or two-dimensional landmarks better for quantifying tarsal morphology? 3. What does tarsal morphology reveal about SANU locomotion?

SANU tarsals are useful for family- and genus-level identification. ANOVA tests revealed highly significant differences between tarsals of all families and genera. Tarsals resampled from a linear discriminant analysis (LDA) were assigned to their correct taxon 71.3% of the time across 8 trials that varied in the method of data collection, tarsal analyzed, and taxonomic level. Astragali and calcanei are equally readily identified and seem equally suited for systematics.

Landmarks outperform linear measurements in capturing tarsal morphology. In 3 of 4 direct comparisons, landmark-based LDAs produced more accurate results than their linear measurement counterparts in assigning resampled tarsals to their correct taxon. Moreover, landmark-based methods are more replicable, faster, and more fully capture complex morphologies than those based on linear measurements.

Morphological disparity and clustering patterns within principal components analysis (PCA) morphospace produced several insights into SANU locomotion. Litopterns exhibited (tense, be consistent throughout) very low disparity even though Proterotheriidae (a litoptern subgroup) was the most diverse family in the sample. Toxodontid calcanei were highly disparate, likely reflecting differing body masses of the two genera considered, *Adinotherium* and *Nesodon*, but curiously, the astragali of these genera overlapped in PCA morphospace. Among typotherians, *Hegetotherium* astragali plotted in a separate region from those of other taxa, a surprising result given that their calcanei overlapped and all typotheres are generally assumed to have locomoted in a similar manner. Plausibly, these differences in astragalar shape may reflect differing habitat preferences given that these typotheres do not vary much in mass.

This study suggests several promising directions for future research in this area. Samples including more closely related taxa than the SANU genera and families in this sample can test the taxonomic specificity with which isolated tarsals can be identified and would better approximate future researchers would attempt to identify isolated tarsals. Expanded sampling to include extant taxa might identify reasonable analogs to SANU locomotor patterns. Broadening sampling of extinct taxa taxonomically, and over a longer temporal range, may shed light on how various SANU lineages and communities responded to long-term environmental changes, including the origin and spread of grasslands.

KEYWORDS

South American native ungulates; geometric morphometrics; ecomorphology; locomotion

INTRODUCTION

Ecomorphology is a paleobiological technique by which the morphology of extinct taxa is used to infer their ecological characteristics through comparisons to living organisms (Barr, 2018a). Based on biological uniformitarianism, ecomorphology assumes that particular morphologies serving specific functions in the present, served similar functions in the past—whether those morphologies are homologous or convergent. Locomotion is one of the most common animal behaviors, so unsurprisingly, it has received a great deal of attention in the ecomorphological literature. Such analyses shed light on a particular taxon's behavior, the selective pressures it faced, and the paleoenvironments it inhabited (e.g., Croft and Anderson, 2008; Cassini et al., 2012a; Chen and Wilson, 2015; Panciroli et al., 2017; Boivin et al., 2019). Ecomorphology is particularly useful to study fossil groups that clearly differ from their close modern relatives or those who have no extant members, such as the South American native ungulates (SANUs) examined herein. Communities, in addition to taxa, can be the subjected to ecomorphological analyses as well, providing insights on trophic interactions and

informing paleoenvironmental reconstructions (e.g., Kovarovic and Andrews, 2007; Plummer et al., 2008, 2015; Polly, 2010; Kay et al., 2012, 2021; Barr, 2015).

Many parts of the appendicular skeleton are used for locomotor ecomorphology, but I have chosen two most-proximal tarsal (ankle) bones, the astragalus and calcaneus, as the subjects of my investigation. The astragalus is the primary articulation of the tibia and the foot. The proximal end of the calcaneus is the anchor for the Achilles tendon. I chose these bones because they are more compact and robust relative to long bones of the appendicular skeleton such as the femur, ulna, or metapodials. Therefore, they are less likely to be damaged by taphonomic processes, increasing potential sample size. Other tarsals and carpals (wrist bones) are similarly compact and robust, but their relatively simple morphologies make them difficult to identify and analyze. Plus, the involvement of the calcaneus and astragalus in foot flexion/extension, a very common and, depending on locomotory style, variable movement, make these bones a common site of locomotory adaptation. Previous ecomorphological studies employing astragali and calcanei have shown correlation between the morphology of these bones and substrate use, locomotory style, and habitat preference in various mammal groups (e.g., Dunn and Rasmussen, 2007; Plummer et al., 2008, 2015; Polly, 2010; Barr, 2014, 2015, 2018a, b; Ginot et al., 2016; Panciroli et al., 2017; Curran, 2018; Boivin et al., 2019; Shelley et al., 2021).

The form of data used in ecomorphological analyses varies. Linear measurements (i.e., length or width) of specific features can be analyzed independently but are usually combined into functional ratios to control for

differences in absolute size (see Dunn, 2018). Angular measurements are often analyzed alongside linear measurements but generally are not converted into ratios. Linear and angular measures (or functional ratios) can be analyzed individually (e.g., Dunn and Rasmussen, 2007; Polly, 2010; Ginot et al., 2016; Barr, 2017; Levering et al., 2017), but often, many are analyzed simultaneously using multivariate techniques such as principal components analysis (PCA), linear discriminant analysis (LDA; also known as discriminant function analysis), or canonical variable analysis (e.g., Croft and Anderson, 2008; Plummer et al., 2015; Panciroli et al., 2017). Geometric morphometrics is a method of recording shape data via points called landmarks and semilandmarks (see Mitteroecker and Gunz, 2009; Curran, 2018). Landmarks are points placed on homologous discrete features across the sample. Semilandmarks consist of sequences of points placed along curved features or surfaces where homologies are difficult to identify. The position of landmarks and semilandmarks, recorded in a Cartesian coordinate system, are subjected to statistical analysis (Adams et al., 2013). Geometric morphometrics can be implemented in two (2D) or three (3D) dimensions. Three-dimensional landmarks capture more morphological information but take longer to record and/or require expensive equipment. 3D data produce stronger signals, but 2D data are sufficient for systematic and ecological purposes (Hedrick et al., 2019; Cardini and Chiapelli, 2020; Wasiljew et al., 2020). Landmark datasets are inherently multivariate because each landmark/semilandmark is a distinct dependent variable/observation.

Genera and species of fossil mammals are nearly always diagnosed by craniodental characters, and as a consequence, isolated tarsals are often identified

only to ‘family’ or ‘order’ (e.g., de Muizon et al., 1998; Shockey and Anaya, 2008; Armella et al., 2016, 2020). The complex morphology of astragali and calcanei potentially holds systematic value, but unlike skulls and teeth, their morphologies vary in continuous, rather than discrete, ways. The ability to identify isolated tarsal elements more precisely will increase the number fossils that are assignable to these more specific levels, aiding paleobiological and paleoecological analyses that require presence/absence or abundance data. Multivariate techniques, whether using linear measurements or landmarks, may allow isolated tarsals to be identified to lower taxonomic levels than has been possible previously.

Here, I analyze the tarsals of notoungulates and litopterns, the two most speciose clades (‘orders’) of South American native ungulates (SANUs). Prior to the late Miocene–Pleistocene Great American Biotic Interchange (GABI), SANUs filled many of the medium and large-bodied herbivore niches in South American ecosystems (Croft et al., 2020). The relationships of SANUs to other placental mammals has long been debated, but recent genetic and proteomic evidence suggests that they are most closely related to perissodactyls among living taxa, with artiodactyls as the next outgroup (Buckley, 2015; Welker et al., 2015; Westbury et al., 2017).

Due to the distant phylogenetic relationships and, in some lineages, vastly different morphologies of SANUs and their nearest extant relatives, ecomorphological analysis is of the best ways to understand SANU paleobiology. Various SANU groups have been qualitatively analogized to artiodactyls, rhinocerotids, and rodents (Scott, 1910, 1912; Croft, 2016; Croft et al., 2020).

Ecomorphology provides a way to quantitatively assess which modern species various SANUs resemble in their appendicular morphology and, presumably, their locomotor behavior. Several locomotor ecomorphological analyses of notoungulates and litopterns have attempted to answer these questions (e.g., Elissamburu, 2004, 2010; Shockey et al., 2007; Croft and Anderson, 2008; Cassini et al., 2012a; Muñoz et al., 2017), but none have focused exclusively on tarsals.

Understanding SANU locomotory paleobiology is important because, by the early Neogene, the medium to large-sized mammal communities of Africa, Eurasia, and North America were made up of the same higher-order clades (e.g., artiodactyls, perissodactyls, proboscideans, and carnivorans; MacFadden, 2000; Turner and Antón, 2004; Fortelius et al., 2014; Saarinen et al., 2020). Until the GABI, South America's mammal faunas were completely different consisting of SANUs, xenarthrans, sparassodonts, and phorusrhacids (Cione et al., 2015; Croft, 2016). Their taxonomic differences notwithstanding, the mammal assemblages of all continents faced experienced similar climatic, vegetational, and geologic changes. Due to their taxonomic homogeneity, the mammal communities of Africa, Eurasia, and North America, likely responded similarly to these changes. Due to the taxonomic distinctiveness of pre-GABI South American mammal communities, their response to these same changes can be viewed as a more 'independent' test of community evolution.

Here, I examine SANUs of the early Miocene Santa Cruz Formation (SCF), which bears arguably the best-studied pre-Quaternary mammal fauna in South America (Vizcaíno et al., 2012c; Croft, 2016). The SCF is fossiliferous across much

of Santa Cruz Province in southern Argentina, but localities spanning ~17.8–15.6 Ma along the Atlantic coast and the Río Santa Cruz, have received the most attention (Fleagle et al., 2012; Perkins et al., 2012; Cuitiño et al., 2016; Trayler et al., 2020). Paleobotanic, sedimentological, and ecometric evidence suggests have suggested that the paleoenvironment of these localities was a mosaic of open and closed habitats with seasonal precipitation (Brea et al., 2012; Kay et al., 2012, 2021; Raigemborn et al., 2015, 2018; Cuitiño et al., 2019; Catena and Croft, 2020). Early Miocene notoungulates are split into two groups: the generally large-bodied toxodontians and the smaller typotherians (Croft et al., 2020). Toxodontians are represented by three 'families' in the SCF: Toxodontidae, Homalodotheriidae, and 'Notohippidae' (which is likely paraphyletic; see Wyss et al., 2018; Martínez et al., 2021). Two typotherian 'families' are recognized from the SCF, Hegetotheriidae and Interatheriidae. Three litoptern 'families' are known from the SCF, Macraucheniidae, Proterotheriidae, and Adianthidae. Another SANU 'order,' Astrapotheria, is found in the SCF but was not included in my sample. 'Notohippids' and adianthids also do not appear in my sample. I explain the reasons for these omissions in the Materials and Methods. See Appendix 3 for a full list of SANU genera known from the SCF and those used in this analysis.

This project is intended as a pilot study that will encourage parallel analyses of other SANUs and herbivorous mammals from different regions and temporal intervals. I recorded the morphology of SANU tarsals from the Santa Cruz Formation using two distinct methods, linear and angular measurements, and 2D landmarks. With these data, I investigate several questions. First, I assess the systematic utility

of isolated tarsals to the family- and genus-levels using ANOVA and linear discriminant analysis. Second, I evaluate linear measurement versus landmark data methodologies and astragali versus calcanei with quantitative tests and my qualitative experience to see if one methodology/bone is superior. Third, although I was unable to incorporate modern mammal tarsals into my sample due to the COVID-19 pandemic, I draw some paleobiological conclusions from the relative position and disparity of SCF SANUs in a principal components analysis morphospace. Finally, I discuss future directions I intend to take this research.

MATERIALS AND METHODS

Sixteen SANU genera are represented in the Santa Cruz Formation. Of these, *Theosodon* Ameghino, 1887 (Macraucheniidae), *Anisolophus* Burmeister, 1879 (Proterotheriidae), *Diadiaphorus* Ameghino, 1887 (Proterotheriidae), *Thoatherium* Ameghino, 1887 (Proterotheriidae), *Homalodotherium* Flower, 1873 (Homalodotheriidae), *Adinotherium* Ameghino, 1887 (Toxodontidae), *Nesodon* Owen, 1846 (Toxodontidae), *Hegetotherium* Ameghino, 1887 (Hegetotheriidae), *Pachyrukhos* Ameghino, 1885 (Hegetotheriidae), *Interatherium* Ameghino, 1887 (Interatheriidae), and *Protypotherium* Ameghino, 1887 (Interatheriidae), are included in the current study (Appendix 3). However, certain genera (*Adianthus* Ameghino, 1891 (Adianthidae), *Patriarchus* Ameghino, 1889 (Interatheriidae), *Notohippus* Ameghino, 1891 (“Notohippidae”), *Icochilus* (Interatheriidae), *Tetramerorhinus*

Ameghino, 1894 (Proterotheriidae), and *Astrapotherium* Burmeister, 1879 (Astrapotheriidae)) are not included. Tarsals of *Adianthus* and *Patriarchus* (Scott, 1910; Fernández et al., 2019a), are unknown, and I was unable to access these elements for *Notohippus* or *Icochilus*. Given the abundance of *Tetramerorhinus* spp. in the SCF and historic referral of some members of this genus to *Proterotherium* Ameghino, 1883 (still seen on many museum labels; see Soria, 2001), it is likely that some tarsals labeled as 'Proterotheriidae indet.' represent *Tetramerorhinus*, but I cannot be certain (Soria, 2001; Schmidt et al., 2019). Although I examined and photographed one *Astrapotherium* calcaneus during the course of this study, its morphology was an outlier relative to the notoungulates and litopterns in my sample — likely owing to *Astrapotherium*'s larger size and distant relations to these taxa (Vizcaíno et al., 2012b; Croft et al., 2020). I omitted this specimen from my analyses to avoid a single, highly divergent specimen overwhelming more subtle patterns in the notoungulate and litoptern samples.

The specimens used in each analysis are given in Table 11. The number of astragali or calcanei used in the linear and landmark analyses differs because some specimens were damaged in a way that made them suitable for collecting one type of data but not the other. Specimens identified only as 'Family indet.' were included in family-level analyses but not in genus-level analyses.

Data Collection

I photographed specimens at the American Museum of Natural History, Museo de La Plata, Museo Argentino de Ciencias Naturales, and Yale Peabody Museum. Each specimen was photographed in dorsal, medial, plantar, and lateral

views. Only the tarsals of skeletally mature individuals were included. Recommendations for making geometric morphometric analyses replicable (Fox et al., 2020), were followed. They were applied to linear measurements as well. The same digital camera (Nikon D90), lens (Nikon AF-S DX Micro NIKKOR 40mm f/2.8G), and photographic protocols were used for all specimens. I was the solely responsible for collecting linear measurement and landmark data.

Linear and angular measurements were taken as shown in Figures 25 and 26, and as described in Appendix 4. (Note: hereafter 'linear measurements' refers to linear as well as angular measurements). Linear measurements were taken in ImageJ (Schindelin et al., 2012). Two angular and 14 linear measurements were collected for each calcaneus, and three angular and 16 linear measurements for each astragalus. The linear measurements were scaled to make the greatest proximodistal length of the tarsal (i.e., A1 or C1) equal to 1, to ensure that differences in shape rather than absolute size would be analyzed. However, linear rescaling does not eliminate allometric shape differences, so size effects still likely impacted the results (Barr, 2018b; Etienne et al., 2020).

I recorded landmark data with tpsDig2 (Rohlf, 2006). If necessary, photographs were reflected so that all specimens appeared to be from the left side. Landmarks and semilandmarks were digitized as shown in Figure 27 and described in Appendix 5. To record semilandmarks, I traced the shape of the curved feature of interest with as many points as needed to accurately capture its shape. This line was then resampled to produce the proper number of semilandmarks. For astragali, nine landmarks and 33 semilandmarks were recorded in plantar view. From calcanei,

eight landmarks and 21 semilandmarks were taken in medial view, and seven and 22 in dorsal view. Data from both views of the calcanei were analyzed simultaneously. Landmark data from all elements were aligned and rescaled with Procrustes analysis using the geomorph package (Adams and Otárola-Castillo, 2013) for R (R Core Team, 2020). Semilandmarks were treated as sliding semilandmarks for the Procrustes alignment. The .tps files containing landmark data from dorsal and medial calcaneal views were Procrustes aligned separately before being combined (as subsets) for the statistical analyses.

Data Analysis

Analyses were conducted in R version 4.0.2 (R Core Team, 2020) with the geomorph (Adams and Otárola-Castillo, 2013), tidyverse (Wickham et al., 2019), caret (Kuhn, 2008), and MASS packages (Venables and Ripley, 2002). All analyses were performed on the linear and landmark datasets for both tarsals at both the family- and genus-level, yielding eight total analyses, unless otherwise noted.

Principal components analysis (PCA) reduces the dimensionality and maximizes variation of multivariate datasets to make clusters of similar observations (i.e., specimens) easier to visualize. These plots offer a first-order, visual approximation of whether SANU taxa can be distinguished from each other, and the disparity of individual taxa. Additionally, the relative position and disparity of taxonomic clusters can be used to infer morphological similarity or divergence.

I tested whether the tarsals of different SANU families and genera could be distinguished using MANOVA (MASS) for linear datasets and Procrustes ANOVA

(geomorph) for landmark datasets. These tests assessed whether SANU tarsals can be distinguished taxonomically.

The efficacy of assigning indeterminate tarsals to family or genus was judged using linear discriminant analysis (LDA). LDA is similar to PCA in that it reduces the dimensionality of the dataset, but unlike PCA, it considers pre-defined group membership and seeks to maximize the clustering of these groups. Specimens were randomly resampled and then were classified using the LDA model. The accuracy of these classifications versus their known assignments was recorded. Assuming that SANU tarsals can be taxonomically distinguished (as shown by the ANOVA tests), this LDA test will assess the reliability of assigning isolated (i.e., unassociated with identifiable craniodental remains) to known taxa.

Lastly, I calculated morphological disparity within each family. This analysis was only performed on the landmark datasets because it is only available in the geomorph package. I did not analyze intra-genus morphological disparity due to the low number of specimens assigned to several genera in my sample (Table 11). The full degree of morphological variation within a taxon cannot be assessed with only a few specimens, so I did not have confidence in any potential results of such analyses.

RESULTS

Spreadsheets containing all linear measurements are provided in Supplementary Files 11 (astragalus) and 12 (calcaneus). Landmark data are given in Supplementary Files 13 (astragalus), 14 (calcaneus in dorsal view), and 15 (calcaneus in medial view).

Principal Components Analysis of SANU Tarsals

I plotted the first two principal components (PCs) of each PCA to visualize patterns of variation among different families (Fig. 28). In all four family-level plots, the two litoptern families, Macraucheniidae and Proterotheriidae, are closely associated and often overlap. Hegetotheriids and interatheriids, the two typotherian clades, also plot closely but less so than the litopterns. In all plots except for 'astragalus landmark' toxodontids are clearly separated from the other families. Interestingly, in the astragalus landmark plot, the overlap is caused by a single outlier toxodontid with a positive value for PC1. Homalodotheriids are clearly separated in the calcaneus plots, but the sample included no homalodotheriid astragali (Table 11).

I made similar PC1 vs. PC2 plots using specimens identified at the genus-level (Fig. 29). Homalodotheriidae (*Homalodotherium*) and Macraucheniidae (*Theosodon*) are represented by single genera in my sample (Table 11; Appendix 3). The two hegetotheriid genera, *Hegetotherium* and *Pachyrukhos*, fall in separate areas of the morphospace in all four plots. *Adinotherium* and *Nesodon*, the two toxodontids, overlap in the astragalus plots but not the calcaneus plots. Interatheriid (*Interatherium* and *Protypotherium*) and proterotheriid (*Anisolophus*, *Diadiaphorus*, and *Thoatherium*) genera are not notably separated by PCs 1 and 2.

Quantitatively Distinguishing SANU Taxa with Tarsals

MANOVA (linear data) and Procrustes ANOVA (landmark data) tests distinguish all SANU families and genera with an extremely high level of confidence ($p<0.001$) for both tarsals and data types (Table 12). Since my sample contained no *Homalodotherium* astragali, I re-ran the calcaneus tests with this taxon removed to more fairly compare the relative performance of these tarsals. These analyses yielded results of similar levels of significance (Supplementary File 6).

Identifying SANU Tarsals using Linear Discriminant Analysis

In total, seven of the eight LDAs had an accuracy greater than 50% (Table 13). Generally, astragali were correctly assigned more often than calcanei when comparing pairings of the same taxonomic level (i.e., genus or species) and data type (i.e., landmark or linear). To test whether the absence of *Homalodotherium* from the astragalar datasets affected these results (Table 11), I re-ran the calcaneal LDA without *Homalodotherium*, and in three of the four calcaneal tests, accuracy improved little (<2%) (Supplementary File 16). Unsurprisingly, given their fewer degrees of freedom, family-level LDAs produced far more accurate classifications than their genus-level counterparts, often by 30% or more when comparing LDA pairs with identical elements (i.e., astragalus or calcaneus) and data types. Landmark LDAs outperformed linear measurement LDAs in three of four pairings where element and taxonomic level were the same.

Intra-Family Morphological Disparity of SANU Tarsals

Despite apparent differences in intra-family disparity in the landmark datasets (Fig. 28B, D), pair-wise ANOVA tests revealed few significant differences (i.e., $p<0.05$; Table 14). The astragali of toxodontids were significantly more disparate than those of other families in my sample. For calcanei, hegetotheriids were more disparate than all other families but only the differences between them and homalodotheriids, macraucheniids, and proterotheriids were significant. These highly disparate families, Toxodontidae and Hegetotheriidae, are represented by multiple genera, which is not true of all families in this analysis (Table 11). However, disparity is not purely a function of diversity as the family with the most genera, Proterotheriidae, (three confirmed in this sample and four in the SCF overall), exhibited low disparity relative to the other families.

DISCUSSION

All families and genera in my sample can be distinguished using either tarsal element or data type (i.e., linear measurement or landmark; Table 12). The pattern of variation in the first two principal components (PCs) suggest that phylogeny, body size, and locomotor behavior all affect tarsal morphology. SANU families recorded in the SCF generally exhibit similar levels of intra-family tarsal morphological disparity despite differing in the number of genera and species (Table 14), suggesting that locomotor disparity and taxonomic diversity are not always correlated.

Paleobiological Inferences

Litopterna—Macraucheniidae and Proterotheriidae are similar in tarsal morphology. Macraucheniidae is represented solely by *Theosodon* in the SCF, whereas four proterotheriid genera are recognized (Appendix 3; Soria, 2001; Schmidt et al., 2019). Macraucheniids and proterotheriids are generally thought to have diverged by the early Eocene, though the uncertain placement of taxa such as *Paranisolambda* Cifelli, 1983, and *Anisolambda* Ameghino, 1901, make this uncertain (see McGrath et al., 2020). Estimates of body mass vary according to the proxy used, but *Theosodon* is generally considered 1.2–2x more massive than the largest proterotheriid from the SCF, *Diadiaphorus majusculus* Ameghino, 1887, which itself is significantly larger than *Thoatherium* and *Anisolophus* (Table 11; Cassini et al., 2012b; Vizcaíno et al., 2012b). The pedal morphology of these clades differ, with macraucheniids being tridactyl and proterotheriids (at least those found in the SCF) being functionally — or, in the case of *Thoatherium*, truly — monodactyl (Scott, 1910; Soria, 2001). Litopterns are generally considered cursorial animals and conservative in their postcranial morphology throughout their history (Scott, 1910; Cifelli, 1983; Cifelli and Villarroel, 1997; Shockey, 1999; Soria, 2001; Cassini et al., 2012a; Gelfo et al., 2016; Croft et al., 2020).

Despite their phylogenetic separation, size differences, and morphological distinctions, macraucheniids and proterotheriids plot closely to each other or overlap in the first two PCs of both tarsals and data types (Fig. 28). At the genus-level, the three proterotheriids are not easily distinguished (Fig. 29), except by ANOVA tests were still (Table 12). These morphospace and morphological disparity patterns (Table 14) support the morphological conservatism noted by previous authors.

Homalodotheriidae—Homalodotheriidae are represented by a single genus in the SCF, *Homalodotherium* (Appendix 3). My sample contained no astragali from this taxon and one or two calcanei for the linear and landmark analyses, respectively (Table 11). *Homalodotherium* was one of the largest-bodied SANUs in the SCF (Table 11) and had long, clawed forelimbs which are believed to have been used to gather vegetation from high in trees as it reared up on its hindlimbs similar to the chalicothere perissodactyls of Africa, Eurasia, and North America, and also to North and South American ground sloths (Coombs, 1983). Unlike other SANUs in this sample, *Homalodotherium* is believed to have been plantigrade rather than digitigrade based on its tarsal and pedal morphology (Elissamburu, 2010).

Given the unusual lifestyle and morphology of *Homalodotherium*, it is unsurprising that its calcanei plot distantly from other SANUs in this sample (Figs. 28–29), reflecting the very different stresses its plantigrade posture and facultative bipedality would have subjected it to.

Toxodontidae—Toxodontids are represented by *Adinotherium* and *Nesodon* in the SCF (Appendix 3). Within Toxodontidae, *Adinotherium* and *Nesodon* are close relatives (Forasiepi et al., 2015; Armella et al., 2018). *Nesodon* and *Adinotherium* are the largest and third-largest taxa in the sample, respectively, though their mass difference is rather large (~4–5x; Table 11). Otherwise, these genera are similar in overall morphology (Scott, 1912). Cassini et al. (2012a) inferred that these taxa had similar styles of locomotion based on comparable values for many functional limb bone indices. Houssaye et al. (2016) observed similarities in limb bone

microstructure in *Nesodon* and extant graviportal rhinoceroses, suggesting that *Nesodon* may have achieved a mass large enough to necessitate postural changes.

Toxodontids are sharply distinct from other families in three of four analyses, the astragalus-landmark analysis being the lone exception (Fig. 28). Toxodontid astragali were one of the few examples where intra-familial disparity was significantly higher than other families (Table 14). high calcaneal disparity appears driven by *Adinotherium* and *Nesodon* plotting separately in the PCA morphospace (Fig. 29C–D). However, they overlap in the astragalar morphospace (Fig. 29A–B). This high disparity, and apparently stark generic differences for calcanei is surprising given the close phylogenetic relationship and similar overall morphology and functional limb bone ratios of these two genera (Scott, 1912; Cassini et al., 2012a; Forasiepi et al., 2015; Armella et al., 2018). Size likely accounts for the separation of these taxa in calcaneal morphospace from each other and other SANUs as a whole. *Adinotherium* and *Nesodon* are the largest SANUs in this analysis save for the macraucheniid *Theosodon* which is intermediate between them (Table 11). Given the highly cursorially-specialized and conservative morphology of *Theosodon* and other litopterns, the disparate positions of *Theosodon* and the toxodontids are expected.

Tarsal morphology, particularly articular facet size, changes with size in rhinocerotids (Etienne et al. (2020), a pattern attributed to the transition to graviportality (i.e., columnar limb posture) in larger-bodied taxa. *Nesodon* is interpreted as having been graviportal, but *Adinotherium* likely was not. Calcanei are proportionately shorter in larger-bodied bovids (Barr, 2018b). Since calcaneal length

(C1) was the measure by which all other calcaneal linear measurements were rescaled (Appendix 4), toxodontid calcaneal disparity being much higher for linear than landmark datasets was expected (Fig. 28C–D). Toxodontidae exhibits the largest relative and absolute mass range of any family in this sample, meaning that allometric effects should be substantial. Later toxodontids, such as *Toxodon*, exceeded 1000 kg in mass, allowing a consideration of the allometric scaling of their tarsals compared to other mammals of similar body size, such as rhinocerotids, proboscideans, or astrapotheres (Fariña et al., 1998; Croft, 2016).

Interatheriidae—Interatheriidae are represented by two genera, *Interatherium* and *Protypotherium*, and the most total specimens in my sample (Table 11). These genera are considered interatheriine interatheriids and are fairly closely related (Vera et al., 2017; Fernández et al., 2019a; Croft and Anaya, 2020). Interatheriids are generally small bodied with *Protypotherium* being larger than *Interatherium* (Table 11). *Protypotherium* is much longer-legged than *Interatherium* (Sinclair, 1909), leading Croft and Anderson (2008) to compare them to an artiodactyl and mustelid, respectively. *Interatherium* has sometimes been considered semi-fossorial or fossorial (Elissamburu, 2004), though others have cast doubt on its digging abilities, arguing that it was likely ambulatory or a generalist locomotor (Cassini et al., 2012a; Muñoz et al., 2017). *Protypotherium* is thought to have been cursorial or favored a ‘bounding’ locomotion (Croft and Anderson, 2008; Cassini et al., 2012a).

Interatheriidae is most closely associated with Hegetotheriidae in the PCA morphospace (Fig 4). *Interatherium* and *Protypotherium* occupy similar areas of the

calcaneus PCA morphospace but are slightly separated in analyses of the astragalus (Fig. 29). Quantitatively, interatheriids exhibited low disparity for both tarsals (Table 14). Nevertheless, the MANOVA and Procrustes ANOVA tests distinguish the two genera in all cases (Table 12). The overlapping position of these genera in the calcaneal morphospaces suggests that they locomoted similarly. Conversely, their slight separation in the astragalus plots suggests there were differences. Given the clear discrepancy in limb length between these genera (Sinclair, 1909; Croft and Anderson, 2008), they almost certainly differed in their locomotor behavior.

Hegetotheriidae—Hegetotheriids, also typotherian notoungulates, are known from the SCF by *Hegetotherium* and *Pachyrukhos* (Table 11; Appendix 3), which are placed in separate 'subfamilies' Hegetotheriinae and Pachyrukhinae, respectively (Seoane et al., 2017; Seoane and Cerdeño, 2019). Both taxa are small bodied, but *Hegetotherium* is ~3x larger than *Pachyrukhos* (Table 11). Otherwise they resemble one another except *Hegetotherium*, especially is notably more robust, particularly its skull (Sinclair, 1909). Hegetotheriids have been interpreted as semi-fossorial (Elissamburu, 2004) or as cursorial or possibly saltatorial (Seckel and Janis, 2008; Cassini et al., 2012a; Macrini et al., 2013; Muñoz et al., 2017). Studies including hegetotheriids and interatheriids have inferred similar locomotory styles for both groups. Cassini et al. (2012a) considered *Pachyrukhos* the most cursorial of all SANUs in the SCF based on functional limb bone ratios.

As stated, hegetotheriids partially overlap interatheriids in PCA morphospace in three of four trials (Fig. 28). Hegetotheriids are highly disparate in PCA

morphospace; their calcanei are significantly more disparate than those of homalodotheriids, macraucheniids, and proterotheriids (Table 14). Like Toxodontidae, the two hegetotheriid genera, *Hegetotherium* and *Pachyrukhos* plot in distinct regions (Fig. 29). *Pachyrukhos* overlaps with interatheriids except for the astragalus-landmark plot, where it overlaps with no other taxa. *Hegetotherium* astragali overlapped with litopterns and toxodontids in the linear and landmark analyses, respectively. Conversely, *Hegetotherium* calcanei plotted very near or overlapped other typotherians. The separation of *Hegetotherium* and *Pachyrukhos*, especially in the astragalus plots, may reflect their size difference as *Hegetotherium* is the largest typothere in the SCF (Table 11). *Hegetotherium* astragali overlap those of litopterns and toxodontids, taxa that outweigh them by an order of magnitude or more, so size is unlikely to be the primary driver of this pattern. Based on limb bone proportions, *Pachyrukhos* has been considered the most cursorial SCF SANU followed by *Hegetotherium* and then *Protypotherium* Cassini et al. (2012a). If differences in cursorial specialization were driving the plotting pattern of these typotherians, then one would not expect the 'intermediate' cursor, *Hegetotherium*, to be the outlier. If the locomotory modes of *Hegetotherium* and *Pachyrukhos* (+ interatheriids) are similar, then choice of habitat may be the cause of this disparity. The astragalar trochlea in *Hegetotherium* is much wider— affecting A3, A4, and Aa1 — than in *Pachyrukhos* and interatheriids. Wide astragalar trochleae are prevalent among closed habitat bovids (Plummer et al. 2008), suggesting a greater emphasis on lateral, rather than purely para-sagittal, movements in closed habitats. The paleoenvironment of the SCF is reconstructed as a mosaic of open and closed

habitats (Brea et al., 2012; Kay et al., 2012, 2021; Cuitiño et al., 2019), so conceivably *Hegetotherium* inhabited forests while other typotherians favored open areas. Most paleodietary studies consider typotheres to have been grazers (Cassini et al., 2011; Cassini, 2013). However, based on its procumbent incisors and robust cranium, McCoy and Norris (2012) envisioned *Hegetotherium* as a "mammalian woodpecker," not unlike *Daubentonia* (aye-aye) and *Dactylopsila* (triok), gnawing through wood to feed on grubs and other invertebrates. If this hypothesis is correct, then it would stand to reason that *Hegetotherium* would inhabit forested areas, which could explain its wide astragalar trochlea.

Relative Utility of Linear and Landmark Data.

I compared linear measurement and landmark methods to determine which is more effective at analyzing tarsal morphology. Both methods produce multidimensional datasets, allowing them to be subjected to many of the same analyses (e.g., PCA, LDA). Obviously, these methods' performance in quantitative analyses is important, but other aspects, such as replicability, applicability to different taxonomic groups, and workflow must also be considered.

Procrustes ANOVA/MANOVA and LDA tests were used to quantitatively assess whether linear measurement or landmark data better at distinguishing and assigning isolated tarsals to taxa. Applying MANOVA (for linear measurement data) and Procrustes ANOVA (for landmark data), the tarsals of different SANU taxa were highly significantly different using both data types. However, the higher F-values of the landmark-based tests suggest that the differences are slightly more pronounced in these analyses (Table 12). Landmark-based LDA models were more successful at

assigning resampled tarsals to their correct taxon in three of four cases, the calcaneus-genus model being the exception (Table 13). However, when *Homalodotherium* was removed from the dataset, the landmark LDA outperformed the linear one (Supplementary File 16). In sum, both landmark and linear measurement datasets performed well, but landmark datasets produced slightly better outcomes in the LDA.

One reason landmark-based methods produce better results is that they are better at capturing complex morphologies and are more applicable to diverse and morphologically disparate samples. Linear measurements and landmarks must be recorded on homologous features across all specimens in the sample, but semilandmarks can record shape data when few or no homologous structures are present. The varying position of *Pachyrukhos* and interatheriid astragali, which overlap in the linear PCA plots, but plot separately in the landmark PCA plots, is a great illustration of the effect of landmarks (Fig. 29). This discrepancy likely reflects the fact that these groups' astragalar articular facets exhibit similar proximo-distal and medio-lateral dimensions but differ in shape. This inconsistency highlights the effectiveness of landmark data in capturing complex morphologies. As samples become more taxonomically diverse and morphologically disparate, discrete homologous structures will diminish in number, and the utility of semilandmarks will become more apparent.

In addition to being more effective, landmark-based methods are more replicable than linear measurement-based ones because Procrustes analysis aligns, rotates, and scales specimens automatically. These steps must be done manually

with linear measurement methodologies. Many linear measurements (e.g., ‘greatest proximo-distal length of astragalus,’ A1 in Appendix 4; Fig. 25) seem simple and intuitive. In practice, recording these measurements is not so simple for asymmetric elements such as tarsals; consistent orientation (i.e., rotation) is critically important. Therefore, orientation must be standardized in some way (see Appendix 4), but differing morphologies among taxa can make this practice difficult. Procrustes analysis is more objective and, therefore, more replicable than manually rotating specimen photos and scaling linear measurements.

Landmark-based methods permit a faster workflow than those based on linear measurements. Linear measurements of both tarsals were taken in four views (dorsal, medial, plantar, and lateral (Figs. 25–26; Appendix 4), whereas landmarks were recorded in two views (medial and dorsal) and one view (plantar) on calcanei and astragali, respectively (Fig. 27; Appendix 5). As seen in Tables 12 and 13, the linear measurement datasets performed equally well or slightly worse than their landmark-based counterparts, so the extra time spent photographing and measuring the additional views used in the linear measurement analyses did not yield better results. Furthermore, Procrustes analysis aligned all specimen photos for the landmark analyses much faster than the manual alignment process I performed for the linear measurement analyses.

In sum, landmark-based methods outperformed linear measurement-based methods in both quantitative (Tables 12–13) and qualitative measures. With landmark-based methods, more of the data processing, such as rotation and scaling, is done by software, making the process more replicable and faster. The use of

semilandmarks reduces the need for the discrete, homologous features required by linear measurements, permitting the analysis of more complex morphologies across more taxonomically diverse and morphologically disparate samples. Panciroli et al. (2017) used both linear measurements and 2D landmark data to assign carnivorans to locomotory categories. They argued that each data type usefully compensates for the other's shortcomings, and for superiority of landmarks in capturing complex morphologies. However, they did not identify the shortcomings of landmarks that the linear measurements compensate for. In my opinion, the easier applicability to wide taxonomic samples, greater replicability, and faster workflow of landmark-based methodologies makes them superior for recording tarsal morphology

Relative Utility of Astragalus and Calcaneus

Astragalus datasets had slightly higher F-values for the ANOVA tests and slightly more accurate LDA classification in three of four data type-taxonomic level pairings than calcaneus datasets (Tables 12–13). This conclusion is tempered by the fact that *Homalodotherium* could not be scored for the astragalus direct comparisons may be unfair since there were no *Homalodotherium* — and therefore no Homalodotheriidae — specimens in the astragalus datasets. Excluding *Homalodotherium* specimens from the calcaneus datasets did not clearly affect the results of the ANOVA tests or LDA resampling classification, except for assigning resampled calcanei to genus-level with landmark data (Supplementary File 16). Given these small differences, it does not appear that either tarsal is clearly more systematically useful than the other.

If the morphologies of astragali and calcanei are controlled by the same factors, then one would expect them to exhibit similar clustering patterns in PCA morphospace and morphological disparity, but this was not the case. Intra-taxon disparity differed between astragalus and calcaneus datasets. Toxodontid astragali were significantly more disparate than those of other families, but hegetotheriids had the most disparate calcanei (Table 14). Interestingly, the lower disparity of toxodontid calcanei relative to astragali — and vice versa for hegetotheriids — does not appear to be reflected in the linear measurement datasets (Fig. 28), though this was not tested quantitatively. Given these differing patterns, it appears that the morphologies of SANU astragali and calcanei are not coupled; they record different paleobiological signals. Further study is needed to assess which tarsal records which signal(s), but the toxodontid results detailed above suggest that calcaneal morphology may correlate with body mass. In sum, one cannot study one tarsal and assume that the other exhibits similar patterns of variation. Both astragali and calcanei should be analyzed when possible.

Use of Tarsals for Systematics

One goal of this study was to assess the taxonomic utility of SANU tarsals. Fossil mammal genus- and species-level diagnoses are based heavily on craniodental characters. Besides obvious size differences, there are few ways to assign mammalian postcranial material below the family-level. My results suggest that isolated calcanei and astragali can be assigned to the family and genus-levels once a sufficient sample of possible taxa to which they might be assigned has been amassed. MANOVA and Procrustes ANOVA tests highlight extremely significant

differences ($p<0.001$) between the tarsals of the SANU families and genera in my sample (Table 12), suggesting that tarsals can be distinguished taxonomically.

LDA models were able to assign resampled tarsals to the correct family over 80% of the time and to the correct genus between 46 and 62% of the time (Table 13). These genus-level results are encouraging despite their lower success rate. Resampling one specimen from a poorly represented genus, (e.g., *Pachyrukhos* or *Thoatherium* (Table 11)), removes a large portion of the taxon's total variation, making it much less likely that the LDA model can correctly reassign the specimen to that taxon. If a taxon represented by a single specimen, such as the calcaneus of *Anisolophus*, is resampled, the classification will be an automatic failure since the new LDA has no '*Anisolophus*' group to assign the specimen to. Given the prevalence of these automatic and near-automatic failures due solely to sample size, I am confident that isolated tarsals can be assigned correctly to the correct genus at an even higher rate than shown in Table 13.

I was unable to assess the utility of tarsals for species-level taxonomy because my sample lacked sufficient specimens identified to this level. Furthermore, the systematics of many SCF SANUs is problematic (e.g., *Theosodon*, *Protypotherium*, *Icochilus*; Fernández et al., 2018, 2019b; McGrath et al., 2018) though the situation is improving (Soria, 2001; Fernández et al., 2019a, 2021; Seoane and Cerdeño, 2019) However, species-level variation may be better modeled with LDA than genus- or family-level variation. Linear discriminant analysis assumes that objects (i.e., specimens) within a class (i.e., taxon) are normally

distributed, which may be a more reasonable assumption for species-level than genus- or family-level variation.

My results demonstrate that isolated tarsals can be assigned to genus-level within faunas where the list of taxa is well-understood, such as the fauna analyzed in this study, the outcrops of the SCF exposed along the Atlantic coast of Santa Cruz Province, Argentina, which has been studied for over a century (Vizcaíno et al., 2012a). Although the list of taxa from this, and other similarly well-studied faunas, is likely near-complete, assigning isolated tarsals to lower-order taxa can aid studies relying on taxonomic abundance or high-resolution biostratigraphy.

A more challenging goal would be to assign isolated tarsals from a poorly understood or newly described fauna to one of a list of plausibly related taxa across a span of geologic time and geographic space (e.g., all Miocene interatheriids. The confidence with which tarsals can be used to identify genera or species that are new to a fauna likely varies by clade. Members of morphologically conservative clades, such as Proterotheriidae (Fig. 28; Table 14), may never be identifiable by isolated tarsals because different species or genera are nearly identical postcranially. If the effort to make tarsals reliably assignable to lower-order taxa proves successful, then, given their abundance in the fossil record, these bones would become a valuable tool for investigating faunas' biochronologic affinities or paleoenvironment.

Future Directions

These results demonstrate that landmark and linear measurement data quantify morphology of SANU astragali and calcanei effectively. Morphological

variation is correlated with phylogeny and, perhaps, locomotor habits. The next steps in this long-term project will be to incorporate modern taxa and other fossil faunas of differing ages and paleoenvironments.

Comparing the morphology of modern species with known lifestyles, behaviors, and habitat preferences, to extinct taxa is the basis of ecomorphology. This approach is especially useful for groups like litopterns and notoungulates which are only distantly related to living groups (Croft et al., 2020). For example, fossil members of the modern horse genus *Equus* can be assumed to have behaved much like living forms. Proteomic and genomic evidence suggests that notoungulates and litopterns are members of a larger clade including Perissodactyla and Artiodactyla (Buckley, 2015; Welker et al., 2015; Westbury et al., 2017). These groups are incredibly diverse in their locomotion and they diverged so long ago that their phylogenetic relationships should not have much influence on our conceptions of their locomotory behavior. The aberrant morphologies of certain SANUs (e.g., hegetotheriids, homalodotheriids) are suggestive of locomotor styles, such as fossoriality or occasional bipedality, that rarely, if ever, occur in modern ‘ungulates’ (Elissamburu and Vizcaíno, 2004; Elissamburu, 2010). Accordingly, I will include extant non-ungulate mammals, such as rodents, lagomorphs, and carnivorans, in future sampling of modern forms, along with ‘ungulates.’ Unfortunately, attempting to draw ecomorphological comparisons across distantly related mammal clades may be difficult. Muñoz (2020) examined a combined humeral and femoral database of small carnivorans and rodents to test whether these clades clustered phylogenetically or if ecomorphological trends were consistent across these groups.

Although the phylogenetic signal was stronger, an overlying ecomorphological signal could be discerned. There are a few ways I could attempt to compensate for this phylogenetic signal. I could treat each clade + locomotory style as a distinct class (e.g., “cursorial ‘ungulates,’” or “burrowing carnivorans”), or I could conduct separate analyses for each major modern clade + SANUs.

Tarsal morphology could also be used to examine broad-scale changes in Cenozoic mammal lineages and communities. The spread of open habitats during the middle to late Cenozoic transformed landscapes, leading to numerous dietary, behavioral, and locomotory specializations among mammals (Strömberg, 2011). Attempts to understand the timing of grassland spread primarily focus on evidence from paleobotany or mammalian dietary reconstructions, and these lines of study sometimes disagree (MacFadden, 2000; Shockey and Anaya, 2011; Strömberg, 2011; Bellosi et al., 2021). Adding an additional line of evidence from mammalian locomotion will certainly be useful in resolving this question. Locomotor features related to open habitats and dental features related to dietary specializations may or may not be tightly linked. Some taxa conceivably developed locomotor capabilities to open habitats prior to the appearance of widespread grasslands. Rather than examining specific lineages, using paleocommunities as the units of interest would provide a different view of how modern ecosystems originated.

CONCLUSIONS

South American native ungulate (SANUs) astragali and calcanei from the Santa Cruz Formation can be securely identified at the family or genus levels. (Table 12). Linear discriminant analysis (LDA) reasonably successfully assigns resampled tarsals to their correct family and genus (Table 13). Several genera in the sample were represented by few specimens, so additional sampling would likely improve LDA performance. Except for toxodontid astragali and hegetotheriid calcanei, SANU families exhibited little intra-familial disparity (Table 14). Landmark and linear measurement-based datasets differed little in performance in my analyses. Landmark methods have the advantage of being more easily replicated, less labor intensive, and better at capturing complex morphologies than linear measurement methods, I would favor landmark methodologies in future analyses. Astragali and calcanei were similarly effective for systematics, but they showed different clustering patterns in the PCA morphospaces (Figs. 28–29), suggesting that they record distinct paleobiological signals. Thus, both are worthy of study.

Despite the small sample sizes for some taxa (Table 11) and lack of modern taxa, several conclusions can be drawn from the quantitative results detailed above, and the clustering of the first two principal components (Figs. 28–29). The two litoptern families, Macraucheniidae and Proterotheriidae, clustered tightly in all PCA plots. They also exhibited low disparity despite Proterotheriidae being represented by more genera than other families in my sample (Tables 11, 14). Homalodotheriids, represented by very few specimens in this analysis, plotted far away from all other taxa, which is expected given their facultative bipedality. Toxodontid astragali were tense highly disparate which, appears driven by body size. Interestingly, toxodontid

genera did not plot as clearly separate in the calcaneus morphospaces, suggesting that astragali are more affected by allometry than calcanei. The two interatheriids in my sample, *Interatherium* and *Protypotherium*, generally overlapped in the PCA morphospace. By contrast, the two hegetotheriids, *Hegetotherium* and *Pachyrukhos*, plotted separately. *Pachyrukhos* tarsals plotted closely with those of interatheriids in linear analyses, but not landmark analyses, suggesting that the landmark data recorded components of morphological variation that linear measurements missed. *Hegetotherium* astragali had tense a broad distribution in the PCA morphospace, an unexpected result surprising, given that only a single species is recorded in the SCF.

These analyses demonstrate that tarsal morphology is sufficient to distinguish isolated SANU tarsals at the family- and genus-levels within known faunas, indicating that such elements may be sufficient to prove the presence of these taxa in a given fauna. The next steps of this analysis will be to compare the SANU tarsals to their counterparts in modern mammals whose locomotor behavior is known. Further goals will be to use tarsal morphology to track the evolution of locomotion in mammal lineages and communities across the grand climatic and vegetational changes of the Cenozoic.

Acknowledgements

I would like to thank the Museo Argentino de Ciencias Naturales “Bernardino Rivadavia,” Museo de La Plata, American Museum of Natural History, and Yale Peabody Museum for allowing me to access their fossil collections to collect data for this project. I would also like to thank Chris Everett for helpful conversations that improved the design of this project and quality of this manuscript.

REFERENCES

Adams, D. C., and E. Otárola-Castillo. 2013. Geomorph: An R package for the collection and analysis of geometric morphometric shape data. Methods in Ecology and Evolution 4:393–399.

Adams, D. C., F. J. Rohlf, and D. E. Slice. 2013. A field comes of age: geometric morphometrics in the 21st century. Hystrix 24:7–14.

Ameghino, F. 1883. Sobre una colección de mamíferos fósiles del piso Mesopotámico de la fomación Patagónica recogidos en las barrancas del Paraná por el profesor Pedro Scalabrini en las barrancas del río Paraná. Boletín de La Academia Nacional de Ciencias de Córdoba 5:101–116.

Ameghino, F. 1885. Nuevos restos de mamíferos fósiles oligocenos recogidos por el profesor Pedro Scalabrini y pertenecientes al Museo Provincial de la Ciudad del Paraná. Boletín de La Academia Nacional de Ciencias de Córdoba 8:5–207.

Ameghino, F. 1887. Enumeración sistemática de las especies de mamíferos fósiles coleccionados por Carlos Ameghino en los terrenos eocenos de la Patagonia austral y depositados en el Museo de La Plata. Boletín Museo de La Pla. Boletín Museo de La Plata 5:445–469.

Ameghino, F. 1889. Contribución al conocimiento de los mamíferos fósiles de la República Argentina. Actas de La Academia Nacional de Ciencias de Córdoba 6:1–1027.

Ameghino, F. 1891. Nuevos restos de mamíferos fósiles recogidos por Carlos Ameghino en el Eoceno inferior de la Patagonia austral. Especies nuevas: adiciones y corecciones. Revista Argentina de Historia Natural 1:289–328.

Ameghino, F. 1894. Ennumération synoptique des espéces de mammiféres fossilies des formations éocénes de Patagonie. Boletín de La Academia Nacional de Ciencias de Córdoba 13:259–445.

Ameghino, F. 1901. Notices préliminaires sur des ongulés nouveaux des terrains crétacés de Patagonie. Boletín de La Academia Nacional de Ciencias de Córdoba 16:349–426.

Armella, M. A., D. A. García-López, M. Lorente, and M. J. Babot. 2016. Anatomical and systematic study of proximal tarsals of ungulates from the Geste Formation (northwestern Argentina). Ameghiniana 53:142–159.

Armella, M. A., D. A. García-López, and L. Dominguez. 2018. A new species of Xotodon (Notoungulata, Toxodontidae) from northwestern Argentina. Journal of Vertebrate Paleontology 38:e1425882.

Armella, M. A., D. A. García-López, M. J. Babot, V. Deraco, C. M. Herrera, L. Saade, and S. Bertelli. 2020. Postcranial remains of basal typotherian notoungulates from the Eocene of northwestern Argentina. Acta Palaeontologica Polonica 65:413–428.

Barr, W. A. 2014. Functional morphology of the bovid astragalus in relation to habitat: controlling phylogenetic signal in ecomorphology. Journal of Morphology 275:1201–1216.

Barr, W. A. 2015. Paleoenvironments of the Shungura Formation (Plio-Pleistocene: Ethiopia) based on ecomorphology of the bovid astragalus. Journal of Human Evolution 88:97–107.

Barr, W. A. 2017. Bovid locomotor functional trait distributions reflect land cover and annual precipitation in sub-Saharan Africa. Evolutionary Ecology Research 18:253–267.

Barr, W. A. 2018a. Ecomorphology; pp. 339–349 in D. A. Croft, D. F. Su, and S. W. Simpson (eds.), Methods in Paleoecology: Reconstructing Cenozoic Terrestrial Environments and Ecological Communities. Springer Nature, Cham, Switzerland.

Barr, W. A. 2018b. The morphology of the bovid calcaneus: function, phylogenetic signal, and allometric scaling. Journal of Mammalian Evolution 27:111–121.

Bellosi, E., J. F. Genise, A. Zucol, M. Bond, A. Kramarz, M. V. Sánchez, and J. M. Krause. 2021. Diverse evidence for grasslands since the Eocene in Patagonia. Journal of South American Earth Sciences 108:103357.

Boivin, M., S. Ginot, L. Marivaux, A. J. Altamirano-Sierra, F. Pujos, R. Salas-Gismondi, J. V. Tejada-Lara, and P.-O. Antoine. 2019. Tarsal morphology and locomotor adaptation of some late middle Eocene caviomorph rodents from Peruvian Amazonia reveal early ecological diversity. Journal of Vertebrate Paleontology 38:e1555164.

Brea, M., A. F. Zucol, and A. Iglesias. 2012. Fossil plant studies from late Early Miocene of the Santa Cruz Formation: paleoecology and paleoclimatology at the passive margin of Patagonia, Argentina; pp. 104–129 in S. F. Vizcaíno, R. F. Kay, and M. S. Bargo (eds.), Early Miocene Paleobiology in Patagonia: High-Latitude Paleocommunities of the Santa Cruz Formation. Cambridge University Press, Cambridge, UK.

Buckley, M. 2015. Ancient collagen reveals evolutionary history of the endemic South American “ungulates.” Proceedings of the Royal Society B: Biological Sciences 282:2014–2671.

Burmeister, H. 1879. Description Physique de La République Argentine d’aprés Des Observations Porsonnelles et Étrangéres 3 (Animaux Vertébrés 1: Mammiféeres Vivants e Éteintes). P. E. Coni, Buenos Aires, Argentina, 555 pp.

Cardini, A., and M. Chiapelli. 2020. How flat can a horse be? Exploring 2D

approximations of 3D crania in equids. Zoology 139:125746.

Cassini, G. H. 2013. Skull geometric morphometrics and paleoecology of Santacrucian (late early Miocene; Patagonia) native ungulates (Astrapotheria, Litopterna, and Notoungulata). Ameghiniana 50:193–216.

Cassini, G. H., M. Mendoza, S. F. Vizcaíno, and M. S. Bargo. 2011. Inferring habitat and feeding behaviour of Early Miocene notoungulates from Patagonia. Lethaia 44:153–165.

Cassini, G. H., E. Cerdeño, A. L. Villafañe, and N. A. Muñoz. 2012a. Paleobiology of Santacrucian native ungulates (Meridiungulata: Astrapotheria, Litopterna and Notoungulata); pp. 243–287 in S. F. Vizcaíno, R. F. Kay, and M. S. Bargo (eds.), Early Miocene Paleobiology in Patagonia: High-Latitude Paleocommunities of the Santa Cruz Formation. Cambridge University Press, Cambridge, UK.

Cassini, G. H., S. F. Vizcaíno, and M. S. Bargo. 2012b. Body mass estimation in early Miocene native South American ungulates: a predictive equation based on 3D landmarks. Journal of Zoology 287:53–64.

Catena, A. M., and D. A. Croft. 2020. What are the best modern analogs for ancient South American mammal communities? Evidence from ecological diversity analysis (EDA). Palaeontologia Electronica 23:1–36.

Chen, M., and G. P. Wilson. 2015. A multivariate approach to infer locomotor modes in Mesozoic mammals. Paleobiology 41:280–312.

Cifelli, R. L. 1983. The origin and affinities of the South American Condylarthra and early Tertiary Litopterna (Mammalia). American Museum Novitates 1–49.

Cifelli, R. L., and C. Villarroel. 1997. Paleobiology and affinities of *Megadolodus*; pp. 265–288 in R. F. Kay, R. H. Madden, R. L. Cifelli, and J. J. Flynn (eds.), Vertebrate Paleontology in the Neotropics: The Miocene Fauna of La Venta, Colombia. Smithsonian Institution Press, Washington, D.C., USA.

Cione, A. L., G. M. Gasparini, E. Soibelzon, L. H. Soibelzon, and E. P. Tonni. 2015. The Great American Biotic Interchange: A South American Perspective (J. Rabassa, G. Lohmann, J. Notholt, L. A. Mysak, and V. Unnithan (eds.)). Springer Earth Systems Sciences, Dordrecht, 97 pp.

Coombs, M. C. 1983. Large clawed mammalian herbivores: a comparative study. Transactions of the American Philosophical Society 73:1–99.

Croft, D. A. 2016. Horned Armadillos and Rafting Monkeys: The Fascinating Fossil Mammals of South America. Indiana University Press, Bloomington, Indiana, USA, 304 pp.

Croft, D. A., and L. C. Anderson. 2008. Locomotion in the extinct notoungulate *Protypotherium*. Palaeontologia Electronica 11:1–20.

Croft, D. A., and F. Anaya. 2020. A new typothere notoungulate (Mammalia:

Interatheriidae), from the Miocene Nazareno Formation of southern Bolivia. Ameghiniana 57:189–208.

Croft, D. A., J. N. Gelfo, and G. M. López. 2020. Splendid innovation: the extinct South American native ungulates. Annual Review of Earth and Planetary Sciences 48:259–290.

Cuitiño, J. I., J. C. Fernicola, M. S. Raigemborn, and V. Krapovickas. 2019. Stratigraphy and depositional environments of the Santa Cruz Formation (early-middle Miocene) along the Río Santa Cruz, southern Patagonia, Argentina. Publicación Electrónica de La Asociación Paleontológica Argentina 19:14–33.

Cuitiño, J. I., J. C. Fernicola, M. J. Kohn, R. Trayler, M. Naipauer, M. S. Bargo, R. F. Kay, and S. F. Vizcaíno. 2016. U-Pb geochronology of the Santa Cruz Formation (early Miocene) at the Río Bote and Río Santa Cruz (southernmost Patagonia, Argentina): implications for the correlation of fossil vertebrate localities. Journal of South American Earth Sciences 70:198–210.

Curran, S. C. 2018. Three-dimensional geometric morphometrics in paleoecology; pp. 319–337 in D. A. Croft, D. F. Su, and S. Simpson (eds.), Methods in Paleoecology: Reconstructing Cenozoic Terrestrial Environments and Ecological Communities. Springer Nature, Cham, Switzerland.

Dunn, R. H. 2018. Functional morphology of the postcranial skeleton; pp. 23–36 in D. A. Croft, D. F. Su, and S. Simpson (eds.), Methods in Paleoecology: Reconstructing Cenozoic Terrestrial Environments and Ecological Communities. Springer Nature, Cham, Switzerland.

Dunn, R. H., and D. T. Rasmussen. 2007. Skeletal morphology and locomotor behavior of *Pseudotomus eugenei* (Rodentia, Paramyinae) from the Uinta Formation, Utah. Journal of Vertebrate Paleontology 27:987–1006.

Elissamburu, A. 2004. Análisis morfométrico y morfofuncional del esqueleto apendicular de *Paedotherium* (Mammalia, Notoungulata). Ameghiniana 41:363–380.

Elissamburu, A. 2010. Estudio biomecánico y morfofuncional del esqueleto apendicular de *Homalodotherium* Flower 1873 (Mammalia, Notoungulata). Ameghiniana 47:25–43.

Elissamburu, A., and S. F. Vizcaíno. 2004. Limb proportions and adaptations in caviomorph rodents (Rodentia: Caviomorpha). Journal of Zoology 262:145–159.

Etienne, C., C. Mallet, R. Cornette, and A. Houssaye. 2020. Influence of mass on tarsus shape variation: a morphometrical investigation among Rhinocerotidae (Mammalia: Perissodactyla). Biological Journal of the Linnean Society 129:950–974.

Fariña, R. A., S. F. Vizcaíno, and M. S. Bargo. 1998. Body mass estimations in Lujanian (late Pleistocene-early Holocene of South America) mammal megafauna. Mastozoologica Neotropical 5:87–108.

Fernández, M., and N.A. Muñoz. 2019. Notoungulata and Astrapotheria (Mammalia, Meridiungulata) of the Santa Cruz Formation (early-middle Miocene) along the Río Santa Cruz, Argentine Patagonia. Publicacion Electronica de La Asociacion Paleontologica Argentina 19:138–169.

Fernández, M., J. C. Fernicola, and E. Cerdeño. 2019a. The genus *Patriarchus* Ameghino, 1889 (Mammalia, Notoungulata, Typotheria), from the Santa Cruz Formation, Santa Cruz Province, Argentina. Journal of Vertebrate Paleontology 39:e1613416.

Fernández, M., J. C. Fernicola, and E. Cerdeño. 2019b. On the type materials of the genera *Interatherium* Ameghino, 1887 and *Icochilus* Ameghino, 1889 (Interatheriidae, Notoungulata, Mammalia) from early Miocene of the Santa Cruz Province, Argentina. Zootaxa 4543:195–220.

Fernández, M., J. C. Fernicola, and E. Cerdeño. 2021. Deciduous dentition and dental eruption sequence in Interatheriinae (Notoungulata, Interatheriidae): implications in the systematics of the group. Journal of Paleontology 1–25.

Fernández, M., J. C. Fernicola, E. Cerdeño, and M. A. Reguero. 2018. Identification of type materials of the species of *Protypotherium* Ameghino, 1885 and *Patriarchus* Ameghino, 1889 (Notoungulata: Interatheriidae) erected by Florentino Ameghino. Zootaxa 4387:473–498.

Fernicola, J.C., J.I. Cuitiño, S.F. Vizcaíno, M.S. Bargo, and R.F. Kay. 2014. Fossil localities of the Santa Cruz Formation (early Miocene, Patagonia, Argentina) prospected by Carlos Ameghino in 1887 revisited and the location of the Notohippidian. Journal of South American Earth Sciences 52:94–107.

Fleagle, J. G., M. E. Perkins, M. T. Heizler, A. a. Tauber, B. Nash, T. M. Bown, M. T. Dozo, and M. F. Tejedor. 2012. Absolute and relative ages of fossil localities in the Santa Cruz and Pinturas Formations; pp. 41–58 in S. F. Vizcaíno, R. F. Kay, and M. S. Bargo (eds.), Early Miocene Paleobiology in Patagonia: High-Latitude Paleocommunities of the Santa Cruz Formation. Cambridge University Press, Cambridge, UK.

Flower, W. H. 1873. On a newly discovered extinct mammal from Patagonia (*Homalodotherium cunninghami*). Proceedings of the Royal Society of London 21:383.

Forasiepi, A. M., E. Cerdeño, M. Bond, G. I. Schmidt, M. Naipauer, F. R. Straehl, A. G. Martinelli, A. C. Garrido, M. D. Schmitz, and J. L. Crowley. 2015. New toxodontid (Notoungulata) from the early Miocene of Mendoza, Argentina. Palaontologische Zeitschrift 89:611–634.

Fortelius, M., J. T. Eronen, F. Kaya, H. Tang, P. Raia, and K. Puolamäki. 2014. Evolution of Neogene mammals in Eurasia: environmental forcing and biotic interactions. Annual Review of Earth and Planetary Sciences 42:579–604.

Gelfo, J. N., G. M. López, and M. Lorente. 2016. Los ungulados arcaicos de América del Sur: “Condylarthra” y Litopterna. Contribuciones Científicas Del Museo

Argentino de Ciencias Naturales “Bernardino Rivadavia” 6:285–291.

Ginot, S., L. Hautier, L. Marivaux, and M. Vianey-Liaud. 2016. Ecomorphological analysis of the astragalo-calcaneal complex in rodents and inferences of locomotor behaviours in extinct rodent species. PeerJ 4:e2393.

Hedrick, B. P., P. Antalek-Schrag, A. J. Conith, L. J. Natanson, and P. L. R. Brennan. 2019. Variability and asymmetry in the shape of the spiny dogfish vagina revealed by 2D and 3D geometric morphometrics. Journal of Zoology 308:16–27.

Houssaye, A., V. Fernandez, and G. Billet. 2016. Hyperspecialization in some South American endemic ungulates revealed by long bone microstructure. Journal of Mammalian Evolution 23:221–235.

Kay, R. F., S. F. Vizcaíno, and M. S. Bargo. 2012. A review of the paleoenvironment and paleoecology of the Miocene Santa Cruz Formation; pp. 331–364 in S. F. Vizcaíno, R. F. Kay, and M. S. Bargo (eds.), Early Miocene paleobiology in Patagonia: High-latitude paleocommunities of the Santa Cruz Formation. Cambridge University Press, Cambridge, UK.

Kay, R. F., S. F. Vizcaíno, M. S. Bargo, J. P. Spradley, and J. I. Cuitiño. 2021. Paleoenvironments and paleoecology of the Santa Cruz Formation (early-middle Miocene) along the Río Santa Cruz, Patagonia (Argentina). Journal of South American Earth Sciences 109:103296.

Kovarovic, K., and P. Andrews. 2007. Bovid postcranial ecomorphological survey of the Laetoli paleoenvironment. Journal of Human 52:663–680.

Kuhn, M. 2008. Building predictive models in R using the caret package. Journal of Statistical Software 28:1–26.

Levering, D., S. Hopkins, and E. Davis. 2017. Increasing locomotor efficiency among North American ungulates across the Oligocene-Miocene boundary. Palaeogeography, Palaeoclimatology, Palaeoecology 466:279–286.

MacFadden, B. J. 2000. Cenozoic mammalian herbivores from the Americas: reconstructing ancient diets and terrestrial communities. Annual Review of Ecological Systems 31:33–59.

Macrini, T. E., J. J. Flynn, X. Ni, D. A. Croft, and A. R. Wyss. 2013. Comparative study of notoungulate (Placentalia, Mammalia) bony labyrinths and new phylogenetically informative inner ear characters. Journal of Anatomy 223:442–461.

Martínez, G., M. T. Dozo, J. N. Gelfo, M. R. Ciancio, and R. González-José. 2020. A new toxodont (Mammalia , Panperissodactyla, Notoungulata) from the Oligocene of Patagonia, Argentina, and systematic considerations on the paraphyletic ‘Notohippidae.’ Journal of Systematic Palaeontology 18:1995–2013.

McCoy, D. E., and C. A. Norris. 2012. The cranial anatomy of the Miocene

notoungulate *Hegetotherium mirabile* (Notoungulata, Hegetotheriidae) with preliminary observations on diet and method of feeding. Bulletin of the Peabody Museum of Natural History 53:355–374.

McGrath, A. J., F. Anaya, and D. A. Croft. 2018. Two new macraucheniids (Mammalia: Litopterna) from the late middle Miocene (Laventan South American Land Mammal Age) of Quebrada Honda, Bolivia. Journal of Vertebrate Paleontology 38:e1461632.

McGrath, A. J., J. J. Flynn, and A. R. Wyss. 2020. Proterotheriids and macraucheniids (Litopterna: Mammalia) from the Pampa Castillo Fauna, Chile (early Miocene, Santacrucian SALMA) and a new phylogeny of Proterotheriidae. Journal of Systematic Palaeontology 18:717–738.

Mitteroecker, P., and P. Gunz. 2009. Advances in geometric morphometrics. Evolutionary Biology 36:235–247.

de Muizon, C., R. L. Cifelli, and L. P. Bergqvist. 1998. Eutherian tarsals from the early Paleocene of Bolivia. Journal of Vertebrate Paleontology 18:655–663.

Muñoz, N. A. 2020. Locomotion in rodents and small carnivorans: are they so different? Journal of Mammalian Evolution 28:87–98.

Muñoz, N. A., G. H. Cassini, A. M. Candela, and S. F. Vizcaíno. 2017. Ulnar articular surface 3-D landmarks and ecomorphology of small mammals: a case study of two early Miocene typotheres (Notoungulata) from Patagonia. Earth and Environmental Science Transactions of the Royal Society of Edinburgh 106:315–323.

Owen, R. 1846. Notices of some fossil Mammalia of South America. British Association for the Advancement of Science Report 1846, Transaction of the Sections 16:65–67.

Panciroli, E., C. Janis, M. Stockdale, and A. Martín-Serra. 2017. Correlates between calcaneal morphology and locomotion in extant and extinct carnivorous mammals. Journal of Morphology 278:1333–1353.

Perkins, M. E., J. G. Fleagle, M. T. Heizler, B. Nash, T. M. Brown, A. A. Tauber, and M. T. Dozo. 2012. Tephrochronology of the Miocene Santa Cruz and Pinturas Formations, Argentina; pp. 23–40 in S. F. Vizcaíno, R. F. Kay, and M. S. Bargo (eds.), Early Miocene paleobiology in Patagonia: High-Latitude Paleocommunities of the Santa Cruz Formation. Cambridge University Press, Cambridge, UK.

Plummer, T. W., L. C. Bishop, and F. Hertel. 2008. Habitat preference of extant African bovids based on astragalus morphology: operationalizing ecomorphology for palaeoenvironmental reconstruction. Journal of Archaeological Science 35:3016–3027.

Plummer, T. W., J. V. Ferraro, J. Louys, F. Hertel, Z. Alemseged, R. Bobe, and L. C. Bishop. 2015. Bovid ecomorphology and hominin paleoenvironments of the

Shungura Formation, lower Omo River Valley, Ethiopia. Journal of Human Evolution 88:108–126.

Polly, P. D. 2010. Tiptoeing through the trophics: geographic variation in carnivoran locomotor ecomorphology in relation to environment; pp. 374–410 in A. Goswami and A. Friscia (eds.), Carnivoran Evolution: New Views on Phylogeny, Form, and Function. Cambridge University Press, Cambridge, UK.

R Core Team. 2020. R: a language and environment for statistical computing.

Raigemborn, M. S., S. D. Matheos, V. Krapovickas, S. F. Vizcaíno, M. S. Bargo, R. F. Kay, J. C. Fernicola, and L. Zapata. 2015. Paleoenvironmental reconstruction of the coastal Monte Léon and Santa Cruz formations (early Miocene) at Rincón del Buque, southern Patagonia: a revisited locality. Journal of South American Earth Sciences 60:31–55.

Raigemborn, M. S., V. Krapovickas, A. F. Zucol, L. Zapata, E. Beilinson, N. Toledo, J. Perry, S. Lizzoli, L. Martegani, D. E. Tineo, and E. Passeggi. 2018. Paleosols and related soil-biota of the early Miocene Santa Cruz Formation (Austral-Magallanes Basin, Argentina): a multidisciplinary approach to reconstructing ancient terrestrial ecosystems. Latin American Journal of Sedimentology and Basin Analysis 25:117–148.

Rohlf, F. J. 2006. tpsDig, digitize landmarks and outlines. .

Saarinen, J., D. Mantzouka, and J. Sakala. 2020. Aridity, cooling, open vegetation, and the evolution of plants and animals during the Cenozoic; pp. 83–107 in E. Martinetto, E. Tschopp, and R. A. Gastaldo (eds.), Nature through Time. Springer Nature, Cham, Switzerland.

Schindelin, J., I. Arganda-Carreras, E. Frise, V. Kaynig, M. Longair, T. Pietzsch, S. Preibisch, C. Rueden, S. Saalfeld, B. Schmid, J. Y. Tinevez, D. J. White, V. Hartenstein, K. Eliceiri, P. Tomancak, and A. Cardona. 2012. Fiji: an open-source platform for biological-image analysis. Nature Methods 9:676–682.

Schmidt, G. I., S. H. Del Pino, N. A. Muñoz, and M. Fernández. 2019. Litopterna (Mammalia) from the Santa Cruz Formation (early-middle Miocene) at the Río Santa Cruz, southern Argentina. Publicacion Electronica de La Asociacion Paleontologica Argentina 19:170–192.

Scott, W. B. 1910. Mammalia of the Santa Cruz beds. Part I. Litopterna. Princeton University Expedition to Patagonia 7:1–156.

Scott, W. B. 1912. Mammalia of the Santa Cruz Beds. Part II. Toxodonta; pp. 111–300 in W. B. Scott (ed.), Princeton University Expedition to Patagonia. vol. 6. Princeton University Press, Princeton, USA.

Seckel, L., and C. Janis. 2008. Convergences in scapula morphology among small cursorial mammals: an osteological correlate for locomotory specialization. Journal of Mammalian Evolution 15:261–279.

Seoane, F. D., and E. Cerdeño. 2019. Systematic revision of *Hegetotherium* and

Pachyrukhos (Hegetotheriidae, Notoungulata) and a new phylogenetic analysis of Hegetotheriidae. Journal of Systematic Palaeontology 17:1415–1443.

Seoane, F. D., S. Roig Juñent, and E. Cerdeño. 2017. Phylogeny and paleobiogeography of Hegetotheriidae (Mammalia, Notoungulata). Journal of Vertebrate Paleontology 37:e1278547.

Shelley, S. L., S. L. Brusatte, and T. E. Williamson. 2021. Quantitative assessment of tarsal morphology illuminates locomotor behaviour in Palaeocene mammals following the end-Cretaceous mass extinction. Proceedings of the Royal Society B: Biological Sciences 288:20210393.

Shockey, B. J. 1999. Postcranial osteology and functional morphology of the Litopterna of Salla, Bolivia (late Oligocene). Journal of Vertebrate Paleontology 19:383–390.

Shockey, B. J., and F. Anaya. 2008. Postcranial osteology of mammals from Salla, Bolivia (late Oligocene): form, function, and phylogenetic implications; pp. 135–157 in E. J. Sargis and M. Dagosto (eds.), Mammalian Evolutionary Morphology: A Tribute to Frederick S. Szalay. Springer Science.

Shockey, B. J., and F. Anaya. 2011. Grazing in a new late Oligocene mylodontid sloth and a mylodontid radiation as a component of the Eocene-Oligocene faunal turnover and the early spread of grasslands/savannas in South America. Journal of Mammalian Evolution 18:101–115.

Shockey, B. J., D. A. Croft, and F. Anaya. 2007. Analysis of function in the absence of extant functional homologues: a case study using mesotheriid notoungulates (Mammalia). Paleobiology 33:227–247.

Sinclair, W. J. 1909. The Santa Cruz Typotheria. Proceedings of the American Philosophical Society 47:64–78.

Soria, M. F. 2001. Los Proterotheriidae (Litopterna, Mammalia), sistemática, origen y filogenia. Monografias Del Museo Argentino de Ciencias Naturales 1–171.

Strömberg, C. A. E. 2011. Evolution of grasses and grassland ecosystems. Annual Review of Earth and Planetary Sciences 39:517–544.

Trayler, R. B., M. D. Schmitz, J. I. Cuitiño, M. J. Kohn, M. S. Bargo, R. F. Kay, C. A. E. Strömberg, and S. F. Vizcaíno. 2020. An improved approach to age-modeling in deep time: implications for the Santa Cruz Formation, Argentina. Geological Society of America Bulletin 132:233–244.

Turner, A., and M. Antón. 2004. Evolving Eden: An Illustrated Guide to the Evolution of the African Large-Mammal Fauna. Columbia University Press, New York, New York, USA, 269 pp.

Venables, W. N., and B. D. Ripley. 2002. Modern Applied Statistics with S, 4th ed. Springer, New York, New York, USA.

Vera, B., M. Reguero, and L. González Ruiz. 2017. The Interatheriinae

notoungulates from the middle Miocene Collón Curá Formation in Argentina. Acta Palaeontologica Polonica 62:845–863.

Vizcaíno, S. F., M. S. Bargo, and R. F. Kay. 2012a. Background for a paleoecological study of the Santa Cruz Formation (late Early Miocene) on the Atlantic Coast of Patagonia; pp. 1–22 in S. F. Vizcaíno, R. F. Kay, and M. S. Bargo (eds.), Early Miocene Paleobiology in Patagonia: High-Latitude Paleocommunities of the Santa Cruz Formation. Cambridge University Press, Cambridge, UK.

Vizcaíno, S. F., G. H. Cassini, N. Toledo, and M. S. Bargo. 2012b. On the evolution of large size in mammalian herbivores of Cenozoic faunas of southern South America; pp. 76–101 in B. D. Patterson and L. P. Costa (eds.), Bones, Clones and Biomes: The History and Geography of Recent Neotropical Mammals. University of Chicago Press, Chicago, Illinois, USA.

Vizcaíno, S. F., R. F. Kay, and M. S. Bargo. 2012c. Early Miocene Paleobiology in Patagonia: High-Latitude Paleocommunities of the Santa Cruz Formation. Cambridge University Press, Cambridge, UK, 369 pp.

Wasiljew, B. D., J. Pfaender, B. Wipfler, I. V. Utama, and F. Herder. 2020. Do we need the third dimension? Quantifying the effect of the z-axis in 3D geometric morphometrics based on sailfin silversides (Telmatherinidae). Journal of Fish Biology 97:537–545.

Welker, F., et al. 2015. Ancient proteins resolve the evolutionary history of Darwin's South American ungulates. Nature 522:81–84.

Westbury, M., et al. 2017. A mitogenomic timetree for Darwin's enigmatic South American mammal *Macrauchenia patachonica*. Nature Communications 8:1–8.

Wickham, H., et al. 2019. Welcome to the tidyverse. Journal of Open Source Software 4:1686.

Wyss, A. R., J. J. Flynn, and D. A. Croft. 2018. New Paleogene notohippids and leontiniids (Toxodontia; Notoungulata; Mammalia) from the early Oligocene Tinguirica Fauna of the Andean Main Range, central Chile. American Museum Novitates 1–42.

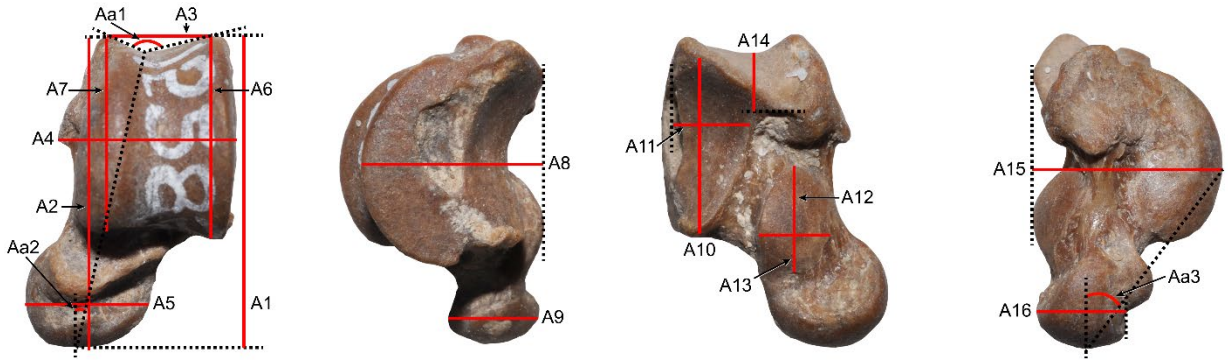

Figure 25: Linear and angular measurements recorded from astragali in (left to right) dorsal, medial, plantar, and lateral views as shown on YPMPU 15285 (*Interatherium* sp.). See Appendix 4 for explanation of measurements and Supplementary File 1 for values. Solid red lines indicate measurements and dashed black lines indicate lines used for alignment.

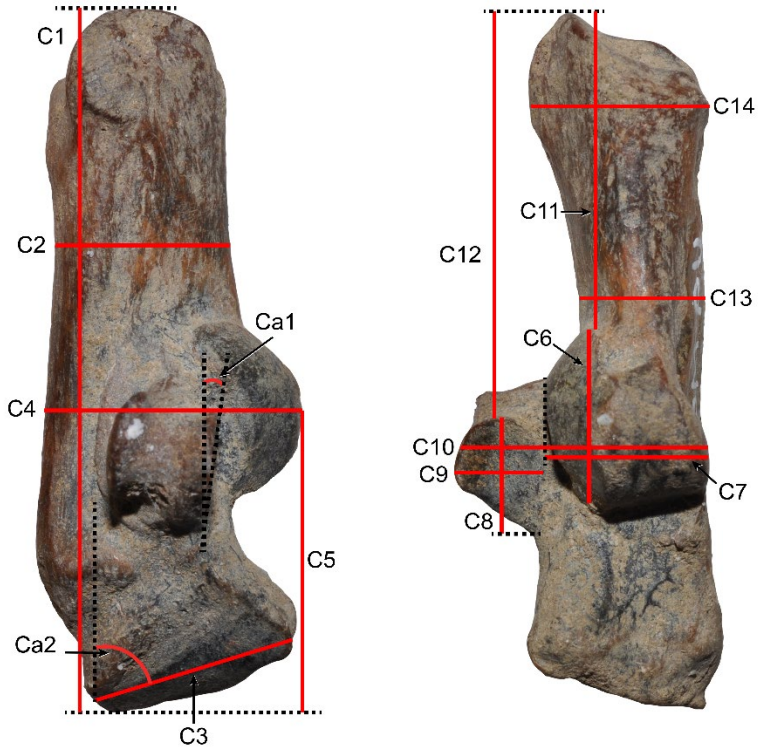

Figure 26: Linear and angular measurements recorded from calcanei in medial (left) and dorsal (right) views as shown on YPM temp 3462 (*Interatherium* sp.). See Appendix 4 for explanation of measurements and Supplementary File 2 for values. Solid red lines indicate measurements and dashed black lines indicate lines used for alignment.

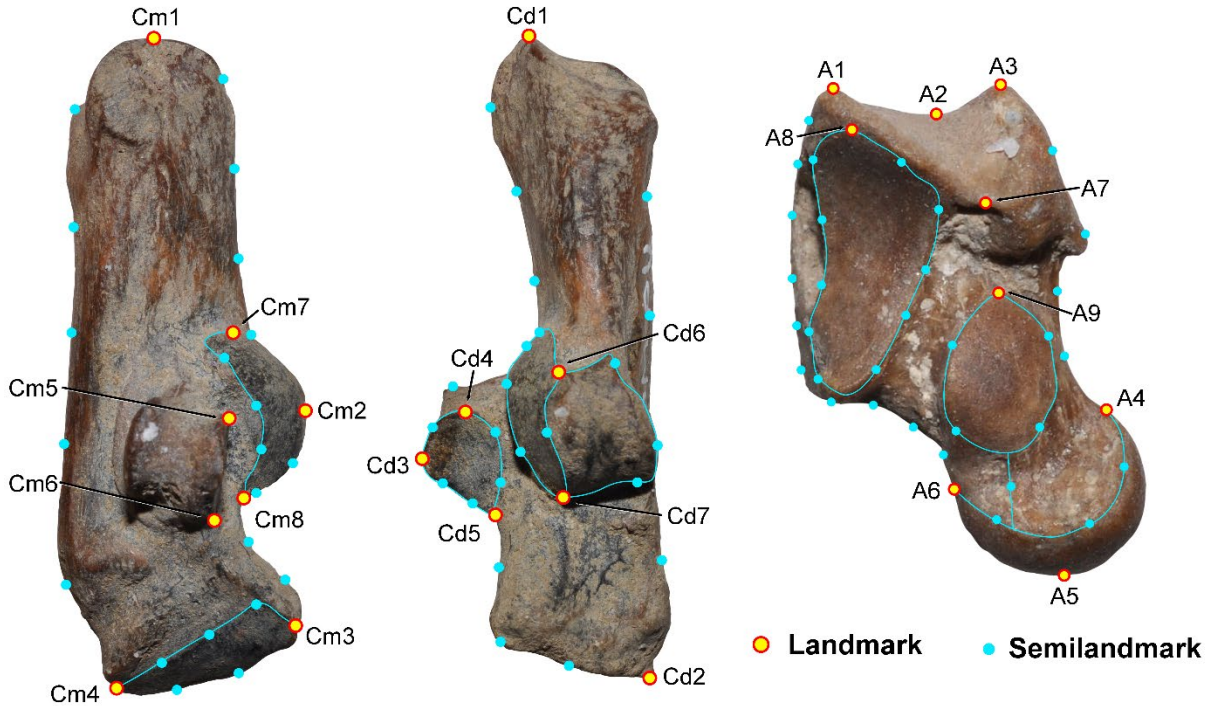

Figure 27: Landmarks and semilandmarks digitized from calcanei in medial (left) and dorsal (center) views (YPM temp 3462; *Interatherium* sp.) and astragali in plantar view (right; YPMPU 15285; *Interatherium* sp.). Labeled yellow and red circles represent landmarks and unlabeled blue circles show semilandmarks. Curves on which semilandmarks are defined are indicated by blue lines when they do not correspond with the external border of the tarsal. See Appendix 5 for explanations of all landmarks and semilandmarks.

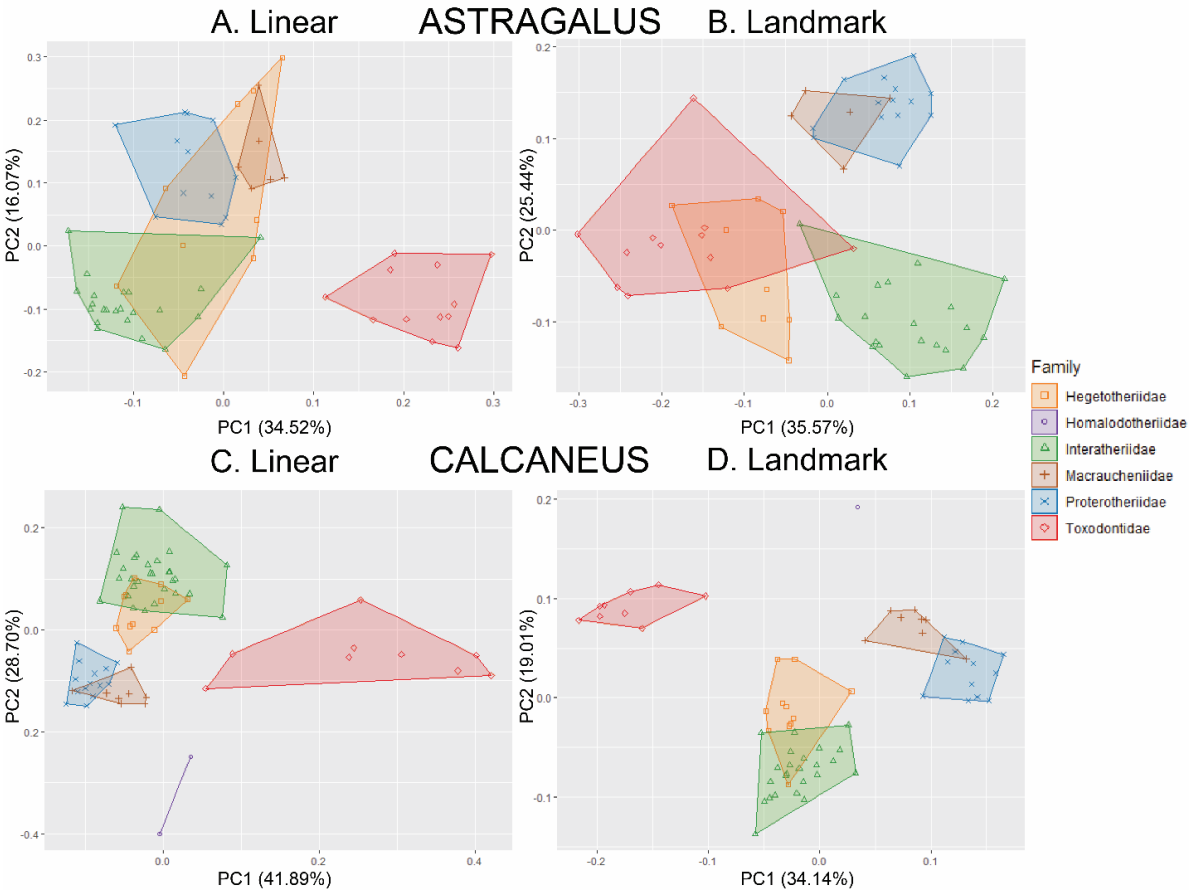

Figure 28: First two principal components of SANU astragali (top) and calcanei (bottom) using linear (left) and landmark (right) techniques grouped according to family.

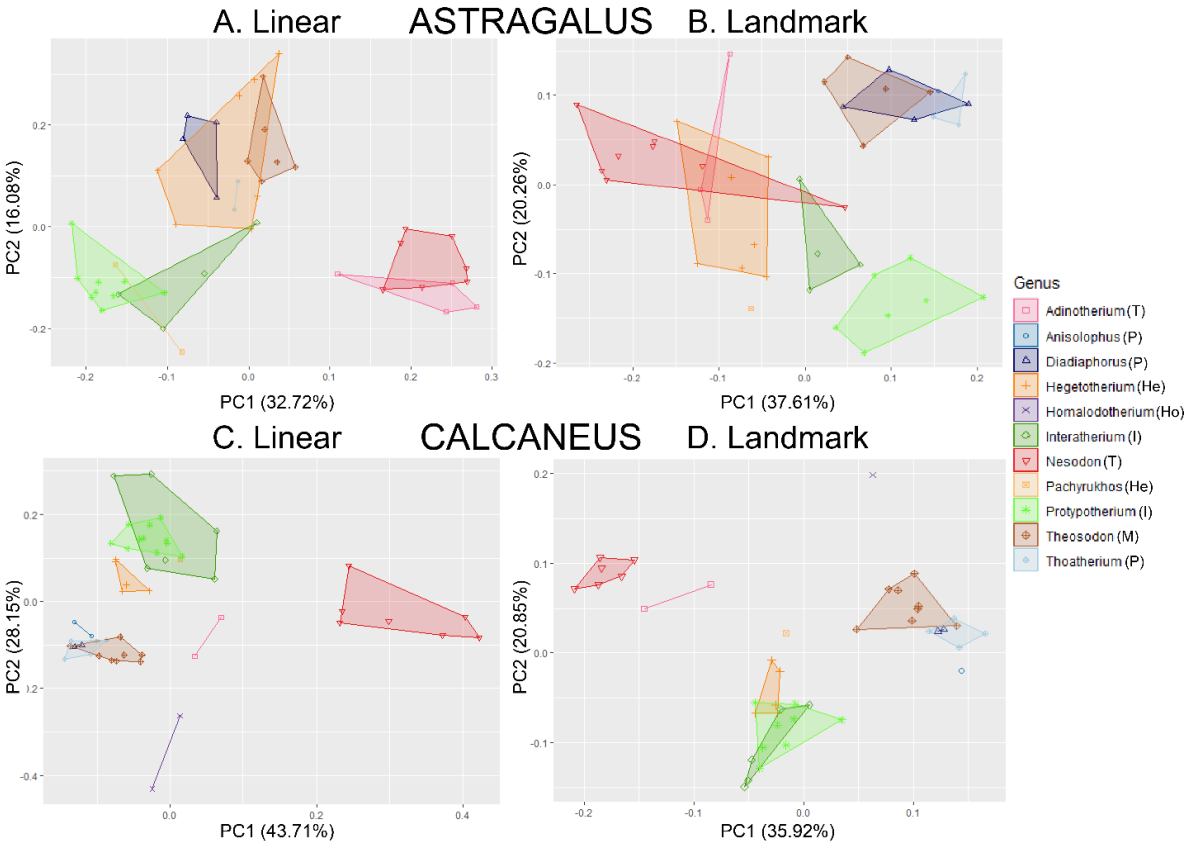

Figure 29: First two principal components of SANU astragali (top) and calcanei (bottom) using linear (left) and landmark (right) techniques grouped according to genus. Abbreviation after genus name indicates family. **Abbreviations:** He–Hegetotheriidae; Ho–Homalodotheriidae; I–Interatheriidae; M–Macraucheniidae; P–Proterotheriidae; T–Toxodontidae.

Table 11: Number of specimens analyzed per taxon and estimated body mass. Body mass estimates are the means cranial-based estimates Cassini et al. (2012b) or mandible-based estimates if cranial estimate was not reported (indicated by *) except for *Homalodotherium* which originated from Vizcaíno et al. (2012b). If Cassini et al. (2012b) calculated mass of multiple species in the genus, the range of means is given. Body mass estimates reported in kg. **Abbreviations:** indet, indeterminate; land, landmark; lin, linear measurement.

Family	**Genus**	**Astragalus**		**Calcaneus**		**Body Mass**
		Lin.	**Land.**	**Lin.**	**Land.**	
Hegetotheriidae	TOTAL	9	9	11	11	—
	Hegetotherium	7	7	5	5	4.67
	Pachyrukhos	2	1	1	1	1.56
	indet	0	1	5	5	—
Homalodotheriidae	TOTAL	0	0	2	1	—
	Homalodotherium	0	0	2	1	340
Interatheriidae	TOTAL	22	20	29	24	—
	Interatherium	4	4	6	5	1.33–1.81
	Protypotherium	9	7	11	8	1.93–3.63
	indet	9	9	12	11	—
Macraucheniidae	TOTAL	6	5	8	8	—
	Theosodon	6	5	8	8	113.09*
Proterotheriidae	TOTAL	12	14	14	12	—
	Anisolophus	0	1	2	1	13.13*
	Diadiaphorus	4	4	2	2	47.49
	Thoatherium	2	3	5	4	19.79
	indet	6	6	5	5	—
Toxodontidae	TOTAL	12	12	9	9	—
	Adinotherium	4	3	2	2	82.06
	Nesodon	7	8	7	6	320.25
	indet	1	1	0	1	—
TOTAL		**61**	**60**	**73**	**65**	

Table 12: Results of MANOVA (linear data) and Procrustes ANOVA (landmark data) tests. *** indicates p-value <0.001.

Element	Level	Data Type	F-value	p-value
Astragalus	Family	Landmark	17.35	***
Astragalus	Family	Linear	10.114	***
Astragalus	Genus	Landmark	5.8759	***
Astragalus	Genus	Linear	2.4178	***
Calcaneus	Family	Landmark	15.949	***
Calcaneus	Family	Linear	8.1091	***
Calcaneus	Genus	Landmark	8.2962	***
Calcaneus	Genus	Linear	2.7123	***

Table 13: Effectiveness of reassigning randomly resampled tarsals to their correct taxon using a linear discriminant model using landmark and linear data. Accuracy indicates percentage of resampling trials where tarsal was classified correctly.

Element	Level	Data Type	Accuracy
Astragalus	Family	Landmark	94.6%
Astragalus	Family	Linear	84.6%
Astragalus	Genus	Landmark	61.6%
Astragalus	Genus	Linear	46.2%
Calcaneus	Family	Landmark	87.3%
Calcaneus	Family	Linear	82.0%
Calcaneus	Genus	Landmark	55.2%
Calcaneus	Genus	Linear	59.2%

Table 14: Intra-family morphological disparity of SANU tarsals using landmark data. Disparity of each family is shown along the diagonal. * indicates a significant difference ($p<0.05$) in intra-familial disparity between families. Abbreviations: Heg, Hegetotheriidae; Hom, Homalodotheriidae; Int, Interatheriidae; Mac, Macraucheniidae; Prot, Proterotheriidae; Tox, Toxodontidae.

ASTRAGALUS					
TAXON	**Heg.**	**Int.**	**Mac.**	**Prot.**	**Tox.**
Heg.	0.01804				*
Int.		0.01733			*
Mac.			0.01055		*
Prot.				0.01282	*
Tox.					0.03420

CALCANEUS						
TAXON	**Heg.**	**Hom.**	**Int.**	**Mac.**	**Prot.**	**Tox.**
Heg.	0.01664	*		*	*	
Hom.		0.01128				
Int.			0.01247			
Mac.				0.00698		
Prot.					0.00695	
Tox.						0.01323

APPENDICES

Appendix 1. Description of characters used in phylogenetic analysis. Characters involving cranial or mandibular dimensions were only recorded on adult specimens (i.e., M3/m3 fully erupted). *–continuous character. †–character adapted from Schmidt (2015).

1. Distance from anterior edge of orbit to tip of rostrum/distance from anterior edge of orbit to posterior edge of cranium. *
2. Dorsoventral height of rostrum (measured perpendicular to plane of tooth row) at distal border of P1/M1 mesiodistal length. *
3. Dorsoventral height of orbit/M1 mesiodistal length. *
4. Width of palate between right and left M1/M1 mesiodistal length. *
5. Mandibular height (measured perpendicular to ventral edge of mandible) at posterior edge of m1/m1 length. *
6. Mandibular height (measured perpendicular to ventral edge of mandible) at distal edge of m3/height at distal edge of p2. *
7. Length of upper incisor–P1 diastema/M1 mesiodistal length. *
8. Mesiodistal length of m1 (mm). *
9. Orbit: open (0); closed (1).
10. Anterior edge of orbit directly over: P4 (0); M1 (1); M2 (2).
11. Posterior edge of infraorbital foramen directly dorsal of: P4 (0); P3 (1).
12. Lateral edges of premaxillae: convergent (0); parallel (1).
13. Posteriormost point of symphysis at level of: p3 (0); p2 (1); p1 (2).
14. Number of upper incisors: three (0); one (1).
15. Upper incisor(s): small and incisiform (0); hypertrophied and tusk-like (1).
16. Number of lower incisors: three (0); two (1).
17. External (distal-most) lower incisor relative to other incisors: subequal (0); significantly larger than internal (mesial) incisor(s) (1).
18. Upper canine: present (0); absent (1).
19. Diastema between P1 and next-most mesial tooth: absent (0); present (1).
20. Lower canine: incisiform (0); tusk-like (1); absent (2).
21. Diastema between c and p1: absent (0); present (1).
22. Cheek teeth: bunodont (0); bunoselenodont (1).
23. P2 protocone: absent (0); present (1).†
24. P3 paracone and metacone: incipient on each other (0); broadly spaced (1).
25. P3 mesiolingual cingulum: not connected to protocone and not forming basin (0); connected to protocone forming basin (1); extends past protocone (2); absent (3).
26. P3 hypocone: absent (0); present (1).†
27. P3 paraconule: absent (0); present (1).
28. P3 metaconule: absent (0); present (1).†
29. P3 parastyle: absent (0); present (1).
30. P3 mesostyle: absent (0); present (1).

31. P4 mesiolingual cingulum: not connected to protocone and not forming basin (0); connected to protocone forming basin (1); extends past protocone (2); absent (3).
32. P4 hypocone: absent (0); present (1).†
33. P4 parastyle: absent (0); present (1).
34. P4 mesostyle: absent (0); present (1).
35. P4 metastyle: absent (0); present (1).
36. P4 metaconule: joined to protocone by crest (0); joined to hypocone by crest (1); absent (2); isolated (3). †
37. M1/P4 linguolabial width: subequal (ratio < or = 1.15) (0); M1 wider (> 1.15) (1).
38. M1–2 metaconule: cuspate (0); absent (1); forming labiolingual crest (2). †
39. M1–2 hypocone: present (0); absent (1).
40. M1–2 paracone and metacone ‘folds’ (ridges between labial styles): strong (0); absent (1); weak (2). †
41. M1–2 paracone and metacone concavities: both weak (0); paracone concavity well-developed (1); both well-developed (2).
42. M1–2 metaconule: more mesial than hypocone (0); at same level as hypocone (1).
43. M1–2 metaconule: joined to protocone (0); joined to hypocone (1); joined to crest uniting hypo- and protocone (2); joined to metacone (3); isolated (4). †
44. M1–2 parastyle and mesostyle: absent (0); present (1). †
45. Relative development of styles in M1–2: mesostyle more developed (0); neither developed (1); parastyle more developed (2); equally developed (3). †
46. Relative development of styles in M3: neither style developed (0); mesostyle more developed (1); equally developed (2); parastyle more developed (3). †
47. M1–2 protocone and hypocone: not directly connected (0); connected by weak crest containing small sulcus (1); connected by complete crest (2). †
48. M1–2 labial cingula: present (0); absent (1). †
49. M3 labial cingulum: present (0); absent (1). †
50. M1 mesiolingual cingulum: not connected to protocone and not forming basin (0); connected to protocone (1); reaches lingual sulcus (2). †
51. M2 mesiolingual cingulum: not connected to protocone and not forming basin (0); connected to protocone (1); reaches lingual sulcus (2). †
52. M3 mesiolingual cingulum: not connected to protocone and not forming basin (0); connected to protocone (1); reaches lingual sulcus (2). †
53. M1 metaconule position: closer to hypocone (0); equidistant (1); closer to protocone (2).
54. M2 metaconule position: closer to hypocone (0); equidistant (1); closer to protocone (2).
55. M1 hypocone: directly distal of protocone (0); positioned more labially than protocone (1).

56. M2 hypocone: directly distal of protocone (0); positioned more labially than protocone (1).
57. M2/M3 coronal area: larger (> or = 1.15) (0); subequal in size (< 1.15) (1).
58. M3 hypocone: present (0); absent (1). †
59. M3 metastyle: absent (0); present (1).
60. M3 distal cingulum: present (0); absent (1).
61. M3 metaconule: connected to protocone by crest (0); absent (1); not connected to protocone (2).
62. Ratio of p2/p1 mesiodistal length: p2/p1 < or = 1.25 (0); p2/p1 > or = 1.45 (1); 1.25 < p2/p1 < 1.45 (2);
63. p1-2 implantation: no diastema (0); diastema between teeth (1); imbricated (2).
64. p2 metaconid: absent (0); present (1).
65. p3 labial cingulid: absent (0); present (1).
66. p3 talonid basin: absent (0); simple crest (1); crescentic loph (2).
67. p3 trigonid basin: mesiodistally longer than talonid basin (0); same length as talonid basin (1).
68. p3 hypoconid: absent (0); lingual of protoconid (1); directly distal of protoconid (2); labial of protoconid (3).
69. p3 hypoconulid: absent (0); present (1).
70. p3 paraconid and metaconid: absent (0); present (1).
71. p3 entoconid: absent or weak (0); well-developed (1).
72. p4 entoconid: absent or weak (0); well-developed (1).
73. p4 labial cingulid: absent (0); present (1).
74. p4 trigonid basin: mesiodistally longer than talonid basin (0); same length as talonid basin (1).
75. p4 hypoconid: lingual of protoconid (0); directly distal of protoconid (1); labial of protoconid (2).
76. m2/m1 mesiodistal length: subequal (ratio is < or = 1.15) (0); m2 larger (> 1.15) (1).
77. Position of paraconid on m1-2: directly lingual of protoconid (0); mesial of protoconid (1); absent (2).
78. Paralophid on m1-2: absent (0); terminates near midline (1); developed and reaching lingual edge of tooth (2). †
79. Entoconid on m1-2: as large as hypoconulid (0); larger than hypoconulid (1); smaller than hypoconulid (2); absent (3). †
80. m1-3 cristids obliquae: connected to metaconid (0); connected to metalophid (1).
81. m1-2 labial cingulids: absent (0); present (1).
82. m3 labial cingulid: absent (0); present (1).
83. m1-2 lingual cingulids: absent (0); present (1).
84. m3 lingual cingulid: absent (0); present (1).

85. Hypsodonty index: HI < 0.85 (0); 0.85 < HI < 1.00 (1); HI > 1.00 (2). †
    Note: Hypsodonty Index was measured only on m3s that were unworn enough so that the lophids were distinguishable from (i.e. thinner than) the cuspids.
86. m3 paraconid: present (0); absent (1).
87. m3 entoconid: isolated (0); connected to hypolophid (1); connected by crest to hypoconulid (2); connected by crest to hypolophulid (3); absent (4). †
88. m1-2 hypoconulid position: not on lingual border of tooth (0); on lingual border of tooth (1).
89. m3 hypoconulid position: not on lingual border of tooth (0); on lingual border of tooth (1).
90. m3 paralophid: absent (0); terminates near midline (1); reaches lingual edge of tooth (2).
91. m3 metaconid: conical (0); mesiodistally extended (1).
92. Manus/pes: Functionally tridactyl (0); functionally or truly monodactyl, as shown by reduced second and/or fourth metapodials (1).

Appendix 2. Notohippidian rodent taxa. “Ameghino’s ‘Notohippidian’” lists all rodent taxa identified by Ameghino (1900-02) as ‘Notohippidian’ but likely includes taxa coming from Río Bote and both the Notohippidian and ‘typical’ Santacrucian layers at Karaiken. “Río Bote” lists all Notohippidian rodents identified by Ameghino (1900-02) that Fernicola *et al.* (2014) determined must come from Río Bote. “Cerro Centinela” lists all rodents that Marshall and Pascual (1977) identify from Cerro Centinela.

Interval/Locality	**Taxon**
Ameghino’s ‘Notohippidian’	*Steiromys duplicatus*
	Acarechimys minutissimus
	Acaremys murinus
	Sciamys principalis
	Adelphomys sp.
	Stichomys sp.
	Spaniomys modestus
	Perimys zonatus
	Eocardia montana
	Schistomys erro
	Phanomys mixtus
	Phanomys vetulus
	Neoreomys australis
Río Bote	*Perimys erutus*
	Schistomys erro
	Phanomys mixtus
	Neoreomys australis
Cerro Centinela	*Stichomys*? sp.
	Adelphomys sp.
	Perimys sp.

Appendix 3. List of all South American native ungulate genera recognized from the Santa Cruz Formation. Genera in bold were included in this analysis. * indicates that *Homalodotherium* calcanei but not astragali were included in this sample. Data taken from (Soria, 2001; Fernicola et al., 2014; Croft, 2016; Cuitiño et al., 2019; Fernández and Muñoz, 2019; Fernández et al., 2019; Schmidt et al., 2019; Seoane and Cerdeño, 2019).

Astrapotheria
- Astrapotheriidae
  - *Astrapotherium* Burmeister, 1879

Litopterna
- Adianthidae
  - *Adianthus* Ameghino, 1891
- Macraucheniidae
  - ***Theosodon*** Ameghino, 1887
- Proterotheriidae
  - ***Anisolophus*** Burmeister, 1879 (*sensu* Soria, 2001)
  - ***Diadiaphorus*** Ameghino, 1887
  - *Tetramerorhinus* Ameghino, 1894 (*sensu* Soria, 2001)
  - ***Thoatherium*** Ameghino, 1887

Notoungulata
- Toxodontia
  - *Notohippus* Ameghino, 1891
  - Homalodotheriidae
    - ***Homalodotherium**** Flower, 1873
  - Toxodontidae
    - ***Adinotherium*** Ameghino, 1887
    - ***Nesodon*** Owen, 1846
- Typotheria
  - Hegetotheriidae
    - ***Hegetotherium*** Ameghino, 1887
    - ***Pachyrukhos*** Ameghino, 1885
  - Interatheriidae
    - ***Interatherium*** Ameghino, 1887
    - *Icochilus* Ameghino, 1889
    - *Patriarchus* Ameghino, 1889 (*sensu* Fernández et al., 2019)
    - ***Protypotherium*** Ameghino, 1887 (*sensu* Fernández et al., 2021)

REFERENCES

Ameghino, F. 1885. Nuevos restos de mamíferos fósiles oligocenos recogidos por el profesor Pedro Scalabrini y pertenecientes al Museo Provincial de la Ciudad del

Paraná. Boletín de La Academia Nacional de Ciencias de Córdoba 8:5–207.
Ameghino, F. 1887. Enumeración sistemática de las Ameghino, F. 1887. Enumeración sistemática de las especies de mamíferos fósiles coleccionados por Carlos Ameghino en los terrenos eocenos de la Patagonia austral y depositados en el Museo de La Plata. Boletín Museo de La Pla. Boletín Museo de La Plata 5:445–469.
Ameghino, F. 1889. Contribución al conocimiento de los mamíferos fósiles de la República Argentina. Actas de La Academia Nacional de Ciencias de Córdoba 6:1–1027.
Ameghino, F. 1891. Nuevos restos de mamíferos fósiles recogidos por Carlos Ameghino en el Eoceno inferior de la Patagonia austral. Especies nuevas: adiciones y corecciones. Revista Argentina de Historia Natural 1:289–328.
Ameghino, F. 1894. Ennumération synoptique des espéces de mammiféres fossilies des formations éocénes de Patagonie. Boletín de La Academia Nacional de Ciencias de Córdoba 13:259–445.
Burmeister, H. 1879. Description Physique de La République Argentine d'aprés Des Observations Porsonnelles et Étrangéres 3 (Animaux Vertébrés 1: Mammiféeres Vivants e Éteintes). Buenos Aires, Argentina:, P. E. Coni, .
Croft, D.A. 2016. Horned Armadillos and Rafting Monkeys: The Fascinating Fossil Mammals of South America. Bloomington, Indiana, USA:, Indiana University Press, .
Cuitiño, J.I., S.F. Vizcaíno, M.S. Bargo, and I. Aramendía. 2019. Sedimentology and fossil vertebrates of the Santa Cruz Formation (early Miocene) in Lago Posadas, southwestern Patagonia, Argentina. Andean Geology 46:383–420.
Fernández, M., and N.A. Muñoz. 2019. Notoungulata and Astrapotheria (Mammalia, Meridiungulata) of the Santa Cruz Formation (early-middle Miocene) along the Río Santa Cruz, Argentine Patagonia. Publicacion Electronica de La Asociacion Paleontologica Argentina 19:138–169.
Fernández, M., J.C. Fernicola, and E. Cerdeño. 2019. The genus *Patriarchus* Ameghino, 1889 (Mammalia, Notoungulata, Typotheria), from the Santa Cruz Formation, Santa Cruz Province, Argentina. Journal of Vertebrate Paleontology 39:e1613416.
Fernández, M., J.C. Fernicola, and E. Cerdeño. 2021. Deciduous dentition and dental eruption sequence in Interatheriinae (Notoungulata, Interatheriidae): implications in the systematics of the group. Journal of Paleontology.
Fernicola, J.C., J.I. Cuitiño, S.F. Vizcaíno, M.S. Bargo, and R.F. Kay. 2014. Fossil localities of the Santa Cruz Formation (early Miocene, Patagonia, Argentina) prospected by Carlos Ameghino in 1887 revisited and the location of the Notohippidian. Journal of South American Earth Sciences 52:94–107.
Flower, W.H. 1873. On a newly discovered extinct mammal from Patagonia (*Homalodotherium cunninghami*). Proceedings of the Royal Society of London 21:383.
Owen, R. 1846. Notices of some fossil Mammalia of South America. British Association for the Advancement of Science Report 1846, Transaction of the Sections 16:65–67.

Appendix 4: Explanation of linear and angular measurements as shown in Figures 1–2. Note the greatest proximodistal length of element (C1 or A1) was recorded in each view to ensure that measurements in each view were equivalent.

CALCANEUS

C1med/C1dor: greatest proximo-distal length of calcaneus in medial (med) and dorsal (dor).

C2: narrowest antero-posterior width of calcaneal tuber (perpendicular to C1med)

C3: antero-posterior length of cuboid facet (greatest length, not necessarily perpendicular to C1med)

C4: antero-posterior width from anterior-most point of ectal facet to posterior edge of calcaneus (perpendicular to C1med)

C5: proximo-distal length from anterior-most point of ectal facet to the distal-most point of calcaneus (parallel to C1 med)

C6: proximo-distal length of ectal facet (parallel to C1dor)

C7: medio-lateral width of ectal facet (perpendicular to C1dor)

C8: proximo-distal length of sustentacular facet (parallel to C1dor)

C9: medio-lateral width of sustentacular facet (perpendicular to C1dor)

C10: greatest medio-lateral width of calcaneus (i.e. across sustentaculum tali; perpendicular to C1dor)

C11: proximo-distal length from proximal-most point of calcaneus to proximal-most point of ectal facet (parallel to C1dor)

C12: proximo-distal length from proximal-most point of calcaneus to proximal-most point of sustentacular facet (parallel to C1dor)

C13: narrowest medio-lateral width of calcaneal tuber (perpendicular to C1dor)

C14: widest medio-lateral width of calcaneal tuber (perpendicular to C1dor)

Ca1: angle formed by sustentacular facet and proximo-distal axis of calcaneus

Ca2: angle formed by cuboid facet (C3) and proximo-distal axis of calcaneus

Note: Calcanei were rotated so that greatest proximodistal axis was vertical. C1med, C2–C5, Ca1, and Ca2 were measured from photographs of calcanei

in medial view. C1dor and C6–14 were measured from photographs of calcanei in dorsal view.

ASTRAGALUS

A1dor/med/pla/lat: length from lateral trochlear ridge to distal-most point of astragalus

A2: length from medial trochlear ridge to distal-most point of astragalus

A3: width between two proximal-most points of trochlear ridges

A4: greatest medio-lateral width across trochlea

A5: medio-lateral width of navicular facet

A6: proximo-distal length of lateral trochlear ridge

A7: proximo-distal length of medial trochlear ridge

A8: greatest dorso-plantar width across lateral trochlear ridge

A9: dorso-plantar width of navicular facet in lateral view

A10: greatest proximo-distal length of ectal facet

A11: greatest medio-lateral width of ectal facet

A12: greatest proximo-distal length of sustentacular facet

A13: greatest medio-lateral width of sustentacular facet

A14: proximo-distal length of trochlea visible in plantar view

A15: greatest dorso-plantar width across medial trochlear ridge

A16: dorso-plantar width of navicular facet in medial view

Aa1: angle formed by ‘vertex’ of trochlear trough and proximal-most points of trochlear ridges

Aa2: angle formed by proximo-distal axis and line connecting ‘vertex’ of trochlear trough and midpoint of navicular facet

Aa3: angle between proximo-distal axis and line connecting dorsal-most point of lateral trochlear ridge and midpoint of navicular facet

Note: Astragali were rotated so that point of greatest curvature on the proximal and distal-most points of the trochlea were aligned vertically in dorsal and plantar views or so that the plantar border of the astragalus was aligned vertically in medial and lateral views. A1dor, A2–A7, Aa1, and Aa2

taken in dorsal view; A1med, A8, and A9 taken in medial view; A1pla and A10–A14 taken in plantar view; A1lat, A15, A16, and Aa3 taken in lateral view.

Appendix 5: Explanation of landmarks and semilandmarks as shown in Figure 3. Curves defining semilandmarks were digitized with as many points as needed to capture shape and then resampled to give the proper number of semilandmarks.

CALCANEUS

Medial View

Landmarks

Cm1: Proximal-most point of calcaneal tuber

Cm2: Dorsal-most point of fibular/ectal facet

Cm3: Dorsal-most point of cuboid facet

Cm4: Plantar-most point of cuboid facet

Cm5: Proximal-most point of sustentacular facet

Cm6: Distal-most point of sustentacular facet

Cm7: Proximal-most point of ectal facet

Cm8: Distal-most point of ectal facet

Semilandmarks

1–4: Dorsal edge of calcaneus from Cm1 to Cm2

5–8: Dorsal edge of calcaneus from Cm2 to Cm3

9–10: Distal edge of calcaneus from Cm3 to Cm4

11–15: Plantar edge of calcaneus from Cm4 to Cm1

16–18: Proximal edge of cuboid facet from Cm3 to Cm4

19–21: Plantar edge of ectal facet from Cm7 to Cm8

Dorsal View

Landmarks

Cd1: Proximal-most point of calcaneal tuber

Cd2: Distal-most point of calcaneus

Cd3: Medial-most point of sustentaculum (may or may not correspond to edge of sustentacular facet)

Cd4: Proximal-most point of sustentacular facet

Cd5: Distal-most point of sustentacular facet

Cd6: Proximal-most point where ectal and fibular facets are joined

Cd7: Distal-most point where ectal and fibular facets are joined

Semilandmarks

1–5: Lateral edge of calcaneus from Cd1 to Cd2

5–8: Medio-distal edge of calcaneus from Cd2 to Cd3

8–12: Medio-proximal edge of calcaneus from Cd3 to Cd1

13–14: Lateral edge of sustentacular facet from Cd4 to Cd5

15–16: Medial edge of sustentacular facet from Cd5 to Cd4

17–19: Proximal, lateral, and distal edges of fibular facet from Cd6 to Cd7

19–21: Distal, medial, and proximal edges of ectal facet from Cd7 to Cd6

22: Junction of fibular and ectal facets from Cd6 to Cd7

ASTRAGALUS (plantar view only)

Landmarks

A1: Proximal-most point of lateral trochlear ridge

A2: Point of greatest curvature in trochlear trough

A3: Proximal-most point of medial trochlear ridge

A4: Proximal-most point of navicular facet along medial edge

A5: Distal-most point of astragalus

A6: Proximal-most point of navicular facet along lateral edge

A7: Distal-most point of trochlea visible on plantar side

A8: Proximal-most point of ectal facet

A9: Proximal-most point of sustentacular facet

Semilandmarks

1–4: Medial edge of astragalus from A3 and A4

6–15: Lateral edge of astragalus from A6 and A1

16–25: Clockwise around ectal facet from A8 to A8

26–29: Medial border of sustentacular facet and possibly proximal edge of navicular facet from A4 to A9. Note: if these facets do not connect (as in Fig. 3), proximal edge of navicular facet was marked until directly distal of A9 then medial edge of sustentacular facet was marked starting directly proximal of this point.

30–33: Lateral border of sustentacular facet and possibly proximal edge of navicular facet from A9 to A6. Note: if these facets do not connect (as in Fig. 3), lateral edge of sustentacular facet was marked until directly distal of A9 then proximal edge of navicular facet was marked starting directly distal of this point.

CAPTIONS FOR SUPPLEMENTARY FIGURES

Figure S1. Fragments of three lower molariform teeth of *Picturotherium* sp. (SGOPV 2158) in occlusal view. Scale bar equals 1 cm.

Figure S2. Maxillary (top) and mandibular (bottom) fragments of Proterotheriidae indet. (SGOPV 2220) in occlusal view. Scale bar equals 1 cm.

Figure S3. Fragment of lower molariform tooth of Proterotheriidae indet. (SGOPV 2416) in occlusal view. Scale bar equals 5 mm.

Figure S4. Strict consensus tree produced by phylogenetic analysis performed after the removal of taxa scored for: **A,** fewer than 33% of characters (four taxa) and **B,** fewer than 50% of characters (ten taxa).

Figure S5. Strict consensus tree produced by phylogenetic analysis when **A,** *Anisolambda* spp.; **B,** *Paranisolambda prodromus*; **C,** *Protheosodon coniferus*; and **D,** all three 'anisolambdids' are constrained to fall outside of clade X. Node X represents the least-inclusive clade that includes all proterotheriids *sensu* Soria (2001).

Figure S6: Tree used for analyses of macraucheniid diversity and body size evolution, based on the phylogenetic analysis of McGrath et al. (2018). Species' known temporal ranges are represented by bold lines. Colored bands indicate time bins. Abbreviations: BAR, Barrancan; CHP, Chapadmalalan; CHS, Chasicoan; CLH, Colhuehuapian; CLL, Colloncuran; DES, Deseadan; HUA, Huayquerian; ITA, Itaboraian; LAV, Laventan; MAR, Marplatan; MAY, Mayoan; MON, Montehermosan; MUS, Mustersan; PLE, Pleistocene; RIO, Riochican; SAN, Santacrucian; TIN, Tinguiririan; VAC, Vacan.

Figure S7: Additional material of the holotype of *Olisanophus riorosarioensis* gen. et sp. nov. (UATF-V-001287) including **1**, partial LM3 (reversed); **2**, right mandibular ramus preserving roots of Rp3–4, partial Rm1–2, and complete Rm3 in occlusal view; **3**, left mandibular ramus preserving roots of Lp2, partial Lp3, and complete Lp4–m3 in labial view. Scale bar = 1 cm.

Figure S8: Additional specimens of *Olisanophus akilachuta* gen. et sp. nov. **1**, partial LM2 of UATF-V-001780. **2**, Right upper molariform (P4 or M1?) of UATF-V-000967. Scale bar = 5 mm.

Figure S9: Partial right mandibular ramus of *Olisanophus akilachuta* gen. et sp. nov. (UATF-V-000987) preserving base of Rm1 and partial Rm2–3. Scale bar = 1 cm.

Figure S10: Referred specimen of *Olisanophus akilachuta* gen. et sp. nov. (UATF-V-001613) including **1**, fragment of RP4 and complete RM1–3 in maxillary fragment in occlusal view and distal right tibia in **2**, distal and **3**, anterior (i.e., dorsal) views. Scale bar = 1 cm.

Figure S11: Associated partial **1**, Lm2 and complete **2**, Lm1 (MNHN BLV 20) referred to *Olisanophus akilachuta* gen. et sp. nov. Scale bar = 1 cm.

Figure S12: Specimens of *Olisanophus* sp. **1**, partial right mandible preserving bases of Rm1–3? (UATF-V-001181) in occlusal (top) and labial (bottom) views; **2**, distal right femur (UATF-V-001907) in anterior view; **3**, distal third metapodial (UATF-V-001999) in (left to right) dorsal, lateral, and plantar views; **4**, distal right tibia (UATF-V-001907) in distal (left) and anterior (i.e., dorsal; right) views. Scale bar = 1 cm.

Figure S13: Partial left mandibular ramus of *Olisanophus* sp. (UATF-V-001562) preserving Lp3–4 in **1**, occlusal and **2**, labial views. Scale bar = 1 cm.

Figure S14: **1**, Strict consensus of twelve most-parsimonious trees of 351.775 steps each with new taxa in bold. **2**, Strict consensus of six most-parsimonious trees of 355.730 steps each with *Protheosodon coniferus* excluded from the clade of ‘traditional proterotheriids’ (i.e., least-inclusive clade that includes all members of Proterotheriidae *sensu* Soria (2001)) with *Neodolodus colombianus* in bold. In both trees, nodes with a Bremer support between 0.500 and 0.999 marked with open circle, and nodes with a Bremer support of 1.000 or larger marked with closed circle.

Figure S15: Results of hierarchical clustering analysis using Jaccard index on Miocene Patagonian rodent communities with provisionally recognized taxa excluded using **A.** genera and **B.** species. Colors and shapes of faunas as in Figure

18. **Abbreviations:** Cc-CILY, Cruces Infinitos and Los Yeguarizos; Cc-CT, Cañadón de Tordillo; Cp-BG, Bryn Gwyn; Cp-CB, Cerro Bandera Formation; Cp-GB-LFZ, lower faunal zone of Colhue-Huapi Member of Sarmiento Formation at Gran Barranca; Sa-GB-UFZ, upper faunal zone of Colhue-Huapi Member of Sarmiento Formation at Gran Barranca; Sa-lmP, lower and middle sequences of Pinturas Formation; Sa-SC-AC, Santa Cruz Formation along Atlantic coast; Sa-SC-RSC, Santa Cruz Formation along Río Santa Cruz; Sa-uP, upper sequence of Pinturas Formation.

Figure S16: Results of hierarchical clustering analysis using Simpson similarity index on Miocene Patagonian rodent communities. **A.** Genera with provisional taxa included; **B.** species with provisional taxa included; **C.** genera with provisional taxa excluded; **D.** species with provisional taxa excluded. **Abbreviations:** Cc-CILY, Cruces Infinitos and Los Yeguarizos; Cc-CT, Cañadón de Tordillo; Cp-BG, Bryn Gwyn; Cp-CB, Cerro Bandera Formation; Cp-GB-LFZ, lower faunal zone of Colhue-Huapi Member of Sarmiento Formation at Gran Barranca; Sa-GB-UFZ, upper faunal zone of Colhue-Huapi Member of Sarmiento Formation at Gran Barranca; Sa-lmP, lower and middle sequences of Pinturas Formation; Sa-SC-AC, Santa Cruz Formation along Atlantic coast; Sa-SC-RSC, Santa Cruz Formation along Río Santa Cruz; Sa-uP, upper sequence of Pinturas Formation.